Imperial College London
Department of the Life Sciences

The anatomy and evolution of "acanthodian" stem-chondrichthyans

Richard P. Dearden

September 2018

Supervised by Martin D. Brazeau

Submitted in partial fulfillment of the requirements for the degree of
Doctor of Philosophy in the Life Sciences of Imperial College London
and the Diploma of Imperial College London

DECLARATION

This thesis comprises my own work. I have acknowledged collaborative parts of the thesis in the "Contributions of authors" section in chapter 1.

Richard Dearden

Copyright Declaration

The copyright of this thesis rests with the author. Unless otherwise indicated, its contents are licensed under a Creative Commons Attribution-NonCommercial 4.0 International Licence (CC BY-NC).

Under this licence, you may copy and redistribute the material in any medium or format. You may also create and distribute modified versions of the work. This is on the condition that: you credit the author and do not use it, or any derivative works, for a commercial purpose.

When reusing or sharing this work, ensure you make the licence terms clear to others by naming the licence and linking to the licence text. Where a work has been adapted, you should indicate that the work has been changed and describe those changes.

Please seek permission from the copyright holder for uses of this work that are not included in this licence or permitted under UK Copyright Law.

The *Cheiracanthus* must have been an eminently handsome little fish...It is, however, a rare matter to find it presenting its original profile in the stone...However perfect the specimen, no part of the internal skeleton is ever found, not even when scales as minute as a pin are preserved, and every spine stands up in its original place.

The Old Red Sandstone or New Walks in an Old Field (3rd ed.)

HUGH MILLER

ACKNOWLEDGEMENTS

Firstly I would like to thank my supervisor, Martin Brazeau, for providing valuable support and advice throughout the project. In particular I have enjoyed the opportunities for fieldwork Martin has provided, notwithstanding my own misadventures with airag and bear spray (separately). Thanks also to my PhD progress panel, Tim Barraclough, Mark Sutton, and Armand Leroi, who provided useful suggestions at progress project reviews. I would also like to acknowledge the European Research Council, who provided the funding upon which my project was based, in addition to a grant from the European Synchrotron Radiation Facility.

Of course, thanks are also due to my Brazeau-lab companions- Anna, Marco, Thomas, and Emma. In them I have found useful advice and valuable friendship, whether visiting Autogrills, dancing in PopWorld, or plumbing The Void. I've also enjoyed working with the many masters students and undergraduates who have passed through the lab - my thanks in particular to Chris Stockey and Andy Ko, who carried out work which has ended up in this thesis.

Throughout the thesis process numerous people have helped me with queries and suggestions regarding my project. I would like to thank Tom Davies and Paul Tafforeau for computed tomography based aid and wisdom. Thanks to Ivan Sansom, Jan den Blaauwen and Plamen Andreev, for help and advice with scale sectioning. Thanks to the numerous staff at museums who have hosted and helped me on collections visits - particularly Emma Bernard at the Natural History Museum and Stig Walsh at the National Museum of Scotland, but also staff at the Senckenberg Frankfurt, Museum of Zoology in Berlin, the Cambridge University Museum of

Zoology, the McManus Gallery in Dundee, and John Bruner and Stephanie Blais at the University of Alberta. Several people have also been generous with their time helping me organise fieldwork - thanks to Bob Davidson, Mike Newman, John Armstrong, and John Flett Brown, as well as Doug Tate and others from Nahanni National Park and Nature Reserve, for help and advice. Many people have also taken the time to give help me with to my projects, whether suggestions or advice or have provided unpublished data for me to refer to. These include Mike Coates, Carole Burrow, Sam Giles, Gavin Hanke, John Maisey, Alan Pradel, Joe Keating, Ben King, and Phil Donoghue. This is almost certainly not an exhaustive list - sorry and thanks to anyone I've forgotten!

Despite regular whinging I have greatly enjoyed my time at Silwood Park and would have enjoyed it far less if not for the people I have met here, so thanks to all of them. One of my greatest pleasures has been putting these gripes into (extremely) amateur dramatic form in the annual Silwood Revue, so thanks to everyone who has got involved in that. The Denizens of the Slodge (variously, Chris, Richard, Jack, and Dylan) have been great to live with, forgiving lapses in kitchen hygiene and finger-based emergencies. Pizza Monday has been fantastic - thanks to Owen, Rishi, and Thomas as much as to the pizza - and has drastically improved my culinary horizons. Silwood *a cappella* has kept me singing during my lunchtimes, if only rarely *a cappella*. My most regular activity has been the Crossword Club, aiding and abetting my morning brain break (procrastination?) over the last four years, and providing me new words to put in my thesis, like dacha, spiv, and mufti.

Thanks also to the support staff that have helped throughout the PhD. In particular this includes Theo, Barbara, and Liz in the library, for helping me acquire arcane tomes ranging from to what seems like the entire back-catalogue of Palaeontographica Abteilung A, to lengthy treatises on ancient Belgic coinage.

Last, but not least, thanks to Amy for putting up with more lengthy soliloquies on fossil fishes (and cathedrals) than any plant scientist should ever have to listen to. Thanks to the collective Deardens - Mum, Dad, Eddie, Lizzie, and Chris (and Pippa the Dog). And thanks to my wider friends and family, in particular my grandfather for getting me interested in this kind of thing in the first place.

ABSTRACT

Acanthodians, an enigmatic grade of Palaeozoic fishes, have loomed large in theories about vertebrate evolution. In recent years evidence has steadily grown that acanthodians, once thought to be a group, are instead a paraphyletic grade comprising the very earliest chondrichthyans (sharks, rays, and elephant sharks). However, the poor preservational potential that once obscured the acanthodians' position in gnathostome phylogeny instead now blights the relationships of stem-chondrichthyans to one another and to the chondrichthyan crown-group. This in turn conceals the history of the assembly of the chondrichthyan body plan. In this thesis I aim to address this by describing the anatomy of three acanthodians from the Devonian (419-359 Mya) of the United Kingdom - *Ptomacanthus*, *Diplacanthus*, and *Vernicomacanthus*. Computed microtomographic imaging of a fossil of *Ptomacanthus* reveals the skeleton of the pharynx, preserved articulated and in three dimensions. Synchrotron microtomographic imaging of a fossil of *Diplacanthus* reveals a crushed branchial, mandibular, and neurocranial skeleton. Comparison of the tissue forming this endoskeleton with new information on endochondral bone in an acanthothoracid placo- derm allows a reassessment of the evolution of endochondral tissues in gnathostomes. I also redescribe *Vernicomacanthus* on the basis of new material and histological study, and assess the comparative anatomy of acanthodian shoulder girdles. Finally, I carry out a reanalysis of stem-chondrichthyan phylogeny in the light of this information. This new information helps constrain changes in the chondrichthyan branchial and neurocranial skeleton to specific parts of the chondrichthyan stem-group. It also adds to a growing body of evidence that "acanthodians" form two distinct grades in the chondrichthyan stem-group: a rump grade at the base of the chondrichthyan stem-group, and a paraphyletic grade of "climatiid" taxa.

Table of Contents

Acknowledgements . . . 5

Abstract . . . 8

Table of Contents . . . 9

List of Figures . . . 12

1 Introduction . . . 1
- 1.1 A chondrichthyan primer . . . 2
- 1.2 The acanthodian fishes . . . 6
- 1.3 Current problems in early chondrichthyan evolution . . . 14
- 1.4 Methods Overview . . . 18
- 1.5 Thesis aims . . . 22
- 1.6 Contribution of authors . . . 23

2 Characters of the chondrichthyan total group. . . . 25
- 2.1 Problems in early chondrichthyan phylogeny . . . 25
- 2.2 What makes a scale chondrichthyan? . . . 26
- 2.3 Characters of chondrichthyans . . . 39
- 2.4 Assessment of fossil taxa . . . 73
- 2.5 Conclusion . . . 80

3 The visceral skeleton of the stem-chondrichthyan *Ptomacanthus* . . . 81
- 3.1 Introduction . . . 81
- 3.2 Materials and Methods . . . 83
- 3.3 Results . . . 85
- 3.4 Discussion . . . 93
- 3.5 Conclusion . . . 104

4 A third "acanthodian" endoskeleton in *Diplacanthus crassisimus* . . . 106
- 4.1 Introduction . . . 106

4.2 Materials and Methods . . . 108
4.3 Results . . . 110
4.4 Discussion . . . 131

5 Endochondral tissues in early vertebrates . . . 142
5.1 Introduction . . . 142
5.2 Materials and Methods . . . 144
5.3 Results . . . 145
5.4 Discussion . . . 153
5.5 Conclusion . . . 158

6 The stem-chondrichthyan genus *Vernicomacanthus* and the early evolution of the chondrichthyan shoulder girdle . . . 159
6.1 Introduction . . . 159
6.2 Materials and Methods . . . 161
6.3 The acanthodian-grade genus *Vernicomacanthus* . . . 163
6.4 Comparative anatomy of two acanthodian shoulder girdles . . . 181
6.5 Discussion . . . 187
6.6 Conclusion . . . 198

7 A phylogenetic exploration of the chondrichthyan stem-group . . . 199
7.1 Introduction . . . 199
7.2 Methods . . . 199
7.3 Results . . . 201
7.4 Discussion . . . 212
7.5 Conclusion . . . 218

8 Conclusion . . . 219

Appendices . . . 253

A Appendix A: Details of phylogenetic analysis for Chapter 3 . . . 253

B Appendix B: Details of phylogenetic analysis for Chapter 7. . . . 260
B.1 Taxa and references . . . 260
B.2 Notes on character derivation . . . 264
B.3 Abbreviations for character sources . . . 264
B.4 Character list . . . 264

C APPENDIX C: DETAILS OF SUPPLEMENTARY INFORMATION 353

List of Figures

FIGURE 1.1 Caption next page 3

FIGURE 1.1 Phylogeny of early gnathostomes, plotted against time. Topology is the strict consensus tree from the dataset of Coates et al. (2018). Dates taken from the literature. Inset is the same scheme of relationships, but simplified. 4

FIGURE 1.2 Caption next page 7

FIGURE 1.2 Selected articulated acanthodian-grade stem-chondrichthyans. Pictured are (a) *Mesacanthus*, an "acanthodiform"; (b) an ischnacanthid; (c) *Diplacanthus*, a diplacanthiform; (d) *Vernicomacanthus*, a "climatiid", and (e) *Brochoadmones*, one of the problematic MOTH taxa 8

FIGURE 2.1 Body scales of select gnathostomes in dorsal view (first column) and bisected through the sagittal plane (second column): (a) the osteichthyan *Psarolepis* from (Qu et al., 2013b); (b) the stem-chondrichthyan *Acanthodes* from (Denison, 1979); (c) the stem-chondrichhyan *Vernicomacanthus* from Chapter 6 of this thesis; (d) the stem-chondrichthyan *Seretolepis* from Karatajūtė-Talimaa (1997); Hanke and Wilson (2010); (e) An elasmobranch chondrichthyan, from (Smith and Hall, 1990). 32

FIGURE 2.1 Caption previous page 33

FIGURE 2.2 Neurocrania and endocasts of select gnathostomes in dorsal view: (a) The stem-gnathostome *Dicksonosteus*, from Goujet (1984); (b) The actinopterygian *Mimipiscis*, from Gardiner (1984); Giles and Friedman (2014); (c) The stem-chondrichthyan *Acanthodes*, from Davis et al. (2012); (d) The holocephalan *Callorhincus* from Coates et al. (2017a); (e) The symmorriiform *Dwykaselachus*, from Coates et al. (2017a); (f) The Palaeozoic "shark" *Cladodoides* from Maisey (2005). 43

FIGURE 2.3 Select gnathostome neurocrania in ventral view: (a) The stem-gnathostome *Dicksonosteus*, from Goujet (1984); (b) The actinopterygian *Raynerius* from Giles et al. (2015b); (c) The stem-gnathostome *Janusiscus* from Giles et al. (2015c); (d) The stem-chondrichthyan *Acanthodes* from Davis et al. (2012); (e) The stem-chondrichthyan *Doliodus* from Maisey et al. (2009); (f) The stem-elasmobranch *Egertonodus* from Maisey (1983); (g) The symmoriiform *Dwykaselachus* from Coates et al. (2017a); (h) The holocephalan *Hydrolagus* from Allis (1917). 44

FIGURE 2.4 Neurocrania and endocasts of select gnathostomes in lateral view: (a) The stem-chondrichthyan *Acanthodes*, from Davis et al. (2012); Miles (1973a); (b) The Palaeozoic "shark" *Cladodoides* from Maisey (2005);(c) The actinopterygian *Mimipiscis*, from Gardiner (1984); Giles and Friedman (2014);(d) The holocephalan *Callorhincus* from Coates et al. (2017a);(e) The symmorriiform *Dwykaselachus*, from Coates et al. (2017a); (f) The stem-elasmobranch *Tribodus*, from Lane (2010).. 46

FIGURE 2.5 Branchial arches in select gnathostomes, laterally flattened, with ventral elements on the left and dorsal on the right: (a) The actinopterygian *Raynerius*, from Giles et al. (2015b); (b) The stem-gnathostome *Paraplesiobatis*, from Brazeau et al. (2017); (c) The stem-gnathostome *Acanthodes*, from Gardiner (1984); Miles (1973b); (d) The symmoriiform *Ozarcus*, from Pradel et al. (2014); (e) The elasmobranch *Scyliorhinus* from Pradel et al. (2014); (f) The holocephalan *Callorhincus* from Pradel et al. (2014). Colour scheme: *red*, basihyal/branchial; *turquoise*, hypobranchial; *purple*, ceratohyal/branchial; *yellow*, epihyal/branchial; *orange*, pharyngohyal/branchial. Lighter shades denote hyoid arch. . . . 48

FIGURE 2.6 Meckel's cartilages from selected gnathostomes: (a) The stem-chondrichthyan *Acanthodes*, from Miles (1973b); (b) The Palaeozoic "shark" *Cladodoides*, from Gross (1938); (c) The stem-holocephalan *Iniopera*, from Pradel (2010); (d) The stem-elasmobranch *Homalodontus*, from Mutter et al. (2007). Arrows denote position of articulation with palatoquadrate. 60

FIGURE 2.7 Bodies of select gnathostomes: (a) The actinopterygian *Mimipiscis*, from Gardiner (1984); (b) The stem-chondrichthyan *Ptomacanthus*, from Brazeau (2012); (c) The stem-holocephalan *Squaloraja*, from Patterson (1965); (d) The crown-elasmobranch *Heterodontus*, from Janvier (1996).. 62
FIGURE 2.8 The neurocrania of select gnathostomes in anterior view: (a) The actinpterygian *Raynerius*, from Giles et al. (2015b); (b) The stem-chondrichthyan *Acanthodes*, from Davis et al. (2012); (c) The stem-holocephalan *Iniopera*, from Pradel (2010); (d) The stem-elasmobranch *Egertonodus*, from Maisey (1983). 67

FIGURE 3.1 (a) Photograph of NHM P.24919a scale bar 20mm; (b) Virtual rendering of pharyngeal skeleton; (c) Drawing of dorsal branchial skeleton from the anatomical left hand side; (d) Drawing of ventral branchial skeleton. Colour scheme: *red*, basihyal/branchial; *turquoise*, hypobranchial; *purple*, ceratohyal/branchial; *yellow*, epihyal/branchial; *orange*, pharyngohyal/branchial. Lighter shades denote hyoid arch, . . . 87
FIGURE 3.2 Caption on next page. 88
FIGURE 3.2 (a) Dorsal view of the ventral branchial skeleton, with the groove in right ceratobranchial II shown (line runs approximately through groove) in (b) dorsal and (c) posterior aspect, (d) Dorsal view of the left hand dorsal branchial skeleton, with views of (e) the right hand anterior dorsal skeleton, (f) displaced fourth epibranchial, and (g) the junction between the fourth and fifth left epi- and pharyngobranchials.. 89
FIGURE 3.3 Caption on next page. 91
FIGURE 3.3 The *Ptomacanthus* visceral skeleton juxtaposed against the mould of the specimen surface (a) with visceral skeleton, (b) with dorsal visceral skeleton, (c) the mould only 92
FIGURE 3.4 Tomograms showing the basihyal in (a) the approximate sagittal plane, and reconstructed section through (b) the approximate transverse plane, and (c) the approximate coronal plane. Abbreviations: br. arch, branchial arch; cerhy., ceratohyal; gul. squam., gular squamation; Mck., Meckel's cartilage. 93

FIGURE 3.5 The consensus tree of the Bayesian analysis, with nodes labelled with posterior probabilities - the percentage of sampled trees recovering that split. 94
FIGURE 3.6 The results of the parsimony analysis (a) the strict consensus tree, (b) the majority rule consensus tree.. 95
FIGURE 3.7 Postero-anterior extent of branchial skeleton in (a) *Dicksonosteus* Goujet (1984),(b) *Raynerius* (Giles et al., 2015b), (c) *Acanthodes* (Miles, 1973b; Davis et al., 2012), (d) *Ptomacanthus* (Brazeau, 2009), (e) *Gladbachus* (Coates et al., 2018), (f) *Ozarcus* (Maisey, 2007; Pradel et al., 2014). Phylogenetic tree congruent with topology described in methods. P indicates a shift of the posterior extent of the branchial skeleton, while A indicates a shift of the anterior extent. Colour scheme: gray, neurocranium; light yellow, hyomandibular; dark yellow, epibranchial; orange, pharyngobranchial; blue, dermal shoulder girdle. 97
FIGURE 3.8 The phylogenetic distribution of branchial arch morphologies in gnathostomes, based on the strict consensus tree derived from the parsimony analysis described in the methods. Character changes of selected pharyngeal arch characters from our analysis are plotted using an ACCTRAN optimisation. Taxa shown are (a) *Cowralepis*Carr et al. (2009), (b) *Paraplesiobatis* (Brazeau et al., 2017), (c) *Raynerius* (Giles et al., 2015b), (d) *Glyptolepis* (Jarvik, 1972), (e) *Acanthodes* (Gardiner, 1984; Miles, 1973b), (f) *Ptomacanthus*, (g) *Gladbachus* Coates et al. (2018), (h) *Triodus* (Heidtke et al., 2004), (i) *Scyliorhinus* (Pradel et al., 2014), (j) *Ozarcus* (Pradel et al., 2014), (k) *Callorhinchus*Pradel et al. (2014), (h) *Debeerius* (Grogan and Lund, 2000). Colour scheme: as in figure 6, with addition of: light turquoise, hypohyal; gray, urohyal. Silhouette from Brazeau (2012); Long (1986a); Schaeffer and Williams (1977); Gardiner (1984), and Phylopic. 100

FIGURE 4.1 Caption on next page. 109

FIGURE 4.1 Entire specimen (a) Photograph of specimen NMS 1891.92.334; (b) close-up photograph of mineralised endoskeleton; (c) entirety of segmented region; exterior view; (d) entirety of segmented region, interior view. Colours: blue, dermal; lilac, neurocranium; purple, branchial; teal, mandibular and hyoid; yellow, vertebral column. 110
FIGURE 4.2 Caption on next page. 112
FIGURE 4.2 Figure 2: Neurocranial and vertebral skeleton in (a) lateral; and (b) medial view; (c) Braincase juxtaposed against mould of surface, showing lateral commisure; Braincase of *Acanthodes* in (d) anterior, and (e) Lateral view showing corresponding details of lateral commissure . Abbreviations as in Figure 2. 113
FIGURE 4.3 Anterior neurocranial mineralisation (a) From internal side against the mould of the specimen surface; (b) From internal side but rotated slightly to show foraminae in surface; (c) From external side, (d) Neurocranium of *Doliodus* in ventral view with subnasal plate highlighted, redrawn from Maisey et al. (2009); (e) Neurocranium of *Cladodoides* in lateral view with anterior orbital wall highlighted, redrawn from Maisey (2005). 114
FIGURE 4.4 Caption on next page. 116
FIGURE 4.4 Attempted reconstruction of left lateral otic region in *Diplacanthus* in (a) lateral view, (b) same lateral view as *in situ*; (c) posterior view; (d) medial view; (e) Photograph of *Acanthodes* cast NHM P.49995, showing comparable region; (f) neurocranium of *Acanthodes* in lateral view with approximate corresponding region highlighted, redrawn from Davis et al. (2012); (g) neurocranium of *Pucapampella* in lateral view, redrawn from Maisey (2001a); (h) neurocranium of *Cladodoides* in lateral view, redrawn from Maisey (2005); (i) neurocranium of *Mimipiscis* in lateral view, redrawn from Gardiner (1984) 117
FIGURE 4.5 Caption on next page. 118

FIGURE 4.5 (a) Right half of basicoccipital of *Diplacanthus* in medial view; (b) Left half of basioccipital of *Diplacanthus* in lateral view; (c) Interpretive drawing of right half of basicoccipital of Diplacanthus in medial view; (d) Interpretive drawing of left half of basioccipital of *Diplacanthus* in lateral view; (e) sagittal section through postero-ventral neurocranium of *Mimipiscis*, redrawn from Gardiner (1984); (f) Lateral view of basioccipital of *Acanthodes*, redrawn from Miles (1973b); (g) Ventral view of basioccipital of Acanthodes, redrawn from Miles (1973b); (h) Putative basioccipital of *Milesacanthus* in ventral (?) view, redrawn from Young and Burrow (2004); (i) Ventral view of basioccipital of *Diplacanthus* 119

FIGURE 4.6 Basioccipital region of selected early vertebrates, showing path of ventral vasculature (a) *Diplacanthus*; (b) The stem-chondrichthyan *Acanthodes*, redrawn from Davis et al. (2012); (c) The stem-chondrichthyan *Doliodus*, redrawn from Maisey et al. (2009); (d) The symmoriiform *Dwykaselachus*, redrawn from Coates et al. (2017a); (e) The actinopterygian *Raynerius*, redrawn from Giles et al. (2015b), (f) The sarcopterygian *Ptyctolepis*, redrawn from Lu et al. (2017), (g) The stem-gnathostome *Dicksonosteus*, redrawn from Goujet (1984), (h) The stem-gnathostome *Janusiscus*, redrawn from Giles et al. (2015c) 120

FIGURE 4.7 Mandibular and hyoid skeleton (a) in lateral view; (b) in medial view; (c) showing postero-medial displacement of metapterygoid relative to quadrate; (d) articulation between the left Meckel's cartilage and palatoquadrate; (e) right Meckel's cartilage in medial view; (f) left Meckel's cartilage in posterior view ; (g) left Meckel's cartilage in lateral view. Abbreviations: L, left; R, right. 122

FIGURE 4.7 Caption on previous page 123

FIGURE 4.8 (a) Entire branchial skeleton from left (internal) side, dermal plate removed; (b) proximal end of ceratobranchial III; (c) proximal end of ceratobranchial II; (d) Interpretation of the branchial skeleton of *Kathemacanthus* from Hanke and Wilson (2010); Epibranchial in (e) lateral, and (f) medial view; Pharyngobranchial IV? in (g) medial, and (h) lateral view; (i) entire branchial skeleton from right (external) side, dermal plate removed. Abbreviations as in Figure 2. 127

FIGURE 5.1 Caption on next page 147

FIGURE 5.1 Tomograms showing different section through tissues in *Diplacanthus crassisimus* NMS 1891.92.334. (a) ceratohyal and opercular plate; (b) mid-section of Meckel's cartilage articular; (c) anterior end of Meckel's cartilage articular; (d) palatoquadrate (below) and the anterior ceratohyal (above); (e) ventral plate of procoracoid, (f) cartilaginous core of procoracoid, (g) dermal plate of procoracoid . Abbreviations: gcc, globular calcified cartilage. 148

FIGURE 5.2 The three dimensional structure of globular calcified cartilage in *Diplacanthus crassisimus*. (a) section through ceratohyal from tomogram; (b-d) 3 dimensional model of tissue with increasing transparency of cartilage; (e) three dimensional model of ceratohyal with approximate plane of section shown. Colours (b-e): grey, cartilage (variance in shade show differences in threshold); red, chondrocyte lacunae. 149

FIGURE 5.3 Endochondral bone in an arthrodire placoderm braincase. (a) ventral view; (b) posterior view of occipital region; (c) dorsal view; (d) endocast in dorsal view; (e) right labyrinth in lateral view; (f) endocast in ventral view, (g) specimen in matrix, (h) close up view of tomogram 152

FIGURE 6.1 Four articulated specimens of *Vernicomacanthus uncinatus*: (a) NMS 1891.92.203; (b) NHM P.1342a; (c) DUNMG Kinnaird 82; (d) NMS 2001.7.4. Scale bar is 5mm in all cases.. 165

FIGURE 6.2 The head of *Vernicomacantus uncinatus*. (a) DUNMG Kinnaird 82, (b) NMS 1891.92.203, (c) NHM P.1342a, (d) Magnified picture of sensory line in NMS 1891.92.203, (e) CT rendered model surface model of NMS 2001.7.4, with SEMS of (f) Postorbital tessera, (g) rostral denticles, (h) head tessera, (i) several head tesserae in articulation, (j) branchial plates. 168
FIGURE 6.3 The shoulder girdle in *Vernicomacanthus uncinatus*: (a) DUNMG Kinnaird 82; (b) NMS 1891.92.203, (c) NMS 1885.54.69a, (d) NHM P.1342a. Abbreviations: R., right; L.,left. All scale bars 50mm. . . 171
FIGURE 6.4 Details of fin spines in *V. uncinatus* NMS 2001.7.4. 173
FIGURE 6.5 Histology in an isolated pectoral fin spine NMS G.2018.18.1 of *V. uncinatus*: (a) Plan of sections through fin spine, with drawings of sections below; (b) section no. 5 at 10x magnification, showing general architecture; (c) section no. 5 at 40x magnification, showing osteodentine; (d) section no. 5 at 40x magnification, showing an ornament ridge; (d) section no. 1 at 40x magnification, note reduced vascularisation and osteocyte lacunae.. 175
FIGURE 6.6 Scanning electron microscope images of scales from across the body of NMS 2001.7.4: (a) Typical flank squamation; (b) Tessera-like scales underneath dorsal fin spine; (c) Scales of the fin web; (d) transitional tessera on posterior of head; (e) exposed underside of flank scale.. 176
FIGURE 6.7 Histology of isolated scale from residues of NMS 2001.7.4: (a-d) CT rendered images in (a) dorsal view; (b) anterior view; (c) dorso-lateral view; (d) Posterior view; (e-g) CT rendered images with outside semi transparent, revealing pulp cavities in (e) dorsal view; (f) anterior view; (g) dorso-lateral view; (h) WRITE THIS BIT 178

FIGURE 6.8 The dermal shoulder girdle of *Ptomacanthus* NHM P.24919a. (a) in ventral view; (b) in dorsal view; (c) in lateral view; (d) right pinnal plate in dorsal view. Colour scheme: Purple, left pinnal plate; Blue, right pinnal plate; Grey, material I interpret as the broken edge of the left pinnal plate and the median prepectoral plate 183
FIGURE 6.9 The procoracoid of *Diplacanthus*. (a) in the specimen; (b) rendered 3D model juxtaposed against specimen surface; (c-f) element in (c) medial, (d) posterior, (e) dorsal, and (f) ventral views; (g) medial view of top of denticulated pad, showing vasculature; (h) medial view of ventral lamina, showing digitate processes and vasculature; (i) photograph and drawing of NHM P.1357a, with articulated procoracoids showing inwards-pointed digitate processes; (j,k) updated reconstruction of the shoulder girdle of *Diplacanthus* in (j) lateral, and (k) ventral views. 185
FIGURE 6.10 Caption on next page. 189
FIGURE 6.10 Selected gnathostome shoulder girdles in lateral view. Depicted are (a) *Vernicomacanthus*, from this chapter; (b) *Dobunnacanthus* gen. nov., from Miles (1973a); (c) Gyracanthides, from Warren et al. (2000); (d) *Lupopsyrus*, from Hanke and Davis (2012); (e) *Climatius*, from Burrow et al. (2015); (f) *Ptomacanthus*, from this chapter, scapulocoracoid inferred from Miles (1973a); (g) *Diplacanthus*, from Miles (1973a) and this chapter; (h) *Uraniacanthus*, from Hanke and Davis (2008); (i) *Acanthodes*, from Miles (1973a); (j) *Cheiracanthus*, from Miles (1973a); (k) *Euthacanthus*, from Miles (1973a); (l) *Ischnacanthus*, from Miles (1973a) (procoracoid conjectural); (m) *Doliodus*, from Maisey et al. (2017); (n) *Onychoselache*, from Coates and Gess (2007); (o) *Akmonistion*, from Coates and Sequeira (2001a); (p) *Mimipiscis*, an osteichthyan, from Miles (1973a). Colours: Green, prepectoral spine 1; Orange, Prepectoral spine 2; Purple, posterolateral angle. 190
FIGURE 6.11 Caption on next page. 194

FIGURE 6.11 Selected gnathostome shoulder girdles in ventral view. Depicted are (a) *Vernicomacanthus*, from this chapter; (b) *Dobunnacanthus* gen. nov., from Miles (1973a); (c) Gyracanthides, from Warren et al. (2000); (d) *Lupopsyrus*, from Hanke and Davis (2012); (e) *Culmacanthus*, from Long (1983); (f) *Diplacanthus*, from Miles (1973a) and this chapter; (g) *Climatius*, from Burrow et al. (2015); (h) *Parexus*, from Miles (1973a); (i) *Ptomacanthus*, from this chapter; (j) *Brachyacanthus*, from Miles (1973a); (k) *Euthacanthus*, from Miles (1973a);(m) *Doliodus*, from Maisey et al. (2017). Colour scheme as for Fig. 6.10 with: Cyan, median plate/spine; Blue, first intermediate ("admedian") spine. 195

FIGURE 7.1 (Caption next page.) 204
FIGURE 7.1 Results of parsimony analysis: (a) strict consensus tree, with Bremer decay indices for each node (b) Adams consensus tree 205
FIGURE 7.2 (Caption next page.) 206
FIGURE 7.2 Majority rule consensus from the Bayesian analysis: node numbers are posterior probabilities as percentages 207
FIGURE 7.3 (Caption next page.) 208
FIGURE 7.3 Chondrichthyan total-group from results of different analyses, with different parts labelled. (a) parsimony strict consensus; (b) parsimony Adams consensus; (c) Bayesian result. Abbreviations: Acantho: acanthodiforms; Dipla, diplacanthiforms; Isch, ischnacanthiforms. Grey blobs are clades with "gyracanthid" characters, Green blob is inferred position of posterior shift of branchial skeleton 209
FIGURE 7.4 Unambiguous synapomorphies plotted on agreement subtree, excluding the chondrichthyan total group.. 210
FIGURE 7.5 Unambiguous synapomorphies of the chondrichthyan total group, plotted on agreement subtree. 211

CHAPTER 1

INTRODUCTION

The jawed vertebrates, or gnathostomes, make up the overwhelming majority of vertebrate diversity and disparity. Gnathostomes have become almost ubiquitous in ecosystems across Earth, with modern forms inhabiting both waters deep and shallow, salty and fresh, lands both arid and wet, cold and hot, and even the sky. This gnathostome success could not have occurred without their mineralised skeleton, which forms the basis for a specialised suite of anatomical features including paired fins (or limbs), and tooth-lined, dorso-ventrally closing jaws. This skeleton also gives the gnathostomes a relatively high propensity to fossilise which, paired with not a little human self-curiosity, has also made them a key study area for scientists trying to understand the mechanics of evolution. The fossil record of gnathostomes chronicles the origins of their anatomy, and also of their success as a clade.

The roots of the gnathostome clade can be found somewhere in the waters of the early Palaeozoic (Fig. 1.1). It is here, in the Silurian (444-419 Mya), that we find the very earliest definite members of the two sister groups that comprise living, crown-group gnathostomes: the osteichthyans, or bony fishes, and the chondrichthyans, or cartilaginous fishes (Zhu et al., 2009; Burrow and Rudkin, 2014). Accompanying these early crown-group members are a host of stem-group gnathostomes, which record the acquisition of gnathostome morphology before the divergence of the two living groups (Janvier, 1996). Each of these three branches incident on the gnathostome crown-node - the osteichthyan, chondrichthyan, and gnathostome stem-groups - are important for understanding the evolution of modern jawed

vertebrate anatomy. In this thesis, I am concerned in particular with one of them: the chondrichthyan stem-group.

1.1 A CHONDRICHTHYAN PRIMER

Living cartilaginous fishes form a numerically minor, but ecologically significant, part of vertebrate diversity of which the majority belong to the familiar Elasmobranchii: sharks, skates, and rays(Fig. 1.1). Elasmobranchs fulfil a wide variety of ecological roles in modern oceans, including raptorial predators, small demersal animals, and enormous filter feeders. The elasmobranch crown-group seems to have had its origins in the Late Palaeozoic (Inoue et al., 2010), with early representatives of most living orders being found at least in the Mesozoic (Janvier and Pradel, 2015). Stem-group elasmobranchs, such as *Synechodus* and hybodontiforms, are known from the Late Palaeozoic and existed well into the Mesozoic (Maisey, 1985; Coates and Gess, 2007). All of these early elasmobranchs are recognisably shark-like in form (eg.Maisey (1982, 1989a)).

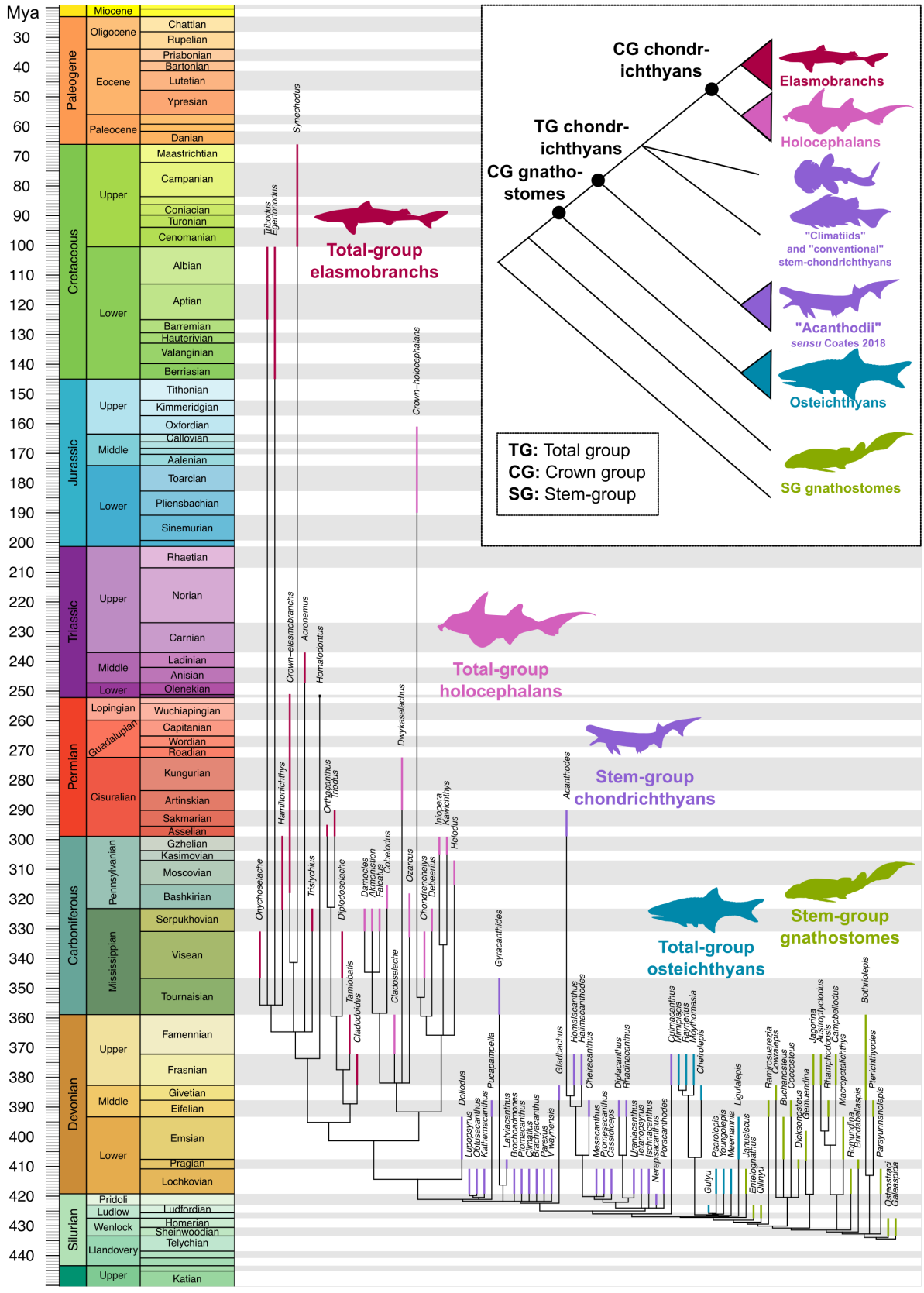


FIGURE 1.1: Caption next page

FIGURE 1.1: Phylogeny of early gnathostomes, plotted against time. Topology is the strict consensus tree from the dataset of Coates et al. (2018). Dates taken from the literature. Inset is the same scheme of relationships, but simplified.

The sister group of the elasmobranchs comprises the far less diverse Holocephali: rat, rabbit, and elephant fishes (Fig. 1.1). Recent holocephalans live close to the seabed, and often dwell at great depth (Didier, 1995). They ply this specialised lifestyle with a correspondingly specialised anatomy, including large dental plates, jaws which are fused to the neurocranium, and a gill skeleton which has been shunted forwards underneath the braincase. Like elasmobranchs the fossil record of crown-holocephalans extends back into the Mesozoic (Janvier, 2015), with molecular data placing the divergence of the crown-group in the Mesozoic (Inoue et al., 2010). A number of Palaeozoic and Mesozoic stem-holocephalans are known, including *Squaloraja*, *Myriacanthus*, iniopterygians, and helodontids (Janvier, 1996, 2015). Similarly to living holocephalans, these are characterised by a durophagous dentition and a set of highly unusual body shapes. The earliest definite stem-holocephalan on which there is broad agreement is the Lower Carboniferous eel-like animal, *Chondrenchelys* (Finarelli and Coates, 2014; Benton et al., 2015).

The combination of living chondrichthyans' ancient pedigree and their seemingly archaic morphology has led to the perception that they are somehow primitive. The most obvious manifestation of this perception is in trashy blockbusters with antediluvian menaces (Turtletaub, 2018). However, it also influences scientific thought; in evolutionary developmental studies chondrichthyans are routinely used as proxies for ancestral gnathostome conditions (eg. Mallatt (1996); Carvalho et al. (2013); Gillis et al. (2009)). Whether living chondrichthyans provide an appropriate model for this is not dependent on a perceived set of primitive characters. Instead it is dependent on how accurately character states in Recent chondrichthyans reflect

those at the gnathostome crown-node, something that can only be discerned with fossil taxa.

The answer to how primitive the character states of living chondrichthyans really are lies with extinct members of the chondrichthyan stem-group. Many candidate stem-group chondrichthyans are found throughout the mid-late Palaeozoic (Fig. 1.1). They include ctenacanths, xenacanths, cladoselachians and symmoriiforms, known from articulated body-fossils (Janvier, 1996), as well as less completely known animals such as *Cladodoides* (Gross, 1937, 1938; Maisey, 2005), *Antarctilamna* (Young, 1982), and *Gogoselachus* (Long et al., 2015). Most of these are ostensibly shark-like, and clearly chondrichthyan on the basis of the prismatic calcified cartilage forming their endoskeleton (Brazeau and Friedman, 2014), but are otherwise neither clearly elasmobranch nor clearly holocephalan. Because of this they have been placed variously in the elasmobranch, holocephalan, and chondrichthyan stem groups (eg. Coates and Sequeira (2001b); Pradel et al. (2011); Grogan et al. (2012)) The most recent new data on this suggests that many of these Palaeozoic "sharks" may lie inside the chondrichthyan crown-group (Coates et al., 2017a).

A smaller number of shark-like animals are more confidently identified as stem-chondrichthyan. *Pucapampella* is based on several isolated braincases with many plesiomorphic characteristics from the Early-Mid Devonian of the Southern hemisphere (Maisey and Anderson, 2001; Maisey, 2001a). *Gladbachus* is known on the basis of a single articulated skeleton from the Middle Devonian (Heidtke and Krätschmer, 2001; Coates et al., 2018) with highly unusual, supposedly placoderm-like, scales (Burrow and Turner, 2013). *Doliodus* comprises a chondrichthyan-like head skeleton (Miller et al., 2003; Maisey et al., 2009, 2014), and more recently a surprisingly plesiomorphic postcranial skeleton (Maisey et al., 2017; Burrow et al., 2017). Between them these three taxa leave a fairly naked chondrichthyan stem-group, with little in the way of information on the postcranium and dermal

integument. In recent years however, this has changed, with a host of new taxa being transplanted onto the chondrichthyan stem-group: the acanthodians.

1.2 THE ACANTHODIAN FISHES

Acanthodians are a collection of prodigiously spinose Palaeozoic fishes, ostensibly united by a shared morphology (Fig. 1.1, 1.2). This morphology includes a suite of fin spines, as well as a body with an almost entirely cartilaginous internal skeleton and covered by tiny scales. The earliest definite acanthodians are known from the Silurian (Burrow and Rudkin, 2014; Hanke et al., 2001b), and they existed throughout the Devonian and Carboniferous until they finally became extinct in the Permian (Janvier, 1996). The acanthodians' heyday however really seems to have come in the Early to Mid Devonian, when they reached the apex of their diversity and disparity (see Fig. 1.1). Unfortunately the cartilaginous skeletons and shark-like shagreens of acanthodians do not lend themselves readily to fossilisation, and acanthodian fossils are notoriously poor, with even articulated body fossils preserving little internal anatomy (Fig. 1.2). Resultantly acanthodians' relationships with one another and with other living jawed vertebrates have been a source of debate for the last 150 years. In recent years even their status as a group has been questioned.

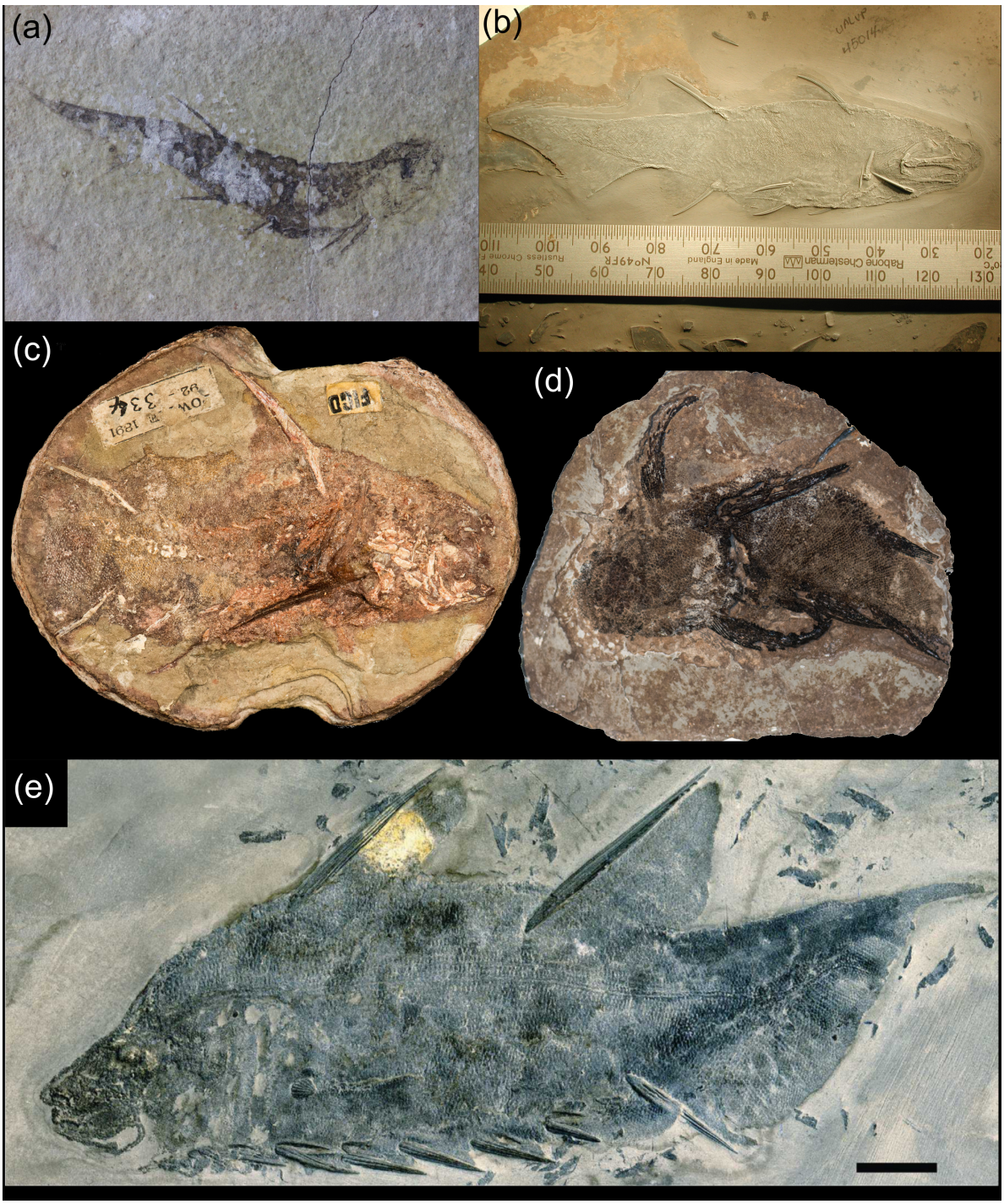


FIGURE 1.2: Caption next page

FIGURE 1.2: Selected articulated acanthodian-grade stem-chondrichthyans. Pictured are (a) *Mesacanthus*, an "acanthodiform"; (b) an ischnacanthid; (c) *Diplacanthus*, a diplacanthiform; (d) *Vernicomacanthus*, a "climatiid", and (e) *Brochoadmones*, one of the problematic MOTH taxa

---

1.2.1 **ORS originals**

The majority of articulated acanthodian taxa known prior to the 21st century came from a range of localities in the Old Red Sandstone (ORS) of the United Kingdom (Fig. 1.2a,c,d). The ORS is a series of rocks cropping out on either side of the Northern Atlantic, which range from Late Silurian to Early Carboniferous in age. Several acanthodian-rich mid-Devonian localities are known from the Middle ORS of Scotland: these are interpreted as being fossilised remnants from a large lake that covered the area (Lake Orcadie) (Dineley and Metcalf S J, 1999). Many localities are also known from the Early Devonian of the Lower ORS, in the Midland Valley of Scotland: these are rich in articulated Lochkovian acanthodians (eg. Tillywhandland (Trewin and Davidson, 1996)). More recently an acanthodian fauna has also been described from the Early Devonian of the Welsh Borders (particularly Wayne Herbert), which is also interpreted as Lochkovian (White, 1935; Miles, 1973a). Between them these Early-Middle Devonian sites preserve a wide diversity of acanthodian forms.

Many articulated acanthodian fossils are known from outside the Devonian of the UK, although not in the same density. Several acanthodians are known from the Devonian of Australia which are comparable to ORS taxa (Burrow et al., 2012; Long, 1983, 1986a,b; Young and Burrow, 2004). European and North American acanthodians are also known, which seem similar to ORS forms (Schultze and Zidek,

1982; Gagnier, 1996). In the Carboniferous a group called gyracanths are common: large bodied forms known largely on the basis of fin spines, but also on the basis of some endoskeletal material (Turner et al., 2005; Warren et al., 2000; Snyder et al., 2017). Many members of the genus *Acanthodes* are known from throughout the Carboniferous and Permian (Zidek, 1976; Heidtke, 2011, 2015). While varying in time and space all of these taxa had anatomies which are largely interpretable in the light of ORS taxa.

Attempts to taxonomically organise acanthodian taxa have been largely based on ORS forms. While formulations have varied (eg. Berg (1940); Miles (1964b); Watson (1937); Woodward (1891)), acanthodians have been broadly organised into three main grades, based on overall similarity. The ischnacanthiforms, typified by *Ischnacanthus*, are marked by their dentigerous jawbone: they are the earliest occurring acanthodians known (Burrow and Rudkin, 2014; Hanke et al., 2001b) (eg. Fig. 1.2b). The acanthodiforms, typified by *Acanthodes*, are slender toothless animals with a reduced fin spine complement: while members of this group are known from the Lower Devonian (eg. Watson (1937)) some represent the youngest-known occurring acanthodians, lasting until the Permian (Janvier, 1996) (eg. Fig. 1.2a). Finally climatiiforms, typified by *Climatius*, are relatively heavily armoured, with plate-like shoulder girdles, numerous spines, and usually having numerous tooth whorls (Janvier, 1996) (eg. Fig. 1.2d). Exact membership of these groups has varied: particularly with respect to problematic forms such as the late-occurring gyracanths and diplacanthids, an Early-Middle Devonian grade. Nonetheless, these three grades encompassed the broad swathe of acanthodian diversity and 19th-20th phylogenetic century debate centred around the relationships between these groups and the placement of an assumed monophyletic Acanthodii (eg. Jarvik (1977); Miles (1973a)).

1.2.2 *Acanthodes* - an acanthodian exemplar?

In debates on acanthodian relationships one european acanthodian in particular has proved disproportionately influential: *Acanthodes*. *Acanthodes* is fairly late occurring taxon (See Fig. 1.1) found throughout the Carboniferous and Permian, and has become something of a catch-all genus for lots of very similar acanthodians in this period (eg. (Zidek, 1976; Heidtke, 2011, 2015)). *Acanthodes* has a somewhat anguiliform body, with a reduced dermal squamation, and lacks teeth. Its late occurring presence in the Permian suggests that it might have been something of a living fossil group at the time. Despite its specialised, late occurring status *Acanthodes* has ended up in some ways representative of acanthodians as a whole.

The reason for this perhaps undue influence can be found in the head of one particular species of *Acanthodes*. *Acanthodes confusus* (formerly *A. bronni* (Heidtke, 2011)) has a remarkably well mineralised endoskeleton for an acanthodian. This endoskeleton is preserved in the form of natural moulds from the Early Permian Lebach ironstone, in Saarland Germany. The moulds record details of the braincase, of the visceral skeleton, and of the shoulder girdle to an extent not seen in any other acanthodian fish Watson (1937); Miles (1973b, 1964a, 1965, 1968); Nelson (1968); Jarvik (1977). The result of this unique preservation is that *Acanthodes* was for a long time more or less the only acanthodian for which any internal information was known.

As the only acanthodian with a well-known endoskeleton, much past debate around acanthodian relationships has revolved around interpretations of these moulds of *Acanthodes*. These debates have centred around whether *Acanthodes* was chondrichthyan-like (eg. Jarvik (1977)), osteichthyan-like (Miles (1973b)), or neither (eg. Watson (1937); Rosen et al. (1981)). Complicating this has been the mouldic preservation of *Acanthodes*, which has hindered easy interpretation and allowed

competing interpretations of its anatomy Miles (1973b); Jarvik (1977); Brazeau and de Winter (2015); Davis et al. (2012). An example of this is the branchial skeleton, which has been reconstructed in more or less every way imaginable (eg. Watson (1937); Rosen et al. (1981); Miles (1973b); Nelson (1968); Miles (1964a)). As *Acanthodes* varied in position in these analyses, other acanthodians tended to be tacked onto its position in a monophyletic group (Miles, 1973b; Jarvik, 1977).

1.2.3 **MOTH madness**

A particularly influential new set of acanthodian forms came with the description of numerous articulated taxa from a Lower Devonian site: the Man On The Hill, or MOTH, locality, in Canada Gagnier and Wilson (1996b); Bernacsek and Dineley (1977); Gagnier and Wilson (1996a, 1995); Hanke et al. (2001a); Hanke (2002); Hanke and Wilson (2004, 2006); Hanke (2008); Hanke and Davis (2008); Hanke and Wilson (2010); Hanke and Davis (2012); Hanke et al. (2013); Blais et al. (2011, 2015); Blais (2017). MOTH revealed a large fauna of articulated acanthodians, thelodonts, osteostracans, and heterostracans (with osteichthyans and placoderms conspicuously absent) (eg. Fig. 1.2b,e). Specimens from MOTH are flattened: while this means endoskeletal information from the locality is limited, the dermal skeletons of acanthodians from the locality are remarkably well preserved. This reveals a diversity of acanthodians equalling that of the Early Devonian of the ORS.

Several of the taxa from MOTH have proved difficult to fit into ORS-based schemes of acanthodian relationships. These include animals such as *Brochoadmones* (Fig. 1.2e) and *Tetanopsyrus*, which display characteristics from several of the putative acanthodian "groups" (Hanke and Wilson, 2006; Hanke et al., 2001a; Gagnier and Wilson, 1996b; Bernacsek and Dineley, 1977). It also contains several taxa which seem to combine crown-chondrichthyan-like monodontode scales with

acanthodian-like bodies (eg. *Lupopsyrus*, *Lupopsyroides*, *Obtusacanthus* (Bernacsek and Dineley, 1977; Hanke and Wilson, 2004; Hanke and Davis, 2012)). The MOTH fauna also includes several animals which were described as stem-chondrichthyans (as opposed to acanthodians). These include *Seretolepis* and *Kathemacanthus* - while these have acanthodian-like fin spine complements they show supposedly "chondrichthyan-like" features of the scales and endoskeleton (Hanke and Wilson, 2010). The description of this MOTH fauna blurred the line between acanthodian groups, and between acanthodians and chondrichthyans.

As different as some these taxa are, the MOTH fauna bears many similarities with that of the UK Lochkovian sites. *Uraniacanthus*, a putative diplacanthid acanthodian, is present both in the ORS and in MOTH (Hanke and Davis, 2008; Newman et al., 2012; Miles, 1973a). Ischnacanthids from MOTH are distinguishable from ORS ischnacanthids (and each other!) only on the basis of minutiae of dentition (Blais et al., 2015) (Fig. 1.2b). *Mesacanthus* from the ORS and *Promesacanthus* from MOTH are almost identical (Watson, 1937; Hanke, 2008). Finally, several of the more unusual taxa from MOTH are known from very similar scales from European localities, such as *Seretolepis*, *Altholepis*, and *Polymerolepis* (Hanke and Wilson, 2010; Hanke et al., 2013; Karatajūtė-Talimaa, 1997; Turner et al., 2017). Lochkovian faunas from around what is now the Atlantic had very similar complements of acanthodians.

1.2.4 **An acanthodian paraphyly**

A major shift in thought on acanthodians (and early vertebrates more generally) came with the identification of a preserved basicranium in a specimen of the "climatiid" *Ptomacanthus* (Brazeau, 2009). Unexpectedly, this did not resemble the neurocranium of *Acanthodes*, with a ventrally narrowed osteichthyan-like

basisphenoid (Davis et al., 2012). Instead the braincase of *Ptomacanthus* more resembled that of a placoderm or chondrichthyan, with a broad basiocciput (Brazeau, 2009). However, more important than the neurocranium itself was the phylogenetic analysis that accompanied it. This recovered acanthodians (and placoderms) not as monophyletic groups as had previously been assumed, but instead as a paraphyletic grade, shared between the osteichthyan and chondrichthyan stem-groups.

The description of *Ptomacanthus* prompted a flurry of analyses over the next decade interrogating gnathostome phylogeny in the light of new fossil discoveries (eg. Giles et al. (2015c); Zhu et al. (2013); Davis et al. (2012); King et al. (2016); Coates et al. (2018, 2017a)). Throughout these analyses acanthodians have remained consistently paraphyletic, but have been alternatively juggled between the osteichthyan, chondrichthyan, and gnathostome stem-groups. The identification of homology between the skull roofs of osteichthyans and "placoderm" stem-gnathostomes led to acanthodians being deposited wholesale onto the chondrichthyan stem-group, as a poorly defined grade (Zhu et al., 2013; Giles et al., 2015c). In more recent analyses this topology has proved resistant to new information (eg. Fig. 1.1).

This stem-chondrichthyan position for acanthodians has since been shored up with a steady stream of further evidence. The "shark-like" character states in the braincase of *Acanthodes* that Davis et al. (2012) identified as gnathostome plesiomorphies are more likely characters of the chondrichthyan total-group. This was backed up by the recharacterisation of the articulation between the neurocranium and hyomandibula of *Acanthodes* as being chondrichthyan-like (Brazeau and de Winter, 2015). It has also emerged that *Doliodus*, long considered to be the "earliest" chondrichthyan Miller et al. (2003), has a remarkably acanthodian-like postcranium (Maisey et al., 2017), as well as similar endoskeletal tissue (Long et al., 2015). This, combined with the anatomy of fauna from MOTH (eg. Hanke and

Wilson (2010)) means that the line between "acanthodians" and "chondrichthyans" is considerably more blurred than it was. It is now widely agreed that acanthodians are in fact a grade comprising some of the earliest cartilaginous fishes.

1.3 CURRENT PROBLEMS IN EARLY CHONDRICHTHYAN EVOLUTION

While there is now a reasonable confidence that "acanthodians" are actually the earliest branching members of the chondrichthyan total-group, relationships within the stem-group remain poorly understood. Generally speaking "conventionally chondrichthyan" stem-chondrichthyan taxa tend to be retrieved relatively more crownwards on the chondrichthyan stem-group, with formerly "acanthodian" taxa relatively stemwards (a notable exception to this is the recent analysis by Coates et al. (2018)). However, beyond this there is extremely poor resolution to the chondrichthyan stem-group. The result is that in most phylogenetic analyses early chondrichthyans emerge as paraphyletic, with topological disagreement between analyses. This means that there is a very limited set of hierarchical characters that can be used to delimit sections of the chondrichthyan stem, hindering efforts to work out how chondrichthyan anatomy evolved.

The one consistent signal in the mess has been a rump of acanthodian taxa which has formed the sister group to all other chondrichthyans, a putative clade which Coates et al. (2018) tentatively term the Acanthodii. Not by coincidence, these Acanthodii largely comprises the taxa which had previously retrieved on the osteichthyan stem-group (Davis et al., 2012; Brazeau, 2009): those placed by previous authors in the ischnacanths, acanthodiforms, and diplacanthids . These taxa tend to be less spinose and less heavily armoured than more crownwards chondrichthyans, and without plentiful tooth whorls. They are also united by a number of dermal characters of fin spines and scales. On the basis of *Acanthodes* -

a member of this group - these also appear to have a distinct internal morphology from more crownwards chondrichthyans (Davis et al., 2012). It remains somewhat unclear however whether this really is a clade, or just a grade with plesiomorphic chondrichthyan characters.

The "climatiids" - another of the original groupings of acanthodian - have decayed entirely in these analyses to form a paraphyly. This paraphyly is poorly defined, but tends to form relatively crownwards to the Acanthodii, below or even intermingled with conventionally defined stem-chondrichthyans (eg. Fig. 1.1). The implication of this is that supposedly "climatiid" characters such as a heavily armoured shoulder girdle and prepectoral spines are instead a suite of character states which are plesiomorphic for chondrichthyans. Further evidence for this the description of pectoral and pelvic spines in both stem-osteichthyans (Zhu et al., 2009; Choo et al., 2017) and in *Doliodus* Miller et al. (2003). However, there is no clear evidence for a climatiid clade (Coates et al., 2018). This leaves the chondrichthyan stem-group with a set of fairly plausible plesiomorphic states, but little to place constituent members in well defined clades.

One part of the solution to these problems is with acanthodians which have combinations of character sets typical for other acknowledged groups. *Euthacanthus* is rather climatiid-like but with a acanthodiform-like head skeleton (Watson, 1937; Newman et al., 2014, 2011). *Latviacanthus* is acanthodiform-like but with a number of climatiid-like characters (Schultze and Zidek, 1982). *Vernicomacanthus* is similar in some respects to the Carboniferous gyracanths, but also to many climatiids (Burrow et al., 2008; Miles, 1973a). *Brachyacanthus* has a markedly acanthodiform-like shoulder girdle, but is otherwise climatiid-like Watson (1937); Miles (1973a). Such problematic taxa provide possible opportunities to bridge morphological gaps between supposed groups of acanthodian in phylogenetic analyses.

Another glaring deficiency in our knowledge is in the structure of the endoskeleton of the head and pharynx in acanthodian-grade animals. These potentially provide a fantastic source of information, as they are broadly comparable with other early vertebrates. *Acanthodes* remains by far the most completely known acanthodian endoskeleton (Davis et al., 2012; Miles, 1973a), but as discussed above its interpretation is still hindered by the mouldic preservation of its fossils. *Ptomacanthus* is known from its basicranium, but very few morphological characters are actually harvestable from what is preserved (Brazeau, 2009). Parts of endoskeletons are known in other taxa, for example, a possible basioccipital in *Milesacanthus* (Young and Burrow, 2004), possible a endocranium in *Protodus* (Burrow and Turner, 2010), and the branchial skeleton in *Kathemacanthus* (Hanke and Wilson, 2010) and in *Halimacanthodes* (Burrow et al., 2012), but these provide limited comparative information. Any detailed head morphology that could be harvested from an acanthodian-grade animal would likely prove valuable.

Although most acanthodian endoskeletons are extremely poorly known, an exception is found in the shoulder girdle. As Miles (1973a) notes, these tend to mineralise more extensively than other parts of the acanthodian endoskeleton, and so are correspondingly well known. The presence of similar shoulder girdles outside the acanthodian grade also means that harvested characters are fairly widely comparable. The dermal armour of the shoulder also has an array of different morphologies, which could be phylogenetically informative (Long, 1986b; Miles, 1973a), particularly now that the shoulder girdle of *Doliodus* is known (Maisey et al., 2017). This preservation is relative however, the shoulder girdle of many acanthodian taxa is still poorly known.

New views on acanthodians has also coincided with efforts to redescribe many of the acanthodian taxa from the ORS of the UK. These studies have aimed to take advantage of the fact that while the endoskeletons of many acanthodians may be

impossible to know, the scales and spines provide a potentially extremely rich source of information that is comparable to other early vertebrates. A broad range of ORS taxa have been described in this way, including *Parexus* (Burrow et al., 2013), *Climatius* (Burrow et al., 2015), *Uraniacanthus* (Newman et al., 2012), diplacanthids (Burrow et al., 2016a), *Euthacanthus*(Newman et al., 2014, 2011), and *Ptomacanthus* (Brazeau, 2012). We now know a great deal about the dermal skeletons of these animals, and the tissues of which they are made. However, continuing to describe dermal material in other taxa provides the opportunity to build a large, valuable comparative dataset.

This is particularly important outside the acanthodian grade. Dermal skeletons in many otherwise articulated fossil "sharks" are extremely poorly known, and could provide important anatomical information for comparison with the growing wealth of acanthodian-based studies. The importance of this was recently brought home by the highly unusual morphology of the dermal skeleton in the stem-chondrichthyan *Gladbachus* (Burrow and Turner, 2013; Coates et al., 2018). It may prove that many of these look more acanthodian-like than previously realised, and uncover new character sets with which to analyse taxa in the chondrichthyan stem-group.

In this thesis I attempt to tackle some of these problems in stem-chondrichthyan phylogeny. In particular I focus on redescribing aspects of the anatomy of several acanthodian taxa from the ORS of the United Kingdom. I do this using a combination of two major techniques: computed tomography and phylogenetic analysis.

1.4 METHODS OVERVIEW

1.4.1 **Tomographic Methods**

Over the last decade and a half, the development of computed tomographic methods have revolutionised the study of early vertebrates. Destructive tomographic methods have a long pedigree in palaeoichthyology, with serial grinding being successfully used throughout the 20th century to reconstruct internal skeletons of fossil fish (Janvier, 1996). Similarly, X-rays have long been used to image specimens, particularly in shale localities with thin sheets (eg. Zangerl and Case (1973)). The coincidence of X-rays and tomography computed tomography has provided new ways of looking at old fossils, revealing material in the matrix previously inaccessible (Sutton et al., 2014; Cunningham et al., 2014).

The most widely used method in these studies is to use v to generate three dimensional images (eg/ Maisey (2005); Giles et al. (2015c)). This approach uses an source to cast X-rays through the object of interest (Sutton et al., 2014). A detector records the attenuation of the x-rays as they pass through the object at different axes of rotation (usually through 360 degrees). The resolution of such a scan is dictated by the resolution of the X-ray source, the size of the object and its distance from the source. A series of variables, such as the length of the scan, and the power, amplitude, and degree of filtration of the x-rays provide additional means of controlling output. The resulting projections are then used to calculate a series of tomograms: slices through the scanned object with the material differentiated by density.

More recently a second computed tomographic method has come to the fore: X-ray synchrotron tomography (eg. (Sanchez et al., 2014; Pradel et al., 2009a; Rücklin et al., 2012)). A synchrotron is a particle accelerator, the use of which generates high energy sychrotron X-rays (Sutton et al., 2014). Synchrotrons can be used to scan

objects in much the same way as X-ray microtomographs, but with the additional advantages of high intensity X-rays and the avoidance of some artifacts. It is particularly effective when used in concert with phase contrast tomography; rather than comparing X-ray attenuation, phase contrast (which can also be implemented in X-ray microtomography) uses the refraction of X-rays at material boundaries to infer transitions in material. This has the effect of distinguishing more clearly between materials with similar compositions. However, the utility of synchrotron tomography is limited by its being enormously less convenient and more expensive than X-ray microtomography.

Once a series of tomograms have been obtained, they must be rendered into three-dimensional models. This is done using one of a wide range of programs - in this thesis the two used are Mimics and VGStudio. The process involves working through the scan data tomogram by tomogram (some level of automation is often possible), "painting" the object of interest using thresholding on the basis of density difference (Sutton et al., 2014). Three dimensional models can then be generated by combining the slices of mask The models can then be exported in a range of file types and put into animation software (in this thesis, Blender) to render realistically lit images.

1.4.2 **Phylogenetic Methods**

Harvesting characters from these models is of no use without placing them in a phylogenetic context. Without genomes, establishing relationships between fossilised animals is entirely dependent on their morphology. To do this morphological characters are recorded, shared states of which act as hypotheses of primary homology (Patterson, 1982). A statistical analysis is then to recover the optimal tree/s for the relationships of taxa, given their character sets. The two most

commonly deployed methods to tackle this are parsimony and Bayesian analysis.

Parsimony methods are based on their eponymous principle: the assumption that the most probable tree is the one with the least change (Lemey et al., 2009). They do this by calculating tree length (ie. how many character state changes are present) for different tree topologies and choosing the tree with the shortest length. While in theory the most thorough way to do this is to test every possible tree topology this is impractical and a variety of heuristic procedures have been developed which attempt to find the shortest tree without exhaustively testing everything. This is done using a combination of a counting algorithm (usually Fitch's algorithm, but weighting procedures also exist) and a branch swapping procedure to find new topologies. The output of parsimony procedures is a tree or a series of trees on which state changes can be mapped to specific branches.

Recently a new set of phylogenetic methods have come to the fore based on Bayesian inference (Lemey et al., 2009). These use Bayes theorem, which essentially allows calculation of the probability that a hypothesis is correct given the data. This probability - the posterior probability - is calculated using a prior probability (ie. the expected result before data collection) and the likelihood of the collected data. A model is used which gives the likelihood of switching between character states; the simplest of these is the Mk model, which has a fixed substitution rate, but models exist which allow for variable rates on different branches of the tree. The posterior probability is estimated, usually using Monte Carlo Markov Chains (MCMC) which sample parameter space until a consistent result is reached. From this a sample of trees is produced, which are sampled in proportion to the trees' posterior probabilities.

Since the advent of Bayesian methods disagreement has arisen about which method set is a more accurate means of recovering trees from morphological

data. Proponents of parsimony argue that Bayesian models are unrealistic for morphological data, and cope poorly with missing data (eg. (Goloboff and Catalano, 2016)). Advocates for Bayesian inference counter that Bayesian models are no less realistic than the central assumptions of parsimony. A steady stream of papers have recently come out comparing these two methods on the basis of simulated data (eg.Wright and Hillis (2014); Puttick et al. (2018); Reilly et al. (2016)). Broadly, these have found that Bayesian inference produces more accurate but less precise trees than parsimony analysis, particularly in datasets with high homoplasy. Nonetheless, in this thesis I have elected to use both methods.

1.4.3 **Supplementary data**

All of the three-dimensional data reconstructed from tomographs in this thesis are available to view on Figshare, both as three dimensional .ply and .stl files, and in animated videos. A list of supplementary figures with links to these videos and modelsis provided in Appendix C.

Also present on Figshare are all of the files necessary to recreate the phylogenetic analyses in Chapters 3 and 7.

1.4.4 **Note on institutional abbreviations**

Various institutions are mentioned in this thesis, which are abbreviated as follows: NMS, National Museum of Scotland, Edinburgh; NHM, Natural History Museum, London; DUNMG, Dundee.

1.4.5 **Attributions for Phylopic images**

Images of *Bothriolepis* and *Callorhinchus milii* used in figures of this thesis were taken from Phylopic and submitted by Ghedoghedo and Tony Ayling (vectorised by Milton Tan) respectively. Both were distributed under a Creative Commons Attribution-ShareAlike 3.0 Unported license (https://creativecommons.org/licenses/by-sa/3.0/).

1.5 THESIS AIMS

The aim of this thesis is to shed light on some of the problems in early chondrichthyan evolution, particularly focussing on the relationships of stem-chondrichthyans, using computed tomographic and phylogenetic techniques. In Chapter 2 I review characters that can be used to identify fossils as stem-group or crown-group chondrichthyans. In Chapter 3 I describe the visceral skeleton of the "climatiid" stem-chondrichthyan *Ptomacanthus* and discuss the evolution of the branchial skeleton. In Chapter 4 I describe the cranial endoskeleton of the diplacanthid stem-chondrichthyan *Diplacanthus* and discuss the putative acanthodian clade, the Acanthodii. In Chapter 5 I compare new data on endochondral tissues in a stem-chondrichthyan (*Diplacanthus*) and in a placoderm grade stem-gnathostome, and discuss the evolution of these tissues in gnathostomes. In Chapter 6 I redescribe the Lochkovian "climatiid" genus *Vernicomacanthus* and discuss the evolution of the chondrichthyan shoulder girdle. In Chapter 7 I reassess the phylogeny of stem-chondrichthyans in the light of this new information, and discuss the implications of the topology I recover for chondrichthyan evolution.

1.6 CONTRIBUTION OF AUTHORS

Chapter 2: Characters of the chondrichthyan total group

Martin D. Brazeau conceived this project. I carried out research, wrote the draft and produced figures and tables. Martin D. Brazeau provided comments and edits on the drafts.

Chapter 3: The visceral skeleton of the stem-chondrichthyan *Ptomacanthus*

Martin D. Brazeau and I conceived the project and conducted CT scanning with Tom Davies. I generated the CT renderings and produced figures and tables. I wrote the description and interpretation of the specimen data. Martin D. Brazeau provided comments and edits on the drafts. Christopher Stockey carried out the initial x-rays of the specimen.

Chapter 4: A third "acanthodian" endoskeleton in *Diplacanthus crassisimus*

Martin D. Brazeau and I conceived the project. An initial session of synchrotron scanning (not directly used in this thesis) was carried out by Martin D. Brazeau, Matt Friedman and Robert C. Atwood. A second session (used in this thesis) was carried out by me, Anna Jerve, and Paul Tafforeau. I generated the CT renderings and produced figures and tables. I wrote the description and interpretation of the specimen data. Martin D. Brazeau provided comments and edits on the drafts. Christopher Stockey carried out the initial x-rays of the specimen.

Chapter 5: Endochondral tissues in early vertebrates

Martin D. Brazeau and I conceived the project. Synchrotron scanning (used in this thesis) was carried out by me, Anna Jerve, and Paul Tafforeau. Anna Jerve generated the CT renderings. I produced figures and tables. I wrote the description and interpretation of the specimen data. Martin D. Brazeau provided comments and edits on the drafts.

Chapter 6: The stem-chondrichthyan genus *Vernicomacanthus* and the early evolution of the chondrichthyan shoulder girdle

Martin D. Brazeau, Carole Burrow, Jan van den Blaauwen, Bob Davidson, and I conceived the project. Acid preparation was carried out by Anna Jerve. CT scanning was carried out by me and Tom Davies. Spine sectioning was carried out by Jan den Blaauwen. Scale sectioning was carried out by Ivan Sansom. Segmenting of the CT data was carried out by Andy Koh. I wrote the description and interpretation of the specimen data. Martin D. Brazeau provided comments and edits on the drafts.

Chapter 7: A phylogenetic exploration of the chondrichthyan stem-group

Martin D. Brazeau and I conceived the project. I carried out experimental design, data collection, and all analysis. I wrote the interpretation of the data.

CHAPTER 2

CHARACTERS OF THE CHONDRICHTHYAN TOTAL GROUP.

2.1 PROBLEMS IN EARLY CHONDRICHTHYAN PHYLOGENY

As I discussed in the introduction, several areas of chondrichthyan phylogeny remain particularly problematic. One such area is in the chondrichthyan stem-group, where the interrelationships between acanthodian-grade taxa and "conventionally chondrichthyan" stem-chondrichthyans is poorly understood (Coates et al., 2018). Another is in the taxa surrounding the chondrichthyan crown-group node: Palaeozoic "sharks" have variably been placed on any one of the three branches incident upon this node (eg. (Coates and Sequeira, 2001b; Pradel et al., 2011; Grogan et al., 2012).) A third such area is in definitively associating isolated scales (eg. mongolepids (Andreev et al., 2016) with any of these groups. These problematic areas ultimately obscure important questions about chondrichthyan evolution.

This chapter aims to assess these problematic areas in early chondrichthyan phylogeny by considering the characters with which we are able to confidently assign taxa to the chondrichthyan clade. Attempts to do this have recently been carried out for osteichthyans (Friedman and Brazeau, 2010), and for Palaeozoic gnathostomes more broadly (Brazeau and Friedman, 2014), but have not been specifically targeted at chondrichthyans for a number of years (Maisey, 1984; Patterson, 1965). First I consider scales, and the criteria that can be used to confidently assign an isolated scale to the chondrichthyan total group. Secondly I consider characters that can be used to place fossils in the chondrichthyan crown-group (ie. elasmobranch and holocephalan total groups), and update the list of

Brazeau and Friedman (2014) for the chondrichthyan total group. Finally I use the character set I arrive at to assess the placement of problematic taxa.

2.2 WHAT MAKES A SCALE CHONDRICHTHYAN?

Despite their weakly mineralised endoskeletons, traces of chondrichthyans abound in the fossil record, in the form of disarticulated parts of the dermal skeleton: spines, plates, teeth, and scales. In and of themselves, the value of this dermal detritus is limited as it is difficult to reliably relate to articulated animals, or even to disarticulated remains from the same site. However, skeletal elements which can confidently be identified as chondrichthyan have the potential to be an important source of information telling us where and when chondrichthyans existed in the past. Of particular interest is exactly when the divergence of chondrichthyans and osteichthyans took place - confidently identified chondrichthyan dermal remains would provide a hard upper limit on this event (Benton et al., 2015).

"Chondrichthyan" remains which could provide this upper limit have been described from throughout the early Palaeozoic. The earliest "conventional chondrichthyan" body fossil is the Middle Devonian *Doliodus*, identified by its precerebral fontanelle and paired foraminae for the lateral dorsal aortae (Miller et al., 2003; Brazeau and Friedman, 2014; Maisey et al., 2009). However, the interpretation of all acanthodians as stem-chondrichthyans pushes this date back to the Late Silurian, with the ischnacanthid acanthodian *Nerepisacanthus* (Burrow, 2011; Burrow and Rudkin, 2014). *Nerepisacanthus* is approximately the same age as the oldest articulated osteichthyan fossil, *Guiyu* (Zhu et al., 2009), providing a conservative upper bound for osteichthyan-chondrichthyan divergence in the Late Silurian (Benton et al., 2015). Isolated dental elements do little to push this back any further, with recognisably chondrichthyan tooth whorls found in the

Lower Devonian of Spain (Botella, 2006; Botella et al., 2009), and ischnacanthid dentigerous jaw bones found as early as the Middle Silurian (Hanke et al., 2001b). Sinacanthid spines, from the Lower Silurian of China, have also been associated with chondrichthyans, although not on the basis of any clear-cut apomorphies (Sansom et al., 2005). However the oldest acanthodian spines are known from the Middle Silurian (Hanke et al., 2001b), and possibly from as far back as the Early Silurian (Fritsch, 1907) .

Possibly pushing these dates back still further are an array of putatively chondrichthyan scales. These are known throughout the Silurian: acanthodian scales have been described from as early as the Lower Silurian (Karatajūtė-Talimaa and Smith, 2003). Mongolepids comprise a supposed clade of isolated scales, mainly from throughout the Silurian, but with some examples from the Upper Ordovician (Andreev et al., 2016; Karatajūtė-Talimaa et al., 1990). Various other Silurian examples include the elegestolepids, a number of shark-like monodontode scales (Andreev et al., 2017). Upper Ordovician scales have also been associated with chondrichthyans, including *Skiichthys* (Smith and Sansom, 1997), *Tezakia*, *Canyonolepis* (Andreev et al., 2015), and the Ordovician mongolepid *Solinalepis* (Andreev et al., 2016) The very earliest is putative chondrichthyan scale is *Tantalepis*, from the Middle Ordovician (Sansom et al., 2012). However, these scales are often assigned more on the basis of overall similarity than on any one character (Brazeau and Friedman, 2014; Benton et al., 2015).

Looming over the diagnosis of many of these microremains has been the "placoid" integument of living chondrichthyans, comprising a shagreen of small, non-growing denticles. In the past these scales have been defined on the basis of a compound set of characters which came to be seen as "chondrichthyan". Placoid scales are formed from a single odontode, are entirely odontogenic, are non-growing, have a basal canal, and have a number of neck canals (Reif, 1978). Because

of the perceived simple structure of these scales and perceived chondrichthyan primitiveness placoid scales have played a major role in hypotheses of dermal integument evolution as models for basic units making up the gnathostome dermal skeleton, most prominently in Reif's Odontode Regulation Theory (Reif, 1982). While there is probably some truth to placoid scales being a comparatively simple scale-type, placoid scales are almost certainly not the ancestral condition for gnathostomes or even chondrichthyans. Overall similarity with placoid scales is a poor diagnostic basis with which to identify scales of the earliest stem-chondrichthyans.

Further muddying these waters are the integuments of the stem-group gnathostomes which would have been coeval with these putative early chondrichthyans. Most glaring of these are the thelodonts, fossils of which almost solely comprise an integument of micromeric, at first glance shark-like scales (Janvier, 1996). While scales of thelodonts have been extensively studied, articulated body fossils are extremely rare, and have turned up unexpected variation. Other jawless stem-gnathostomes -galeaspids, osteostracans, anaspids and heterostracans - seemingly have a more osteichthyan-like body integument of interlocking rhomboidal scales. However, this is based on a very small collection of few specimens with articulated body squamations, even fewer of which have been studied in detail (Qu et al., 2015a; Wang et al., 2005). This even extends to mandibulate "placoderm" stem-gnathostomes, which the scales of which have only really been studied in two studies (Burrow and Turner, 1998, 1999). This is particularly worrying in the absence of early members of each of these clades in the earliest parts of their evolutionary range (Sansom et al., 2014).

So how can one confidently identify an isolated scale as being chondrichthyan? Here I review characters of morphology, histology and growth that might be used to identify an isolated scale as belonging to the chondrichthyan total-group. I do this

using only scales which are definitively associated with a body skeleton, and based on the assumption that all acanthodians are stem-chondrichthyans, osteichthyans are the sister group to chondrichthyans, and that "placoderms" and "ostracoderms" form a stem-gnathostome grade with "placoderms" sharing a more recent common ancestor with the crown-group. Because the assumption is that scales are isolated I accept only characters which are unique to the chondrichthyan total group. Finally, I assess whether Ordovician and Silurian micro-remains meet the resulting criteria.

2.2.1 **Scale structure**

The head skeletons of crown-gnathostomes are characterised by one of two states: osteichthyans are macromeric, with large, locationally specialised dermal plates covering the head, and chondrichthyans are micromeric, covered in a pelt of numerous, tiny denticles (Janvier, 1996). Mandibulate stem-gnathostomes are also macromeric, and the likely homology of their bones with those of osteichthyans means that a macromeric head skeleton is probably the ancestral state for crown-gnathostomes (Zhu et al., 2013, 2016; Giles et al., 2015c). A third state, sometimes termed mesomery, also exists, where parts of the head skeleton are formed from interlocking tesserae which are unspecialised in shape but nonetheless larger than micromeric denticles. This is common in the skull roof of stem-chondrichthyans, particularly "climatiid" acanthodians such as *Climatius* and *Parexus* (Burrow et al., 2015; Miles, 1973a; Burrow et al., 2013) in which heads are roofed with stellate tesserae while the rest of the head is covered with more specialised scales, including elongated branchial plates superficially like those of osteichthyans. Tesserae also seem to be broadly common in acanthodians generally being present, although less well characterised, in diplacanthids (Burrow et al., 2016a; Hanke and Davis, 2008; Young and Burrow, 2004; Long, 1983), in ischnacanthids (Blais et al., 2015), and in acanthodiforms and putative kin Gagnier and Wilson (1996b); Hanke (2008).

Very similar tesserae have also been reported in the possible crown-chondrichthyan *Tamiobatis* (Williams, 1998), and it is possible that they are underreported in early chondrichthyans. However, isolated tesserae are not necessarily chondrichthyan, as a tessellate head skeleton is also present in some stem-gnathostomes: osteostracans, galeaspids, and some placoderms (Janvier, 1996).

The distribution of body scale forms in gnathostomes is less well understood. As with the head skeleton, crown-gnathostomes have two clear conditions: osteichthyans have a covering of large, interlocking scales, whereas chondrichthyans have a shagreen of micromeric denticles (Janvier, 1996). Interlocking body scales are widespread in the gnathostome stem-group, in placoderms such as *Sigaspis* (Goujet, 1973), as well as in osteostracans and anaspids (Janvier, 1996). However micromeric squamations are also common in the gnathostome stem-group. Stem-gnathostome thelodonts have a pelt of disorganised dermal denticles sufficient for past authors to have linked them to chondrichthyans (Traquair, 1899). Micromery has been reported in osteostracans, and figured isolated galeaspid scales are small enough that they could be considered micromeric (eg. Wang et al. (2005) Fig.1). Even in some placoderms, scales described are relatively small, and would probably be considered micromeric if found on a chondrichthyan (eg. scales in Burrow and Turner (1998)) Scale size alone is insufficient to identify a scale as being chondrichthyan.

Another common feature of chondrichthyan scales not present in osteichthyans is a "neck": a marked waist between the crown and the base of the scale (Fig. 2.1). A neck is ubiquitous in chondrichthyan scales, both in stem- and crown-group members (Denison, 1979; Cappetta, 1987; Zangerl, 1981). This constrasts with the condition in osteichthyans and stem-gnathostomes in which scales are flattened with the crown usually sits on a flat dermal base with no intervening constriction (eg. *Raynerius* (Giles et al., 2015b), osteostracans (Qu et al., 2015a)). However, there are exceptions: the Palaeozoic osteichthyan *Psarolepis* has a neck alongside its otherwise

osteichthyan-shaped scales (Qu et al., 2013c), as does the actinopterygian *Cheirolepis* (Pearson and Westoll, 1979). In mandibulate stem-gnathostomes necks are found in some buchanosteids (eg. Burrow and Turner (1998) Fig. 9), *Brindabellaspis* (Burrow and Turner, 1998), as do some rhenanids (Denison, 1978). In jawless stem-gnathostomes necks are present in thelodonts (Märss et al., 2007), and arguably in some figured galeaspid scales (Wang et al. (2005) Fig. 1). Necks do not identify isolated scales as chondrichthyan.

A further set of characters used in phylogenetic analysis of early vertebrates considers the shape of the scale base. Many stem-chondrichthyans have a rounded, convex base - this is apparent in "classic" acanthodian scales (Denison, 1979), but also the relatively more crownwards taxon *Gladbachus* (Coates et al., 2018; Burrow and Turner, 2013) (Fig. 2.1). Contrastingly in many more crownwards chondrichthyans the base is flat or concave, for example in *Vernicomacanthus* (Chapter 6), *Seretolepis* (Hanke and Wilson, 2010), and *Brochoadmones* (Hanke and Wilson, 2006). The scale bases of osteichthyans such as *Raynerius* (Giles et al., 2015b) are instead flattened, which is also the state in osteostracans Qu et al. (2015a). However, in stem-gnathostome placoderms the shape varies, with both bulging and convex-based scales (Burrow and Turner, 1998, 1999). The gnathostome stem has both thelodonts and placoderms with bulbous bases, and flat-based osteostracan scales (Qu et al., 2015a; Märss et al., 2007; Burrow and Turner, 1999). Moreover these states are often labile within one taxon: in several taxa (eg. *Ptomacanthus* (Brazeau, 2012), and *Diplacanthus* (Burrow et al., 2016a)) flattened or bulging bases coexist in the same taxon.. Scale base shape seems to be labile enough that it has no use in identifying isolated scales.

FIGURE 2.1: Body scales of select gnathostomes in dorsal view (first column) and bisected through the sagittal plane (second column): (a) the osteichthyan *Psarolepis* from (Qu et al., 2013b); (b) the stem-chondrichthyan *Acanthodes* from (Denison, 1979); (c) the stem-chondrichhyan *Vernicomacanthus* from Chapter 6 of this thesis; (d) the stem-chondrichthyan *Seretolepis* from Karatajūtė-Talimaa (1997); Hanke and Wilson (2010); (e) An elasmobranch chondrichthyan, from (Smith and Hall, 1990).

Passages from the pulp cavity onto the surface of the neck - neck canals - have also often cited as a sign of chondrichthyan affinity in isolated scales (Sansom et al., 2012) (Fig. 2.1e). These canals are present in the placoid scales of living chondrichthyans, in which they transmit vasculature through the scale (Reif, 1978). However neck canals are actually widely present in the gnathostome total-group (Coates et al., 2018). They are present throughout chondrichthyan total-group for example in Palaeozoic "sharks" such as *Akmonistion* (Coates and Sequeira, 2001a), although are notably absent in *Gladbachus* (Coates et al., 2018). However they are common in acanthodian grade stem-chondrichthyans with a variety of different scale morphologies such as *Diplacanthus* (Burrow et al., 2016a), *Euthacanthus* (Newman et al., 2014), and *Vernicomacanthus* (see Chapter 6). Moreover the scales of the osteichthyans *Psarolepis* (Fig. 2.1a) and *Andreolepis* have a series of neck canals communicating with the internal vasculature (Qu et al., 2013b,a), suggesting the state is present in stem-group osteichthyans (Brazeau and Friedman, 2014). As Hanke and Wilson (2010) suggest, the presence of neck canals can probably vary dependent on the depth of insertion of the scale. This, combined with their broad phylogenetic distribution means that neck canals seem to be a generalised feature of early crown-group gnathostomes, and do not provide a confident chondrichthyan assignation for a scale.

Another vascular character of chondrichthyan scales is a ventral opening of the pulp cavity onto the base of the scale (Reif, 1978) (Fig. 2.1). As well as being a feature of "placoid" scales, a basal pore is also widely present in Palaeozoic "sharks",

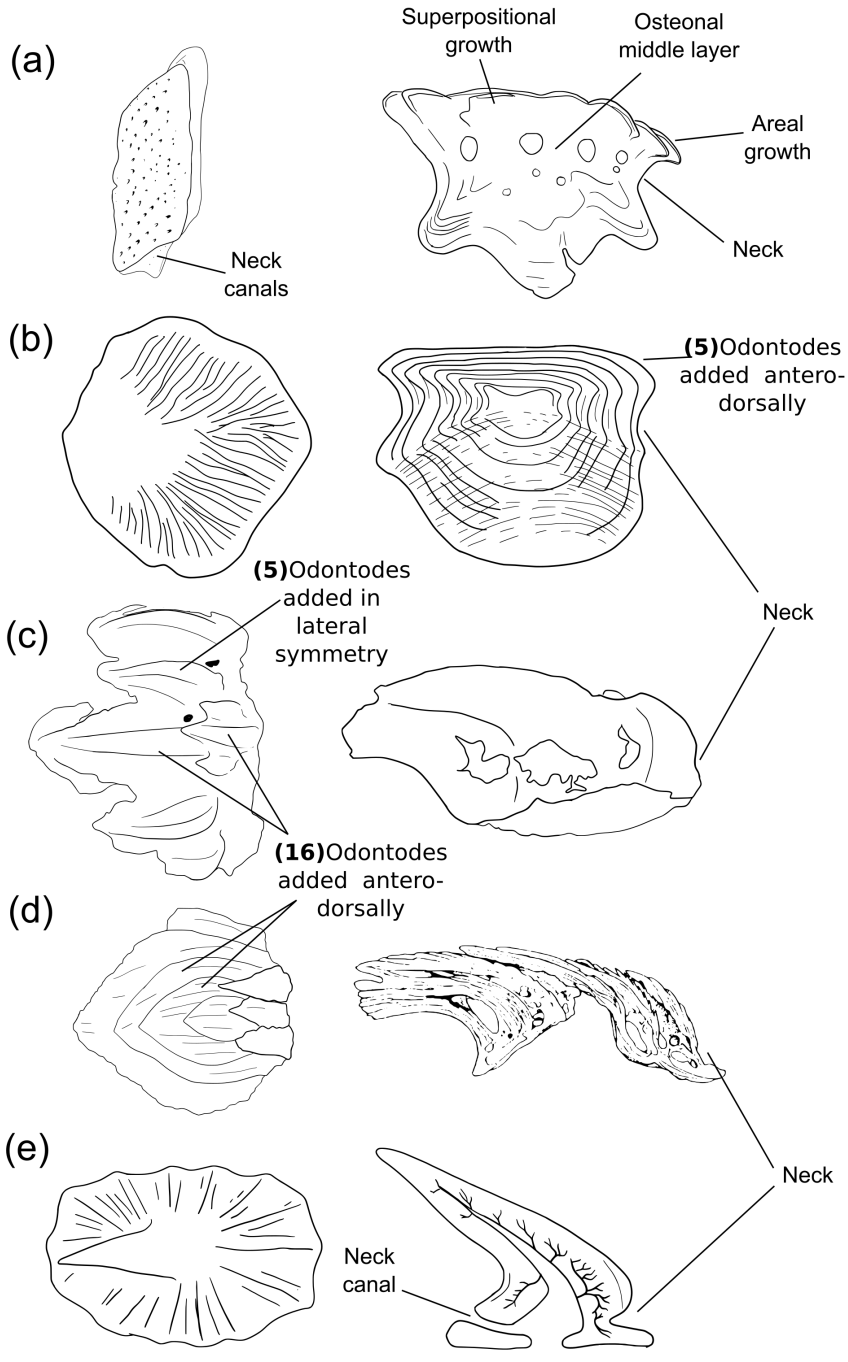


FIGURE 2.1: Caption previous page

both monodontode and polyodontode Zangerl (1981). Most osteichthyan scales, including the otherwise plesiomorphic scales of *Psarolepis*, lack a basal pore (Qu et al., 2013c). However, they are present in *Andreolepis* - an otherwise osteichthyan-like scale (Qu et al., 2013a). It is also apparently absent in the few described placoderm scales (Burrow and Turner, 1998, 1999). Notably a basal pore is absent in some members of the chondrichthyan stem-group, such as *Brochoadmones* (Hanke and Wilson, 2006), *Gladbachus* (Coates et al., 2018), and *Vernicomacanthus* (Chapter 6), meaning that its presence may diagnose a relatively crownwards position on the chondrichthyan stem-group. However, a basal opening of the pulp cavity is widely present in thelodont scales (Märss et al., 2007). Numerous vasculatory openings have also been reported in the base of the scales of osteostracans (Qu et al., 2015a). Because of this it cannot be used to confidently identify an isolated scale as belonging to a chondrichthyan.

2.2.2 **Histology**

The dermal bone of early vertebrates is formed from a diverse range of tissue-types, a result of early evolutionary experimentation in skeletogenesis (Donoghue et al., 2006). These varied tissues can be understood within a framework of three tissue layers: a superficial odontocytic layer, a middle osteonal layer, and an underlying laminated layer (Giles et al., 2013). Some stem-gnathostomes have more esoteric dermal histologies, like the "galeaspidin" of galeapids and the "aspidin" of heterostracans (Wang et al., 2005; Keating and Donoghue, 2016; Keating et al., 2015). However, these can be interpreted as corresponding to the layers of a three-layered model (Keating and Donoghue, 2016). A trio of corresponding layers are found in early osteichthyans, for example the scales of Psarolepis (Qu et al., 2013b), as well as in placoderm-grade stem-gnathostomes (Giles et al., 2013). Contrastingly the placoid scales of living chondrichthyans are instead composed of a single

odontogenic layer, with no underlying laminar or osteonal layer (Gillis et al., 2017). Notably, scales in some batoids have been shown to have an intermediate osteonal layer (Reif, 1979). While in the past this has been used to argue for its primitiveness, the distribution makes it clear that this is in fact a derived state. A three-layered structure is likely to be the plesiomorphic state of the dermal skeleton at the crown-gnathostome node (Giles et al., 2013).

While the crown-chondrichthyan dermoskeleton is reduced to a single superficial layer (Gillis et al., 2017), this is not true of stem-group, or of many early crown-group chondrichthyans. The supposedly quintessential onion-skin type scales of many acanthodians have dentinous crowns and a lamellar bony base (Denison, 1979) which may correspond to the topmost and lowermost layers of the plesiomorphic vertebrate skeleton (Giles et al., 2013). This also seems the most sensible way of interpreting the multicuspid scales of other acanthodians and early chondrichthyans which have a base with several generations of odontodes deposited on top (eg. *Seretolepis* (Karatajūtė-Talimaa, 1997; Hanke and Wilson, 2010)). In the plates and stellate tesserae of the head of acanthodians -perhaps more comparable to the dermal plates of other gnathostomes a similar pattern is also found - odontodes overlie a sheet of lamellar bone, with no intermediate osteonal layer (eg. *Climatius* (Burrow et al., 2015)). Even in the stem-chondrichthyan *Gladbachus*, noted for its unusual supposedly "placoderm-like" scale morphology,the scales that cover the body and head lack an osteonal middle layer between the lamellar base and overlying odontodes (Burrow and Turner, 2013; Coates et al., 2018). Because of this it seems likely that, within the gnathostome crown-group, the loss of this middle layer is a chondrichthyan synapomorphy. Thelodonts also arguably have a basal layer (their growing base) Because of this, while the absence of an osteonal middle layer is probably sufficient to diagnose a mandibulate gnathostome as chondrichthyan, it is insufficient to diagnose a disarticulated scale as such.

The dentinous tissue that forms the scale crown in gnathostomes vary in the relationships of dentine tubules and in the polarity and presence of the cell spaces that feed into them. Typically these variables are summarised into three broad groupings (with various overlapped and additional types): mesodentine, semidentine, and orthodentine (Janvier, 1996). Orthodentine comprises unipolar dentine tubules, with no cell lacunae present within the dentine - this is common in many crown-gnathostome scales (eg. the osteichthyan *Mimipiscis*, some acanthodians (Denison, 1979), and living chondrichthyans (Reif, 1979)). Mesodentine comprises a network of tubules and cell spaces - this is also common in the scales of many acanthodians (eg. *Climatius* (Burrow et al., 2015), *Diplacanthus* (Burrow et al., 2016a)) as well as in osteostracans Qu et al. (2015b) Semidentine comprises unipolar dentine tubules but with cell spaces within the dentine: it is theoretically limited to placoderm-grade stem-gnathostomes, but as Brazeau and Friedman (2014) note similar tissues are present in other stem-gnathostomes and putative acanthodians (Sansom et al., 2013; Karatajūtė-Talimaa and Smith, 2003). The only one of these tissues that might be a candidate for identifying isolated chondrichthyan scales is mesodentine - however the presence of this in stem-gnathostomes precludes the use of this as an identifying character.

2.2.3 **Mode of growth**

The placoid scales of Recent chondrichthyans are monodontode - that is, they comprise only one unit of crown growth based around a single papillum (Reif, 1978). Once this odontode is formed, no further growth takes place, with the scale eventually being shed and replaced by a younger scale. This condition is also widespread amongst fossil crown-chondrichthyans (Dick, 1978; Maisey and Denton, 2016). Similar scales are present in the presumed stem-chondrichthyans *Lupopsyrus*, *Lupopsyroides*, and *Obtusacanthus* (Hanke and Wilson, 2004; Hanke and

Davis, 2012), in which they have been taken as evidence of a close relationship with crown-group chondrichthyans. Monodontody is not however limited solely to chondrichthyans - the stem-gnathostome thelodonts also have scale crowns with a single pulp cavity (Märss et al., 2007). Monodontody is not sufficient to classify a scale as chondrichthyan.

Despite the ubiquity of monodontode scales in Recent chondrichthyans the scales of many fossil chondrichthyans are polyodontode, comprising several sequentially added crown growth units. Within animals conventionally considered "chondrichthyans" this is most obvious in "ctenacanthid"-like scales, in which new odontodes are added laterally, in *Ctenacanthus* and *Tamiobatis* (Reif, 1978; Williams, 1998). Outwardly similar scales to this have been described in *Antarctilamna* (Young, 1982) and *Doliodus* (Miller et al., 2003), and *Protacrodus* (Gross, 1938). However, scales of this type are poorly understood histologically. Polyodontode scales with a different growth pattern are also found in several MOTH taxa: *Kathemacanthus*, *Seretolepis*, and *Brochoadmones* (Hanke and Wilson, 2006, 2010). "Climatiid" acanthodians such as *Parexus* (Burrow et al., 2013), *Climatius* (Burrow et al., 2015), and *Ptomacanthus* (Brazeau, 2012), as well as *Vernicomacanthus* in Chapter 6 of this thesis. Polyodontody is also the norm outside the chondrichthyans total group, with the scale crowns of many stem-gnathostomes and osteichthyans comprising complexes of multiple odontodes (Gardiner, 1984; Burrow and Turner, 1999).

Confusing this distribution however are stem-chondrichthyans with an "onion-skin" type growth pattern which fits clearly into neither polydontody nor monodonotody. These scales have a single pulp cavity at the centre, surrounded by an original "odontode". However, rather than growing by the addition of odontodes areally, additional generations of growth are layered concentrically around the original odontode, giving the scale an onion-skin like pattern in cross

section (Denison, 1979). This pattern is widespread in certain acanthodian-grade chondrichthyans, in particular acanthodiforms (Denison, 1979), diplacanthiforms (Burrow et al., 2016a), and ischnacanthiforms (Gross, 1973). However, it also exists outside these groups, with its presence reported in the acanthodians *Euthacanthus* (Newman et al., 2014), and in some scales of *Ptomacanthus* (Brazeau, 2012). Whether this condition is more rightly considered polyodontode or monodontode is uncertain. Like polyodontode scales, the scales have several discrete growth stages. However, like monodontode scales, they originate from a single papillum of growth, with a single central pulp cavity. Given the several discrete growth stages I consider it more likely that they should be considered to by polyodontode, like the superpositional growth in non-chondrichthyans Qu et al. (2013c).

I believe that these polyodontode patterns of growth can be divided into two characters that are unique to chondrichthyans, partially derived from the "areallly apposed growth" character of Brazeau and Friedman (2014). The first, and more inclusive, of these is the antero-dorsal addition of odontodes: where a new odontode is added directly over the previous one, in the sagittal plane (eg. Figure 2.1). This can be seen in the scales of *Parexus* (Burrow et al., 2013), *Brochoadmones* (Hanke and Wilson, 2006), *Seretolepis*, and *Kathemacanthus* (Hanke and Wilson, 2010) where leaf-shaped odontodes are added one over the other, in the sagittal plane. The scales of *Vernicomacanthus* (Chapter 6) also demonstrates this growth in its central row of three odontodes It also seems likely to be the case in the "ctenacanth-type" scales common in Palaeozoic chondrichthyans (Williams, 1998), as well as in *Protacrodus*, a poorly understood total-group chondrichthyan (Gross, 1938). I would also argue that the "onion-skin" type growth of some acanthodians conforms with this pattern (eg. *Diplacanthus* in Burrow et al. (2016a)), while in these taxa the additional generations of growth surround one another completely, seemingly in synchronicity with the base growth, each new generation does grow on top of the previous one, in a symmetrical superposition. Contrastingly while new odontodes in the scales

of many osteichthyans grow superpositionally (eg. *Psarolepis* in Qu et al. (2013c)), or linearly (eg. *Andreolepis* in Qu et al. (2013a)) there are no instances these are not added antero-dorsally. The same is true in those stem-gnathostome placoderm scales which have been described (Burrow and Turner, 1998, 1999) Notably, this is also the same mode by which chondrichthyan tooth whorls grow. This pattern of growth seems to be unique to chondrichthyans.

The second character is the symmetrical addition of lateral odontode generations. This characterises many chondrichthyan scales, including those of *Tamiobatis* (Williams, 1998), *Diplodoselache* (Dick, 1981), and *Doliodus* (Miller et al., 2003). It is also common in the scales of "climatiid" acanthodians such as *Climatius* (Burrow et al., 2015) and *Ptomacanthus* (Brazeau, 2012) and, as I show in (Chapter 6), *Vernicomacanthus*. It is not present in typical onion-skin-like acanthodian scales, nor is it present in some stem-chondrichthyan scales like those of *Parexus* (Burrow et al., 2013), *Brochoadmones* (Hanke and Wilson, 2006), *Seretolepis*, and *Kathemacanthus* (Hanke and Wilson, 2010). A similar character to this is presumably referred to in the "symmetrical growth" character proposed by Andreev et al. (2016). While odontode generations are added in the scales of osteichthyan and stem-group gnathostomes, sometimes areally (eg. *Psarolepis* Qu et al. (2013b)), these never seem to be added in lateral symmetry. This seems to form a slightly less inclusive state than the previous growth character.

2.3 CHARACTERS OF CHONDRICHTHYANS

2.3.1 **Aims, assumptions, and methods**

The following section aims to summarise characters that can be used to confidently place a fossil in the chondrichthyan total group. I have updated the list of Brazeau and Friedman (2014) for characters that can be used to place animals in

the chondrichthyan total-group, and split it into characters that can place taxa in the chondrichthyan total-group generally, and those which can place a fossil crownwards of *Acanthodes*. I also consider characters that can confidently be used to place a fossil in the chondrichthyan crown-group, in either the holocephalan total-group or in the elasmobranch total-group. Following the methods of Friedman and Brazeau (2010) and Brazeau and Friedman (2014) I have done this by using the first doublet rule of Maddison et al. (1984), ie. that for a character state to be considered apomorphic, the converse state must be present (and applicable) in two consecutive outgroups.

I also make a number of assumptions about the relationships of the groups involved:

1. That chondrichthyans are monophyletic, comprising elasmobranchs and holocephalans as monophyletic sister groups.
2. That osteichthyans are the monophyletic sister-group to chondrichthyans
3. That all acanthodians are stem-group chondrichthyans
4. That "placoderm" and "ostracoderm" taxa are stem-group gnathostomes

2.3.2 **Characters that can place a fossil in the chondrichthyan total group**

These characters can place a fossil in the chondrichthyan total group, and are also present (or impossible to rule out) in *Acanthodes*.

1. Precerebral fontanelle
2. Dorsal otic ridge
3. *Hyoid articulates ventrally or laterally to the path of the jugular vein groove
4. Skull roof lacks sutured plates
5. *Odontodes added to body scales antero-dorsally
6. *Spines on coracoid shoulder girdle
7. *Intermediate spines
8. Dorsal scapular blade
9. Lateral sensory line passing between flank scales

Characters with an * have been added to the list of Brazeau and Friedman (2014).

NEUROCRANIUM — The precerebral fontanelle, a large, anterior opening on the ethmoid region into the cerebral cavity, is an extremely consistent feature of chondrichthyan neurocrania (Schaeffer, 1981; Maisey, 1984, 2004; Brazeau and Friedman, 2014) (Fig. 2.2). Whilst in living chondrichthyans it is found only in elasmobranchs, it is almost ubiquitous amongst extinct shark-like chondrichthyans (Schaeffer, 1981). In the past this has led to its being proposed as a synapomorphy uniting these shark-like fossil taxa with elasmbranchs, to the exclusion of holocephalans (Maisey, 2005).. Parallels have long been drawn between the precerebral fontanelle and the holocephalan ethmoid canal (De Beer and Moy-Thomas, 1935; Schaeffer, 1981), although this homology has been disputed on the

basis of the ethmoid canal being a roofed over extra-cranial space (Maisey, 2005; Didier, 1995). The precerebral fontanelle is also present in the stem-chondrichthyans, such as *Doliodus* (Maisey et al., 2009). Although there has been one dubious report of a putative precerebral fontanelle in *Protodus* (Burrow and Turner, 2010), in better preserved acanthodian braincases the ethmoid region is unknown (Brazeau, 2009; Davis et al., 2012). Due to this uncertainty, as well as the lack of information about the condition in acanthodians,in which , it is here conservatively maintained as a chondrichthyan, rather than an elasmobranch, character, following Brazeau and Friedman (2014).

A dorsal otic ridge is a broadly acknowledged feature of chondrichthyan neurocrania (Brazeau and Friedman, 2014; Maisey, 2001a; Schaeffer, 1981) (Fig. 2.2). It is widely present in Palaeozoic sharks (eg. Schaeffer (1981)) as well as in *Acanthodes* (Davis et al., 2012). It is absent in placoderms and in osteichthyans, although I note the misgivings of Brazeau and Friedman (2014) about taxa with strongly attached skull roofing bones. Also, as noted by Brazeau and Friedman (2014) a similar structure is present on the neurocranium of the acatinopterygian *Lawrenciella*. Notably, a posterior ridge also appears to be present on the neurocranial roof of the stem-gnathostome *Romundina* Dupret et al. (2017), although from the material it is unclear if this is limited to the occiput, or extends onto the otic region If the former is the case it is more similar to the pronounced occipital crest of some chondrichthyans (eg. Schaeffer (1981); Finarelli and Coates (2014)). I have retained dorsal otic ridge as a character here, although with these reservations.

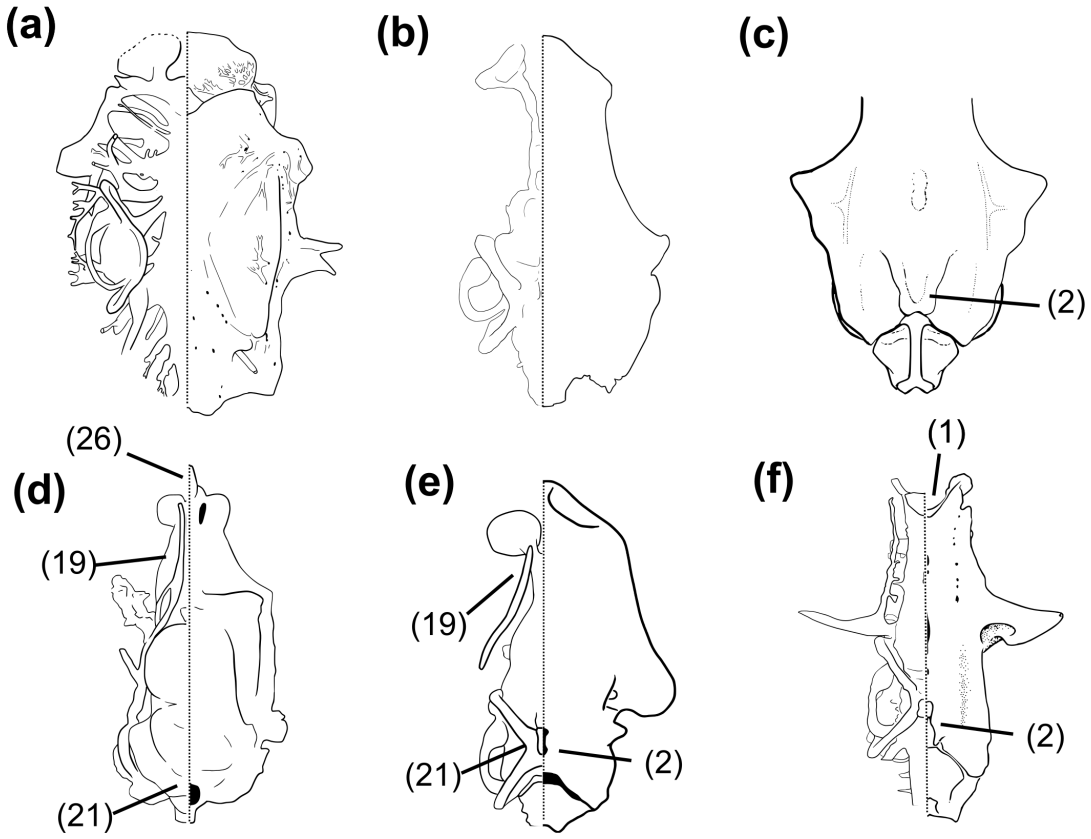


FIGURE 2.2: Neurocrania and endocasts of select gnathostomes in dorsal view: (a) The stem-gnathostome *Dicksonosteus*, from Goujet (1984); (b) The actinopterygian *Mimipiscis*, from Gardiner (1984); Giles and Friedman (2014); (c) The stem-chondrichthyan *Acanthodes*, from Davis et al. (2012); (d) The holocephalan *Callorhincus* from Coates et al. (2017a); (e) The symmorriiform *Dwykaselachus*, from Coates et al. (2017a); (f) The Palaeozoic "shark" *Cladodoides* from Maisey (2005).

In chondrichthyans the hyoid arch articulates with the neurocranium ventrally to the path of the jugular vein groove (Maisey, 2004; Brazeau and de Winter, 2015) (Fig. 2.4). This morphology can be seen in a broad range of fossil chondrichthyan taxa such as *Cladodoides*, *Pucapampella*, and *Orthacanthus* (Maisey, 2005, 2001a; Schaeffer, 1981). Contrastingly, in osteichthyans such as *Mimipiscis* (Gardiner,

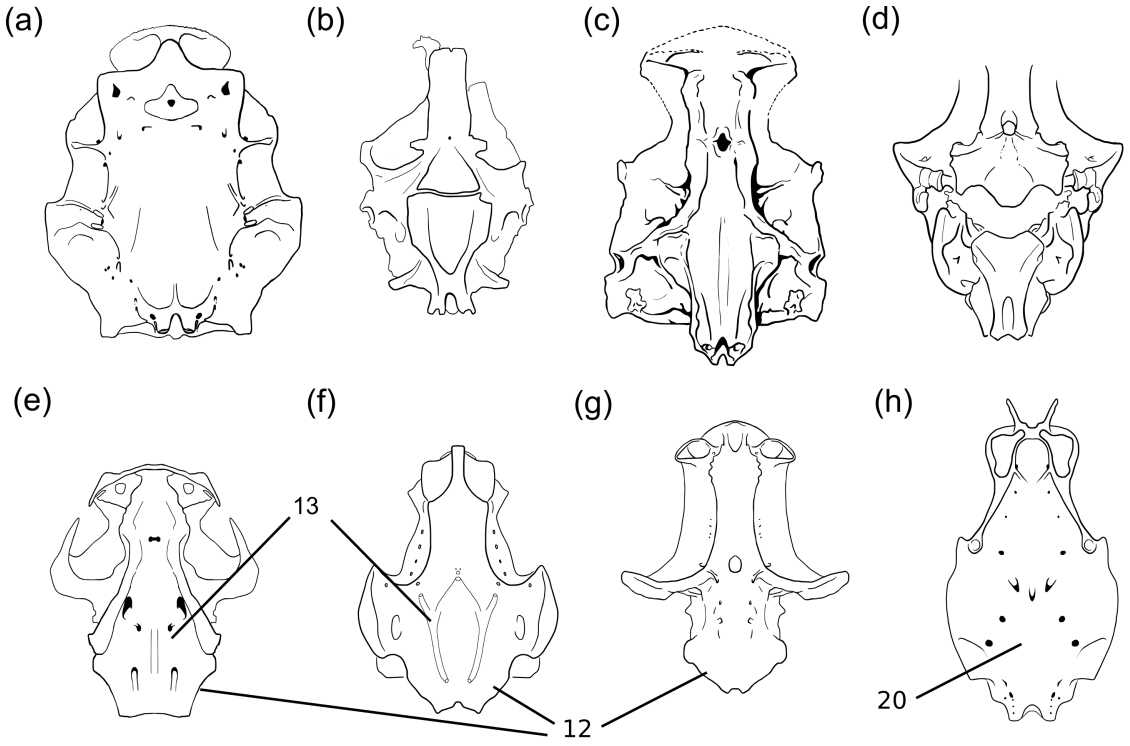


FIGURE 2.3: Select gnathostome neurocrania in ventral view: (a) The stem-gnathostome *Dicksonosteus*, from Goujet (1984); (b) The actinopterygian *Raynerius* from Giles et al. (2015b); (c) The stem-gnathostome *Janusiscus* from Giles et al. (2015c); (d) The stem-chondrichthyan *Acanthodes* from Davis et al. (2012); (e) The stem-chondrichthyan *Doliodus* from Maisey et al. (2009); (f) The stem-elasmobranch *Egertonodus* from Maisey (1983); (g) The symmoriiform *Dwykaselachus* from Coates et al. (2017a); (h) The holocephalan *Hydrolagus* from Allis (1917).

1984) and placoderms such as *Dicksonosteus* (Goujet, 1984), the hyoid arch instead articulates with the neurocranium on a process that overlies the path of the jugular canal dorsally (Brazeau and de Winter, 2015). The condition in acanthodians, typified by *Acanthodes*, has been a source of debate between parties arguing for the chondrichthyan (Jarvik, 1977) and the osteichthyan (Miles, 1973b; Davis et al., 2012) states. However, recent redescription of the condition in *Acanthodes* showed that it lies ventrally to the jugular vein, in the chondrichthyan condition (Brazeau and

de Winter, 2015). This seems to be a fairly clear cut chondrichthyan synapomorphy.

The glossopharyngeal (IX) nerve exits the neurocrania of gnathostomes in a variety of different ways (Pradel et al., 2013). In elasmobranchs and holocephalans it exits via the remnants of the metotic fissure, through the glossopharyngeal canal in elasmobranchs or through a foramen in holocephalans (Pradel et al., 2013). It also exits through the metotic fissure in Palaeozoic "sharks" such as *Akmonistion* (Coates and Sequeira, 1998), as well as *Acanthodes*. Contrastingly, in osteichthyans it exits through a posteroventral foramen in the otic wall, and does the same in stem-gnathostomes such as *Dicksonosteus* (Goujet, 1984). One exception is in *Ligulalepis*, in which it is presumed to have exited through the metotic fissure as in chondrichthyans due to the absence of a foramen Clement et al. (2018). The exit through the metotic fissure is possibly a derived trait of chondrichthyans. However due to the uncertain state in *Ligulalepis* I have elected not to include it as a character.

VISCERAL ARCHES — In some sarcopterygians, rather than contacting the unpaired basibranchial skeleton, the fourth hypobranchial instead contacts the anterior paired section of the fourth branchial arch (eg. *Glyptolepis*(Jarvik, 1972)) (Fig. 2.5). This is distinct from the condition in chondrichthyans and in actinopterygians, in which these do not contact one another, instead contacting the unpaired basibranchial skeleton (eg. *Mimipiscis*(Gardiner, 1984)). The broad presence of this state across sarcopterygians living and extinct has led to its being proposed as a sarcopterygian synapomorphy. However, the recent description of a very similar state in the stem-gnathostome *Paraplesiobatis* raises the possibility that the union of the posteriormost branchial arches is fact plesiomorphic for crown-gnathostomes (Brazeau et al., 2017). As it stands two equally parsimonious scenarios exist: the first that this condition was independently derived in sarcopterygians and *Paraplesiobatis*, and the second that this condition was present amongst stem-group gnathostomes,

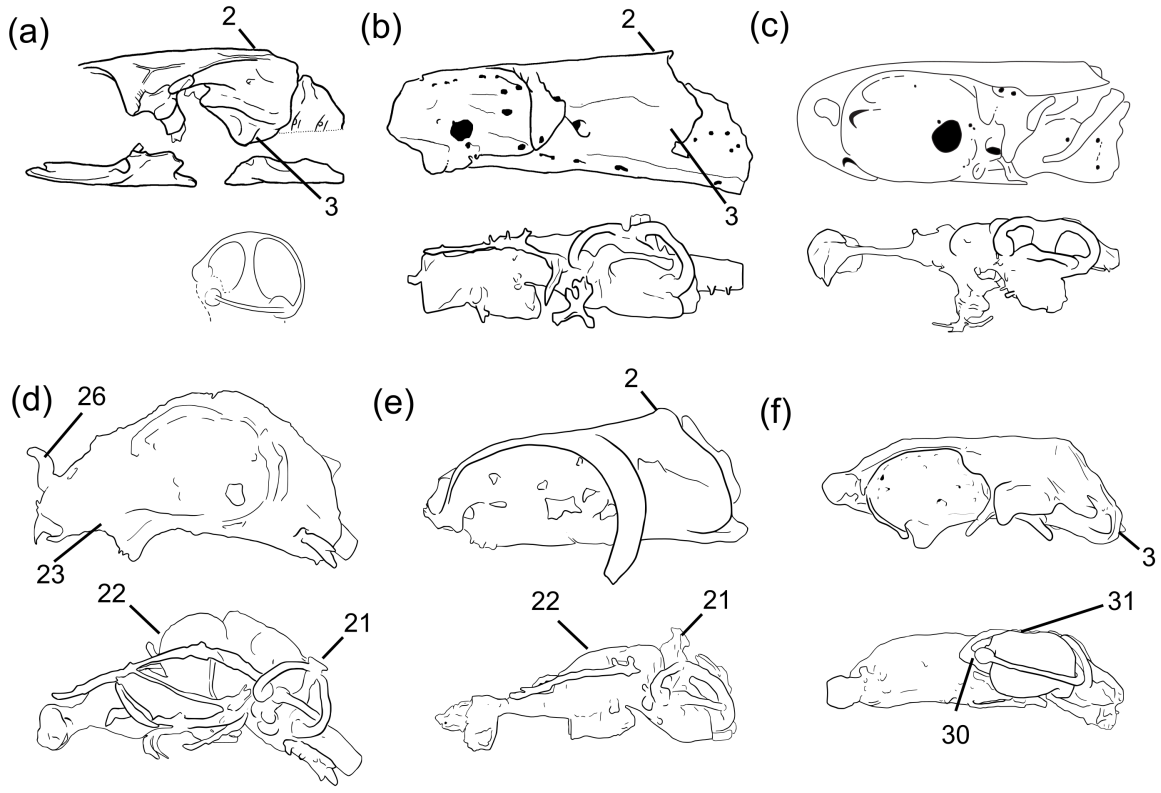


FIGURE 2.4: Neurocrania and endocasts of select gnathostomes in lateral view: (a) The stem-chondrichthyan *Acanthodes*, from Davis et al. (2012); Miles (1973a); (b) The Palaeozoic "shark" *Cladodoides* from Maisey (2005);(c) The actinopterygian *Mimipiscis*, from Gardiner (1984); Giles and Friedman (2014);(d) The holocephalan *Callorhincus* from Coates et al. (2017a);(e) The symmorriiform *Dwykaselachus*, from Coates et al. (2017a); (f) The stem-elasmobranch *Tribodus*, from Lane (2010).

and lost in both actinopterygians and chondrichthyans. To distinguish between these two scenarios more information is required from one of the three stem-groups incident on the gnathostome crown-node. However, if the second proves to be correct, the ventral separation of the posteriormost paired elements of the branchial arches would be a chondrichthyan synapomorphy. Here I have elected not to

include it however, due to its sparse distribution.

Coates et al. (2018) identify two epibranchial characters which may be synapomorphies for chondrichthyans. The first of these is the presence of an epibranchial on the posteriormost branchial arch. This is present in chondrichthyans including *Acanthodes* (Davis et al., 2012): it is also present in living osteichthyans but is probably secondarily derived (Carvalho et al., 2013). The second is a pronounced flange along the posterior margins of epibranchials - this can be seen in *Acanthodes*, *Gladbachus*, and *Ozarcus*, (Coates et al., 2018; Pradel et al., 2014), and is absent in Palaeozic osteichthyan gill skeletons Giles et al. (2015b); Gardiner (1984); Jarvik (1980). This may be a plesiomorphic feature of crown-chondrichthyan gill skeletons. Unfortunately, because these are present in *Acanthodes*, and because of the absence of any stem-gnathostome "placoderm" dorsal branchial skeletons (Brazeau et al., 2017), the polarity of these characters is not possible to resolve.

SKELETON — A micromeric skull was cited by Brazeau and Friedman (Brazeau and Friedman, 2014) as a character that can place a fossil in the chondrichthyan total group, and which is also shared by acanthodians. In recent years evidence has come to light that the macromeric skeletons of osteichthyans and placoderms are homologous in the form of likely stem-gnathostomes with osteichthyan-like dermal head armour such as *Entelognathus* and *Janusiscus* (Zhu et al., 2013; Giles et al., 2015c; Zhu et al., 2016) . Whether or not these animals were stem-gnathostomes, or very early members of the gnathostome crown-group, it does seem increasingly likely that the plesiomorphic condition for crown-group gnathostomes was a macromeric exoskeleton, and the micromeric dermal head skeleton of chondrichthyans and some acanthodians is secondarily derived. In this scenario the larger plates that are present in the head skeletons of many acanthodians, for example *Culmacanthus* (Long, 1983), may be retained from the plesiomorphic gnathostome condition.

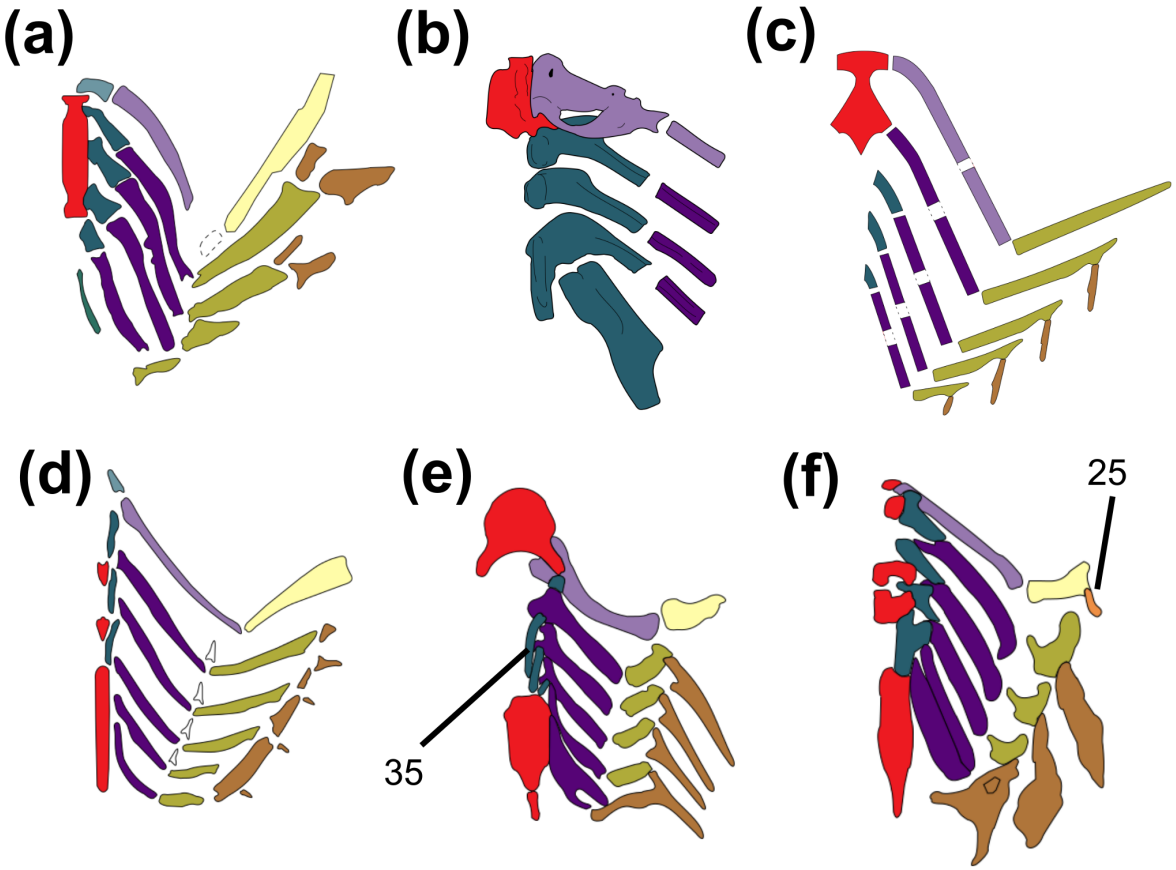


FIGURE 2.5: Branchial arches in select gnathostomes, laterally flattened, with ventral elements on the left and dorsal on the right: (a) The actinopterygian *Raynerius*, from Giles et al. (2015b); (b) The stem-gnathostome *Paraplesiobatis*, from Brazeau et al. (2017); (c) The stem-gnathostome *Acanthodes*, from Gardiner (1984); Miles (1973b); (d) The symmoriiform *Ozarcus*, from Pradel et al. (2014); (e) The elasmobranch *Scyliorhinus* from Pradel et al. (2014); (f) The holocephalan *Callorhincus* from Pradel et al. (2014). Colour scheme: *red*, basihyal/branchial; *turquoise*, hypobranchial; *purple*, ceratohyal/branchial; *yellow*, epihyal/branchial; *orange*, pharyngohyal/branchial. Lighter shades denote hyoid arch.

Macromeric elements of the head skeleton are also present in the headshields of some stem-holocephalans such as *Menaspis*; given the phylogenetic position of these

taxa they are likely secondarily derived (Patterson, 1965).

Despite this there is some difficulty settling on the most inclusive state for this character. Tesserae are broadly present across the gnathostome total group, in ostracoderms, some placoderms, and osteichthyans (Janvier, 1996). Moreover, it is not really true to say that the skull roof of acanthodian-grade taxa is unpatterned - the tesserae of acanthodian heads are definitely regionalised, with different plate types occurring in different places (eg. *Climatius* in Miles (1973a), *Vernicomacanthus* in this thesis, Chapter 6). However, what they do lack is large sutured plates: I have elected to modify this character to be based on the absence of sutured plates.

As discussed previously in this chapter, I also consider scale growth by the antero-dorsal addition of odontodes to be a characters shared by *Acanthodes* and chondrichthyans more broadly.

SPINES — Anterior to the pectoral fin spines in many acanthodian-grade stem-chondrichthyans are one or two pairs of small spines, over the coracoid region of the shoulder girdle (Miles, 1973a) (Fig. 2.7). These are widespread amongst acanthodians, (eg. *Gladiobranchus*(Hanke and Davis, 2008), *Promesacanthus*(Hanke, 2008), *Climatius*(Miles, 1973a), *Acritolepis*(Valiukevičius, 2003)). These are also present in *Doliodus* (Pradel et al., 2016) and are probably plesiomorphic for the chondrichthyan total-group. Both osteichthyans (eg. *Guiyu* (Zhu et al., 2009)) and stem-gnathostomes (eg. *Entelognathus*(Zhu et al., 2013)) have pectoral fin spines, but in no case is there a prepectoral projection. Thus, contingent on acanthodians being stem-chondrichthyans this can be considered a character identifying a taxa as chondrichthyan.

Another characteristic of acanthodian-grade members is a pair of rows of spines running ventrally between the pectoral and pelvic girdles (Fig. 2.7). These intermediate (or prepelvic) spines vary in number, but are widespread amongst acanthodians, (eg. *Gladiobranchus*(Hanke and Davis, 2008), *Promesacanthus*(Hanke, 2008), *Climatius*(Miles, 1973a)). In most taxa (the notable exception being *Brochoadmones*(Hanke and Wilson, 2006; Gagnier and Wilson, 1996b)) these are not associated with any kind of fin web. No articulated osteichthyans or stem-gnathostomes (eg. *Mimipiscis*(Gardiner, 1984), *Coccosteus*(Miles and Westoll, 1968)) show a similar morphology and they are probably peculiar to chondrichthyans.

2.3.3 Characters that can place a fossil in the chondrichthyan total group, crownwards of *Acanthodes*

These characters can place a fossil in the chondrichthyan total group, crownwards of *Acanthodes*.

10. Tessellate prismatic calcified cartilage
11. *Canal for efferent pseudobranchial artery
12. *Laterally broad basioccipital
13. Canals for lateral dorsal aortae in basioccipital
14. *Anteriorly abbreviated notochord
15. Tooth files with unfused bases
16. *Laterally symmetrical areal growth
17. Denticles on fin side of dorsal fin spines
18. Pelvic claspers

TISSUES — Tessellate prismatic calcified cartilage lines the perichondrium of skeletal elements in all living chondrichthyans (Dean and Summers, 2006). The tissue is also present (usually being a key identifying feature) in Palaeozoic sharks (Schaeffer, 1981). It is completely unknown in any osteichthyans or stem-gnathostomes (Maisey, 2013). It is also unknown in any acanthodian-grade taxa, with a single report in *Traquairichthys* by Fritsch (1895) considered suspect by Ørvig (1951). The absence of this tissue in *Doliodus* (Long et al., 2015) and the unusual perichondrial calcification in *Gladbachus* Coates et al. (2018) leave its precise origins uncertain. However its presence indicates a phylogenetic position crownwards of *Acanthodes* on the chondrichthyan stem-group.

NEUROCRANIAL — In chondrichthyans the efferent pseudobranchial arteries enters the basicranium through paired foraminae before passing over the trabeculae to meet the internal carotids (Maisey, 2005, 2007; Schaeffer, 1981). This is the case in total-group elasmobranchs and Palaeozoic chondrichthyans (eg.(Maisey, 2004, 1983; Schaeffer, 1981; Maisey, 2007)). Although in holocephalans internal carotids are absent, the pseudobranchial arteries enter through paired foraminae widely separated from the median of the basicranium, so they seem certain to have originally displayed the wider chondrichthyan condition (Pradel, 2010). Contrastingly, in osteichthyans, the efferent pseudobranchial arteries pass along grooves in the basicranium, before entering with the internal carotids (eg. (Gardiner, 1984; Maisey, 2007)). This second state also seems to be the case in placoderm grade stem-gnathostomes, some of which have ventral grooves for what are inferred to be the pseudobranchial arteries (Young, 1986). *Acanthodes* too, has grooves in the basisphenoid inferred to be for the pseudobranchial arteries (Miles, 1973b). This character thus seems to group chondrichthyans crownwards of *Acanthodes*.

In living elasmobranchs the parachordal plates forms a broad surface below the otic region, the hypotic lamina (eg. in *Notorynchus* (Maisey, 2004)) (Fig. 2.3). While this is absent in holocephalans(De Beer and Moy-Thomas, 1935) a similar broad basioccipital region is widely present in Palaeozoic chondrichthyans including *Doliodus*, *Pucapampella Dwykaselachus*, and *Orthacanthus* (Maisey et al., 2009; Coates et al., 2017a; Schaeffer, 1981; Maisey, 2001a), and so is probably plesiomorphic for the chondrichthyan crown-group. A similar condition is probably also present in the the acanthodian-grade *Ptomacanthus* (Brazeau, 2009) Contrastingly, in *Acanthodes* Miles (1973b) and *Diplacanthus* (see Chapter 4), the basiocciput is laterally restricted underneath the otic region. The same, laterally constricted condition to this is also found in osteichthyans (eg. *Mimipiscis* (Gardiner, 1984)), as well as in the likely stem-gnathostome *Janusiscus* (Giles et al., 2015c). In most stem-gnathostomes though, the basiocciput is broad (eg. *Dicksonosteus* (Goujet, 1984)). However, it satisfies multiple

outgroups and so I have accepted a broad basiocciput as a chondrichthyan character.

A consistent feature of chondrichthyan braincases is that the notochord is anteriorly abbreviated, terminating in a relatively shallow occipital condyle (Maisey, 2001a). This can be seen across a broad range of crown-chondrichthyans including elasmobranchs *Tristychius* and *Notorynchus* (Coates and Tietjen, 2018; Maisey, 2004), and in holocephalans *Iniopera* and *Hydrolagus* (Pradel, 2010; Allis, 1917), It is also present in Palaeozoic sharks such as *Dwykaselachus*, *Cladodoides*, and *Ozarcus* (Coates et al., 2017a; Maisey, 2005, 2007). In the stem-chondrichthyan *Pucapampella* the notochord appears similarly abbreviated ending about halfway along the length of the parachordal plate (Maisey, 2001a). Contrastingly in osteichthyans the notochordal tunnel is far more extensively developed - in early actinopterygians it proceeds into the braincase up to the level of the posterior dorsal fontanelle (Gardiner, 1984; Giles et al., 2015b; Pradel et al., 2016), while in sarcopterygians it passes through the occipital region entirely, ending in the notochordal pit on the underside of the ethmosphenoid (eg *Gogonasus* in (Long and Barwick, 1997)). Similarly in stem-gnathostomes the notochord is not anteriorly delimited, extending fairly far anteriorly underneath the neurocranium (eg (Goujet, 1984; Giles et al., 2015c)). Notably Miles (1973b) also interprets *Acanthodes* as diplaying a similar morphology. This then, could be a character uniting chondrichthyans lying crownwards of *Acanthodes*.

MANDIBULAR ARCH — Brazeau and Friedman (2014) considered that tooth whorls with unfused bases could place a fossil relatively crownwards on the chondrichthyan stem-group. These are present in the majority of chondrichthyans (Zangerl, 1981). Contrastingly, in acanthodians and in the stem-chondrichthyan *Doliodus*, tooth whorls have fused bases (eg.Maisey et al. (2014); Burrow et al. (2015)). Another, less inclusive aspect of this not considered by (Brazeau and Friedman,

2014) is tooth retention. In both stem-chondrichthyans with tooth whorls and in many Palaeozoic sharks, teeth were retained in the mouth, rather than being shed as in living elasmobranchs (Williams, 2001). It is possible the presence or absence of this character has some phylogenetic importance within the chondrichthyan total group(Williams, 2001). However, the more inclusive state seems to be the fused tooth bases character adopted by Brazeau and Friedman (2014).

POSTCRANIAL — In living fishes pelvic claspers are unique to chondrichthyans, and they were listed as a chondrichthyan character by Brazeau and Friedman (2014) (Fig. 2.7). As they noted pelvic claspers are present in a broad array of placoderm, grade taxa: since, they have also been described in antiarchs (Long et al., 2014). This means claspers are now broadly present in the gnathostome stem-group - in arthrodires, antiarchs, and ptyctodonts - and may be plesiomorphic for crown-group gnathostomes (Long et al., 2014; Ahlberg et al., 2009; Trinajstic et al., 2014). Notably though, stem-gnathostome claspers do not appear to be part of the pelvic girdle, unlike those of chondrichthyans (Trinajstic et al., 2014). Because the character still satisfies my outgroup criteria, being absent in acanthodians and osteichthyans, I have retained it as a character.

2.3.4 **Characters of total group holocephalans**

19. Superficial ophthalmic trunks situated dorsal to telencephalon
20. No entry for internal carotids in basicranium
21. External opening of endolymphatic ducts anterior to entry of anterior semicircular canal into sacculus
22. Mesencephalon and cerebellum roof higher than semicircular canal

23. Palatoquadrates fused to neurocranium
24. Jaw articulation at rearmost extremity of mandible
25. Pharyngohyal
26. Unpaired cartilage articulating on ethmoid region of neurocranium
27. Prepelvic tenaculae
28. Dorsal fin spine at pectoral level only

NEUROCRANIUM — In all living holocephalans the superficial ophthalmic trunk passes through a foramen in the anterior of the orbit and is carried by an enclosed tube, the ethmoid canal, onto the surface of the ethmoid region. This is certainly apomorphic for holocephalans: in elasmobranchs, and many Palaeozoic sharks and osteichthyans rami of the superficial ophthalmic complex instead exit the orbits dorsally and pass through an array of foramina onto the roof of the neurocranium (eg.*Notorynchus* (Maisey, 2004), *Cladodoides* (Maisey, 2005), *Tamiobatis* (Romer, 1964; Schaeffer, 1981), *Orthacanthus* (Schaeffer, 1981), *Lawrenciella* (Pradel et al., 2016), and *Kentuckia* (Rayner, 1951)). However, it is difficult to distill into a useful character with which to diagnose fossils as holocephalan: the ethmoid canal itself is an extremely non-inclusive character, which is absent in most stem-holocephalans (Pradel, 2010; Patterson, 1965) and its homology with other structures in the chondrichthyan head has been much debated (Finarelli and Coates, 2014; Patterson, 1965). RecentlyCoates et al. (2017a) argued that the central position of the ophthalmic trunks over the telencephalon in the putative stem-holocephalan *Dwykaselachus* was homologous with that of holocephalans (Fig. 2.2). This seems to be a convincingly holocephalan character, and is also far more inclusive and clear than any based on the ethmoid canal itself.

In most gnathostomes the internal carotid arteries supply blood to the brain. They do this either by entering the neurocranium via paired internal carotid foramina - eg. some stem-gnathostomes (eg. *Buchanosteus* (Young, 1979)), some "acanthodians" (eg. *Ptomacanthus* (Brazeau, 2009)), and some chondrichthyans (eg. *Egertonodus* (Maisey, 1983)) - or by entering through the buccohypophyseal foramen - eg. osteichthyans (eg. *Cheirolepis*), some chondrichthyans (eg. *Cladodoides*), stem-gnathostomes (eg. *Janusiscus*), and some "acanthodians" (eg. *Acanthodes*). However, in Recent holocephalans the internal carotids do not supply the brain, instead either being aborted during development (Sansom et al., 2012) or, in the case of *Rhinochimaera* exist but without a role in brain supply (Stahl, 1967) - correspondingly there are no foramina for the internal carotids and the hypophyseal foramen is closed (Allis, 1917) (Fig. 2.3). A similar arrangement has been reported in a likely stem-holocephalan sibyrhynchid (Pradel, 2010) which lacks foramina through which the internal carotid arteries could have entered the braincase. This then seems plausible as a character uniting iniopterygians and living holocephalans (Pradel, 2010), inferred in the iniopterygian on the basis of the absence of any kind of foramen that the internal carotids could plausibly enter. Some fossil total-group elasmobranchs lack a buccohypophyeal opening (*Synechodus*) (Maisey, 1985) while others possess both a buccohypophyseal opening and internal carotids (Maisey, 1983). Acanthodians seem to be similarly varied, with a buccohypophyseal entry in *Acanthodes* (Davis et al., 2012), and apparent paired internal carotid foramina in *Ptomacanthus* (Brazeau, 2009). Only in holocephalans however is there no entry for the internal carotids in the basicranium.

In extant holocephalans, as well as extant elasmobranchs, the dorsal aorta is uninvested in the basicranium (De Beer and Moy-Thomas, 1935; Didier, 1995) (Fig. 2.3). However, in the stem-holocephalan *Helodus* there is a single canal for the median dorsal aorta at the extreme posterior of the basicranium (Patterson, 1965) (Moy-Thomas, 1936). A similar canal for the dorsal aorta is found in symmoriiform

sharks, such as "*Cobelodus*" (Maisey, 2007), *Akmonistion* Coates and Sequeira (1998, 2001a), and *Cladoselache* (Maisey, 2007). This differs from the condition in most other Palaeozoic chondrichthyans in which the lateral dorsal aortae are invested in a pair of canals, but the median dorsal aorta is not. A groove for the median dorsal aorta seems widespread (Coates and Sequeira, 1998) - in *Acanthodes* (Miles, 1973b; Davis et al., 2012) sarcopterygians such as *Youngolepis* (Chang, 1982) and chondrichthyans such as *Falcatus* (Lund, 1985). A canal for the median dorsal aorta is also found in some actinopterygians - *Moythomasia*, *Mimipiscis*, and *Kentuckia* (Gardiner, 1984) (Rayner, 1951). Furthermore the basicranial circuit in *Helodus* and Palaeozoic "sharks" differ in that the median dorsal aorta of *Helodus* apparently does not split into two divergent lateral dorsal aortae (Pradel et al., 2011). The identification of a canal for the median dorsal aorta in the basioccipital of the "acanthodian" *Diplacanthus* in Chapter 4 however. While this is probably a character uniting holocephalans with some Palaeozoic "sharks" I have rejected it as the situation in the chondrichthyan stem-group is unclear.

In holocephalans, the endolymphatic duct has a relatively anterior position in the neurocranium, rising vertically from anterior to the level of the *crus commune* (Coates et al., 2018) (Fig. 2.2, 2.4). This contrasts with the duct's position in elasmobranchs, in which it lies posteriorly to the *crus commune* (eg. *Notorynchus* Maisey (2004)). This second condition is common in Palaeozoic sharks in which it is known, including *Orthacanthus* (Schaeffer, 1981) and *Cladodoides* (Maisey, 2005). It is also implied along the chondrichthyan stem-group in the relative positions of the labyrinth and the posterior dorsal fontanelle in *Acanthodes* and *Pucapampella* (Davis et al., 2012; Maisey and Lane, 2010). The same is true in osteichthyans (eg. *Raynerius* Giles et al. (2015b)) and in stem-gnathostomes (eg. *Dicksonosteus* Goujet (1984)). This anterior position can confidently be identified as a holocephalan character: so as to make it applicable to elasmobranchs (which lack a *crus* between the anterior and posterior canals) I have defined it as being level with the entry into the sacculus

of the anterior semicircular canal.

The endocavities of holocephalan braincases are characterised by a unique morphology of the mesencephalon and telencephalon (Fig. 2.4). The mesencephalon is extremely elevated relative to the rest of the endocavity, rising above the labyrinth (eg. in *Callorhincus* (Coates et al., 2017a)), with telencephalon is ventrally offset relative to the mesencephalon (Coates et al., 2017a). These morphologies are absent in elasmobranchs (eg. *Notorynchus* (Maisey, 2004)) and in most Palaeozoic "sharks" (eg. *Cladodoides*(Maisey, 2005)). While little is known about the endocast of *Acanthodes*, the relative positions of its semicircular canals and the braincase roof appear inconsistent with a high mesencephalon (Davis et al., 2012), and osteichthyans consistently display the non-holocephalan condition (Giles and Friedman, 2014). (Coates et al., 2017a, 2018) atomise this into two separate characters in their morphological matrices, telencephalon offset and mesencephalon height, and it seems probable that they are part of a to a broader scale reorganisation of the skull in holocephalans. However, the mesencephalon height seems the easier character to diagnose, as it only relies on the preservation of the labyrinth and mesencephalon.

VISCERAL ARCHES — Perhaps the most obvious character of holocephalans is a holostylic jaw suspension, whereby the palatoquadrates are fused to the neurocranium and the hyoid arch plays no role in suspending the jaws, instead articulating on an operculum (Didier, 1995) (Fig. 2.4). This condition is also present in numerous stem-holocephalans (Patterson, 1965; Finarelli and Coates, 2014). In elasmobranchs the palatoquadrates are separate from the neurocranium, articulating with some combination of processes and the hyoid arch (Maisey, 2004). This is also the case in Palaeozoic “sharks” such as *Cladodoides* (Maisey, 2005), and acanthodians such as *Acanthodes* (Miles, 1973b), as well as osteichthyans

(Gardiner, 1984) and placoderms (Denison, 1978). There are other examples of fusion of the palatoquadrates and neurocranium in vertebrates - in both dipnoans and in tetrapods. However, this is certainly an evolutionarily distinct occurrence, sometimes distinguished from the holocephalan condition as “autostyly” due to differences in the role of the hyomandibular cite (Wilga, 2002). The holostylic condition has often in the past been used, alongside the position of a durophagous dentition, to place fossil chondrichthyans in the holocephalan stem-group (Janvier, 1996). Various of these groups however - namely iniopterygians (Zangerl and Case, 1973) and eugeneodontids (Janvier, 1996) - have members with a holostylic neurocranium and members without, meaning that the character distribution is unlikely as clear cut as one might like. Despite this it stands as strong evidence of affinity with holocephalans.

Another peculiarity of the lower jaw of holocephalans is probably linked to the overall anterior movement of the visceral arches: the articulation on the articular of the mandible is situated on the extreme posterior of the Meckelian element (Fig. 2.6). This condition is present in living holocephalans (Didier, 1995), as well as in the Palaeozoic taxa *Chondrenchelys* (Finarelli and Coates, 2014), *Helodus* (Patterson, 1965), *Debeerius* (Grogan and Lund, 2000) and iniopterygians (Pradel, 2010). Conversely in elasmobranchs it is situated subterminally on the dorsal edge of the element (eg. hybodonts (Maisey, 1982)). This is also the case in Palaeozoic "sharks" like *Orthacanthus* (Schaeffer, 1981), as well as in acanthodian-grade stem-chondrichthyans (eg. *Acanthodes* (Miles, 1968), *Diplacanthus* in Chapter 4 of this thesis, and *Taemasacanthus* (Long, 1986b)). It also lies in this position in osteichthyans (eg. *Mimipiscis* (Gardiner, 1984)), in placoderms it is situated facing dorsally but in a lower position (Hu et al., 2017). This is sufficient evidence for it to be accepted as a holocephalan character.

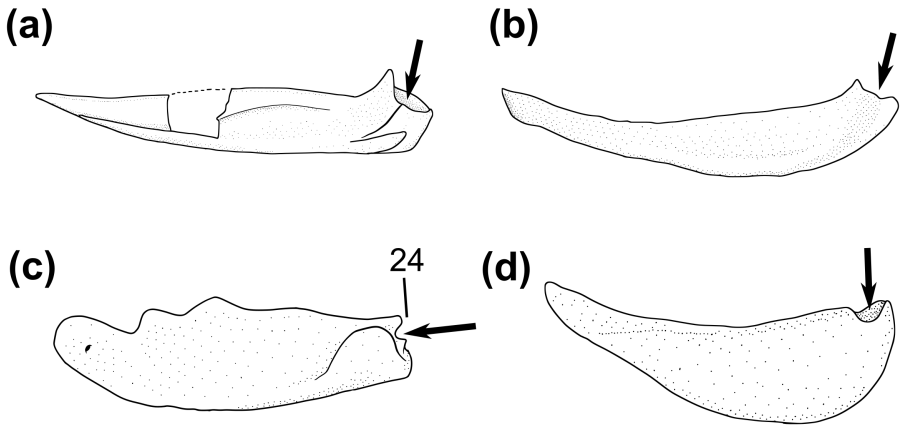


FIGURE 2.6: Meckel's cartilages from selected gnathostomes: (a) The stem-chondrichthyan *Acanthodes*, from Miles (1973b); (b) The Palaeozoic "shark" *Cladodoides*, from Gross (1938); (c) The stem-holocephalan *Iniopera*, from Pradel (2010); (d) The stem-elasmobranch *Homalodontus*, from Mutter et al. (2007). Arrows denote position of articulation with palatoquadrate.

The hyoid arch of holocephalans bears an additional element called the pharyngohyal dorsally to the epihyal (hyomandibular) (Didier, 1995) (Fig. 2.5). This is unlike all other living gnathostomes, in which the hyoid arch terminates at the epihyal (Nelson, 1969). A pharyngohyal is also absent in all known fossil osteichthyans such as *Raynerius* (Giles et al., 2015b), as well as fossil chondrichthyans such as *Ozarcus* (Pradel et al., 2014). *Acanthodes* does have an upper hyoid arch divided into two elements, but these are two ossification centres of the epihyal rather than two separate hyoid bones (Miles, 1973b). However, the Carboniferous chondrichthyan *Debeerius* is described as having a pharyngohyal (Grogan and Lund, 2000). Because of the presumed serial homology of the hyoid arch with the posterior branchial arches, the holocephalan hyoid arch is sometimes described as "morphologically complete" and assumed to represent the primitive state of the hyoid arch (De Beer and Moy-Thomas, 1935; Grogan and Lund, 2000). However,

evidence for this is limited, and it is likely a derived condition (Maisey, 1984). Whichever may be the case it is only known in holocephalans, and may be use as a character in our scheme.

TISSUES — The dentition of living holocephalans takes the form of three pairs of tooth-plates - two upper pairs and a lower pair - which, unlike those of elasmobranchs, are monophyodont (Didier, 1995). These are formed mainly of trabecular dentine, tubules of which become parallel as they approach the surface, similarly to the condition in other durophagous fishes including some rays, sharks, and lungfishes (Patterson, 1965; Didier, 1995). On the oral surface of these tooth plates are found patches of a hypermineralised tissue known as tritors, which wear out of the toothplate during use (Patterson, 1965). These are formed from a tissue known as pleromin, distinguished from enameloid on the basis of it having an exclusively mesenchymal origin. A similar histological set up is found in dipnoans, in which are found tubular dentine with patches of hypermineralised tissue - "pleromin", or "petrodentine". As tubular dentine is found in rays, and there is not a comparable hypermineralised tissue in acanthodian teeth (Burrow et al., 2015) I have omitted any characters based on this.

GIRDLES — Holocephalans are notable for their development of a wide array of cartilages associated with the front of the neurocranium (Patterson, 1965). Labial cartilages in association with the oral cavity are also found in crown- and stem-elasmobranchs (Maisey, 1983), as well as in Palaeozoic chondrichthyans, and possibly acanthodians (Burrow et al., 2015) and stem-gnathostomes (Gross, 1962; Pradel et al., 2009b) but in holocephalans both extinct and extant they are developed to a great extent (Patterson, 1965; Didier, 1995). Holocephalans also have an unpaired rostral cartilage flanked by a pair of lateral rostrals, particularly

impressively in the extant *Rhinochimaera* and the Mesozoic stem-holocephalans *Squaloraja* and *Metopacanthus* (Patterson, 1965), but this is also the case in some elasmobranchs (Patterson, 1965). Both of these assemblages of cartilages are difficult to distill into a distinct character due to the presence of labial cartilages in elasmobranchs (Maisey, 2004).

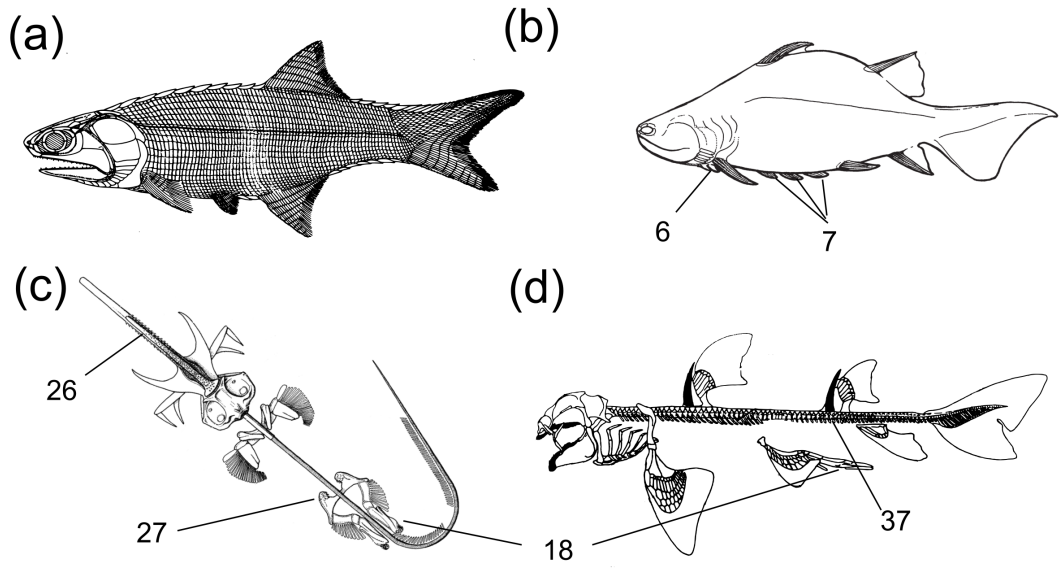


FIGURE 2.7: Bodies of select gnathostomes: (a) The actinopterygian *Mimipiscis*, from Gardiner (1984); (b) The stem-chondrichthyan *Ptomacanthus*, from Brazeau (2012); (c) The stem-holocephalan *Squaloraja*, from Patterson (1965); (d) The crown-elasmobranch *Heterodontus*, from Janvier (1996).

However, also found in holocephalans is a frontal tenaculum, or clasper - an unpaired, and mobile, cartilage ornamented with denticles which articulates on the ethmoid region of males, and thought to be associated somehow with copulation (Didier, 1995) (Fig. 2.4 2.2). Similar unpaired structures are found attached to ethmoid regions of the stem-holocephalans *Squaloraja* (De Beer and Moy-Thomas, 1935; Patterson, 1965), *Metopacanthus* (Patterson, 1965), *Acanthorhina* (Patterson,

1965), and *Traquairichthys* (Lund and Grogan, 2004). Ostensibly similar, but paired, structures are found articulating on ethmoid region of neurocrania of the putative stem-holocephalans *Harpacanthus* (Lund and Grogan, 2004), *Menaspis* (Patterson, 1965) and *Harpagofutator*(Lund, 1982). It is possible that these structures are homologous with extant holocephalans' frontal tenaculae - they articulate with the same region of the braincase, and in the cases of *Harpacanthus* and *Harpagofutator* bear denticles(Lund and Grogan, 2004; Lund, 1982) Because of this, we propose the presence of cartilages articulating on the ethmoid region of the braincase as a character that can place taxa on the holocephalan stem.

In addition to pelvic claspers and a frontal clasper male holocephalans have cartilaginous clasping organs, ornamented with scales, which articulate anteriorly on the pelvic girdle Patterson (1965); Didier (1995) (Fig. 2.7). Similar structures are found on the pelvic girdles of some fossil holocephalans such as *Squaloraja* and *Metopacanthus*, although in the former the cartilage is only an anterior pelvic girdle process and in the latter there is no process, only a patch of enlarged scales (Patterson, 1965). Nonetheless, no similar structures are known in either acanthodians or in elasmobranchs, and enlarged scales associated with the anterior of the pelvic girdle seem to be unique to holocephalans. As this character is extremely restrictive, and difficult to polarise as acanthodians and osteichthyans lack claspers of any any kind, I have chosen to omit it.

Iniopera described by Pradel et al. (2010) has an unpaired cartilage in the ventral part of the shoulder girdle - the intercoracoid element. While in living holocephalans the scapulocoracoids are ventrally fused, (Pradel et al., 2010) note that an unpaired element does exist in the Jurassic holocephalan *Ischyodus*, as well as in other iniopterygians and in the eugeneodontid *Ornithoprion* (Zangerl, 1966). Unpaired cardiobranchial cartilages are also described in the possible Bear Gulch holocephalans *Debeerius* (Grogan and Lund, 2000) and *Harpacanthus* (Lund and

Grogan, 2004), although how closely these are associated with the scapulocoracoids is unclear from the photographs. However, most acanthodians (Miles, 1973a) have paired procoracoids, while the majority of elasmobranchs lack separate coracoid elements, some hexanchiforms (including *Notorynchus*) have an unpaired "sternal" element. This means that the outgroup comparison does not allow the ancestral condition to be safely established.

The sensory canals of living holocephalans are lined by crescent-shaped scales (Didier, 1995). This is also the case in the fossil holocephalan taxa *Squaloraja*, *Myriacanthus*, *Metopacanthus* and *Menaspis* (Patterson, 1965). In elasmobranchs and acanthodians the sensory canals instead pass between the scales, and in osteichthyans they pass through the scales themselves. However, similar ring shaped scales are found in some Mesozoic elasmobranchs such as *Protospinax* (Woodward, 1919; Pradel et al., 2011). Some acanthodiform acanthodians also have similar scales carrying the lateral lines of the head (eg. *Acanthodes* (Zidek, 1976), *Homalacanthus* (Gagnier, 1996)) Because of this I would advocate caution in assuming this character is strictly holocephalan - I have not accepted it as a character.

A few vertebral characters also distinguish holocephalans from elasmobranchs. Posterior to the occiput of Recent holocephalans is a synarcual, upon which the dorsal fin spine and its basal plate articulate - this is also found in a number of stem-holocephalans including *Metopacanthus*, *Myriacanthus* and *Helodus* (Patterson, 1965). Synarcuals are also found in rays, in which they play a part in the expanded pectoral endoskeleton (Patterson, 1965), as well as in placoderms, in which they aid articulation between the head and thorax (Denison, 1978). However they are absent in stem-elasmobranchs (eg. *Hamiltonichthys* (Maisey, 1989a)), as well as in acanthodians (Miles, 1970). Because of the presence in rays I have omitted it as a character.

With the exception of the *Callorhincus* the notochordal sheath of living holocephalans is calcified, forming a series of rings (Didier, 1995; Patterson, 1965). Uniquely these rings are polyspondylous, ie. not organised with body segments. This polyspondyly is also found in the notochordal calcifications of the fossil holocephalan taxa *Squaloraja*, *Myriacanthus*, *Metopacanthus* and *Acanthorhina* (Patterson, 1965). *Chondrenchelys* also has a calcified notochordal sheath, divided into rings, which also appears to be polyspondylous (Finarelli and Coates, 2014). *Helodus* and *Menaspis* apparently have no notochordal calcifications whatsoever (Patterson, 1965). Elasmobranchs and osteichthyans have vertebral calcifications organised with body segments (Janvier, 1996), as it seems do acanthodians (Miles, 1970). Unfortunately it is difficult to confidently diagnose polyspondyly in fossils, unless muscle segments are preserved. It is also difficult to clearly establish an outgroup condition for the notochordal sheath, due to the centrae of elasmobranchs. Because of this I have not accepted either as a character in my scheme.

Despite having two dorsal fins, holocephalans have only one dorsal fin spine, at the level of the pectoral fins (Didier, 1995). Contrastingly, elasmobranchs with fin spines (eg. *Hamiltonichthys*(Maisey, 1989a)) have two dorsal fin spines. The same is true of all known acanthodians-grade stem-chondrichthyans with two dorsal fins (eg. *Parexus*, *Diplacanthus*(Watson, 1937)), as well as *Doliodus* (Maisey et al., 2017). While some acanthodians have only one dorsal fin spine, it is usually well posterior to the pectoral level and highly unlikely to be homologous with the condition in holocephalans (eg.*Acanthodes* (Watson, 1937)). Osteichthyans with dorsal fin spines also have two (Zhu et al., 2009; Choo, 2011). This seems to be a character unique to holocephalans.

2.3.5 **Characters of total group elasmobranchs**

29. Downturned postorbital process
30. Labyrinth projects between otic capsules
31. Isolated posterior semicircular canal
32. Chondrified medial capsular wall
33. Perilymphatic fenestrae
34. Palatoquadrate symphysis
35. Posteriorly directed hypobranchials
36. Constricted vertebral notochord

These morphological characters can place a taxon within the chondrichthyan crown-group, specifically on the elasmobranch stem, that is sharing a more recent common ancestor with crown-elasmobranchs than with crown-holocephalans.

NEUROCRANIUM — A downturned postorbital process with a pronounced anhedral angle has been noted as a possible character uniting some early elasmobranchs (Maisey, 2011; Coates and Tietjen, 2018) (Fig. 2.8). In neurocrania with this morphology the postorbital process turns ventrally relative to the basicranium, forming a pronounced angle with the basicranial floor. An anhedral angle can be clearly seen in the hybodont *Egertonodus* (Maisey, 1983), as well as in the putative stem-chondrichthyans *Acronemus* and *Tristychius* (Maisey, 2011; Coates and Tietjen, 2018). An absent lateral commissure in living chondrichthyans means that they are considered to be inapplicable for this character by (Coates and Tietjen, 2018). Notably however the remaining upper part of the postorbital process in *Notorynchus* does angle ventrally like in fossil taxa with an anhedral angle (Maisey, 2004). In Recent holocephalans an anhedral angle is absent (Coates et al., 2017b).

While Palaeozoic iniopterygians do have orbits that extend ventrally relative to the basicranium the upper orbit is level relative to the roof of the neurocranium (Pradel, 2010). Meanwhile in *Acanthodes* and osteichthyans such as *Mimipiscis* the postorbital processes are level relative to the rest of the braincase (Davis et al., 2012; Gardiner, 1984). Because of this I consider a downturned postorbital processes to be a diagnostic character of elasmobranch neurocrania.

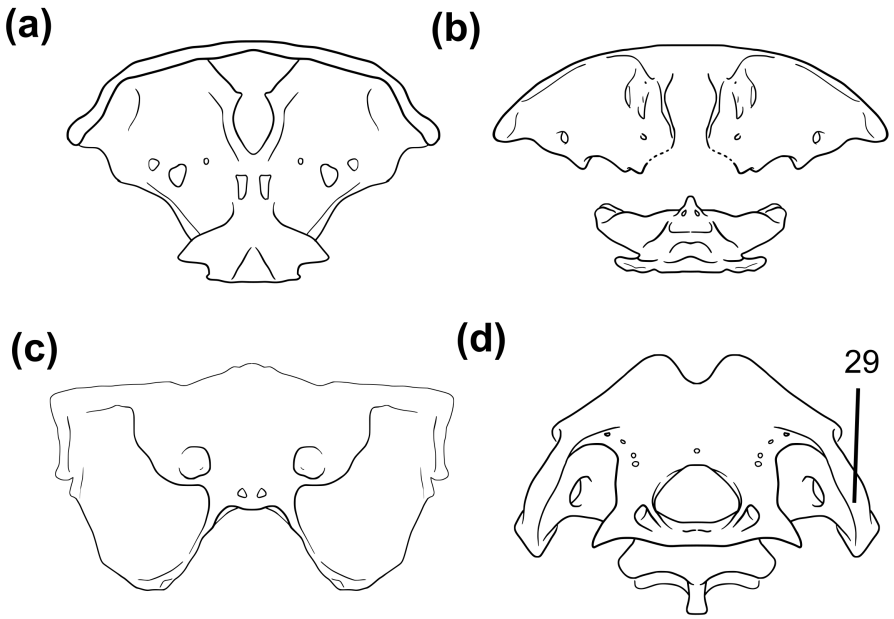


FIGURE 2.8: The neurocrania of select gnathostomes in anterior view: (a) The actinpterygian *Raynerius*, from Giles et al. (2015b); (b) The stem-chondrichthyan *Acanthodes*, from Davis et al. (2012); (c) The stem-holocephalan *Iniopera*, from Pradel (2010); (d) The stem-elasmobranch *Egertonodus*, from Maisey (1983).

Coates and Tietjen (2018) argue that a neurocranial hyomandibular articulation beneath a laterally projecting shelf is another character uniting certain total-group elasmobranchs. This feature is present in hybodonts *Tribodus* and *Egertonodus* (Lane, 2010; Maisey, 1983), as well as in *Acronemus* and *Tristychius* (Maisey, 2011;

Coates and Tietjen, 2018): in these taxa the hyomandibular articulates underneath a lateral projection of the otic shelf. Conversely, in many Palaeozoic "sharks" the hyomandibular articulates on a lateral otic process positioned ventrolaterally to the otic shelf (Schaeffer, 1981). A relatively ventral articulation is also present in stem-chondrichthyan *Acanthodes* (Brazeau and de Winter, 2015), as well as in *Pucapampella*, and *Gladbachus* (Coates et al., 2018; Maisey, 2001a; Brazeau and de Winter, 2015). Unfortunately the lack of a hyomandibular attachment on the braincase of holocephalans makes incomparable for this character. This is also true of osteichthyans and placoderms due to the relatively anterior position of the hyomandibular articulation. Because of this confident polarisation of the character is impossible: while I consider this character likely to be an elasmobranch synapomorphy I have omitted it from my list.

A further neurocranial character cited as a synapomorphy of elasmobranchs is a “bell-shaped” basicranial circuit Schaeffer (1981); Maisey (1984, 1986). This is formed by the lateral dorsal aortae swinging laterally to meet with the efferent hyoidean arteries, and the internal carotids converging almost head on, for example in *Notorynchus* (Maisey, 2004). The bell-shape is in contrast to the "spindle-shaped" arrangement of many extinct chondrichthyans, such as the hybodont *Egertonodus* Maisey (1983). While this does seem to characterise elasmobranchs, this morphology results from a compound set of characters, and decomposes into convergent internal carotids and laterally swinging dorsal aortae. Holocephalans have no basicranial circuit (Didier, 1995), so are incomparable, and it could be argued that head on convergence of internal carotids is found in the acanthodian *Ptomacanthus* (Brazeau, 2009), as well as in placoderms such as *Buchanosteus* (Young, 1979). I have not included this as a character.

The otic capsules in elasmobranchs project anteriorly between the postorbital processes (Coates et al., 2018) (Fig. 2.4). This is visible in living elasmobranchs

such as *Notorynchus* and *Squalus*, where the anterior ampullae lie well forward of the postorbital processes' posterior margins (Maisey, 2004). It is also the case in the hybodont *Egertonodus*, as well as in the putative elasmobranch *Acronemus* (Maisey, 1983, 2011). In Recent holocephalans the anterior ampulla (Coates and Tietjen, 2018) is not located this far forward, and even in iniopterygians in which the orbit is very large the anterior ampulla barely extends between them (Pradel, 2010). *Acanthodes* and osteichthyans also lack this (Davis et al., 2012), giving a clear outgroup condition, so I have accepted it..

The posterior semicircular canal of elasmobranchs is unique amongst vertebrates in that it forms an almost complete loop in isolation from the anterior and exterior canals, and which enters the vestibular region via a single opening (Maisey, 2001b; Maisey and Lane, 2010) (Fig. 2.4). Furthermore a *crus* is present between the anterior and external canals, the saccular and utricular regions are separated, and the *crista neglecta* is enlarged (Maisey, 2001b). This contrasts with the anatomy of holocephalans and osteichthyans in which the posterior semicircular canal meets with the anterior semicircular canal at the *crus commune* (Maisey, 2001b). *Acanthodes* shares the osteichthyan/holocephalan condition (Miles, 1973b; Davis et al., 2012). A whole suite of additional characters have been drawn from the highly specialised elasmobranch inner ear (Maisey, 2001b; Maisey and Lane, 2010). However, many of these are linked to the isolation of the posterior canal (eg. a single opening into the vestibular region), and still others are difficult to detect even in material from extant chondrichthyans (eg. a *crus* between the anterior and posterior canals) (Maisey, 2001b). The isolation of the posterior semicircular canal seems to be the most obvious and easily detectable character in fossils, although I acknowledge that it is part of a wider apomorphic suite of morphologies.

The otic capsule in elasmobranchs is completely separated from the endocranial space by a heavily chondrified medial capsular wall (Maisey, 2001b): this is apparent

in living chondrichthyans such as *Notorynchus* (Maisey, 2004). In holocephalans and osteichthyans this wall is membranous (Maisey, 2001b), and is not preserved in fossil osteichthyans such as *Mimipiscis* or *Moythomasia* (Gardiner, 1984), nor in the acanthodian *Acanthodes* (Davis et al., 2012). While a medial capsular wall is present in stem-gnathostomes such as *Macropetalichthys* (Stensiö, 1925a) it is likely derived in chondrichthyans due to its absence in early chondrichthyan taxa like *Pucapampella* (Maisey and Anderson, 2001; Maisey, 2001a) and *Cladodoides* (Maisey, 2005), as well as in the two successive outgroups to elasmobranchs - *Acanthodes* and holocephalans (Maisey, 2001b). It satisfies criteria to be accepted as an elasmobranch character.

Uniquely amongst vertebrates elasmobranchs have perilymphatic fenestrae: a pair of openings extending from the posterior semicircular canals onto the roof of the neurocranium, separately from the endolymphatic ducts (Maisey and Lane, 2010). As well as being present in living elasmobranchs, these have been identified in hybodonts *Tribodus* and *Egertonodus* (Maisey and Lane, 2010), as well as *Tristychius* and *Acronemus* (Dick, 1978; Coates and Tietjen, 2018; Maisey, 2011). They are absent in living holocephalans, as well as extinct members of the group (Coates et al., 2018). They are also absent in osteichthyans (eg. *Mimipiscis* (Gardiner, 1984)); while their absence in *Acanthodes* is equivocal they seem unlikely to be present given the arrangement of the endolymphatic region. I have accepted this as a character.

The occipital region of the elasmobranch braincase is distinctively wedged between the otic capsules, which has been proposed as an elasmobranch synapomorphy (Schaeffer, 1981; Maisey, 1986, 1984, 2001b). A range of extinct taxa share this state to some extent, including hybodonts (Maisey, 1983), xenacanths (Schaeffer, 1981), and *Cladodoides* (Maisey, 2005). However, it also seems to some extent to be present in holocephalans (see (Allis, 1926; Coates et al., 2017a)) A more restrictive sense of this character identified in recent phylogenetic analyses has been

the wedging only of the dorsal part of the occipital between the otic capsules (eg. (Coates et al., 2017a, 2018)). This appears only in elasmobranchs (Maisey, 1983), as well as some Palaeozoic sharks (eg.xenacanths (Schaeffer, 1981), and *Cladodoides*). However, as this character varies by degrees the degree of wedging in taxa like *Acanthodes* is difficult to judge, so I have not accepted it as a character, although it may be an elasmobranch synapomorphy. Because of this I have not accepted it here as a character.

VISCERAL ARCHES — In elasmobranchs the palatoquadrates meet and are fused, and carry a continuous dental arcade. A continuous dental arcade seems to be plesiomorphic for chondrichthyans (Maisey, 1980), being present in the early chondrichthyan *Doliodus* (Maisey et al., 2009), the xenacanth *Triodus* (Maisey et al., 2014) as well as in the acanthodian *Ptomacanthus* (Brazeau, 2009). However, an actual symphysis between the palatoquadrates is unique to elasmobranchs. While extant holocephalans are holostylic, with their palatoquadrates fused to the neurocranium, the possible Carboniferous holocephalan *Debeerius* has separate palatoquadrates which are separated by the ethmoid region (Grogan and Lund, 2000). This separation is also apparent in osteichthyans (Gardiner, 1984), as well as many extinct chondrichthyans, for example *Xenacanthus* (Schaeffer, 1981). Although Jarvik (1980) argued that *Ptomacanthus* also possessed this symphysis, there is no evidence for it in the fossil (Brazeau, 2009), and it is also lacking in *Acanthodes* (Miles, 1968, 1973b).

The gill skeleton of modern elasmobranchs are unique in that most of the ventralmost paired gill-arch elements, the hypobranchials, are directed posteriorly (Pradel et al., 2014; Nelson, 1969; Maisey, 1984) (Fig. 2.5). In holocephalans, as well as in osteichthyans, the hypobranchials are instead all directed anteriorly (Nelson, 1969). There is no evidence for posterior direction in *Acanthodes* (Miles, 1973b),

or in the Palaeozoic "sharks" *Gladbachus* (Coates et al., 2018) or *Ozarcus* ((Pradel et al., 2014)). In osteichthyans the hypobranchials are also anteriorly directed, both in actinopterygians(Giles et al., 2015b) and in sarcopterygians (Jarvik, 1972) This character is a clear apomorphy of elasmobranchs.

In the teeth of elasmobranchs a triple-layered tooth enameloid has been cited as an elasmobranch dental synapomorphy. This enameloid has been divided into three tissues: shiny layered enameloid (SLE), tangled bundled enameloid (TBE) and Parallel bundled enameloid (PBE) Gillis and Donoghue (2007); Enault et al. (2015). Enault *et al.* Enault et al. (2015) recently split these tissues into two groups: Gillis and Donoghue's Gillis and Donoghue (2007) single crystallite enameloid (SCE), comprising the SLE, and bundled crystallite enameloid (BCE), comprising the TBE, PBE, and radial bundled enameloid (RBE). SCE likely forms the plesiomorphic state of chondrichthyan enameloid being present in a wide range of "shark-like" fossil taxa. The latter BCE may thus be autapomorphous for elasmobranchs Cuny et al. (2009): while Recent holocephalans lack enameloid Didier (1995), its presence in the toothplates of the stem-holocephalan *Helodus* demonstrates that SCE has existed in the clade Gillis and Donoghue (2007). Unfortunately acanthodians lack enameloid in their teeth entirely Ørvig (1973) meaning that they cannot be used as a point of comparison, and the homology of chondrichthyan and osteichthyan enamel/enameloid Donoghue et al. (2006) is a matter of debate: it is entirely absent from the teeth of the putative stem-osteichthyans *Psarolepis*, *Andreolepis*, and *Lophosteus*. Qu et al. (2015b). As such it does not meet the necessary criteria for outgroup comparison, and is rejected as a diagnostic character.

POSTCRANIAL — Elasmobranchs have calcified vertebral centrae, with a constricted notochord (Maisey, 1984, 1986) (Fig. 2.7). As well as in living elasmobranchs this is also present in the extinct *Palaeospinax* and *Synechodus*

(Maisey, 1977) Contrastingly the vertebrae of holocephalans lack centrae Didier (1995); Patterson (1965). The same is true of the several known acanthodian vertebral columns (Miles, 1970) (also see Chapter 4 of this thesis). Calcified vertebral centrae are present in both teleosts and in tetrapods (Janvier, 1996). However, their absence in two outgroups allows me to include it in my character scheme.

2.4 ASSESSMENT OF FOSSIL TAXA

2.4.1 **Possible total-group chondrichthyans**

The two earliest occurring scale based taxa identified as belonging to the acanthodian grade are *Tchunacanthus* and *Lenacanthus*, from the Lower Silurian of Siberia (Karatajūtė-Talimaa and Smith, 2003). Both *Tchunacanthus* and *Lenacanthus* have scale crowns which exhibit symmetrical superpositional growth, ie. odontodes are added in the sagittal plane (Karatajūtė-Talimaa and Smith, 2003). Areal growth is also present, for example a scale of *Lenacanthus* in which odontodes are added laterally to a primordial odontode (Karatajūtė-Talimaa and Smith (2003), Fig. 8c). Because of this I agree that these scales can be placed in the chondrichthyan total group with reasonable confidence. Their shape and mode of growth is consistent with that of other acanthodian grade stem-chondrichthyan scales (Valiukevičius, 2004).

Elegestolepids are a collection of taxa known from monodontode scales from throughout the Silurian and into the Early Devonian, including the eponymous *Elegestolepis*, *Kannathalepis*, *Deltalepis*, and *Ellesmeria* (Andreev et al., 2017; Karatajūtė-talimaa, 1973; Märss and Gagnier, 2001). They comprise a monodontode crown, attached to a bony base - unusually both crown and base were growing (Andreev et al., 2017). Elegestolepid scales are considered chondrichthyan on the basis of their neck canals, as well as their lack of an osteonal middle layer. Notably some

specimens of *Kannathalepis* do exhibit several odontodes fused together, although Andreev et al. (2017) consider these to be aberrant fusions of scales, rather than polyodontody, as they do not share a base. By my scheme, this is insufficient evidence with which to place elegestolepids in the chondrichthyan total group. The only other group with growing odontodes is the thelodonts (Andreev et al., 2017; Märss et al., 2007), and that while elegestolepis could be chondrichthyan they are just as likely to be a hitherto unknown stem-gnathostome with neck canals in a monodontode scale.

Several other monodontode scales are known from Silurian strata, excluded by Andreev et al. (2017) from the elegestolepids on the basis of their non-growing odontodes. *Frigorilepis* is outwardly similar to *Kannathalepis*, and is known from articulated patches of squamation (Märss et al., 2002, 2006). *Wellingtonella* is from the same site (Märss et al., 2002, 2006), and is similar in morphology. *Pilolepis*, a genus based on isolated scales and a spine and identified as a bradydont by Thorsteinsson (1973) also lacks any clearly chondrichthyan growth characters. None of these scales have sufficient characters to be safely considered chondrichthyan.

Mongolepids are a variety of putatively chondrichthyan scale types sharing polyodontode scale crowns with an unusual atubular dentine ("lamellin") (Andreev et al., 2016; Karatajūtė-Talimaa, 1995). Originally they were erected on the basis of isolated scales from the Lower Silurian of Mongolia (Karatajūtė-Talimaa, 1995), but since then have been found more widely, with the earliest putative mongolepid being *Solinalepis* from the Harding Sandstone (Andreev et al., 2016). The Silurian mongolepids have odontodes organised in the sagittal plane, providing evidence of their being chondrichthyan. However, rather than growing by the addition of odontodes mongolepids instead grow with the addition of odontodes posteriorly in parallel lines (Andreev et al., 2016). This mode of scale growth is not the same as the mode which I have identified as a chondrichthyan character, where odontodes are

placed on top or infront of the preceding odontode. While mongolepids do appear to have symmetrical lateral addition of odontodes, they are added in an offset manner, rather than laterally as in chondrichthyans. Other characters "uniting" mongolepids with chondrichthyans are found in other parts of the gnathostome total group. Mongolepids could be considered chondrichthyan on the basis of their lateral odontode addition. However, I would advocate some caution in a confident diagnosis, as they lack the seemingly more inclusive symmetrical superposition of odontodes.

In addition to *Solinalepis* other scales are known from the Ordovician Harding Sandstone which have been identified as chondrichthyan (Andreev et al., 2015; Smith and Sansom, 1997). *Skiichthys* is a poorly understood scale without a confident assignation Smith and Sansom (1997)- it lacks any clearly chondrichthyan characters. *Tezakia* and *Canyonlepis* both have laterally growing odontodes and could be chondrichthyan - however notably these are also offset from the central odontode, like those of mongolepids. However, as with mongolepids they lack the symmetrical superposition of odontodes that appears to be a more inclusive chondrichthyan character. As with mongolepids these taxa could be chondrichthyans, but I would advocate caution in a confident diagnosis.

Tantalepis is the oldest putative chondrichthyan scale, from the Middle Ordovician of central Australia (Sansom et al., 2012). It comprises isolated scales, which outwardly appear to be polyodontode on the basis of possibly several ventrally opening canals and an ornament of several ridges. If so the lateral position of the odontodes would be similar to that of chondrichthyans. However, the scales are far from confidently identifiable as polyodontode- placoid elasmobranch scales commonly have an ornament of multiple ridges (eg. in Maisey (1977) I would advocate caution in diagnosing *Tantalepis* chondrichthyan.

While not an isolated scale, this review provides a chance to reassess the scales of the probable stem-chondrichhtyan *Gladbachus*. When originally described, the scales of *Gladbachus* were framed as being "placoderm-like", with bulging bases, and an areally growing crown (Burrow and Turner, 2013). However these scales appear to come from the head region, and in fact appear fairly similar to "acanthodian" head tesserae in that they lack an osteonal middle layer, and are formed from cellular bone and dentine (Coates et al., 2018). The main distinction from tesserae is their bulging base, which as discussed above appears to be quite a labile character. Meanwhile body scales in *Gladbachus* have a central row of odontodes with anterioposteriorly aligned crowns, which could conceivably be growing in a similar way to other chondrichthyan scales (Coates et al. (2018) Supp. Fig. 3d). While *Gladbachus* has an unusual scale morphology for a chondrichthyan, I would argue that in terms of individual character states it fits into the known range of chondrichthyan scale types.

2.4.2 **Problematic crown-group chondrichthyans**

These characters also provide an opportunity to reassess the characters of various problematic Palaeozoic sharks.

Symmoriiforms are a putative grouping of various Palaeozoic "sharks" nominally split into stethacanthids and symmoriids - on the basis of the presence and absence respectively of large dermal dorsal fin ornament. However, the almost identical endoskeletons in these two groups suggests that in at least some cases this split might be artificial and based on sexual dimorphism (Maisey, 2009) - this is clearly the case in at least *Falcatus* in which male and female forms co-occur (Lund, 1985). Coates et al. (2017a) convincingly argued that on symmoriiform *Dwykaselachus* is a stem-holocephalan on the basis of its neurocranial morphology: it demonstrates an elevated mesencephalon, medially constrained superficial

ophthalmic nerves, and an endolymphatic duct that opens anteriorly relative to the *crus commune*. A caveat is that there is no postcranial material associated with *Dwykaselachus*. I consider that symmoriiforms are likely stem-holocephalans as argued by Coates et al. (2017a).

Cladoselache has an iconic status as "the" Devonian shark - however its relationships within the chondrichthyans remain opaque. Coates et al. (2017a) recovered it as a stem-holocephalan, placed with the symmoriiforms. Although the skull of *Cladoselache* is broadly symmoriiform-like, it lacks any clear cut holocephalan apomorphies. Postcranially, *Cladoselache* shares several similarities with edestids, a poorly known group of sharks which have been associated with holocephalans (Zangerl, 1981; Janvier, 1996), but which also lack clear holocephalan characters (except possibly for some taxa being holostylic (Zangerl, 1981)). The similarities between edestids and *Cladoselache* include plate-like caudal supraneurals and the organisation of the pectoral fin. On this basis I consider it quite likely that *Cladoselache* and edestids are stem-group holocephalans, however there are no clearly polarised characters uniting it with them.

Cladodoides is a Palaeozoic shark comprising an extremely well-preserved neurocranium, with associated visceral arches Maisey (2005); Gross (1937, 1938). It clearly qualifies as a chondrichthyan, but beyond that is uncertain - Coates et al. (2017a) recover it as a stem-group elasmobranch. The main elasmobranch-like character that *Cladodoides* displays is a dorsal wedging of the occiput between the otic capsules However, I as I discussed above, I consider this character dubious. Beyond this, *Cladodoides* lacks any clear elasmobranch synapomorphies as detailed here. Becasue this character can vary by degrees I am wary of definitively agreeing that *Cladoselache* lies in the elasmobranch crown-group.

Xenacanths and ctenacanths are two "groups" of Palaeozoic-Mesozoic chondrichthyan. Neurocrania from both groups are well known on the basis of grinding series (Schaeffer, 1981) and their postcrania are fairly well known too. Coates et al. (2018) recover both groups as stem-elasmobranchs. As in *Cladodoides* only clear elasmobranch-like character that *Cladodoides* displays is a dorsal wedging of the occiput between the otic capsules However they have none of the clear elasmobranch characters I list, and I would be cautious of placing them in the crown-group.

Acronemus* and *Tristychius are two Palaeozoic/Mesozoic taxa associated with hybodonts and elasmobranchs Coates and Tietjen (2018) argue that both taxa are stem-group elasmobranchs on the basis of several characters. Several of these characters have been adopted into my list, and *Acronemus* and *Tristychius* show several elasmobranch characters that can be confidently polarised. These include a downturned postorbital process, , the projection of the labyrinth between the otic capsules, a chondrified medial capsular wall, an isolated posterior semicircular canal, and perilymphatic fenestrae. On the basis of these character, I agree with Coates et al. (2018) that these taxa are stem-group elasmobranchs.

2.4.3 Further discussion

Individually, all characters of "placoid scales" used to identify scales as chondrichthyan are inadequate to do so. Characters of scale shape vary widely amongst gnathostomes, and neck canals are widespread throughout gnathostome phylogeny. Basal openings of the pulp cavity and the loss of an osteonal middle layer are possibly chondrichthyan apomorphies within the gnathostome crown-group; however due to homoplasy in stem-gnathostomes they are useless for identifying scales in isolate. Because of this the only chondrichthyan characters I have identified

are of growing, polyodontode scales.

An obvious problem resulting from this is with the identification of putatively chondrichhtyan monodontode scales. Nothing precludes some early chondrichthyan scales from being monodontode- indeed, at an early enough ontogenetic stage all polyodontode scales are presumably monodontode. However, there are no characters which can identify monodontode scales as being definitively chondrichthyan. While monodontode Early Palaeozoic scales may be chondrichthyan, they could equally well have belonged to stem-gnathostomes unknown from articulated remains. This is not unlikely given the low chances for a micromeric taxon with no mineralised internal skeleton to fossilise in articulation.

One possible solution to this would be collecting data on comparative dermal data in articulated Palaeozoic chondrichthyan fossils. While the lack of endoskeletal data in stem-chondrichthyans is often bemoaned (for example, in the Introduction to this thesis), data on the dermal skeletons of chondrichthyans with preserved endoskeleton is equally sorely needed Brazeau and Friedman (2014), and should be substantially easier to collect. As the unusual morphology of scales in *Gladbachus* shows, an effort like this might reveal hitherto unexpected diversity which may shed light on some isolated "chondrichthyan" remains. Many articulated Palaeozoic chondrichthyans would be key target animals for such efforts. This includes taxa lacking definitive crown-chondrichthyan characters, but which have "ctenacanthid" scales, such as *Tamiobatis* (Williams, 1998), *Diplodoselache* (Dick, 1981), and *Doliodus* (Miller et al., 2003). These animals remain likely candidates for being relatively crownwards stem-chondrichtyans, or as early crown-group members, and proper description of their scales might reveal more characters with which to test phylogenetic relationships within articulated animals, and with isolated "chondrichthyan" scales. It would also be worth better characterising scales in articulated early crown-group members, such as stem-holocephalans

and stem-elasmobranchs, many of which are monodontode (eg. *Akmonistion*, *Tristychius* Coates and Sequeira (2001a); Dick (1978)). This data would complement an ever-growing body of information on the scales of acanthodian-grade stem-chondrichthyans (eg. Burrow et al. (2016a)).

2.5 CONCLUSION

Here I review characters that can be used to identify taxa as total-group and crown-group chondrichthyans, as well as characters of chondrichthyan scales. *Tchunacanthus* and *Lenacanthus* are the earliest isolated scale taxa I would confidently identify as chondrichthyan, placing an upper bound to chondrichthyan-osteichthyan divergence in the Lower Silurian. Symmoriiforms appear likely to be stem-group holocephalans (Coates et al., 2017a), and *Acronemus* and *Tristychius* appear likely to be stem-group elasmobranchs (Coates and Tietjen, 2018). I have found no clear evidence that some shark-like taxa - xenacanths, ctenacanths, and *Cladodoides* - lie in the chondrichthyan crown-group. Describing the scales of these animals would likely provide important data to weigh as evidence in this matter.

CHAPTER 3

THE VISCERAL SKELETON OF THE STEM-CHONDRICHTHYAN *Ptomacanthus*

3.1 INTRODUCTION

The network of endoskeletal elements that support the gills in gnathostomes are functionally essential to feeding and respiration, and have played a critical part in hypotheses of the evolution of jaws and paired fins (Gegenbaur, 1878; Mallatt, 1996; Gillis et al., 2009, 2013) (Gegenbaur, 1878). The diversity of these elements' shape and arrangement further provides a rich resource for comparative morphology, with fundamental differences distinguishing the two crown-gnathostome clades (Pradel et al., 2014). These comprise numerous differences in the pattern of individual gill elements, as well in the position of the gill skeleton with respect to the posterior boundary of the braincase (Nelson, 1969). Without access to readily comparable outgroups (Mallatt, 1996) or fossil taxa showing intermediate conditions, many aspects of the ancestral gnathostome gill skeleton are impossible to infer from extant taxa alone. Nevertheless, it is not uncommon for comparative analyses based on living taxa to presuppose that modern chondrichthyan anatomical conditions are a model of ancestral conditions (Mallatt, 1996; Gillis et al., 2009; Carvalho et al., 2013). In spite of this, it is generally well understood that these propositions may not be phylogenetically sound, and paleontological studies are beginning to overturn many aspects of the shark-like model for early gnathostome morphology (Zhu et al., 2013; Giles et al., 2015c).

Fossils of early chondrichthyan endoskeletons might help resolve the question of primitive pharyngeal pattern characters in gnathostomes. However, until recently, well-preserved fossils of chondrichthyan pharyngeal skeletons from early in the group's history have been largely unknown, owing to poor fossilization potential of their cartilaginous structure. The gill skeleton of *Acanthodes* has long been central to this question, but there has been reciprocal ambiguity over the correct life reconstruction of its components and the phylogenetic relationships of the taxon itself (Miles, 1973b; Rosen et al., 1981; Watson, 1937; Nelson, 1968). Recent discoveries aided by X-ray computed microtomography have revealed important new data points from definitive Paleozoic chondrichthyans *Ozarcus* and *Gladbachus* (Pradel et al., 2014; Coates et al., 2018). *Ozarcus* has a strikingly osteichthyan gill skeleton (Pradel et al., 2014), however phylogenetic ambiguity limits its use as a proxy for stem-chondrichthyan conditions, as it may instead be a stem-holocephalan (Coates et al., 2018). Meanwhile *Gladbachus*, a more likely stem-group candidate, is limited by a branchial skeleton that already shows many crown-group states (Coates et al., 2018). Thus use of these known fossils is limited.

In addition to the patterning of elements, a major difference in the gill skeleton of gnathostomes is in its position relative to the neurocranium, which displays two markedly contrasting conditions. In osteichthyans and holocephalans the pharynx is compact, situated below the braincase, and is covered by an external opercular valve with a single main opening, Contrastingly the pharynx of sharks is caudally extended, situated behind the neurocranium, and opens in a row of external slits. A key argument of many past analyses of the evolution of the pharynx is that the "elasmobranch" condition is plesiomorphic for gnathostomes, on the basis of the perceived primitiveness of chondrichthyans as well as its apparent similarity to the condition in cyclostome outgroups (Mallatt, 1996; Gillis et al., 2009; Carvalho et al., 2013). However, comparison with the compact, subcranial, osteichthyan-like pharynx in stem-gnathostomes suggests this is unlikely. Conditions in the

chondrichthyan stem-group, which could arbitrate on this disagreement, have remained indecisive. Extinct chondrichthyans in which the gill skeleton is well known, such as *Gladbachus* and *Ozarcus*, display conditions identical to living chondrichthyans, with a posteriorly placed, caudally extended, non-operculate pharynx (Coates and Tietjen, 2018; Pradel et al., 2014). *Acanthodes* also appears to have a caudally extended pharynx like chondrichthyans (Miles, 1973b). Thus the evolution of this character is difficult to delimit to a particular part of the chondrichthyan stem-group.

Here I considerably expand the record of early gnathostome branchial morphologies by describing the pharyngeal skeleton of *Ptomacanthus anglicus* Miles (1973a), an acanthodian-grade stem-chondrichthyan from the Lochkovian (419.2-410.8 Mya) of Herefordshire, UK. *Ptomacanthus* displays the earliest three-dimensionally articulated branchial skeleton known in a gnathostome. This supplies a unique and sorely needed point of reference with which to interpret those early chondrichthyan branchial skeletons we already have, and more broadly to reconstruct the ancestral condition of the branchial skeleton in gnathostomes.

3.2 MATERIALS AND METHODS

3.2.1 **Specimen**

The specimen I used in this study is *Ptomacanthus anglicus* (Miles, 1973a) NHM specimen P.24919a, comprising the anatomically ventral half of a siltstone concretion containing the head and pharynx of a fish. This specimen has been previously described by Miles (1973a) and Brazeau (2009, 2012). The part has been etched using hydrochloric acid, leaving moulds of parts of the endoskeleton on the surface (Miles, 1973a). An x-ray of the specimen revealed that the concretion held additional

skeletal material within, leading to this study.

3.2.2 **Geological context**

P.24919a was originally collected from a siltstone lenticle in Wayne Herbert Quarry, Herefordshire, UK (Miles, 1973a; White, 1935). This locality is interpreted as having been fluvial on the the basis of isotopic and sedimentological evidence (Schmitz et al., 1991; Allen and Tarlo, 1963). In addition to further specimens of *P. anglicus* Wayne Herbert has yielded a number of other articulated acanthodians, as well as articulated osteostracans and heterostracans, and pieces of articulated thelodont (Miles, 1973a; White, 1935). The site lies within the *Rhinopteraspis crouchi* zone, and so is Lochkovian in age (419.2-410.8Mya) (White, 1935).

3.2.3 **Micro computed-tomography scanning**

P.24919a was scanned using a Nikon XT H 225 ST at 224kV and 240μA, with a 39μm voxel size. Data were segmented with Mimics v.18 (biomedical.materialise.com/mimics; Materialise, Leuven, Belgium). Segmented models were then imported into Blender (blender.org) to acquire images.

3.2.4 **Phylogenetic analysis**

Both parsimony and Bayesian analyses were run, on a matrix of 88 taxa and 267 characters. This matrix was adapted from Coates et al. (2018) with the addition of information on the branchial skeleton of *Ptomacanthus*, a reworking of characters related to the branchial skeleton, and the addition of two taxa - *Paraplesiobatis* and *Euthacanthus*. Details of these modifications are available in Appendix A.

The parsimony analysis was run in tnt 1.5 Goloboff and Catalano (2016) using a parsimony ratchet with 10,000 iterations, holding 100 trees each iteration, and using TBR branch swapping. Galeaspida was set as an outgroup and the constraint (Galeaspida (Osteostraci (Mandibulate gnathostomes))) was enforced.

The Bayesian analysis was run in MrBayes v. 3.2.6. Mandibulate gnathostomes were constrained as monophyletic and Galeaspida were set as the outgroup. I then carried out the search for 10,000,000 generations, sampling a tree every 1,000 generations, and calculated a majority rule consensus tree with a relative burnin of 25%.

3.3 RESULTS

3.3.1 **Visceral morphology in *Ptomacanthus***

Almost the entire visceral skeleton of *Ptomacanthus* is preserved: Meckel's cartilages, the hyoid arch, and five branchial arches on either side (Fig.3.1, 3.2, 3.3). The specimen preserves some information on the mandibular arch. Meckel's cartilages are visible overlapping slightly at the front of the specimen (Fig. 3.1), although their exact shape is difficult to determine due to interference in the tomograms from the underlying gular squamation. There is no evidence for their ossification in two parts as described by Miles (1973a) supporting the argument of Brazeau (2009) that this effect is created in NHM P.19999 by a stump of matrix. Both ventral tooth rows are preserved within the matrix, having become tipped and partially dissociated from the cartilage to varying degrees; these extend for at least half of the length of the mandible, diminishing in size posteriorly (Fig. 3.1).

Posteriorly to Meckel's cartilages lie paired ceratohyals - two elements that are probably hyomandibulae are preserved in articulation with them, although

another plausible interpretation would be that these are the posterior parts of the palatoquadrates, (Fig.3.1, 3.2, 3.3). In the latter interpretation the hyomandibulae could be represented by some flattened material anterior to the epibranchials. The ceratohyals' boundary with the posterior border of the Meckel's cartilages is difficult to see clearly, but from their narrow articulation with the epihyal they broaden to meet the anterior corners of the basihyal (Fig. 3.1 b,d). A discontinuity in the dorsal surface of the right ceratohyal is likely taphonomic - the globular calcified cartilage below it is continuous, the element is entirely aligned on either side of the discontinuity, and there is no corresponding break in the left ceratohyal. This confirms the absence of hypohyals. Between the ceratohyals of *Ptomacanthus* lies a trapezoidal, flattened basihyal (Fig. 3.1, 3.2a). Unlike most of the rest of the pharyngeal skeleton this is preserved largely as what I infer to be globular calcified cartilage (Figs. 3.1b,d, 3.4). No clear surface features, articulatory or otherwise, are visible; if they ever were present they were likely lost due to incomplete mineralisation or flattening. The anterior corners of the basihyal are closely associated with the ceratohyals, overlying the tip of the left ceratohyals, and lying laterally to the right. This suggests that it lay dorsal to the ceratohyals in life as in chondrichthyans (Pradel et al., 2014), although the specimen's flattening makes its exact life position difficult to determine. Posteriorly this basihyal lies next to, and presumably also articulated with, the anteriormost branchial arch (Fig. 3.1, 3.2a). There is no evidence for unpaired or paired medial mineralisations posterior to the basihyal. However, a broad space between the ventral paired elements of the gill skeleton leaves the possibility open that these were once present, but not preserved in the fossil.

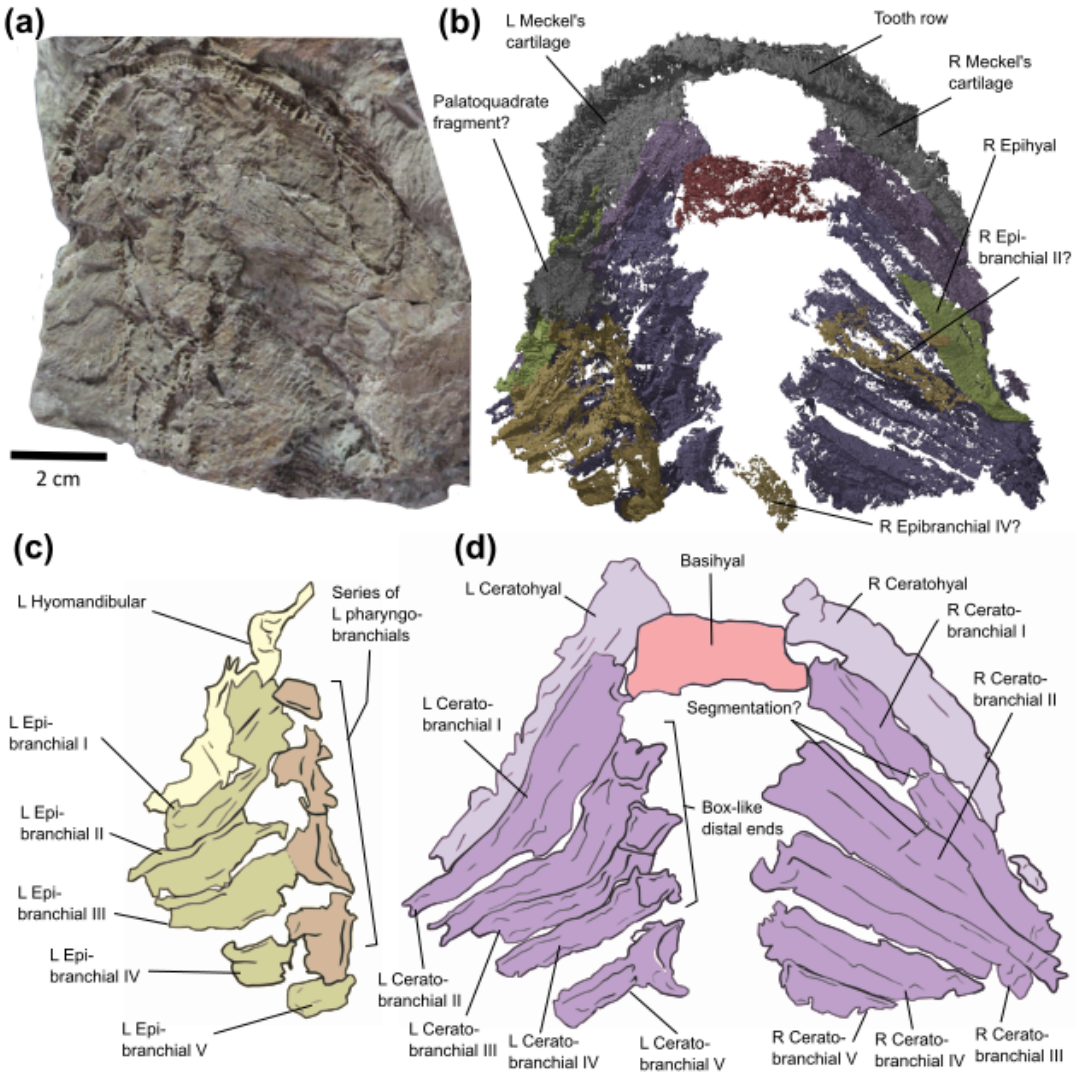


FIGURE 3.1: (a) Photograph of NHM P.24919a scale bar 20mm; (b) Virtual rendering of pharyngeal skeleton; (c) Drawing of dorsal branchial skeleton from the anatomical left hand side; (d) Drawing of ventral branchial skeleton. Colour scheme: *red*, basihyal/branchial; *turquoise*, hypobranchial; *purple*, ceratohyal/branchial; *yellow*, epihyal/branchial; *orange*, pharyngohyal/branchial. Lighter shades denote hyoid arch,

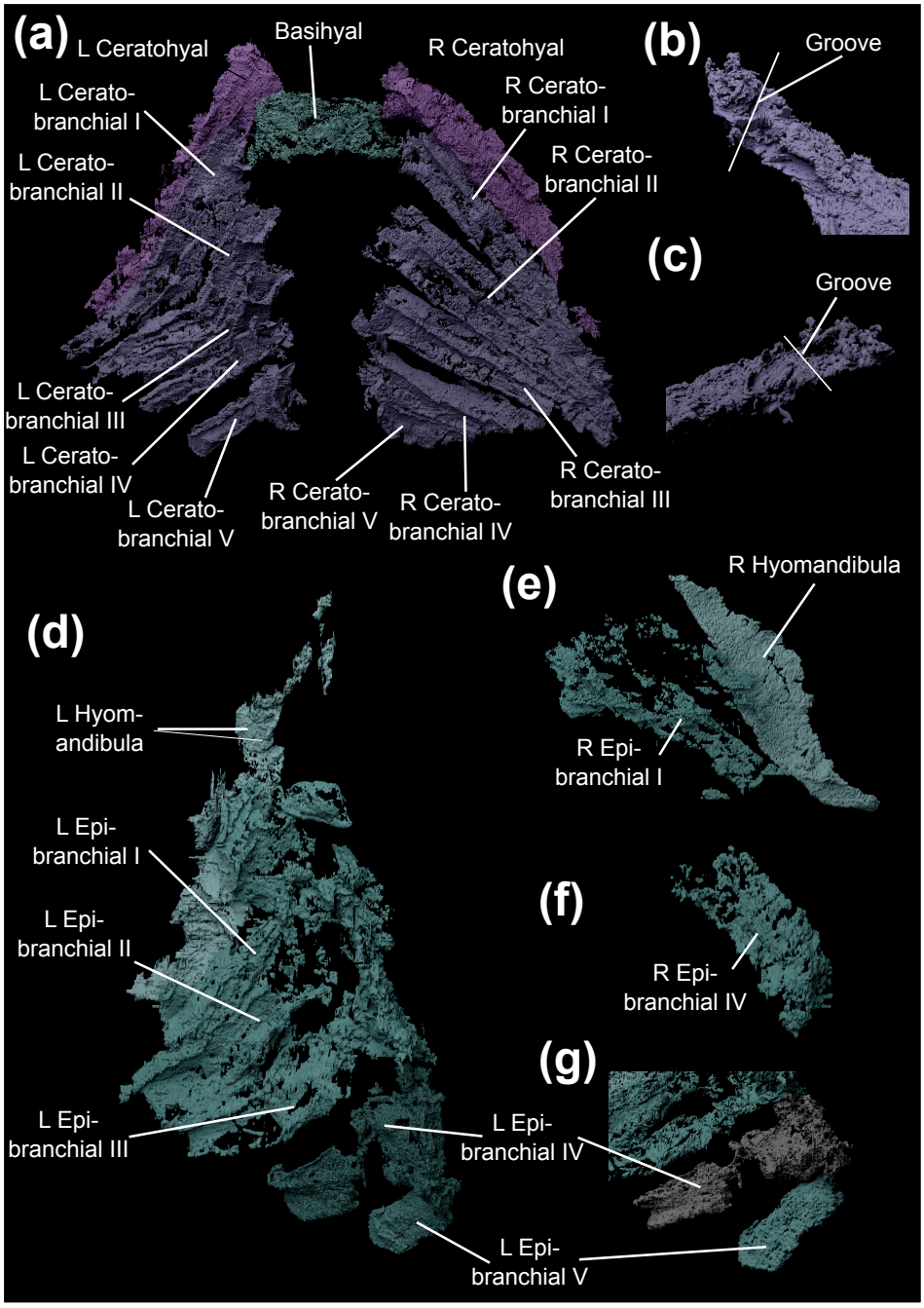


FIGURE 3.2: Caption on next page

FIGURE 3.2: (a) Dorsal view of the ventral branchial skeleton, with the groove in right ceratobranchial II shown (line runs approximately through groove) in (b) dorsal and (c) posterior aspect, (d) Dorsal view of the left hand dorsal branchial skeleton, with views of (e) the right hand anterior dorsal skeleton, (f) displaced fourth epibranchial, and (g) the junction between the fourth and fifth left epi- and pharyngobranchials.

The branchial skeleton is positioned ventrally relative to the neurocranium; only the two posteriormost dorsal arches lie posterior to the occiput (Fig.3.3). Posterior to the Meckelian cartilages are the first pair of epibranchials, with corresponding pharyngobranchials - these lie at approximately the anterior extent of the parachordal plates. Posteriorly to these the morphology of the dorsal branchial skeleton can be seen mainly on the anatomical left hand side.

The frontmost arches, including the first, are extremely crushed and difficult to distinguish from one another, particularly distally, but posteriorly the elements three-dimensional nature can be seen more clearly(Fig. 3.1, 3.2d). Each element is posteriorly grooved, and curves ventrally to meet its corresponding ceratobranchial - no posterior flange is visible (Coates et al., 2018), although its presence could have been obscured by flattening. The distal ends of the elements are expanded and appear to link antero-posteriorly - I interpret these as pharyngobranchials, although any separation from their corresponding epibranchials is unclear. The pharyngobranchials are antero-posteriorly ridged and the more anterior elements are smaller, with the anteriormost element being small and capsular in shape. The fifth epibranchial lacks an expanded upper part, and instead articulates with the posterior end of the fourth pharyngobranchial (Fig.3.2d,g). On the anatomical right-hand side of the specimen the first, second and third elements are largely preserved as moulds on the surface of the matrix (Fig. 3.3) (Miles, 1973a; Brazeau, 2009). However, on this side some remnants are left of several epibranchials, and both a

posteriorly displaced fourth epibranchial, and a small anterior pharyngobranchial are present within the matrix (Fig. 3.1a,3.2e,f).

The ventral halves of all five of the branchial arches in *Ptomacanthus* are separate, and comprise a parallel series of long, curved, posteriorly grooved ceratobranchials (Fig.3.1b,d, 3.2a). The arches taper to meet the upper branchial elements - this proximal region is more intact on the anatomical right-hand side of the specimen where a canal running oblique to the direction of the arch is visible on the first and second arches (Fig.3.2b,c). On the anatomical right hand side of the branchial skeleton each lower element is divided by a break oblique to the element's direction (Figs. 3.1b,d, 3.2a). On the anatomical left hand side this division is not apparent, but does correspond with a point at which the arches sharply kink. Distally the arches terminate with box like ends - a large gap, posterior to the basihyal element separates the left and right sides. The anatomical left-hand posteriormost arch's lower element terminates in a particularly large dorsally-placed crescentic structure. No corresponding element is visible on the right hand side.

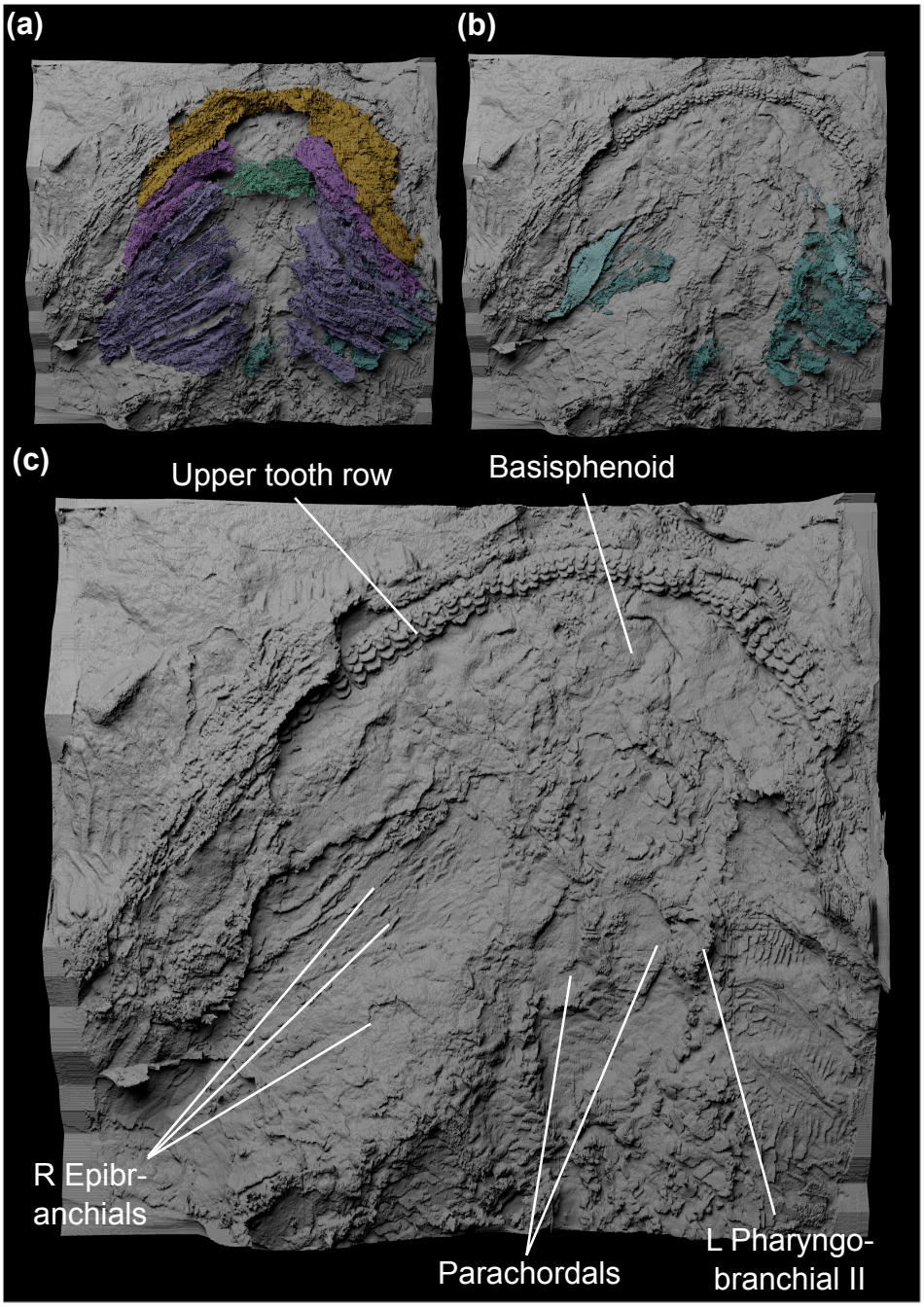


FIGURE 3.3: Caption on next page

FIGURE 3.3: The *Ptomacanthus* visceral skeleton juxtaposed against the mould of the specimen surface (a) with visceral skeleton, (b) with dorsal visceral skeleton, (c) the mould only

---

3.3.2 **Phylogenetic analysis**

Including this new information in the recent dataset of Coates and Tietjen (2018), a recent investigation into stem-chondrichthyan interrelationships, affected the topology of the chondrichthyan stem-group (Fig.3.5, 3.6). The parsimony analysis resulted in 88631 most parsimonious trees, with a length of 701 steps. In the strict consensus tree there is almost no resolution of the chondrichthyan stem-group (Fig. 3.6a). However, in the Adams consensus the stem-chondrichthyan *Gladbachus* is recovered as lying crownwards on the chondrichthyan stem-group relative to *Ptomacanthus*, with a similar result is recovered by the Bayesian analysis (Fig.3.5, 3.6b). This is *contra* Coates and Tietjen (2018) who recovered it in the chondrichthyan stem-group in a relatively less crownwards position than *Ptomacanthus*. All acanthodians are recovered as stem-chondrichthyans, with *Ptomacanthus* and other climatiid taxa lying in a paraphyly relatively crownward to diplacanthids, ischnacanthids and acanthodids, including *Acanthodes*. Also recovered in a relatively crownwards position on the stem-group are the "shark-like" taxa *Lupopsyrus*, *Obtusacanthus*, *Kathemacanthus*, and *Pucapampella*, and *Doliodus* is recovered as the sister taxon to crown-chondrichthyans. Within the crown-group relationships symmoriiformes are recovered as stem-holocephalans, and hybodonts, ctenacanths and xenacanths as stem-elasmobranchs.

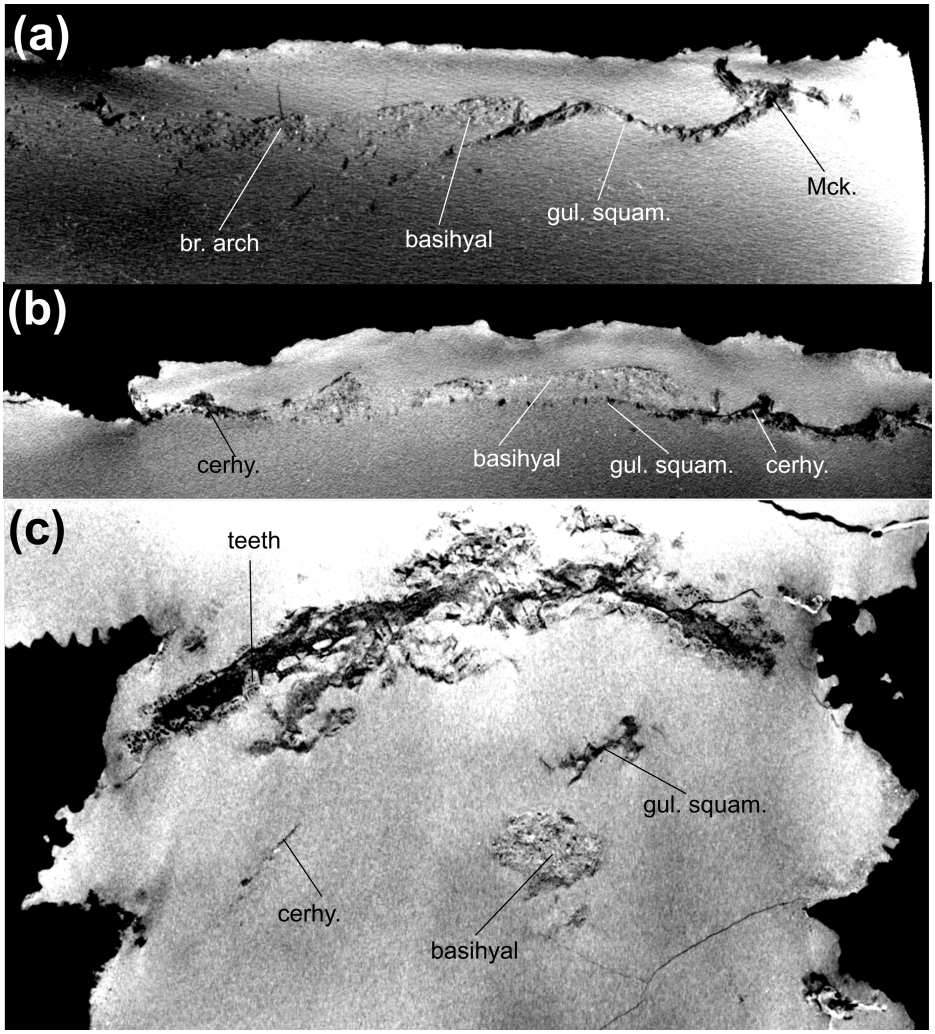


FIGURE 3.4: Tomograms showing the basihyal in (a) the approximate sagittal plane, and reconstructed section through (b) the approximate transverse plane, and (c) the approximate coronal plane. Abbreviations: br. arch, branchial arch; cerhy., ceratohyal; gul. squam., gular squamation; Mck., Meckel's cartilage.

3.4 DISCUSSION

3.4.1 **Phylogenetic implications of branchial arch position**

The data from *Ptomacanthus* presented here fits into an emerging picture of ancestral gnathostome conditions. Mounting evidence places acanthodians in the

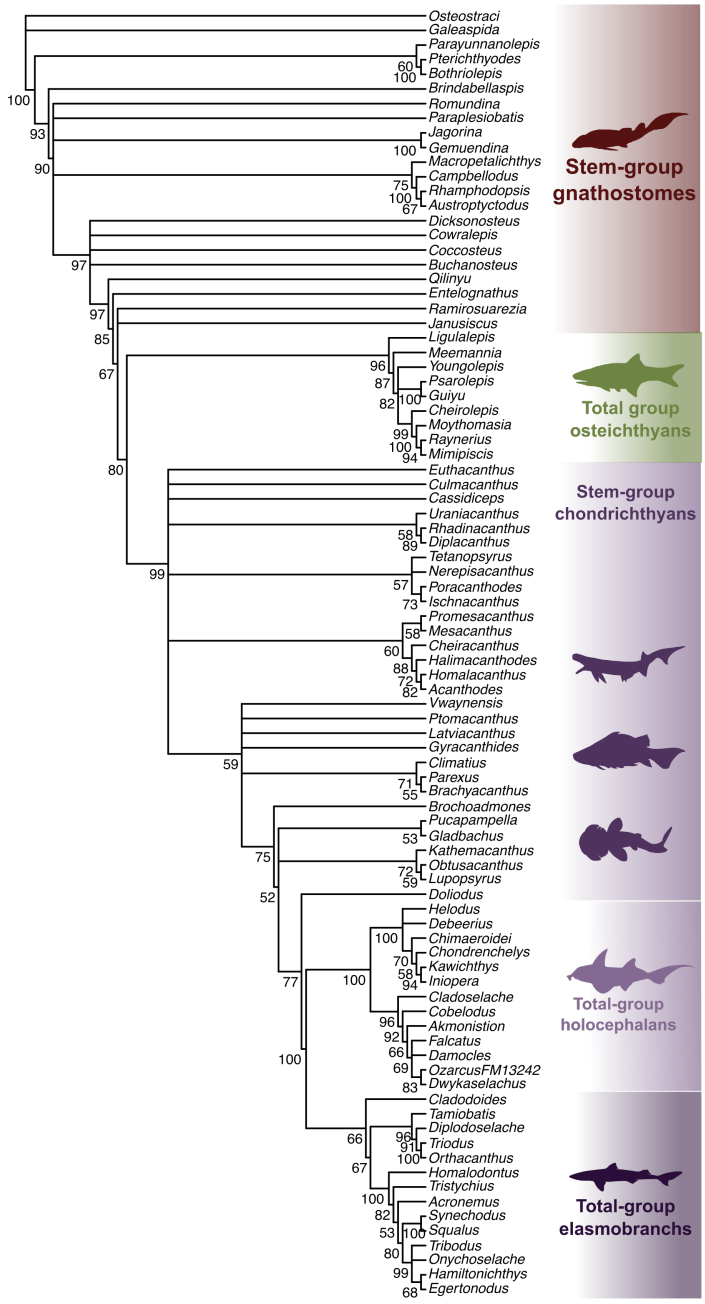


FIGURE 3.5: The consensus tree of the Bayesian analysis, with nodes labelled with posterior probabilities - the percentage of sampled trees recovering that split.

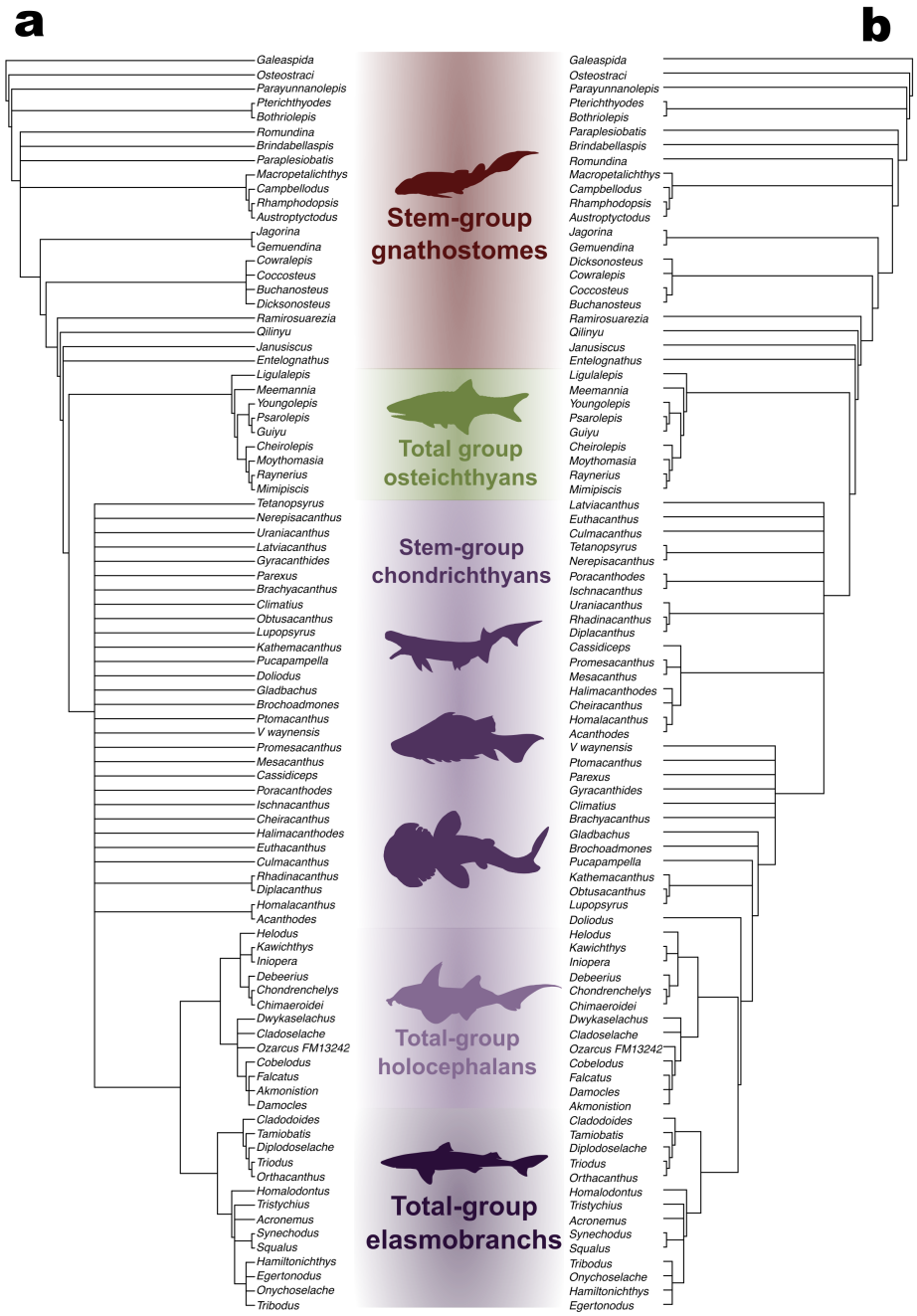


FIGURE 3.6: The results of the parsimony analysis (a) the strict consensus tree, (b) the majority rule consensus tree.

chondrichthyan stem-group, a result that has been repeatedly corroborated in phylogenetic analyses of early gnathostomes (Zhu et al., 2013; King et al., 2016; Brazeau and de Winter, 2015; Giles et al., 2015c; Coates and Tietjen, 2018). Combined with data from stem-group gnathostomes this has prompted a reassessment of plesiomorphic gnathostome anatomy. The osteichthyan-like conditions that led to the placement of acanthodians with bony fishes now instead appear likely to be gnathostome symplesiomorphies. Meanwhile some states assumed to be plesiomorphic due to their presence in "primitive" chondrichthyans are instead probably chondrichthyan synapomorphies.

This data from *Ptomacanthus*, together with our phylogenetic analysis, shows definitively that a compact, positionally osteichthyan-like branchial skeleton was present in some chondrichthyan stem-group members. This compact state is then incident on the gnathostome crown-node on all three branches, confirming that it was plesiomorphic for crown-group gnathostomes. This constrains the development of an "elasmobranch"-like pharynx to relatively more crownwards on the chondrichthyan stem-group, between *Ptomacanthus* and *Gladbachus*. However, the elasmobranch condition seemingly present in *Acanthodes* remains difficult to square with this Davis et al. (2012).

Closer examination of the two osteichthyan-like and elasmobranch-like conditions reveals that they can be split into three linked morphological variables. Firstly the anterior extent of the branchial arches: in osteichthyans (eg. *Raynerius* (Giles et al., 2015b)) and stem-gnathostomes (eg. *Dicksonosteus* (Goujet, 1984)) the arches anteriorly to the parachordal plates, where they articulate on the basicranium. In chondrichthyans there is no articulation and in most the anteriormost branchial arch lies posterior to the otic capsule (eg. *Gladbachus* (Coates and Tietjen, 2018)). Secondly the degree of posterior extension: in osteichthyans and stem-gnathostomes (where known) the arches all lie ventrally relative to the neurocranium (eg. *Raynerius*

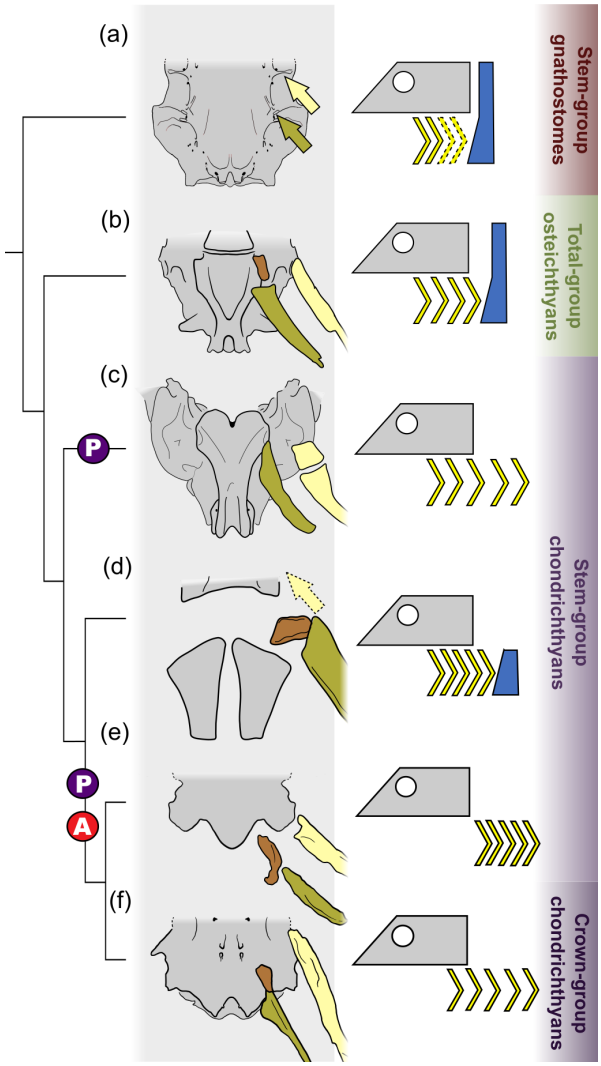


FIGURE 3.7: Postero-anterior extent of branchial skeleton in (a) *Dicksonosteus* Goujet (1984),(b) *Raynerius* (Giles et al., 2015b), (c) *Acanthodes* (Miles, 1973b; Davis et al., 2012), (d) *Ptomacanthus* (Brazeau, 2009), (e) *Gladbachus* (Coates et al., 2018), (f) *Ozarcus* (Maisey, 2007; Pradel et al., 2014). Phylogenetic tree congruent with topology described in methods. P indicates a shift of the posterior extent of the branchial skeleton, while A indicates a shift of the anterior extent. Colour scheme: gray, neurocranium; light yellow, hyomandibular; dark yellow, epibranchial; orange, pharyngobranchial; blue, dermal shoulder girdle.

(Giles et al., 2015b)). In most chondrichthyans they extend caudally (eg. *Ozarcus* (Pradel et al., 2014)). Finally the presence or absence of an operculum: in osteichthyans and stem-gnathostomes bony plates cover the gill arches as part of a functionally-linked complex of dermal bones covering the head and shoulder girdle (eg. *Mimipiscis* Gardiner (1984)). Contrastingly in most chondrichthyans a series of gill slits are present with no macromeric operculum (eg. *Ozarcus* Pradel et al. (2014)).

Of these three conditions *Acanthodes* is chondrichthyan-like in the second respect - the branchial skeleton has a marked caudal extension (Coates et al., 2018). The presence of an operculum is moot - while it had branchial plates, they did not cover the entire pharynx and it seems likely that posterior gill slits were present. However, the anterior extent of the branchial arches in *Acanthodes* is osteichthyan-like: the anterior branchial arch extended underneath the neurocranium, articulating with the basishpenoid (Miles, 1973b). Rather than having a completely elasmobranch-like pharynx, instead *Acanthodes* had a branchial skeleton that is chondrichtyan in some, but not all, respects.

I reformulated the branchial character list on the basis of this in my phylogenetic analysis, and consequently the caudally extended branchial skeleton of *Acanthodes* (and other acanthodiforms such as *Halimacanthodes* (Burrow et al., 2012)) is implied to be homoplasious. It is possible that this is linked to the anguilliform body shape of *Acanthodes*, as suggested by Miles (1968). Extant eels exhibit dissociation of the cranium and shoulder girdle, as well as posterior displacement of the gill arches (Nelson, 1966), both of which are observed in *Acanthodes* (Miles, 1968) .

Another notable affect of these changes to the dataset of Coates et al. (2018) is that the stem-chondrichthyan *Gladbachus* is recovered relatively crownwards to *Ptomacanthus* and other "climatiids" on the chondrichthyan stem-group. This contrasts with the result of Coates et al. (2018), who recovered *Gladbachus*

amongst the "acanthodian" grade. However, the recovery of *Gladbachus* in this position is consistent with a host of other characters grouping *Gladbachus* with the chondrichthyan crown-group to the exclusion of climatiids. These include extensively calcified cartilage, a head skeleton lacking interlocking tesserae, and the absence of any kind of large dermal cranial ossification or paired fin spines (Coates and Tietjen, 2018).

3.4.2 **Pharyngeal patterning**

The mineralisations that together form the gill skeleton vary in their shape and arrangement in different gnathostome taxa. As well as serving a functional role in these animals the variation provides morphological characters that can be diagnostic for their relationships. *Acanthodes*, because of its rare endoskeletal preservation, has in the past been key to interpreting these characters in the very earliest gnathostomes. However, multiple interpretations of the branchial skeleton in *Acanthodes* exist, with differing implications for the early evolution of the branchial skeleton (Watson, 1937; Gardiner, 1984; Miles, 1973a; Nelson, 1968). As well as helping us interpret these patterns in and of itself, *Ptomacanthus* provides an important reference for interpreting patterns of the branchial elements in *Acanthodes*, particularly with regards to the mineralisations forming the ventral gill skeleton.

A broad median element articulating with the ceratohyals and often the first branchial arch - a basihyal - forms part of the anterior pharyngeal floor in some gnathostomes. While in living jawed vertebrates a basihyal is only present in chondrichthyans (eg. *Scapanorhynchus* (Garman, 1913)), in early gnathostomes it is far more widespread. As well as being present in early crown-group and stem-group chondrichthyan branchial skeletons (eg. *Gladbachus* (Heidtke and Krätschmer, 2001; Coates et al., 2018), *Doliodus* (Miller et al., 2003), *Debeerius*

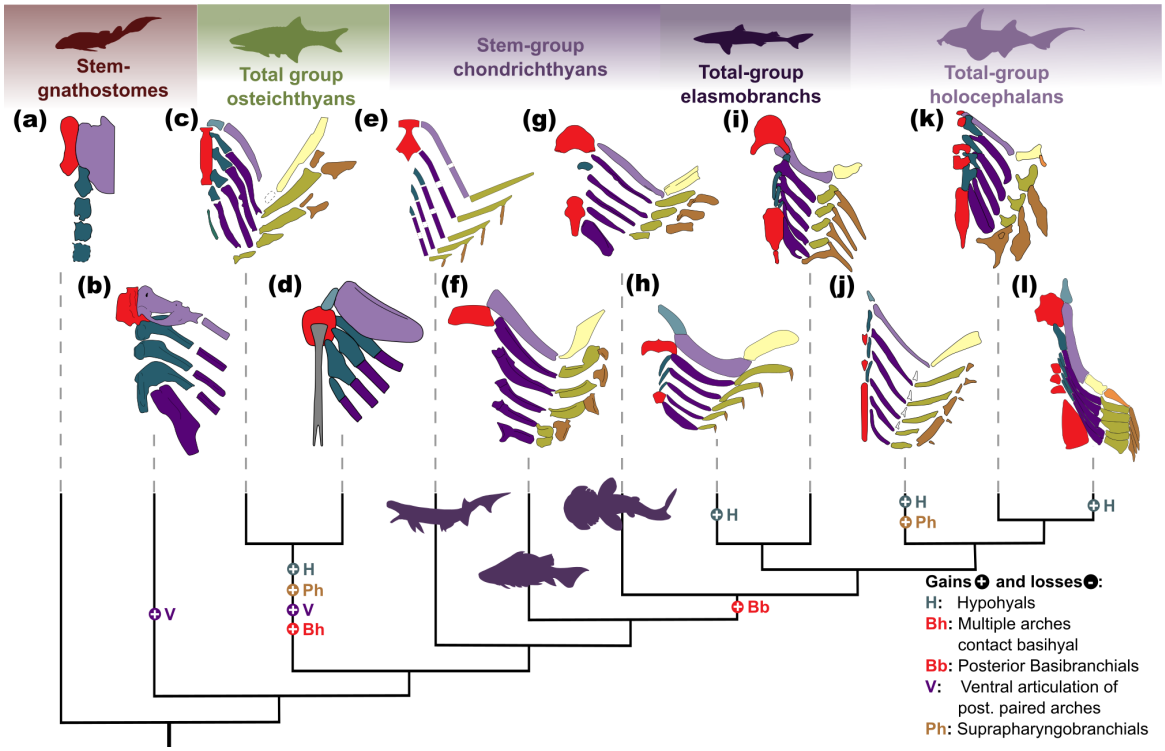


FIGURE 3.8: The phylogenetic distribution of branchial arch morphologies in gnathostomes, based on the strict consensus tree derived from the parsimony analysis described in the methods. Character changes of selected pharyngeal arch characters from our analysis are plotted using an ACCTRAN optimisation. Taxa shown are (a) *Cowralepis*Carr et al. (2009), (b) *Paraplesiobatis* (Brazeau et al., 2017), (c) *Raynerius* (Giles et al., 2015b), (d) *Glyptolepis* (Jarvik, 1972), (e) *Acanthodes* (Gardiner, 1984; Miles, 1973b), (f) *Ptomacanthus*, (g) *Gladbachus* Coates et al. (2018), (h) *Triodus* (Heidtke et al., 2004), (i) *Scyliorhinus* (Pradel et al., 2014), (j) *Ozarcus* (Pradel et al., 2014), (k) *Callorhinchus*Pradel et al. (2014), (h) *Debeerius* (Grogan and Lund, 2000). Colour scheme: as in figure 6, with addition of: light turquoise, hypohyal; gray, urohyal. Silhouette from Brazeau (2012); Long (1986a); Schaeffer and Williams (1977); Gardiner (1984), and Phylopic.

(Grogan and Lund, 2000) and in *Triodus* (Heidtke et al., 2004) a very similar element is also present in placoderm-grade stem-gnathostome branchial skeletons (eg. *Paraplesiobatis* (Brazeau et al., 2017) [Fig. 3], *Cowralepis* (Carr et al., 2009), *Tapinosteus* Stensiö (1969), and *Pseudopetalichthys* Gross (1962); Brazeau et al. (2017). This

phylogenetic distribution suggests that perhaps the presence of a basihyal is the ancestral state for gnathostomes, retained in chondrichthyans. The basihyal in *Ptomacanthus*, contacting the ceratohyals and first branchial arch, fits this pattern. It also adds credence to Gardiner's reconstruction of *Acanthodes*, with a similar arrangement contacting the hyoid and first branchial arch. From my observations of *Acanthodes* casts at the NHM, Gardiner's reconstruction seems to me to be the most credible. Early examples of osteichthyan branchial skeletons also often have a single median element - the "basibranchial" (eg. *Raynerius* (Giles et al., 2015b) *Glyptolepis* (Jarvik, 1972) [Fig. 3]. This is distinct from a basihyal in articulating with the hyoid arch via hypohyals, contacting more than one branchial arch, and extending further posteriorly in the pharynx. However it is possible that this and the symplesiomorphic basihyal are homologous.

In living osteichthyans an additional pair of bony struts - the hypohyals - connect the ceratohyals with the median basibranchial. Hypohyals have long been identified as an unambiguous synapomorphy of osteichthyans (Schaeffer, 1968; Friedman and Brazeau, 2010), as they are entirely absent in extant chondrichthyans (Garman, 1913). The report of hypohyal-like structures in various early chondrichthyans - particularly symmoriids (Coates and Sequeira, 2001a; Pradel et al., 2014), but also more widely (Grogan and Lund, 2000; Heidtke, 1999) has led to the suggestion that they are instead a gnathostome symplesiomorphy (Pradel et al., 2014). Evidence against their homology comes from found in the distinct anatomical differences in arrangement of osteichthyan and chondrichthyan hypohyals (Giles et al., 2015c). The absence of mineralised hypohyals in *Ptomacanthus* again corresponds with Gardiner's reconstruction of *Acanthodes*, as well as with the absence in *Gladbachus* (Coates et al., 2018). This apparent absence of hypohyals on the chondrichthyan stem, their apparent absence in placoderms, and the topology recovered in our phylogenetic analysis suggest that osteichthyan hypohyals are apomorphic for the clade, and that chondrichthyan hypohyals are homoplasious, and apomorphic for

early holocephalans.

A succession of paired and unpaired mineralisations support the floor of the pharynx posterior to the basihyal in living chondrichthyans. Paired elements - hypobranchials - are present in crown-chondrichthyans (and osteichthyans), with their posterior orientation in elasmobranchs possibly synapomorphic (Pradel et al., 2014). Meanwhile an unpaired basibranchial copula element is present in living holocephalans and elasmobranchs, as well as in fossil taxa including *Ozarcus*, *Gladbachus*, and *Triodus* Pradel et al. (2014); Coates et al. (2018); Heidtke et al. (2004), and could be apomorpic for a subset of total-group chondrichthyans. *Ptomacanthus* is distinct from these chondrichthyans in lacking any mineralised basi- or hypobranchial elements, at least not preserved in the fossil. Gardiner's reconstruction of *Acanthodes* also lacks posterior basibranchial elements, although does possess paired hypobranchials on the posterior three branchial arches. Like *Ptomacanthus* and *Acanthodes*, "placoderm"-grade stem-gnathostomes also seemingly lack an unpaired mineralisation posterior to the basihyal (Brazeau et al., 2017; Carr et al., 2009; Stensiö, 1969). Instead a series of paired ventral elements with no space for median elements in between is present (Brazeau et al., 2017). The homology of these elements is unclear - they are possibly homologous with median basibranchials Carr et al. (2009) but in other taxa more closely resemble ceratobranchials (Brazeau et al., 2017). While the homology of paired elements is poorly understood, a basibranchial copula is likely derived in chondrichthyans.

Other patterns comparable to other chondrichthyans can be observed in more dorsal parts of the gill skeleton of *Ptomacanthus*. Despite the incompleteness of the pharyngobranchials, they seem to form an antero-posterior chain with dorsal ridges, like those in *Acanthodes*, *Ozarcus*, and *Gladbachus* (Pradel et al., 2016; Coates et al., 2018). Like living chondrichthyans, *Ptomacanthus* possesses five epibranchials (Carvalho et al., 2013). The articulation of the posteriormost two of these on the

same pharyngobranchial is very similar to the condition in *Ozarcus* (Pradel et al., 2014), and is comparable to that in modern chondrichthyans where epibranchial V is fused to pharyngobranchial IV and articulates with epibranchial IV (Carvalho et al., 2013). Finally the lack of any articulation between the two posteriormost ventral paired branchial arches in *Ptomacanthus* constrasts with a condition shared by *Paraplesiobatis* (Brazeau et al., 2017), and in various sarcopterygians such as *Glyptolepis* (Jarvik, 1972), which may prove to be a gnathostome symplesiomorphy.

3.4.3 **A model for early gnathostome branchial architecture**

The jaws, hyoid arch, and branchial arches are widely thought to be serially homologous - that is, originating from the same developmental pattern that has been repeated and modified along the pharynx. Since Gegenbaur (1878) first suggested this, support has been found in evidence of molecular mechanisms shared between the different pharyngeal arches (Gillis et al., 2013). Consequently it has been assumed that the ancestral pharyngeal skeleton must have been morphologically complete, with one of every part that we observe in branchial arches (hypo-, cerato-, epi-, pharyngo-, etc.) in every other pharyngeal arch. This has formed the basis of attempts to reconstruct the evolution of the gnathostome jaw suspension using a "morphologically complete" hyoid arch with pharyngo- and hypohyals (Grogan and Lund, 2000), as well as in the sporadic revival of the aphetohyoidean hypothesis- the expectation that we should observe a fully functional hyoid gill slit in "primitive" gnathostomes (Watson, 1937; Zangerl and Case, 1976; Pradel et al., 2014).

However, neither the ancestral branchial skeleton I reconstruct here, nor the earliest fossil gnathostome branchial skeletons show any evidence for being "morphologically complete". They lack features that might be expected in such a

skeleton, for example hypo- and pharyngohyals, and display anatomical conditions that are difficult to interpret in terms of living gnathostome branchial skeletons. This is still consistent with a serial homology between arches- however, it illustrates that all serial homologues need not necessarily correspond on some type of morphologically complete, archetypal level. The earliest branchial skeletons should not necessarily be expected to be morphologically complete, and nor should apparently morphologically complete branchial skeletons necessarily be expected to exhibit plesiomorphy.

3.5 CONCLUSION

This new information from *Ptomacanthus* provides an important cipher for interpreting the branchial skeletons of other early gnathostomes. It implies an ancestral gnathostome branchial skeleton that lay almost entirely ventral to the neurocranium, which lacked hypohyals, and which possessed a large median basihyal articulating with the hyoid arch and one branchial arch, possibly with the posteriormost two branchial arches articulating. The possession of five epibranchials, the posteriormost two of which share a pharyngobranchial, is likely to be at some level apomorphic for crown-chondrichthyans plus some stem-group members, as are posteriorly oriented pharyngobranchials and a basibranchial copula. Posteriorly oriented hypobranchials remain a likely elasmobranch synapomorphy, and hypohyals are probably homoplasious in osteichthyans and some early crown-group chondrichthyans. The stem-chondrichthyan *Gladbachus* is found to lie more crownwards in the chondrichthyan stem-group than initial analysis implied, consistent with its otherwise relatively derived character states. Notably the ancestral branchial skeleton we reconstruct is no more like that of chondrichthyans than it is like that of osteichthyans, and does it resemble some kind of morphologically complete archetype. Extant chondrichthyans should not be

used as a model for the ancestral gnathostome branchial skeleton.

CHAPTER 4

A THIRD "ACANTHODIAN" ENDOSKELETON IN *Diplacanthus crassisimus*

4.1 INTRODUCTION

Although the body of data on the dermal skeletons of acanthodian-grade taxa is growing, very little is known about the anatomy of their endoskeletons. Information is limited entirely to *Ptomacanthus* and *Acanthodes*, which show two quite contrasting anatomies both in terms of their endoskeletons and in general (Brazeau, 2009; Davis et al., 2012; Watson, 1937; Brazeau, 2012). These taxa are also recovered relatively far apart in the chondrichthyan stem-group (eg. in Coates et al. (2018)) meaning that their endoskeletons have little to offer in providing information on the interrelationships of putative acanthodian-grade subgroups. Describing the endoskeletal anatomy of acanthodian-grade animals with differing dermal anatomies would complement the information from *Acanthodes* and *Ptomacantus*, and provide endoskeletal context for another group of acanthodians known entirely from dermal skeletons.

One such taxon is *Diplacanthus crassisimus* (Duff, 1842), an acanthodian found at a range of Middle Devonian sites in Scotland (Burrow et al., 2016a). Figured in Hugh Miller's Old Red Sandstone (Miller, 1841), and first described by Duff (1842), the taxon is mentioned in various 19th century texts (reviewed in Burrow et al. (2016a)). The most complete description of its gross anatomy came from Watson (1937), with an updated description of its shoulder girdle from Miles (1973a). A further, largely histological, revision was then provided by Burrow et al.

(2016a). Although *Diplacanthus crassisimus* is one of the best known Middle Old Red Sandstone acanthodians, no detailed information on its endoskeletal head or pharynx is known.

More broadly *Diplacanthus* is part of a wider grade of acanthodians known as diplacanthids, characterised by deep bodies, expanded anterior and posterior circumorbital bones, smooth dermal plates in the mouth, finely striated dorsal fin spine insertions, and distinctively flanged scapulocoracoids (Burrow et al., 2016a). Phylogenetically diplacanthids are often allied with ischnacanthids and acanthodids (including *Acanthodes*) (Coates et al. (2018)). Together these groups possibly comprise a clade forming the sister group to all other chondrichthyans, including both the crown and a portion of the stem-group inhabited by "climatiid" acanthodians such as *Ptomacanthus* as well as more conventional stem-chondrichthyans such as *Doliodus* Coates et al. (2018). Coates et al. (2018) suggest naming this clade "Acanthodii".

The position of *Diplacanthus* as an acanthodian which is neither a climatiid nor an acanthodid, coupled with our relatively good understanding of its overall anatomy, makes it an prime candidate taxon for uncovering endoskeletal anatomy. Here I use X-ray synchrotron tomography to reveal the neurocranial and visceral skeleton of *Diplacanthus crassisimus*. Parts of the braincase are preserved, as well as parts of the mandibular and branchial skeleton. As well as being only the third "acanthodian" endoskeleton described, it is the first with three-dimensionally preserved component elements. The anatomy of *Diplacanthus* is compared to that of other acanthodian and stem-chondrichthyan endoskeletal material. It also has features that bear comparison with early vertebrates more widely.

4.2 MATERIALS AND METHODS

4.2.1 **Specimen**

The specimen I describe is National Museum of Scotland (NMS) specimen 1891.92.334, *Diplacanthus crassisimus*, a stem-chondrichthyan from the Middle Devonian of Tynet Burn, UK (Fig.4.1a). The specimen was originally described by Watson, and noted as having "very massive ossifications in the head skeleton, vertebral column and bases of the fins" that were unfortunately "so crushed as to be almost incapable of interpretation" (Watson, 1937)(Fig.4.1b). In this regard NMS 1891.92.334 is unique amongst its species, and very unusual amongst acanthodians more widely. The counterpart to the specimen has been missing at least since Watson's description (Watson, 1937), and possibly was never originally collected.

4.2.2 **Synchrotron tomography**

The specimen was imaged on Beamline 19 of the European Synchrotron Radiation Facility, using propagation phase-contrast synchrotron microtomography. A voxel size of 2.26 μm was achieved, using an energy of 116keV. The resulting tomograms were then segmented using Mimics v.18 (biomedical.materialise.com/mimics; Materialise, Leuven, Belgium). Models were then imported into Blender (blender.org) to acquire images.

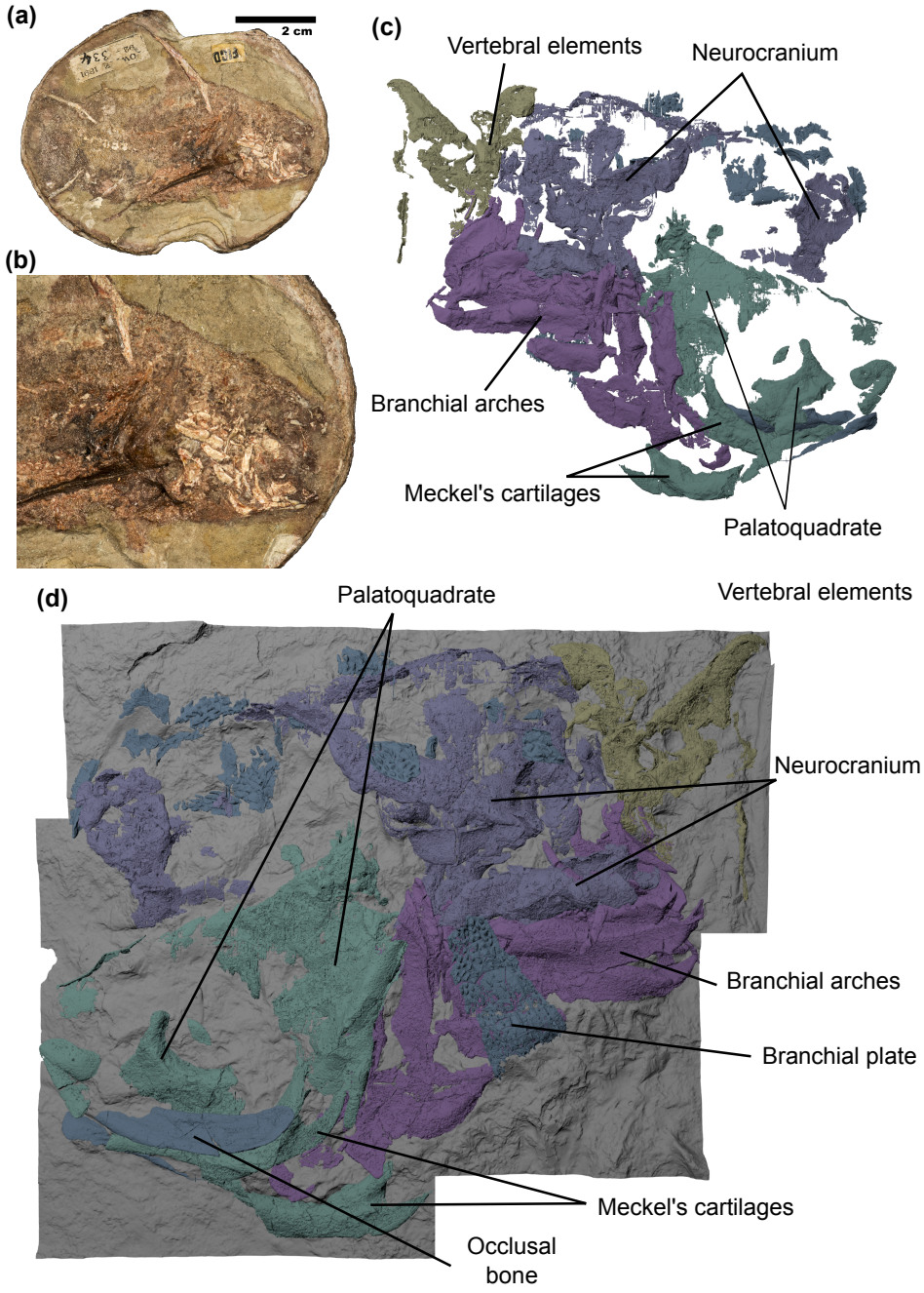


FIGURE 4.1: Caption on next page

FIGURE 4.1: Entire specimen (a) Photograph of specimen NMS 1891.92.334; (b) close-up photograph of mineralised endoskeleton; (c) entirety of segmented region; exterior view; (d) entirety of segmented region, interior view. Colours: blue, dermal; lilac, neurocranium; purple, branchial; teal, mandibular and hyoid; yellow, vertebral column.

4.3 RESULTS

Scanning reveals a large part of the head and pharynx of Diplacanthus (Fig.4.1c,d). Interpretation of this is hindered somewhat by asymmetric distortion and the absence of the counterpart. However parts can be identified by position, particularly with reference to the endoskeleton of *Acanthodes*, which it seems to resemble quite closely. Much of the ventral branchial skeleton is preserved, as well as the entire left hand mandibular arch. Some of the neurocranium is also preserved, comprising part of the ethmoid/anterior orbital region, parts of the left hand border of the otic region, a complete basioccipital element, and an occipital plate. Also preserved is part of the vertebral column, the anterior part of which is in the scanned region. The procoracoid element is described in chapter 6, which deals more broadly with the acanthodian shoulder girdle. The structure of the cartilaginous tissue forming the endoskeleton is discussed in chapter 5, which deals with skeletal tissues in early gnathostomes.

4.3.1 **Braincase**

The braincase of *Diplacanthus* is mineralised in several parts, like that of *Acanthodes* (Davis et al., 2012) (Fig. 4.2). A large circular space anteriorly marks the location of the orbit - this is confirmed by the presence of dermal circum-orbital bones antero-

dorsally to it (Watson, 1937; Burrow et al., 2016a). One chondrified fragment lies anteriorly to the orbit, presumably either anterior orbital or ethmoid. Posterior to the orbit lie parts of the postorbital and otic region. Posterior to this is a basioccipital plate, preserved ventrally to the otic and occipital parts. Notably a basisphenoid is absent - presumably lost to the counterpart. Proportionally the braincase appears similar to that of *Acanthodes* (Davis et al., 2012).

The anteriormost part of the neurocranium is fragmented and flattened, but when reassembled would have had a gently convex spoon-shaped surface, oriented medially (Fig.4.3a-c). Two openings are present in this surface: a larger, irregular opening is probably due to wear at the surface, however a smaller opening posterior to it is clearly a foramen (Fig.4.3b). Although the border is mostly curved, a marked angle is present postero-ventrally (Fig.4.3c). At its ventral border the element expands to form an oblique medial shelf. Below this shelf the element expands further to form a crushed pyramidal region, punctured by a foramen on its postero-lateral side (Fig.4.3b). This region reveals that the element was part of a larger whole, due to sheets of cartilage extending posteriorly and mouldic imprints on the surface of the matrix (Fig.4.3a).

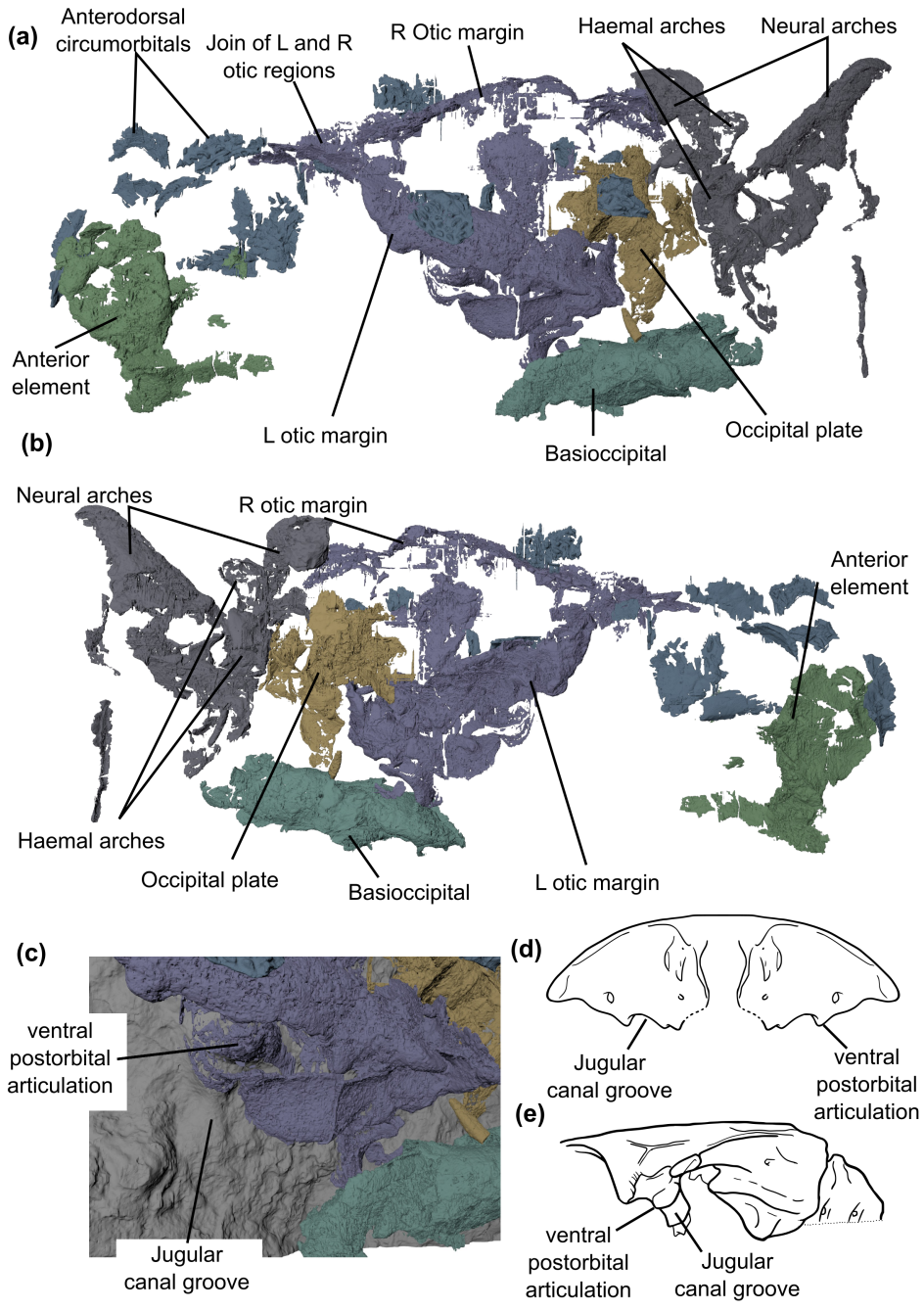


FIGURE 4.2: Caption on next page

FIGURE 4.2: Figure 2: Neurocranial and vertebral skeleton in (a) lateral; and (b) medial view; (c) Braincase juxtaposed against mould of surface, showing lateral commisure; Braincase of *Acanthodes* in (d) anterior, and (e) Lateral view showing corresponding details of lateral commissure . Abbreviations as in Figure 2.

I am unable to identify this elements confidently due to its partial preservation and the absence of the corresponding mineralisation in *Acanthodes* (Davis et al., 2012). One possibility is that it is a subnasal plate like that in the stem-chondrichthyan *Doliodus* and the stem-gnathostome *Janusiscus* (Maisey et al., 2009; Giles et al., 2015c) (Fig. 4.3d). Another is that it is part of the anterior orbital wall - it roughly resembles that of *Cladoides* in general shape (Fig. 4.3e).

The postero-dorsal margin of the orbit is demarcated by sheets of cartilage forming the supraorbital shelf 4.2. These are posteriorly continuous with the lateral and posterior margins of the otic region, comprising a large, L-shaped chondrification 4.2,4.4. On the anterior part of this chondrification there is a pronounced lateral process, which could either be the margin of the postorbital process or the dorsal articulation of the palatoquadrate (Fig.4.4a). The chondrification above this point is punctured by a foramen, which may have carried a branch of the superficial ophthalmic complex from the orbit onto the roof of the neurocranium (Fig.4.4a) (eg. *Cladodoides* (Maisey, 2005)). Posteriorly to this process is a broad, convex surface, which narrows to form a pronounced dorsolateral ridge Miles (1968) (or supraotic crest (Miles, 1973b)) which curves ventrally forming a lateral fossa (4.4a,b). The posterior face of the otic element would have formed the anterior margin of the otic fissure - crossing it is a distinct, horizontal groove, probably for passage of the vagus (IX) nerve (Fig.4.4a-c). Dorsally to this groove is an oval, pad-like protruberance, the identity of which is uncertain. Associated with the rear part of this is a small process, which may be the articulation for the

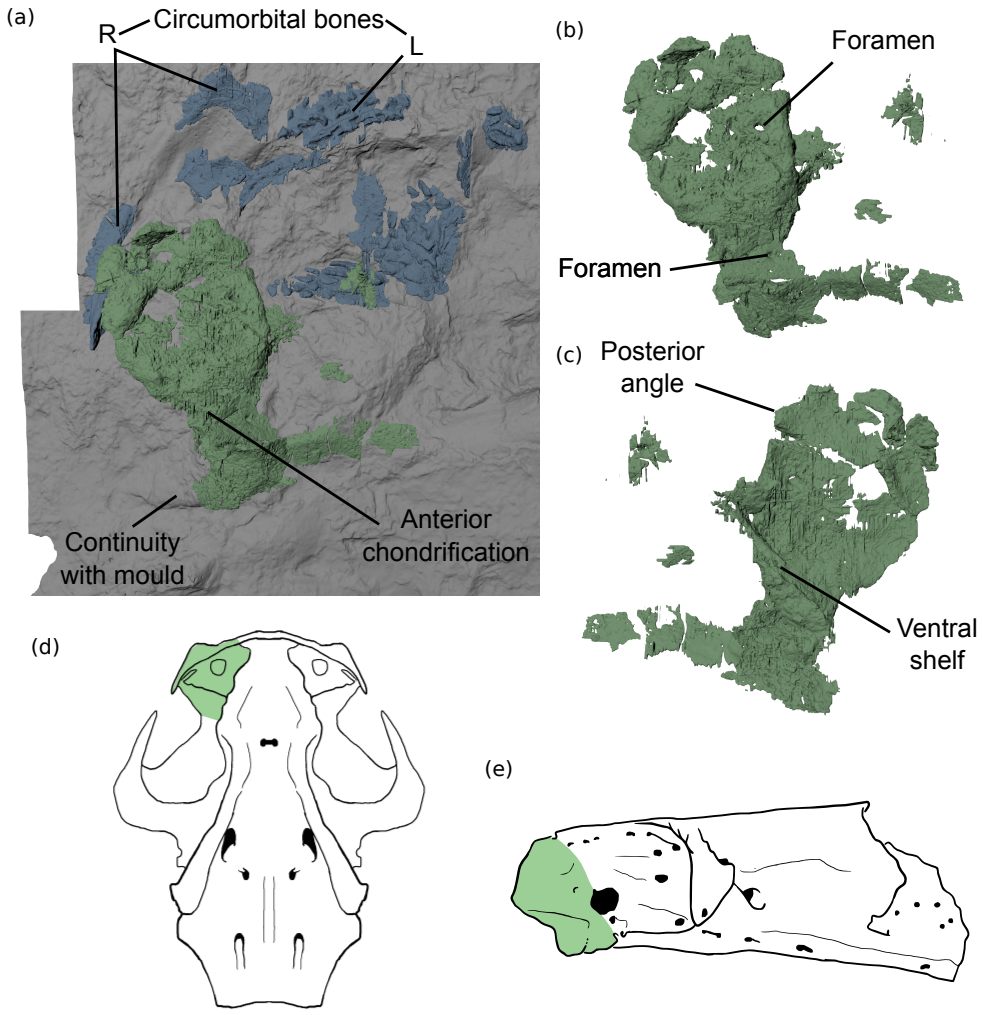


FIGURE 4.3: Anterior neurocranial mineralisation (a) From internal side against the mould of the specimen surface; (b) From internal side but rotated slightly to show foraminae in surface; (c) From external side, (d) Neurocranium of *Doliodus* in ventral view with subnasal plate highlighted, redrawn from Maisey et al. (2009); (e) Neurocranium of *Cladodoides* in lateral view with anterior orbital wall highlighted, redrawn from Maisey (2005).

hyomandibular (Brazeau and de Winter, 2015) (Fig.4.4 a,b).

In the matrix overlying left otic margin and the surface of the specimen are a number of crushed cartilages. These are continuous with mouldic impressions on the surface of the specimen and by comparison with *Acanthodes* (Davis et al., 2012) these are probably the remains of the left hand lateral commissure of *Diplacanthus*. The ventral articulation of the palatoquadrate is preserved as a broken, subhemispherical cartilage. Below this the mould forms a distinct notch is preserved which I interpret as the roof of the jugular canal.

The right hand equivalent of this otic margin is probably represented as a series of crushed cartilaginous sheets which extend posterioirly from the supraorbital shelf 4.4. These are approximately the same length as the left otic chondrification, terminating in a posterior angle. This implies a poorly mineralised roof of the braincase, like in *Acanthodes* (Davis et al., 2012). Between the left and right otic margins is a large, poorly preserved chondrification. From its position this presumably formed part of the dorsal braincase, but it is difficult to determine exactly what. Associated with it are a number of isolated sections of neurocranial canal - one of these is tripartite, and so may be part of the trigeminal (V) or facial (VII) nerve, which would correspond with its position in the braincase (Davis et al., 2012).

Posterior to the otic region is a lateral occipital plate 4.2. It has a similar axehead shape to that of *Acanthodes* (Davis et al., 2012), with a thin posterior end. Some foraminae appear to be present in it, although unclearly. The separation of this from the otic ossification indicates the presence of an otico-occipital fissure, consistent with the condition in other stem-chondrichthyans and osteichthyans (Maisey, 2005; Giles et al., 2015b).

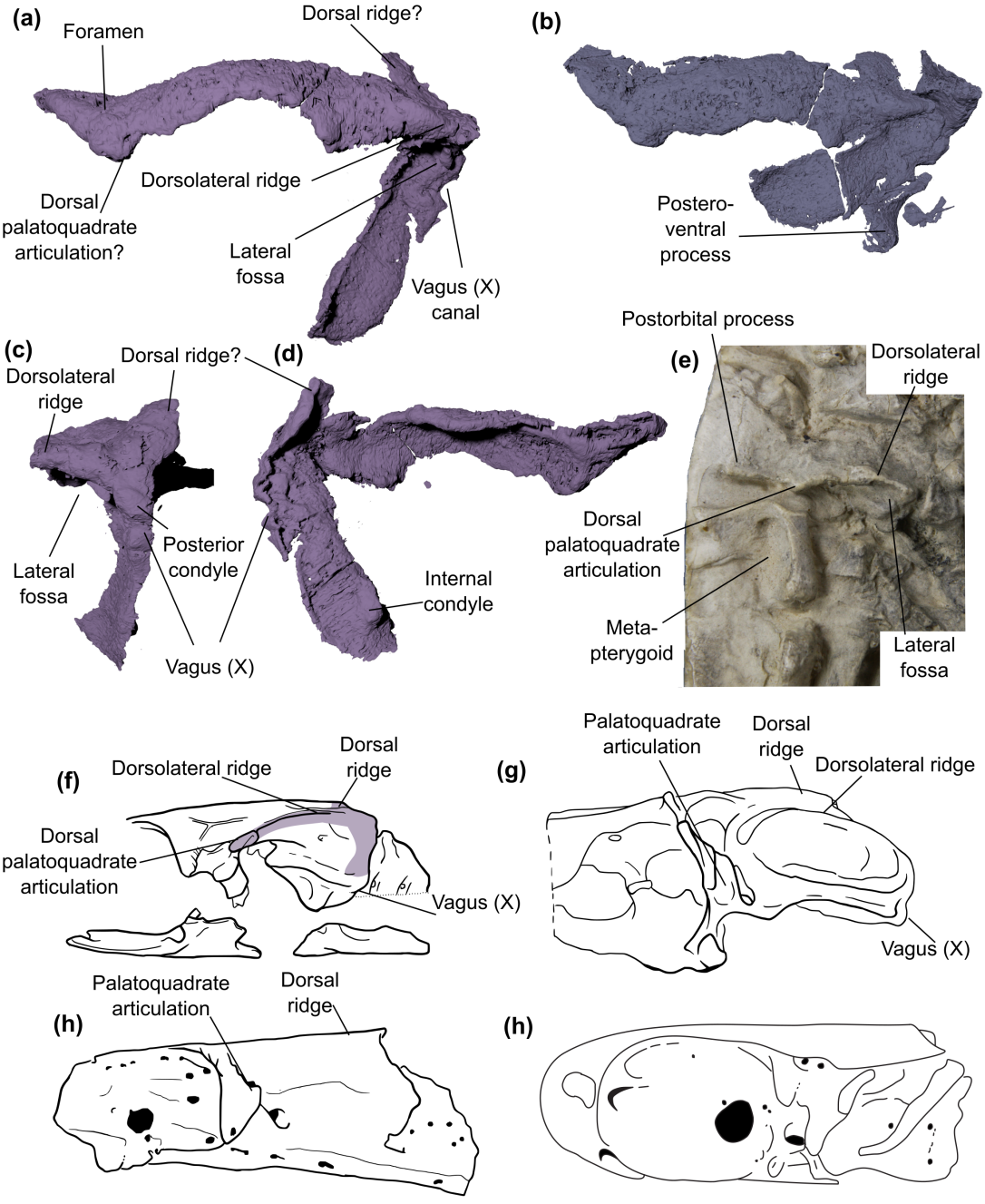


FIGURE 4.4: Caption on next page

FIGURE 4.4: Attempted reconstruction of left lateral otic region in *Diplacanthus* in (a) lateral view, (b) same lateral view as *in situ*; (c) posterior view; (d) medial view; (e) Photograph of *Acanthodes* cast NHM P.49995, showing comparable region; (f) neurocranium of *Acanthodes* in lateral view with approximate corresponding region highlighted, redrawn from Davis et al. (2012); (g) neurocranium of *Pucapampella* in lateral view, redrawn from Maisey (2001a); (h) neurocranium of *Cladodoides* in lateral view, redrawn from Maisey (2005); (i) neurocranium of *Mimipiscis* in lateral view, redrawn from Gardiner (1984)

.

The basioccipital is preserved lying between the otic region and the branchial arches (Fig.4.24.5). It has been mediolaterally crushed and is somewhat fragmented. In lateral view it is similar in shape to that of *Acanthodes* (Miles, 1970, 1973b), tapering anteriorly. As in *Acanthodes* and osteichthyans the basioccipital of *Diplacanthus* is mediolaterally narrowed, rather than as broad as the otic capsules like in stem-gnathostomes (eg. *Buchanosteus* Young (1979)) and other chondrichthyans (eg. *Doliodus* Maisey et al. (2009)). In ventral view it lacks the hourglass-shape seen in the basioccipital of *Acanthodes* and a possible basioccipital element associated with Milesacanthus (Young and Burrow, 2004), although this may be due to lateral crushing. The element has a distinct postero-ventral notch, like that seen a wide range of early gnathostomes. The posterior border of the element is difficult to determine due to the fragmentary nature of the cartilaginous sheets forming its boundary.

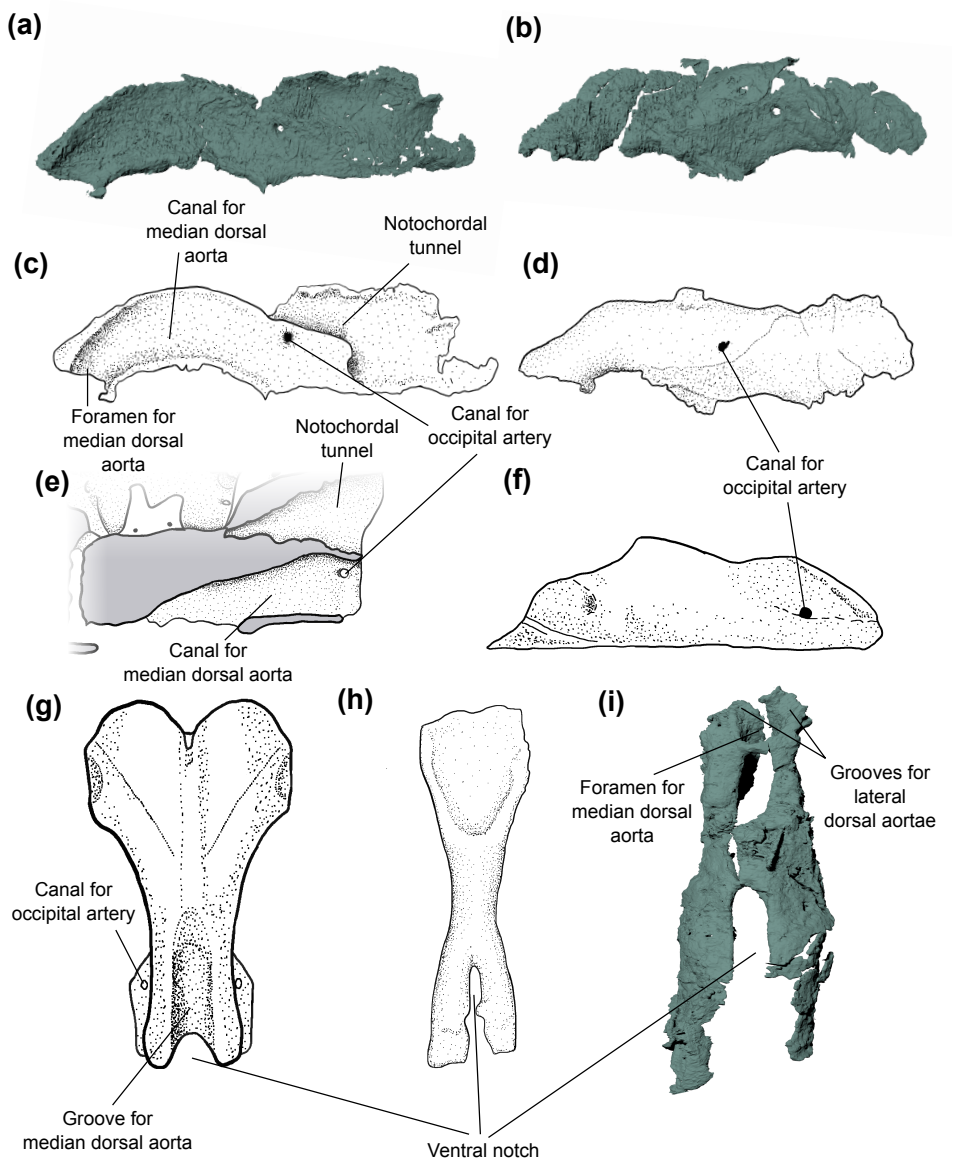


FIGURE 4.5: Caption on next page

FIGURE 4.5: (a) Right half of basicoccipital of *Diplacanthus* in medial view; (b) Left half of basioccipital of *Diplacanthus* in lateral view; (c) Interpretive drawing of right half of basicoccipital of Diplacanthus in medial view; (d) Interpretive drawing of left half of basioccipital of *Diplacanthus* in lateral view; (e) sagittal section through postero-ventral neurocranium of *Mimipiscis*, redrawn from Gardiner (1984); (f) Lateral view of basioccipital of *Acanthodes*, redrawn from Miles (1973b); (g) Ventral view of basioccipital of Acanthodes, redrawn from Miles (1973b); (h) Putative basioccipital of *Milesacanthus* in ventral (?) view, redrawn from Young and Burrow (2004); (i) Ventral view of basioccipital of *Diplacanthus*
.

Internally the basioccipital of *Diplacanthus* carries a canal for the median dorsal aorta - this is formed by mesial antero-posteriorly oriented grooves either half of the element (Fig.4.5a,c). This canal passes dorsally relative to the ventral notch and carried the median dorsal aorta to a well-defined circular foramen at the extreme anterior of the ventral surface. The antero-lateral margins of this foramen are marked by paired grooves, marking the divergence of the median dorsal aorta into lateral dorsal aortae (Fig.4.5i). Posteriorly this canal is punctured by a pair of lateral canals for occipital arteries, which travel perpendicularly relative to the direction of the canal onto the lateral surfaces of the element. Posterior to these foraminae, in the interior of the element, are a pair of pits which would have formed part of the ventral border of the notochordal tunnel, lying dorsal to the aorta (Fig.4.5a,c). This anatomy is closely comparable to the arrangement in stem-actinopterygians such as *Mimipiscis* (Fig.4.5a,c) (Gardiner, 1984) and *Lawrenciella* (Pradel et al., 2016), in which a median dorsal aortic canal lies ventrally relative to the notochordal canal, and where it is punctured in the dorsal margin by a pair of canals for the occipital arteries.

A similar arrangement of canals was also described in the basioccipital of *Acanthodes* (Miles, 1970, 1973b) (Fig. 4.5d,g). In his accounts of the casts Miles describes an internal canal that runs anteroposteriorly along the length of the

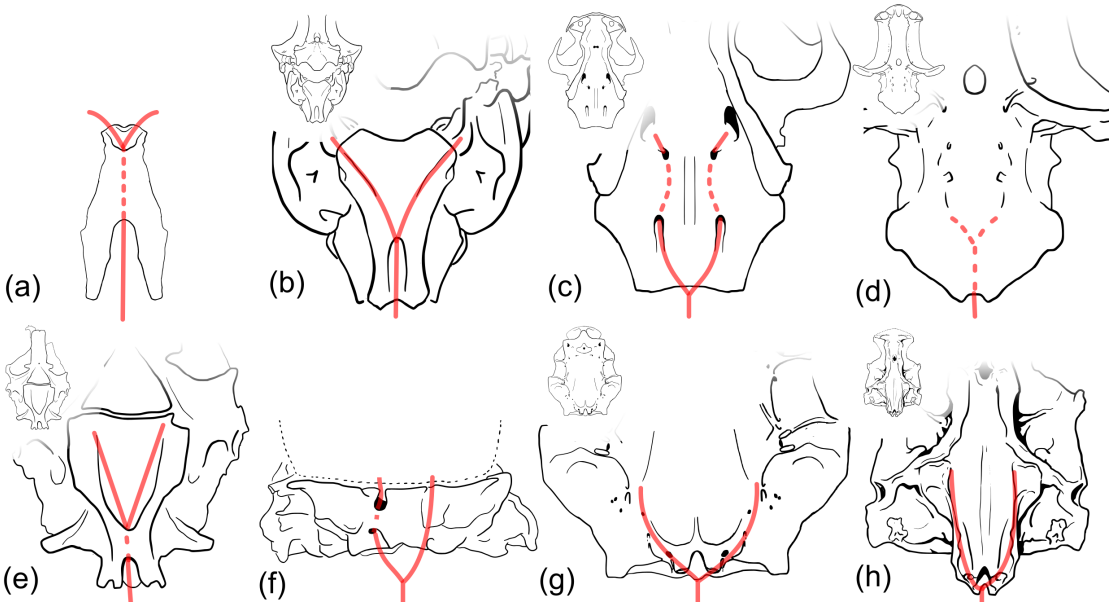


FIGURE 4.6: Basioccipital region of selected early vertebrates, showing path of ventral vasculature (a) *Diplacanthus*; (b) The stem-chondrichthyan *Acanthodes*, redrawn from Davis et al. (2012); (c) The stem-chondrichthyan *Doliodus*, redrawn from Maisey et al. (2009); (d) The symmoriiform *Dwykaselachus*, redrawn from Coates et al. (2017a); (e) The actinopterygian *Raynerius*, redrawn from Giles et al. (2015b), (f) The sarcopterygian *Ptyctolepis*, redrawn from Lu et al. (2017), (g) The stem-gnathostome *Dicksonosteus*, redrawn from Goujet (1984), (h) The stem-gnathostome *Janusiscus*, redrawn from Giles et al. (2015c)

basioccipital. This canal is punctured by a pair of perpendicularly oriented canals which exit onto the lateral surfaces of the element. Although Miles considered that this internal canal would have carried the median dorsal aorta, he eventually concluded that it was instead likely to be the notochordal canal, due to his interpretation of a postero-ventral groove on the base of the element as having carried the median dorsal aorta instead. On the basis of the anatomy of *Diplacanthus* it seems possible that the notochordal canal of Miles was instead the canal for the median dorsal aorta, punctured laterally by occipital arteries, in which case the groove on the ventral surface could then instead be a partially mineralized

ventral notch. However, this is difficult to confirm either way from casts I have studied. A putative basioccipital has also been described (Fig. 4.5h), associated with *Milesacanthus*, a diplacanthid from the Middle Devonian of Antarctica (Young and Burrow, 2004). This bone is also hourglass-shaped, with an almost barrel-shaped middle region like *Diplacanthus*, and a marked posterior notch.

4.3.2 **Vertebral elements**

Ossifications of the vertebral column are preserved posterior to the braincase (Fig. 4.14.2). These comprises paired neural and arches, corresponding to the decription of Watson (1937) (corroborated by Miles (1970)). The most complete neural arch is preserved dorso-ventral to the neurocranium. It is shallowly convex on one side, suggesting it likely comes from the right hand side of the vertebral column. It has a pronounced neural spine and two ventral processes joined by a fragmentary sheet. Anteriorly to this is what I consider to be its likely left antimere, although it is incomplete. Ventral arches are also present; however *contra* Watson (1937) and Miles (1970) these appear more similar to lower arches carrying the notochord than to haemal arches. One half of the best preserved ventral arch is preserved ventral to the neural arches, again from the left-hand side of the vertebral column. This is stout and has a marked groove in the internal face. Flattened examples lie more posteriorly in the vertebral column (Fig. 4.1a) Miles (1970) suggests that this joined with its right hand half below the notochord. The right hand half of the element is crushed anteriorly to it.

4.3.3 **Mandibular skeleton**

The palatoquadrate of *Diplacanthus* resembles that of *Acanthodes* comprising quadrate, metapterygoid, and autopalatine parts, with a pronounced otic process

FIGURE 4.7: Mandibular and hyoid skeleton (a) in lateral view; (b) in medial view; (c) showing postero-medial displacement of metapterygoid relative to quadrate; (d) articulation between the left Meckel's cartilage and palatoquadrate; (e) right Meckel's cartilage in medial view; (f) left Meckel's cartilage in posterior view ; (g) left Meckel's cartilage in lateral view. Abbreviations: L, left; R, right.
.

(Fig. 4.7) Miles (1973b). The quadrate is tall, slightly concave laterally, and has a pronounced extrapalatoquadrate ridge. In cross section it is formed from chondrified walls, with an irregularly chondrified core - similar patterns of chondrification have been reported in the palatoquadrate of *Climatius* and *Gogoselachus* (Burrow et al., 2015; Long et al., 2015). Like *Acanthodes*, at its proximal end it has a large post-articular process, and a piece of overlying cartilage that we interpret as a disarticulated prearticular process (Fig. 4.7d). Antero-dorsally to the quadrate the dorsal part of the metapterygoid is preserved - unlike *Acanthodes* this does not appear to have a pronounced continuation of the extrapalatoquadrate ridge on the dorsal side. The metapterygoid is continued as a mould in the surface of the specimen suggesting that it extended ventrally to at least some extent (Fig. 4.7c). In the dorsal part of the metapteryogoid is a foramen, like that seen in *Acanthodes* and proposed by Miles to carry the mandibular branch of the trigeminal (V) nerve (Fig. 4.7a). A concavity on the dorso-anterior face is the otic cotylus, and a cone-like concavity ventral to it may be an auxiliary otic cotylus. The autopalatine is solidly chondrified, with a pronounced basal process (Fig. 4.7a) - presumably this comes from the left side of the animal, but it is not impossible that it is the right autopalatine. It is broad dorsally, with the upper surface forming a shelf below the basal process- this is punctured by two foraminae, possibly for the maxillary nerve. Its profile tapers ventrally to a blade-like ventral margin.

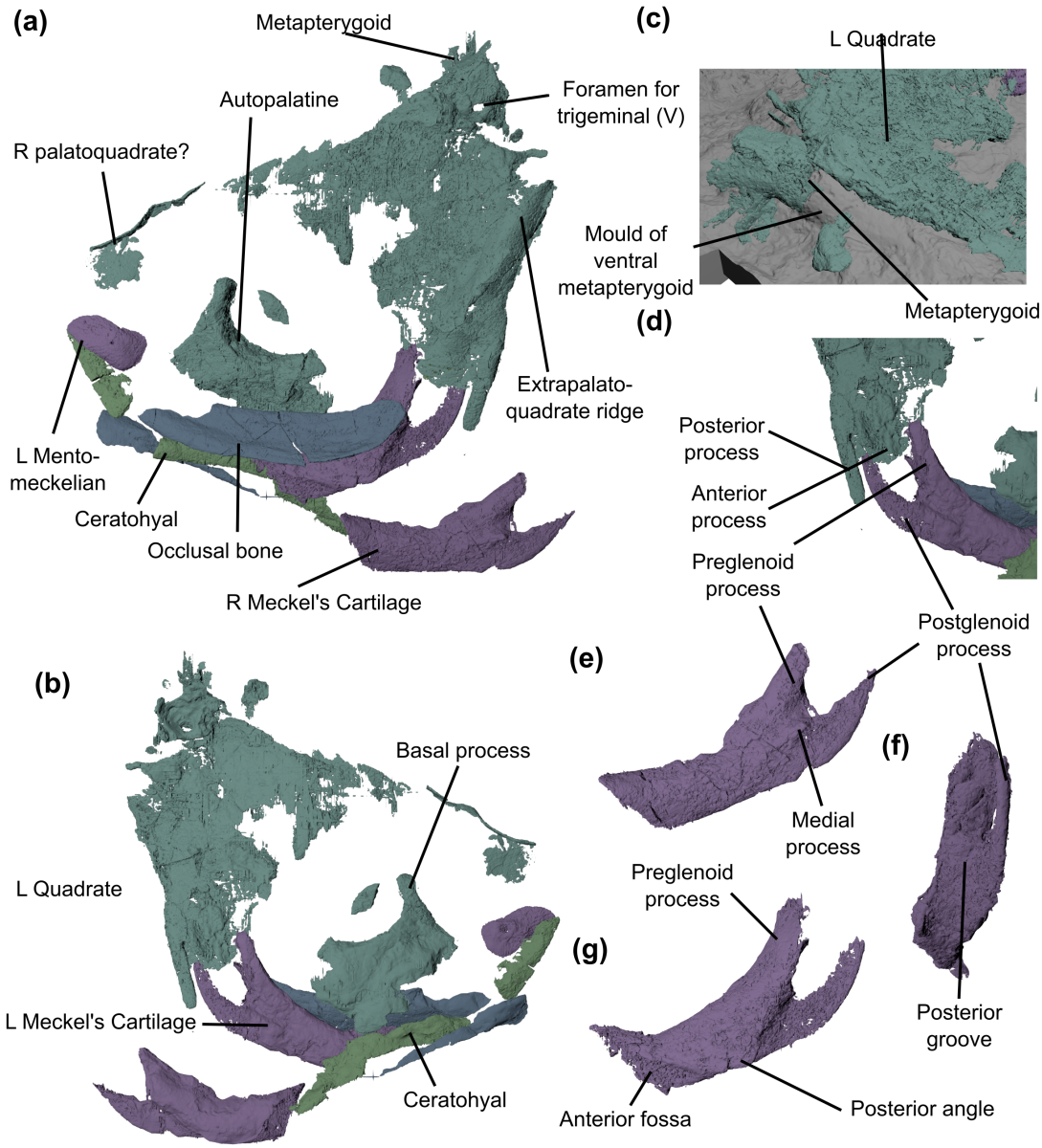


FIGURE 4.7: Caption on previous page

Diplacanthus preserves the articular part of both left and right Meckel's cartilage (Fig. 4.7e-g). The left of these is preserved in approximately life position, ventral to the palatoquadrate, whereas the right is displaced ventrally. While both are worn at the surface of the specimen, the sides facing into the matrix allow reconstruction of the entire element. The cartilage is short and deep relative to its width, and gently curved. At its proximal end it is strongly forked into pronounced pre- and post-glenoid processes. The larger of these, the pre-glenoid process, forms an oblique flange across the width of the element(Fig. 4.7g). The postglenoid process is thinner and curves postero-dorsally from the mesial side of the element. The depth of the glenoid fossa and the poor mineralisation within suggest that the articulation itself might have been on a shallower, unmineralised surface. Postero-ventrally to the glenoid fossa the pre- and post-glenoid processes flank a posterior groove that travels around and underneath the back of the articular, shallowing out about half way along the ventral side of the element (Fig. 4.7f). The lateral face of the Meckelian element, the surface of which which is continuous with that of the pre-glenoid process, forms an elbow laterally to this trough, below which the adductor mandibulae would have attached. Anteriorly the dorsal surface tapers to a point, demarcating the top of an anterior fossa facing laterally on the distal end of the element. The medial face of the cartilage is convex with a small, medially oriented process which forms the beginning of a short antero-posterior ridge. The medial surface tapers anteriorly to form the medial border of the antero-ventral fossa's. Broadly speaking, the cartilage is similar to that of *Tetanopsyrus* (Hanke et al., 2001a; Gagnier and Wilson, 1995), with a high profile, large pre- and post-glenoid processes, and a pronounced postero-lateral angle.

Variable borders in the anterior fossa of either antimere suggest that the middle portion of Meckel's cartilage was unmineralised. This is similar to conditions in various other stem-chondrichthyans, including *Acanthodes* (Watson, 1937), *Tetanopsyrus* (Hanke et al., 2001a; Gagnier and Wilson, 1995) and in *Gladbachus*

(Coates et al., 2018). The surface of the cartilage is smooth, and there is no evidence for any kind of dental groove or sulcus like that found in many Palaeozoic chondrichthyans (e.g. (Pradel et al., 2014; Gross, 1938)). Well anterior to these elements is a small subrectangular chondrification which I interpret as the anterior, or mentomandibular, part of the left Meckel's cartilage (Fig. 4.7a,b). At its anterior extent it pinches in laterally, forming a medially inturned lateral blade, and it is punctured by a single canal, which has a thin lateral foramen and a far wider medial foramen, probably for a ramus of the mandibular sensory canal. Associated with this are parts of thin rod-like chondrifications which probably constituted either one or both ceratohyals - these are two fragmented to describe in detail, but seem similarly proportioned to ceratohyals in *Acanthodes*, which are also somewhat rod-like (Miles, 1973b). There is no evidence for a ventral mandibular splint, like that found in ischnacanthids and in acanthodids (Watson, 1937). Mandibular splints are poorly typified: while described as dermal in some accounts (Watson, 1937) sectioning of that of *Acanthodopsis* revealed it to be endoskeletal (Burrow, 2004): its possible that they represent a combination of misidentified gular dermal elements and ceratohyals in different taxa. The jaw articulation of *Diplacanthus* comprises a pre- and postarticular process on the palatoquadrate articulate with a fossa on the Meckel's cartilage between the pre- and post-glenoid processes (Fig. 4.7d). This style of articulation seems broadly similar to the condition in *Acanthodes* (Miles, 1973b, 1968).

Lying along the lateral side of the left Meckel's cartilage is a dermal plate - the "occlusal" plate identified in other specimens of *Diplacanthus* (Burrow et al., 2016a). The plate is gently curved and convex in crosssection, with the concave side facing laterally, away from Meckel's cartilage. It extends from the level of the preglenoid fossa beyond the articular - the exact anterior boundary is lost. There is no saddle over Meckel's cartilage, like that in ischnacanthid dentigerous jaw bones (Burrow, 2004). The histology of the bone is not readily visible in the scan, but

it is clearly not globular calcified cartilage, and some kind of lamellar layering is visible in some tomograms. Similar dermal plates in the region of the jaw are also found in various acanthodians associated with "diplacanthiforms"- *Tetanopsyrus* Hanke et al. (2001a), *Culmacanthus* (Burrow and Young, 2012), *Uraniacanthus* (Newman et al., 2012; Hanke and Davis, 2008), *Milesacanthus* (Young and Burrow, 2004), and *Rhadinacanthus* (Burrow et al., 2016a). The position of this bone in *Diplacanthus* confirms the interpretation of Burrow et al. (2016a), that rather than being an external mandibular bone this is was in fact within the gape, and so was presumably involved in food processing. It also confirms that *Diplacanthus* lacked a "coronoid process" to this dermal bone Burrow et al. (2016a), like that described in *Uraniacanthus* (Newman et al., 2012; Hanke and Davis, 2008) and in *Culmacanthus* (Burrow and Young, 2012).

4.3.4 **Branchial skeleton**

The branchial skeleton is preserved mainly as a series of robust ceratobranchial cartilages, associated with likely pharyngo- and epi-branchials (Fig. 4.8). No hypobranchial or basibranchial elements are recognisable, although they could be present in the counterpart or have not mineralised. The overall aspect of the branchial skeleton is difficult to make out due to uncertain symmetry and the missing parts. Unfortunately this precludes identifying very many of the character states associated with branchial skeletons, many of which rely on overall arrangement. However, the anatomy of individual elements is preserved in great detail.

Ceratobranchials are the best preserved of the branchial elements in *Diplacanthus*, with five preserved on the left hand side. The ceratobranchials are curved, and posteriorly grooved for the carriage of the afferent branchial arteries and branchial

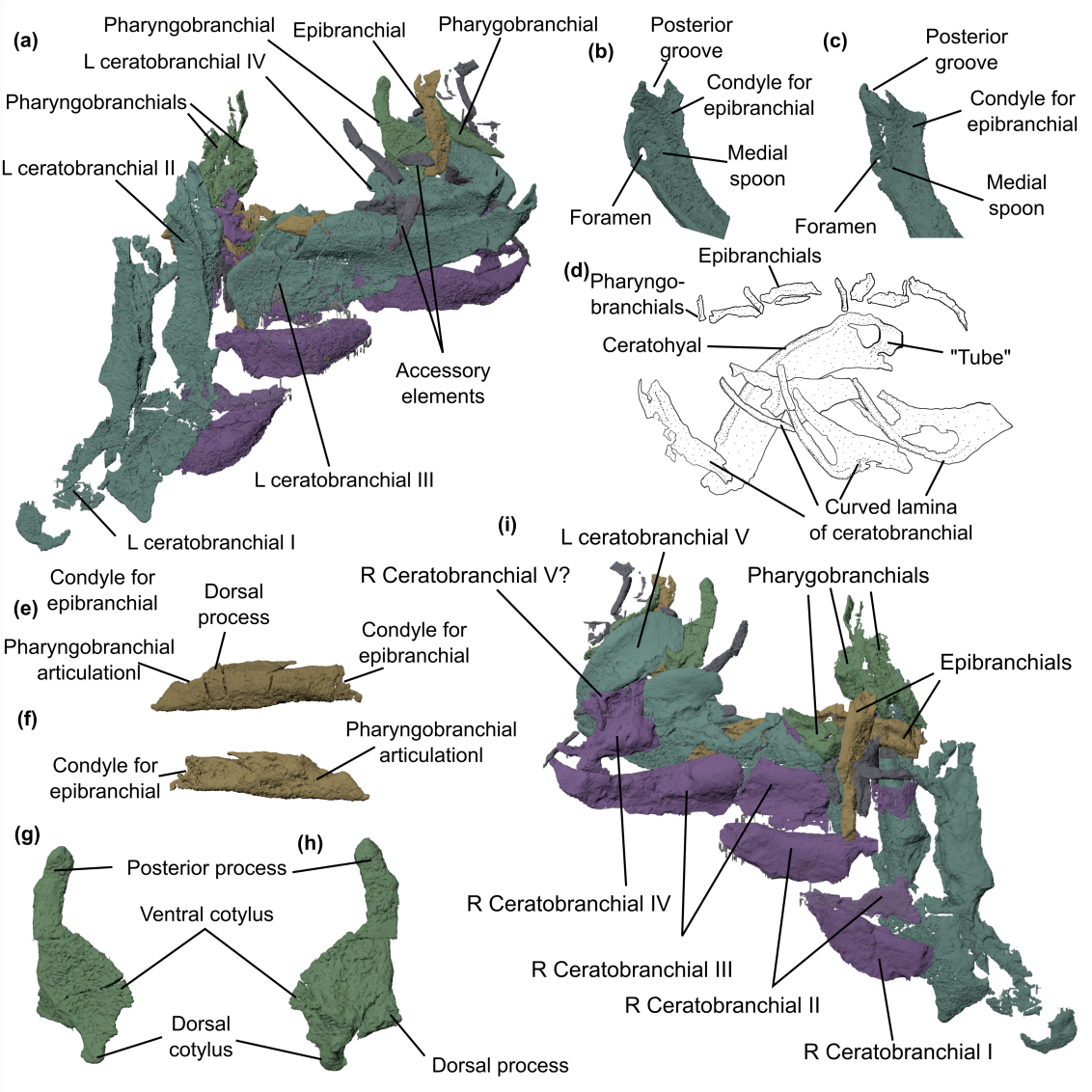


FIGURE 4.8: (a) Entire branchial skeleton from left (internal) side, dermal plate removed; (b) proximal end of ceratobranchial III; (c) proximal end of ceratobranchial II; (d) Interpretation of the branchial skeleton of *Kathemacanthus* from Hanke and Wilson (2010); Epibranchial in (e) lateral, and (f) medial view; Pharyngobranchial IV? in (g) medial, and (h) lateral view; (i) entire branchial skeleton from right (external) side, dermal plate removed. Abbreviations as in Figure 2.

nerve (Gardiner, 1984). The anterior surface is smooth, with no evidence of gill rakers. The proximal ends of the ceratobranchials are square in cross-section - each corner of this square forms a short rounded process, creating between them a cotylus for articulation with the epibranchial (Fig. 4.8b,c). Ventromedially to this cotylus is a spoon-shaped concavity, lying on the antero-dorsal surface of the element just distally to the articulatory condyle, and punctured by a foramen (Fig.4.8b,c) Presumably this foramen transmitted either the vasculature or the nerves - given its size and the continuation of the groove posterior to it probably a nerve. The posterior two corners of the condyle mark the uppermost extent of two ridges that sweep down the ceratobranchial, between them delimiting the posterior groove. As they sweep distally, the ridges turn laterally - combined with the progressive flattening of element's square cross-section this creates a curved sheet-like distal portion of the element. The fifth, ceratobranchial element has a far simpler structure, but contains key elements of its fellows' design, comprising only a curved sheet and a proximal cotylus.

In the second ceratobranchial of *Diplacanthus* the posterior groove is so pronounced proximally that it forms three quarters of a tube, which extends slightly dorsally to the condyle for the epibranchial (Fig. 4.8c). A similar structure is visible in the preserved branchial skeleton of the stem-chondrichthyan *Kathemacanthus*, at the dorsal end of what is labelled by Hanke and Wilson (2010) as a "?scapulocoracoid" (Fig. 4.8d). I suggest instead that this is the ceratohyal which has become posteriorly displaced, with a similar dorsal tube to that of *Diplacanthus*. The "hypobranchial or ceratobranchial cartilages" labelled by Hanke and Wilson (2010) then seem likely to be ceratobranchials, possibly also with as similar spoon shape, or sweeping distal lamina of *Diplacanthus*. Notably the ceratohyal of *Gladbachus* also bears a spoon-shaped concavity at its proximal end - however this appears to be on the lateral side of the element so may not be related Coates et al. (2018).

A number of smaller cartilaginous structures are present at the posterior end of the branchial material (Fig. 4.8a,i). These are thin with rounded off ends but are otherwise featureless. These are associated with the proximal ends of the ceratobranchials - while not articulated with anything I consider the most plausible explanation to be that they are accessory elements, similar to those in Ozarcus, and in extant actinopterygians Pradel et al. (2014).

Four rod-like structures are present which I interpret as epibranchials - these are disarticulated from their arches and so it is impossible to know which arch they belong to (Fig.4.8a,e,f,i). The best preserved of these is trapped between two of the left hand ceratobranchials, and is similar to that of *Acanthodes* Miles (1973b) (Fig. 4.8 e,f). It is short and stout relative to the ceratobranchials, with an approximately elliptical cross section. At its distal end it has a pronounced fossa, oriented dorso-medially, for articulation with the pharyngobranchial. This fossa is delimited posteriorly by a small dorsal process, and anteriorly by an extended ventral process. At its proximal end it has a fossa, cornered by four short processes. Between these fossae runs a shallow posterior groove, which would have carried the branchial nerves and efferent branchial artery. Based on this morphology three of these are probably from the left hand side of the branchial skeleton and one from the right.

Another probable epibranchial is anterior to this, preserved on the surface overlying the ceratobranchials. This element is far larger, suggesting that its well preserved ceratobranchial is one of the more posterior elements. Little morphology is preserved, except for a marked increase in width in the upper two thirds of the element that might be an epibranchial flange, like that seen in *Acanthodes* and *Gladbachus* (Coates et al., 2018). A shallow fossa is also present on the upper face, suggesting that it belongs to the left hand series. Two more possible epibranchials are also present. One of these lies anterior to the others and is probably the head of

a right hand epibranchial - it has a significantly larger cotylus. The posteriormost epibranchial candidate is smaller, and lies between two pharyngobranchials. It is extremely short and has a large fossa on its medial side.

Towards the posterior of the skeleton are two pharyngobranchials in series oriented slightly anteriorly (Fig 4.8 a, g-i). The anterior of the two is the larger (Fig. 4.8g,h)- it comprises a kite-shaped overall shape, the dorsal "tail" of which tapers and bends slightly, with a rounded off end. The element is flat, but thicker at its base, and is slightly concave - whether this concave is true to life or caused by a break at the base of the tail is uncertain. A ridge curves sinusoidally down the side of the element to a slightly bulbous ventral process. Above this the element has a complicated surface. On the side preserved pointing anteriorly a groove runs down the element, flanked where the element thickens a lateral triangular ridge. On the opposite side is another triangular ridge, without a corresponding groove. The smaller pharyngobranchial roughly corresponds with the morphology of the larger one - dorsal and ventral processes are joined by a sinusoidal groove, flanked by a ridge with corresponding triangular process. This posterior pharyngobranchial is not as robust, and the triangular process located more dorsally relative to its height. Throughout the anterior branchial skeleton are a number of other elements which are probably pharyngobranchials. These are however insufficiently well preserved to make a good account of their morphology.

None of the pharyngobranchials in *Diplacanthus* are preserved in articulation with the rest of their gill arch. However, morphologically they and the epibranchials are very similar to the pharyngobranchials of *Acanthodes*, as described by Miles Miles (1973b). In this case, in *Diplacanthus* the dorsal process of the pharyngobranchial would be the posterior process of Miles (1973b), the triangular ridge the dorsal process, and the ventral cotylus the dorsal cotylus (Fig. 8g,h). Miles (1973b) considered that this arrangement resulted in posteriorly pointing

pharyngobranchials in *Acanthodes*. From my examination of *Acanthodes* moulds (eg. NHM P.34914) I believe that this is the more convincing interpretation. If so this seems likely to have also been the case in *Diplacanthus*.

4.3.5 **Dermal skeleton**

Overlying the branchial chamber was a denticulated dermal plate, described by Watson (1937) as an "opercular" bone (Fig. 4.1c). This bone is quite thin - sufficiently so to have been deformed and crushed by the underlying branchial arches. It is wedge shaped, with the wider end ventrally. The denticles are widely spaces and in the ventral part form rows. From its preserved location, overlying several of the ceratobranchials, it seems likely to have been part of the operculum, as Watson (1937) reconstructed it. No grooves for sensory lines are visible, unlike the cheek plate of Culmacanthus, and contra the assertion in Long (1983).

4.4 DISCUSSION

4.4.1 ***Diplacanthus* and a resurrected Acanthodii**

While stem-chondrichthyan phylogeny remains poorly understood, some patterns consistently emerge in phylogenetic analyses. The most glaring of these is a split between crown-chondrichthyans and some stem-chondrichthyans on the one hand, and on the other a rump of acanthodian taxa at the base of the chondrichthyan stem-group Coates et al. (2018). This rump typically comprises taxa usually considered to be diplacanthiforms, ischnacanthiforms, and acanthodiforms, variably arranged as either a clade or a paraphyletic grade: Coates et al. (2018) propose terming this clade the Acanthodii. Establishing whether or not this clade exists, and the arrangement of taxa within it, has important implications for character states in the chondrichthyan

stem-group, such as the plesiomorphic nature of the chondrichthyan dentition.

The current evidence for the existence of this Acanthodii clade comes from dermal characters of spines and scales. The fin spines ornament of ischnacanthids, diplacanthids, and acanthodids has a pronounced anterior ridge (eg. *Diplacanthus* (Burrow et al., 2016a), *Nerepisacanthus* (Burrow and Rudkin, 2014), and *Halimacanthodes* (Burrow et al., 2012)), unlike the more evenly ridged spines in other stem-chondrichthyans (eg. *Climatius* (Burrow et al., 2015)). The scales of these three putative groups also have a distinctive anvil-shape, with a constricted neck, and grow by the concentric "onion-skin" mode of growth supposedly typical of acanthodians (Denison, 1979; Burrow et al., 2016a). More generally these animals tend to lack tooth whorls and have a reduced complement of spines and dermal armour compared to more crownwards taxa (Miles, 1973a).

Comparison of the endoskeletons of *Diplacanthus* and *Acanthodes* add further possible characters supporting this rump grade. An osteichthyan-like basioccipital, which is constricted relative to the overlying otic region, is shared by *Diplacanthus*, *Acanthodes*, and probably *Milesacanthus* (Miles, 1973b; Young and Burrow, 2004). This contrasts with the laterally broad basioccipital region in crown-chondrichthyans, *Doliodus* (Maisey et al., 2009), *Gladbachus* (Coates et al., 2018), *Pucapampella* (Maisey and Anderson, 2001; Maisey, 2001a), and probably *Ptomacanthus* (Brazeau, 2009), which is likely a chondrichthyan synapomorphy. This is borne out by the presence of a laterally restricted condition in the putative stem-gnathostomes *Janusiscus* (Giles, Friedman, et al. 2015) and *Ramirosuarezia* (Pradel, Maisey, et al. 2009). In the mandibular skeleton the preglenoid process of both *Acanthodes* and *Diplacanthus* forms an oblique flange, rather than a more rounded shape as in more crownwards chondrichthyans (Coates et al., 2018) (this is inapplicable in known ischnacanthids, which lack a preglenoid process (Long,

1986b)).

The endoskeleton of *Diplacanthus* also provides some evidence for the relative relationships of the constituent groups in the Acanthodii. A perforation in the metapterygoid, likely for the mandibular branch of the trigeminal nerve (V), is present in several possible acanthodiforms: *Acanthodes*, *Cheiracanthus*, and *Homalacanthus* (Watson, 1937; Miles, 1973b; Gagnier, 1996). In metapterygoids of *Ischnacanthus* I have observed (eg. NHM P7000) I have found no evidence of any such perforation, and more crownwards chondrichthyans also lack it. This could then be a character uniting diplacanthiforms and acanthodiforms to the excluion of ischnacanthids and other chondrichthyans. Similarly present in *Diplacanthus* and *Acanthodes* is the separate mineralisation of the autopalatine, quadrate, and metapteryoid (Miles, 1973b), which is also absent in ischnacanthids and other stem-chondrichthyans (eg. Coates et al. (2018)).

The placement of the Acanthodii in phylogenetic analyses points towards their emergence from an early chondrichthyan stem-group with "climatiid"-like plesiomorphies. Many of the morphologies seen in these "climatiids", such as prepectoral spines (eg. Hanke and Davis (2008); Hanke (2008)) and large cranial roofing tesserae , are also found in some ischnacanthiforms, acanthodiforms, and diplacanthiforms (eg. Hanke and Davis (2008); Hanke (2008); Valiukevičius (2003)). Some acanthodians have proved difficult to fit into established groupings, such as *Euthacanthus* and *Latviacanthus* (Watson, 1937; Newman et al., 2011, 2014; Schultze and Zidek, 1982) due to their combination of climatiid-like and acanthodiform-like character states. Similarly there exist some obscure taxa poorly represented by articulated remains, such as *Acanthodopsis*, an acanthodid with ischnacanthid-like teeth (Burrow, 2004), and *Acritolepis*, a supposed ischnacanthid with a climatiid-like shoulder girdle (Valiukevičius, 2003). Fleshing out our understanding the anatomy of these acanthodians will be crucial to untangling the interrelationships of the three

grades that form the Acanthodii, and their relationship to chondrichthyans as a whole.

4.4.2 **Are diplacanthids a clade?**

A number of articulated taxa have been associated with *Diplacanthus* in the past, in the putative diplacanthiform group. Most similar to the several species of *Diplacanthus* is the Middle Devonian ORS genus *Rhadinacanthus* (Burrow et al., 2016a), which only really differs in the dermal ornament. *Milesacanthus* is another Middle Devonian (Givetian) taxon, which has also been linked to diplacanthids, although differing in the form of its branchiostegal plates (Young and Burrow, 2004). From the Lochkovian of the MOTH locality and the ORS is *Gladiobranchus*, which also looks diplacanthid-like but with branchiostegal plates (Miles, 1973a; Newman et al., 2012; Hanke and Davis, 2008; Bernacsek and Dineley, 1977). Two more dubious members, which are often not recovered with *Diplacanthus* in phylogenetic analyses (eg. Giles et al. (2015c)) are the Lochkovian *Tetanopsyrus*, also from the MOTH site (Hanke et al., 2001a; Gagnier et al., 1999; Gagnier and Wilson, 1995), and the Early-Middle Devonian *Culmacanthus*, from the Bunga beds of New South Wales (Long, 1983; Burrow and Young, 2012).

Beyond overall similarity several characters have been proposed which unite these diplacanthiforms to the exclusion of other "acanthodians". Deep fin spine insertions are present in all of these taxa, with the exception of *Tetanopsyrus* (Hanke et al., 2001a). These insertions also have a characteristic ornament of fine longitudinal striations (Burrow et al., 2016a). Another commonality is the presence of "occusal" smooth dermal plates (Newman et al., 2012), many of which were originally misreported as Meckelian cartilages (eg. Hanke and Davis (2008)) or as mandibular splints (eg. Watson (1937)). These have also been identified in all of the

above taxa, with the presence or absence of a dorsal process on the bone possibly holding further grouping information. The scapulocoracoid of *Diplacanthus* has a pronounced posterior flange, which also appears to be present in *Uraniacanthus*, *Rhadinacanthus*, *Culmacanthus*, and possibly *Milesacanthus* (Hanke and Davis, 2008; Young and Burrow, 2004; Burrow and Young, 2012; Burrow et al., 2016a). Finally an enlarged circum-orbital tessera, antero-dorsal to the orbit, is present in *Diplacanthus*, and also seems to be shared with other diplacanthiforms (Hanke and Davis, 2008).

A core of articulated diplacanthiform taxa exists which can be united with reasonable confidence. *Diplacanthus* genera are found both in the Middle Devonian of both Scotland and Canada, and seem similar in anatomy. *Rhadinacanthus*, also Middle Devonian, also seems extremely likely to be a member of a diplacanthiform clade, sharing all of the above features with *Diplacanthus*. While *Uraniacanthus* retains a number of probably plesiomorphic traits, such as prepectoral spines and branchiostegal plates, it too shares all of the above characters with *Diplacanthus* (Miles, 1973a; Newman et al., 2012; Hanke and Davis, 2008; Bernacsek and Dineley, 1977). The same is also probably true of *Milesacanthus*: although less well known than *Uraniacanthus*, it has a deep fin spine insertion, smooth occlusal plates, and a remarkably similar looking procoracoid to *Diplacanthus* (Miles, 1973a; Young and Burrow, 2004).

While the placement of *Tetanopsyrus* with these taxa is less safe, it also has a set of diplacanthiform-like characters in addition to some possible acanthodian plesiomorphies. It has a large tessera antero-dorsal to the orbit, as well as smooth occlusal plates (Hanke et al., 2001a): the presence of these on both the upper and lower jaws may be plesiomorphic if they are homologous with those of ischnacanthids. The lack of a deep dorsal fin spine insertion may be another plesiomorphic character. What is known of the endoskeleton of *Tetanopsyrus* looks rather like that of *Diplacanthus*. The articular of the Meckel's cartilage has a deeply

forked glenoid, as well as a pronounced ventro-posterior angle (Gagnier and Wilson, 1995). The palatoquadrate was interpreted by Brazeau as being placoderm-like, with no otic process (Brazeau, 2009). Comparison with *Diplacanthus* suggests to me that instead what is preserved is the quadrate, with the low anterior area being the upper occlusal plate.

Culmacanthus is another taxon which has been associated with diplacanthiforms (Long, 1983) - however it has a tendency to be recovered apart from them in phylogenetic analyses. Burrow and Young (2012) identify an occlusal plate in *Culmacanthus*. They also reinterpret one of the original specimens as upside-down - this has the effect of showing that the deeply inserted "pectoral spine" originally described is in fact a deeply inserted dorsal fin spine, with longitudinal striations (Burrow and Young, 2012; Long, 1983). What Long (1983) describes as a circumorbital ring in this specimen is in morphology more similar to the sclerotic ring of other stem-chondrichthyans (see examples in Burrow et al. (2011)), being smooth and surrounding the orbit. The reinterpretation by Burrow and Young (2012) has the effect of shifting a denticulated bone which long identified as circum-orbital antero-dorsally to the orbit - I suggest that this is in fact a diplacanthid-like antero-dorsal circumorbital. Following this interpretation, *Culmacanthus* is indeed likely to be a diplacanthiform, with the enlarged circum-orbital tessera, and diplacanthid-like spines and shoulder girdle (Burrow and Young, 2012).

An unexpected ally of the diplacanthiforms in some recent phylogenetic analysis has been the enigmatic Middle Devonian *Ramirosuarezia* (Pradel et al., 2009a). *Ramirosuarezia* has been recovered in some recent analyses (Qiao et al., 2016; Zhu et al., 2016) among stem-chondrichthyans, particularly diplacanthiforms, although notably not by (Coates et al., 2018). I consider this placement is erroneous, and mainly based on the mis-scoring of the dorsal process as putatively homologous with that of *Uraniacanthus*. In fact, the two bones are clearly not homologues - that of

diplacanthids is a dermal bone, whereas that of *Ramirosuarezia* is toothplate-bearing and presumably Meckel's cartilage (Pradel et al., 2009a). As Pradel et al. (2009b) observe, no acanthodian-like scales are visible in the nodule, and there is no great resemblance between the braincase of *Ramirosuarezia* and what is known in acanthodians, so this identification is probably wrong.

4.4.3 **Broader implications for gnathostome endoskeletal architecture**

These new data from *Diplacanthus* fit into a broader emerging picture of early vertebrate evolution, with all acanthodian-grade taxa situated in the chondrichthyan stem-group (Brazeau and de Winter, 2015). In many respects the endoskeleton in *Diplacanthus* is consistent with expectations drawn from this. A ventral fissure separating the basioccipital and basisphenoid regions is also present in early osteichthyans such as *Raynerius* (Giles et al., 2015b), as well as in the early chondrichthyans *Pucapampella* (Maisey and Anderson, 2001; Maisey, 2001a), *Acanthodes* (Davis et al. 2012), and probably *Ptomacanthus* (Brazeau, 2009). Meanwhile an otico-occipital fissure is widely present in early osteichthyans such as *Mimipiscis* (Gardiner, 1984) and *Eusthenopteron* (Jarvik, 1980), and in early chondrichthyans such as *Dwykaselachus*, *Cladodoides*, *Pucapampella* and *Acanthodes* (Coates et al., 2017a; Maisey, 2005; Maisey and Anderson, 2001; Maisey, 2001a; Davis et al., 2012). A pronounced otic process of the palatoquadrate is also widespread in early chondrichthyans and osteichthyans - the placoderm-like low palatoquadrate of *Tetanopsyrus* is probably not as interpreted by (Brazeau, 2009) (see above). All of these features are almost certainly symplesiomorphic for crown-gnathostomes, uniting taxa crownwards of placoderms (Brazeau and Friedman, 2014).

A preglenoid process in *Diplacanthus*, meanwhile, provides further evidence of the chondrichthyan affinities of acanthodians. In chondrichthyans and *Acanthodes*

the mandibular knob (preglenoid process) of Meckel's cartilage inserts into a cotylus in the palatoquadrate, with a condyle on the palatoquadrate inserting into a cotylus on the Meckel's cartilage (Lane and Maisey, 2012; Hotton, 1952). In contrast, osteichthyans lack a preglenoid process, having a bipartite convex articulation on the Meckel's cartilage (eg. (Gardiner, 1984; Jarvik, 1953; Friedman and Brazeau, 2010)), while in arthrodire "placoderms" the quadrates articulates with a condyle on the Meckel's cartilage, bounded by a lateral flange (Hu et al., 2017). Notably ischnacanthid acanthodians also lack a preglenoid process, instead having a single process of the articular which inserts into a concavity on the quadrate (Watson, 1937; Burrow, 2004; Long, 1986b; Gagnier and Wilson, 1995). *Poracanthodes* is described as having an articular process that extends into a recess in the Meckel's cartilage (Valiukevičius, 1992), which Gagnier and Wilson (1995) believe is a modified *Acanthodes*-like articulation: however this is poorly figured (Friedman and Brazeau, 2010). Regardless, the preglenoid process in acanthodians is probably homologous with that of other chondrichthyans.

A feature common to *Diplacanthus* and some stem-group chondrichthyans is a pronounced dorsolateral ridge of the otic capsule. This is present in *Acanthodes*, although the lateral fossa it creates is considerably less marked (Davis et al., 2012). It is also present in the stem-chondrichthyan *Pucapampella* (Maisey, 2001a; Maisey and Anderson, 2001). In *Doliodus* a lateral projection of the cranial roof on the left hand side appears curves down slightly in what might be the same structure (Maisey et al., 2009), although the flattening of the specimen makes this difficult to confirm. This ridge is clearly absent in most other chondrichthyan braincases, for example in *Cladodoides*, *Orthacanthus*, and *Dwykaselachus*, where the neurocranial roof instead slopes between the dorsal otic crest and the lateral otic ridge (Maisey, 2005; Schaeffer, 1981; Coates et al., 2017a). It is also absent in osteichthyans such as *Raynerius* (Giles et al., 2015b) and *Ligulalepis* (Basden and Young, 2001), and in *Janusiscus* (Giles et al., 2015c). Notably however a broad extension of the otic region

is present in the stem-group elasmobranchs *Tristychius* and *Acronemus* (Coates and Tietjen, 2018; Maisey, 2011), although its homology with the lateral otic ridge is unclear (Coates and Tietjen, 2018) This seems to be a widespread feature of chondrichthyan neurocrania, possibly plesiomorphic for the crown-group.

While the branchial arches of *Diplacanthus* are disarticulated, they are interpretable with respect to *Acanthodes* and seem to be broadly similar in form. Like *Acanthodes* (Miles, 1973b), *Ptomacanthus* (Chapter 3), *Gladbachus* (Coates et al., 2018), and *Ozarcus* (Pradel et al., 2014) a dorsal ridge is present on the pharyngobranchials. A major source of debate in reconstructing the branchial arches of *Acanthodes* has been whether the pharyngobranchials are oriented anteriorly, as in osteichthyans, or posteriorly, as in chondrichthyans (Miles, 1973b; Pradel et al., 2014). *Diplacanthus* offers no decisive information on this, however structures I interpret as pharyngobranchials at the anterior of the branchial chamber are posteriorly oriented. Meanwhile, the similarity of the posterior pharyngo- and epibranchials to those of *Acanthodes* does suggest that they might configure similarly to the reconstruction of Miles (1973b). This is similar to the state observable in many *Acanthodes* specimens, such as NHM P.34914, in which the pharyngobranchials do appear to point posteriorly.

The curious morphology of the heads of the ceratobranchials in *Diplacanthus* bears comparison with some other stem-chondrichthyans. The presence of tube at the top of a ventral visceral element in both *Diplacanthus* and *Kathemacanthus* (Hanke and Wilson, 2010) suggests that it might be part of a more widespread stem-chondrichthyan branchial anatomy, although there is no evidence for similar morphology in *Gladbachus*, *Ptomacanthus*, or *Acanthodes* (Coates et al., 2018; Miles, 1973b) (Chapter 3). Spoon-shaped heads of ceratobranchials are possibly present in *Kathemacanthus* (Hanke and Wilson, 2010). The spoon-shaped heads of the ceratobranchials are very similar to what appears to be a spoon-shaped head of the

ceratohyal head in *Gladbachus* (Coates et al., 2018) - notably however, in *Gladbachus*, this spoon is on the lateral, rather than the medial, side of the element. A ceratohyal fossa is present in several chondrichthyans (Long et al., 2015; Coates et al., 2018) - it is possible that the spoon is a shallower prelude to this morphology.

One aspect of the anatomy of *Diplacanthus* is less easily interpretable as part of a shared early chondrichthyan anatomy. The investment of the median dorsal aorta in the floor of the braincase is a classic actinopterygian synapomorphy (Schaeffer, 1968; Friedman and Brazeau, 2010), present in Palaeozoic members of the clade (Giles et al., 2015b; Gardiner, 1984), as well as in living polypterids (Allis, 1922). Although the condition is unknown in possible stem-osteichthyans *Ligulalepis*, *Guiyu*, *Psarolepis* and *Achoania* (Basden et al., 2000; Basden and Young, 2001; Clement et al., 2018; Zhu et al., 2009, 1999, 2001), its absence in early actinopterygians such as *Cheirolepis* (Giles et al., 2015a) suggests it is apomorphic in actinopterygians rather than plesiomorphic for osteichthyans. The condition is actually also already present in the chondrichthyan total-group, in symmoriiforms (eg. *Dwykaselachus* (Coates et al., 2017a)). However the presence of this condition in an acanthodian-grade stem-chondrichthyan is curious, particularly given its apparent absence in *Acanthodes*, and raises the possibility that it is a crown-gnathostome symplesiomorphy.

Really however this character atomises into two separate characters, as recognised in recent phylogenetic character sets (Coates et al., 2018, 2017a). The first is the point at which the median dorsal aorta splits into lateral dorsal aortae underneath the braincase. This split can either occur either underneath the braincase, as in *Diplacanthus*, *Acanthodes*, symmoriiformes and actinopterygians, or posterior to it, as in most other chondrichthyans (eg. *Doliodus* (Maisey et al., 2009)), sarcopterygians (eg. *Ptyctolepis* (Lu et al., 2017)), and stem-gnathostomes such as *Janusiscus* (Giles et al., 2015c) and *Buchanosteus* (Young, 1979). The second is the investment of the aorta (whether single or paired) in the basicranium. In

many osteichthyans and chondrichthyans it is invested, (eg. *Doliodus*(Maisey et al., 2009), *Raynerius*(Giles et al., 2015b)), whereas in stem However this investment is variable and probably dependent on the mineralisation of the basicranium - in the sarcopterygian *Ptyctolepis* one lateral dorsal aorta is invested and another is not (Lu et al., 2017), and the investment of the median dorsal aorta varies in specimens of *Cladoselache* (Maisey, 2007). Of these characters then the first seems more reliable: it is possible that this anteriorly positioned split of the dorsal aorta represents a shared character between early stem-chondrichthyans and actinopterygians, but conditions in stem-osteichthyans really need to be established to resolve this.

4.4.4 **Conclusions**

Diplacanthus reveals only the third well-known endoskeleton from an "acanthodian" stem-chondrichthyan. The similarity of this skeleton to that of *Acanthodes*, and their shared dissimilarities with the endoskeletons of other early vertebrates, lends support to the existence of the Acanthodii *sensu* Coates et al. (2018). This similarity also reassuringly bolsters the suitability of *Acanthodes* as a proxy for anatomical conditions in the Acanthodii, in agreement with other Palaeozoic acanthodiforms (Burrow et al., 2012). Within these Acanthodii there is some evidence for diplacanthids as a clade, or at least a cohesive grade. *Diplacanthus* also allows us to identify some patterns within early chondrichthyan endoskeletons the importance of which may be boosted by the discovery of further material.

CHAPTER 5

ENDOCHONDRAL TISSUES IN EARLY VERTEBRATES

5.1 INTRODUCTION

The internal skeletons of gnathostomes are built from a combination of two tissues: cartilage and bone. The distribution of these tissues is more complicated than the etymologies of the cartilaginous chondrichthyans and bony osteichthyans would at first suggest. Endoskeletal bone is found in many members of the chondrichthyan total group (eg. *Akmonistion* (Coates et al., 1998), *Scyliorhinus* (Peignoux-Deville et al., 1982)). Meanwhile in many osteichthyans the endoskeleton is largely formed from cartilage (Hall, 2015). While the dermal tissues of the gnathostome skeleton have been studied in great detail by palaeontologists, far less attention has been lavished upon the tissues of the endoskeleton.

Cartilages are widespread throughout Metazoa, but cartilage homologous with that of gnathostomes is probably restricted to gnathostomes, cephalochordates, hagfishes, and lampreys (Hall, 2015). Plesiomorphically for chordates the entire endoskeleton comprises only cartilage, although some stem-group and crown-group gnathostomes, it merely acts as a precursor to endoskeletal bone. However, it is usually only preserved in fossils when mineralised (examples in Ørvig (1951)). The cartilage that forms the skeleton of crown-group chondrichthyans is a highly specialised mineralised cartilage, covering bones in a mosaic of prismatically calcified tesserae. Far the more phylogenetically widespread mineralised cartilage is globular calcified cartilage, which comprises microscale globules of cartilage mineralised by nanoscale spherules of hydroxyapatite (Dean and Summers, 2006;

Ørvig, 1951). In living chondrichthyans globular calcified cartilage forms a component of their cartilaginous tesserae (Dean and Summers, 2006), hoever it is also found more widely in the chondrichthyan stem-group and in osteichthyans (Sanchez et al., 2014), as well as in various stem-group gnathostomes (Ørvig, 1951; Janvier and Arsenault, 2002; Johanson et al., 2010; Wang et al., 2005) There are some notable differences in the structure of these cartilages (for example in *Palaeospondylus* Johanson et al. (2010) and *Euphanerops* (Janvier and Arsenault, 2002)), however due to the sparsity of sampling these have not been widely used to inform phylogenetic analyses.

Ossified skeletons have a more restricted distribution in gnathostomes, particularly endochondrally ossified skeletons. Perichondral bone, covering the surface of skeletal elements, is still widespread in gnathostomes, being found in chondrichthyans (Coates et al., 1998; Peignoux-Deville et al., 1982; Burrow et al., 2015), osteichthyans (Gardiner, 1984; Sanchez et al., 2014), and in osteostracan and placoderm-grade stem-gnathostomes (Janvier, 1996). Endochondral bone - a network of bony trabeculae inside skeletal elements - is far more restricted in distribution. This tissue is often extensive in osteichthyans, and has been thought to be restricted to the osteichthyan clade (Gardiner, 1984; Smith and Hall, 1990). Others have reported it in stem-gnathostomes (Wängsjö, 1952; Dunkle and Bungart, 1940, 1942, 1943, 1945), meaning it could possibly represent a gnathostome plesiomorphy - however in most of these cases it is poorly documented (Ørvig, 1951). An exception to this is the recent report of endochondral bone by Charest et al. (2018) in the endoskeleton of *Bothriolepis*. While this tissue demonstrates endochondral trabeculae it is in a thin, plate-like bone, and an extensive endochondral matrix like that in osteichthyans does not appear to be present.

Here we attempt to clarify the distribution of endochondral tissues in gnathostomes by describing endochondral tissues in two Devonian gnathostomes

on the basis of three-dimensional tomographic data. The first, *Diplacanthus crassisimus*, is a diplacanthid "acanthodian" with an endoskeleton formed from globular calcified cartilage and perichondral bone. The second is a partial isolated "placoderm" stem-gnathostome braincase, which is formed from an extensive trabecular tissue we identify as endochondral bone. Using this data we re-evaluate the evolution of endochondral tissues in jawed vertebrates.

5.2 MATERIALS AND METHODS

5.2.1 *Diplacanthus*

The *Diplacanthus* material described herein is from NMS specimen 1891.92.334. The presence of unusual mineralisation was noted by Watson (1937), who described "ossification" of the endoskeleton in this specimen. However no attempt that we know of has been made to characterize this tissue, presumably due to the unique nature of the specimen. The specimen is from Tynet Burn, the geological setting of which is described in Chapter 4. The gross morphology of the endoskeleton in this specimen is described in Chapter 4 (braincase and visceral skeleton) and Chapter 6 (procoracoid).

Diplacanthus specimen NMS 1891.92.334 was imaged on Beamline 19 of the European Synchrotron Radiation Facility, using propagation phase-contrast synchrotron microtomography. A broad scale scan with a voxel size of 2.26 μm was carried out, imaging the entire head of the specimen, with an energy of 116keV . We also performed a spot scan at a higher resolution, achieving a voxel size of 0.55 μm. The resulting tomograms were then processed using VG StudioMax 2.2 (Volume Graphics, Germany), and images made in Blender (https://www.blender.org).

5.2.2 **Fragmentary placoderm braincase**

This is an uncatalogued fragmentary braincase [Field number: YG2012.MB.14] from Yamaat Gol, Uvs Province, Mongolia. Yamaat Gol is Early Devonian in age (Alekseeva, 1993) and otherwise preserves invertebrates and numerous placoderm elements as well as minor acanthodian and osteichthyan fragments. This fauna is the subject of ongoing work by Martin Brazeau. This is the only braincase known so far from the locality. It is preserved partially within the matrix, and partially as a mould on the surface, and is quite severely weathered.

The placoderm braincase was imaged using CT (computed tomography) at the University of Bristol in a Nikon XT H 225 ST scanner. The specimen was imaged at 355μA and 222keV, with a 1.5mm copper filter, achieving a voxel size of 66μm. 3D models were rendered in VG StudioMax 2.2 (Volume Graphics, Germany), and the resulting models processed in Blender (https://www.blender.org).

5.3 RESULTS

5.3.1 **Diplacanthus**

The preserved internal skeleton of *Diplacanthus* is mainly formed from calcified cartilage. This tissue forms the visceral arches and braincase, as well as part of the shoulder girdle (Fig. 5.1, 5.2). In the visceral arches and braincase, this tissue is unaccompanied by perichondral bone, and there no obviously distinct perichondral tissue present. Elements of the visceral arches display a common pattern of the cartilage, where an outer layer of calcified cartilage surrounds an inner core (Fig. 5.1a-d). In some areas a very thin sheet of the cartilage forms the outside surface of the object with infill either absent or partial (for example the palatoquadrate or parts of the neurocranium) (Fig. 5.1d). This suggests that elements tended to mineralise perichondrally first, or possibly that the outer part was more heavily

mineralised and that internal parts decalcified during preservation. The cartilage lacks the granular surface texture which authors have used to diagnose the presence of calcified cartilage in other stem-chondrichthyans (eg. in Burrow et al. (2015); Burrow (2004); Long et al. (2015); Hanke and Wilson (2010)).

Internally, the tissue comprises an avascular matrix punctured by chondrocyte lacunae (Fig. 5.1, 5.2). These lacunae vary between about 15 and 40 μm in size (Fig. 5.1, 5.2), although size can varies dependent on the location of the lacuna, and some individual lacunae can get as large as 60μm (Fig. 5.1d). The lacunae are surrounded by radii of cartilage growth, visibly distinct from the interstitial matrix (Fig. 5.1a-d). Rings and lines of Liesegang are visible in parts of the tissue, indicating incremental growth of the cartilage (Hall, 2015; Ørvig, 1951). In some areas the cartilage globules are organised into stacks, in what are likely chondrons like those observed in the cartilage of living jawed vertebrates (Hall, 2015) (Fig. 5.2). Notably there is no evidence for "cell nests" like those observed in the stem-gnathostome *Euphanerops* and cyclostomes (Janvier and Arsenault, 2002). Nor are the chondrocyte lacunae greatly enlarged as in the calcified cartilage of the problematic, possibly chondrichthyan, *Palaeospondylus* (Johanson et al., 2010, 2017).

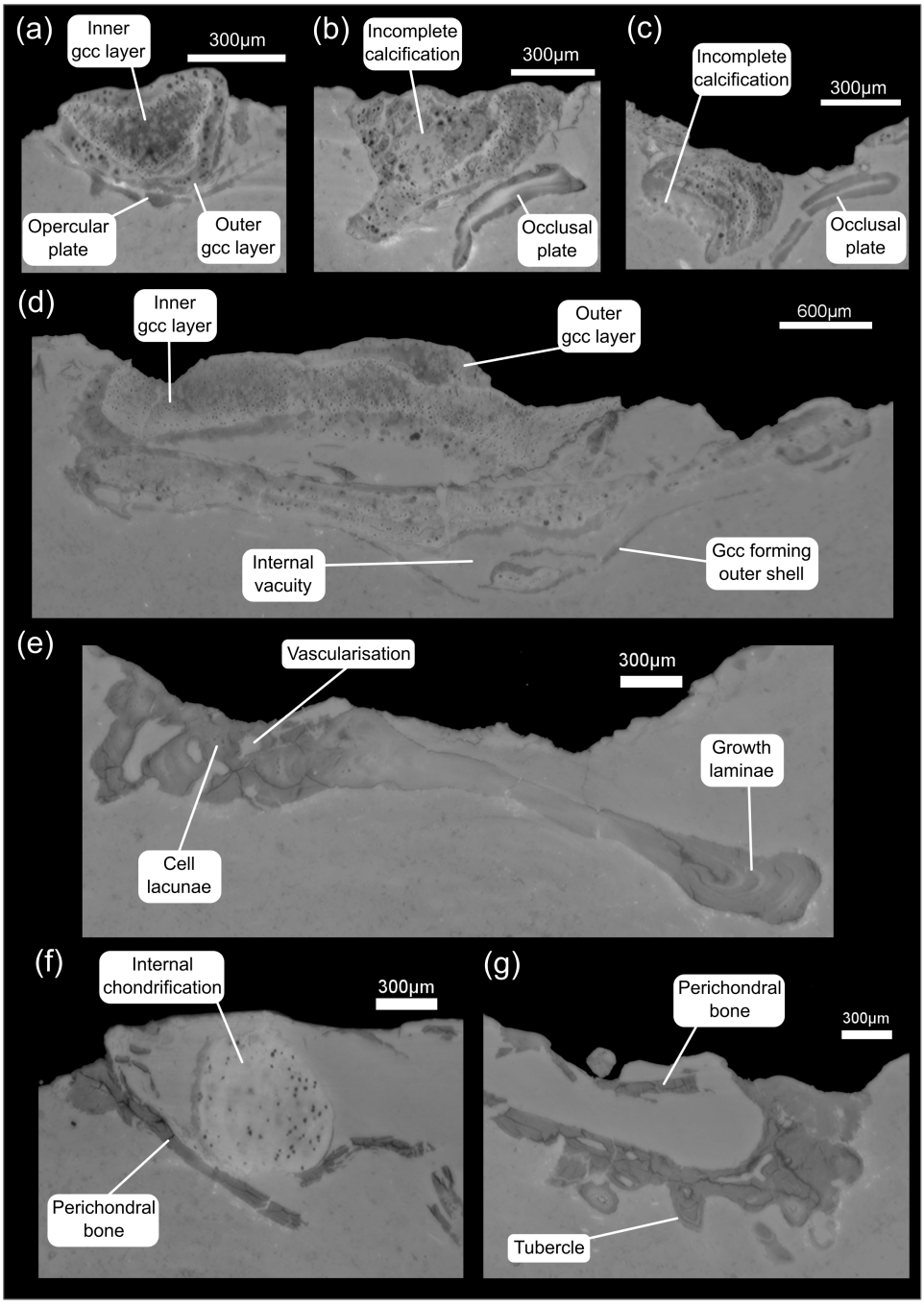


FIGURE 5.1: Caption on next page

FIGURE 5.1: Tomograms showing different section through tissues in *Diplacanthus crassisimus* NMS 1891.92.334. (a) ceratohyal and opercular plate; (b) mid-section of Meckel's cartilage articular; (c) anterior end of Meckel's cartilage articular; (d) palatoquadrate (below) and the anterior ceratohyal (above); (e) ventral plate of procoracoid, (f) cartilaginous core of procoracoid, (g) dermal plate of procoracoid . Abbreviations: gcc, globular calcified cartilage.

The pattern of preservation in *Diplacanthus* indicates that parts of the skeleton were formed from unmineralised cartilage. Like *Acanthodes* (Miles, 1973b), the Meckelian cartilage of *Diplacanthus* is mineralised in two parts: an anterior mentomeckelian and a posterior articular (see Chapter 4). The anterior part of the articular is poorly defined, and isolated chondrocytes radially surrounded by matrix suggest that the calcified cartilage graded into an uncalcified median section of the element (Fig. 5.1c). Internal vacuities in certain elements such as the Meckelian cartilage and the autopalatine, which were presumably filled with unmineralised cartilage in life, contain similar isolated lacunae surrounded by cartilage (Fig. 5.1b). This preservational pattern confirms that preserved tissue in *Diplacanthus* is mineralised cartilage, rather than uniquely well-preserved unmineralised cartilage.

Amongst the skeleton of the head are various dermal elements. The opercular plate is thin - like head tesserae in other acanthodians (Fig. 5.1a), and unlike the dermal bone of most gnathostomes it appears to lack a spongiose inner layer (Giles et al., 2013). The occlusal plate shows little detail, but shows lamellae of growth in places (Fig. 5.1b,c).

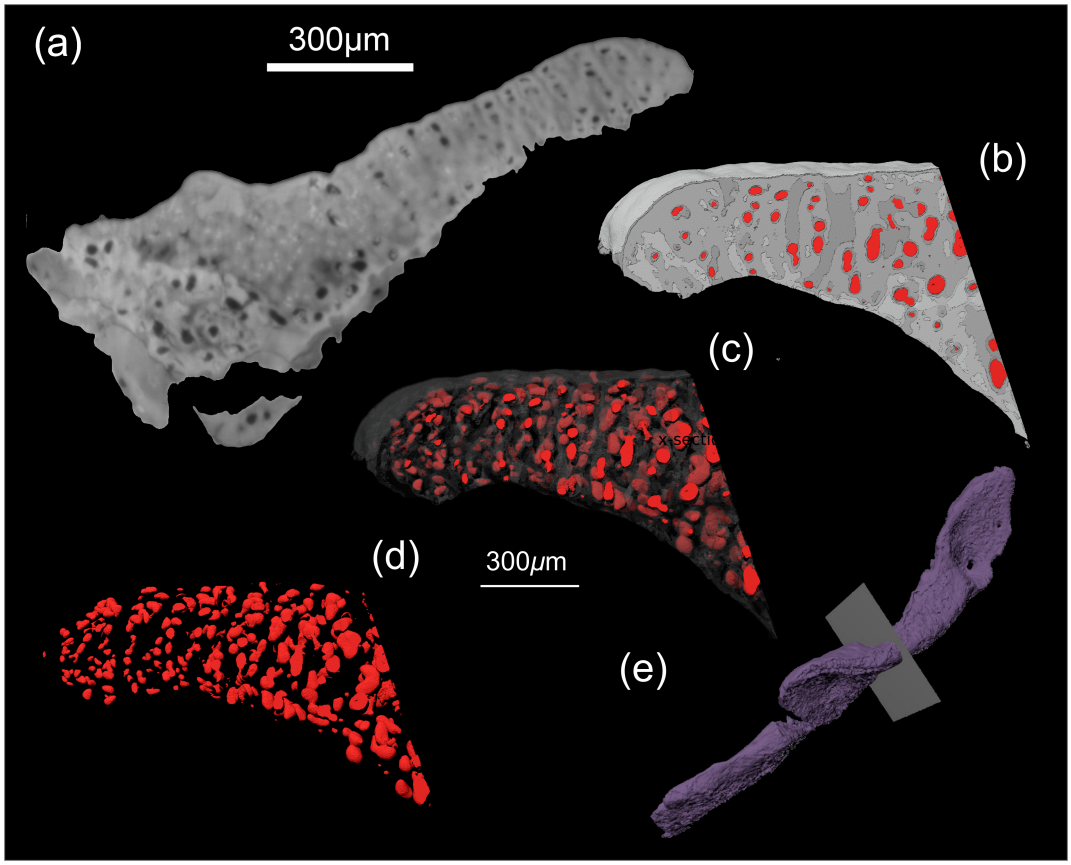


FIGURE 5.2: The three dimensional structure of globular calcified cartilage in *Diplacanthus crassisimus*. (a) section through ceratohyal from tomogram; (b-d) 3 dimensional model of tissue with increasing transparency of cartilage; (e) three dimensional model of ceratohyal with approximate plane of section shown. Colours (b-e): grey, cartilage (variance in shade show differences in threshold); red, chondrocyte lacunae.

Unlike other parts of the skeleton the procoracoid is formed from a combination of calcified cartilage, perichondral bone, and dermal tubercles (Fig. 5.1 e-g, also see full procoracoid model in Chapter 6). Few details of the perichondral bone are visible, but in places growth lamellae are visible. (Fig. 5.1e) The bulk of the tissue appears to be acellular, but in places small spaces around 10μm are visible, which could be osteocyte lacunae(Fig. 5.1e). Shoulder girdles in acanthodian-grade

stem-chondrichthyans are often well mineralised in comparison to the rest of the endoskeleton, and perichondral ossification is a widely accepted explanation for this (Miles, 1973a). A boundary between the tuberculated pad on the procoracoid and the underlying perichondral bone is not visible, but presumably existed. Pulp cavities and growth generations of the tubercles are visible on the tuberculated pad (Fig. 5.1g).

This is the only *Diplacanthus* specimen, from Tynet Burn or anywhere else, known to exhibit such an extensively preserved mineralisation of the internal skeleton. As Watson (1937) notes, the specimen is not particularly large compared to *Diplacanthus* from the same site, so it seems unlikely that its mineralised skeleton is due to the advanced age of the animal. One other Tynet Burn specimen - *Cheiracanthus* NMS 1884.60.3 - also preserves parts of the branchial arches which appear to be mineralised (also uniquely amongst its genus) (Watson, 1937). It is possible that certain concretions from the site have a unique geochemistry preserving calcified cartilage. Unfortunately no record was kept of the specific beds from which specific Tynet Burn specimens were collected in the 19th century (Dineley and Metcalf S J, 1999) so it is difficult to establish whether this is due to conditions in a certain part of the Tynet Burn site.

5.3.2 **Placoderm braincase**

The fragmentary braincase can be identified as an arthrodire or acanthothoracid placoderm-grade stem-gnathostome on the basis of a number of morphological features (Fig. 5.3). The dermal integument is formed from large, macrosquamose plates ornamented with tubercles, characteristic of stem-gnathostomes (Janvier, 1996) (Chapter 5.3b). Although no boundaries between separate plates are visible, based on their relationship to the underlying endocranium they likely comprise

the nuchal plate and part of the paranuchal plates, and possibly parts of the centrals anteriorly (see *Buchanosteus* and *Dicksonosteus* (Young, 1979; Goujet, 1984) . The endocranium is incompletely preserved, but clearly exhibits a large foramen magnum (Fig. 5.3a,b). Characteristic of stem-gnathostomes the notochord is relatively small and continues anteriorly at least until the level of the otic capsules (Fig. 5.3a,b,d). Paired occipital facets appear to be present, along with the weathered remnant of a craniospinal process, both common features of placoderm-grade stem-gnathostome neurocrania (Giles et al., 2015c) (Fig. 5.3a,b). Internally the endocast is comparatively well-preserved, with the two incomplete sides together giving a complete picture of the structure up to the level of the trigeminal (V) nerve. (Fig. 5.3d,e,f) The facial nerve splits deep within the postorbital region, like in crown- and relatively crownwards lying stem-gnathostomes (Brazeau and Friedman, 2014). The otic capsules are widely spaced, like those of other stem-gnathostomes - no sinus superior is present at the *crus commune* and parts of an external semicircular canal are visible (Fig. 5.3d,e,f). The occipital region is elongate with many (five?) spino-occipital nerves, a characteristic of arthrodire placoderms (Young, 1979; Goujet, 1984) (Fig. 5.3d,f). The proportions of the braincase recall those of other acanthothoracid placoderm such as *Romundina* Dupret et al. (2017).

The endochondral part of this braincase is formed from a cancellous tissue (Figure 5.3h), which I identify as endochondral bone. The cancellae within this tissue are irregular in shape and variable in size, but generally have a diameter of approximately 1-2mm. This tissue is distinctly unlike the calcified cartilage of *Diplacanthus* in appearance, consisting of a far less continuous matrix. It also appears unlike more problematic endochondral tissues in animals such as *Palaeospondylous* which is formed from regularly patterned oval spaces (Johanson et al., 2010). The tissue extends throughout the entire braincase, forming an extensive matrix of trabeculae. Notably, this is far more extensive than the isolated trabeculae identified as endochondral bone in *Boreaspis* and *Bothriolepis* (Wängsjö, 1952; Charest et al.,

2018). The margins of the braincase, and of the endocast within is formed from a thicker tissue which we interpret as perichondral bone similarly to other stem-gnathostomes. This suggests that this tissue is osteichthyan-like endochondral bone, with an ossified perichondrium.

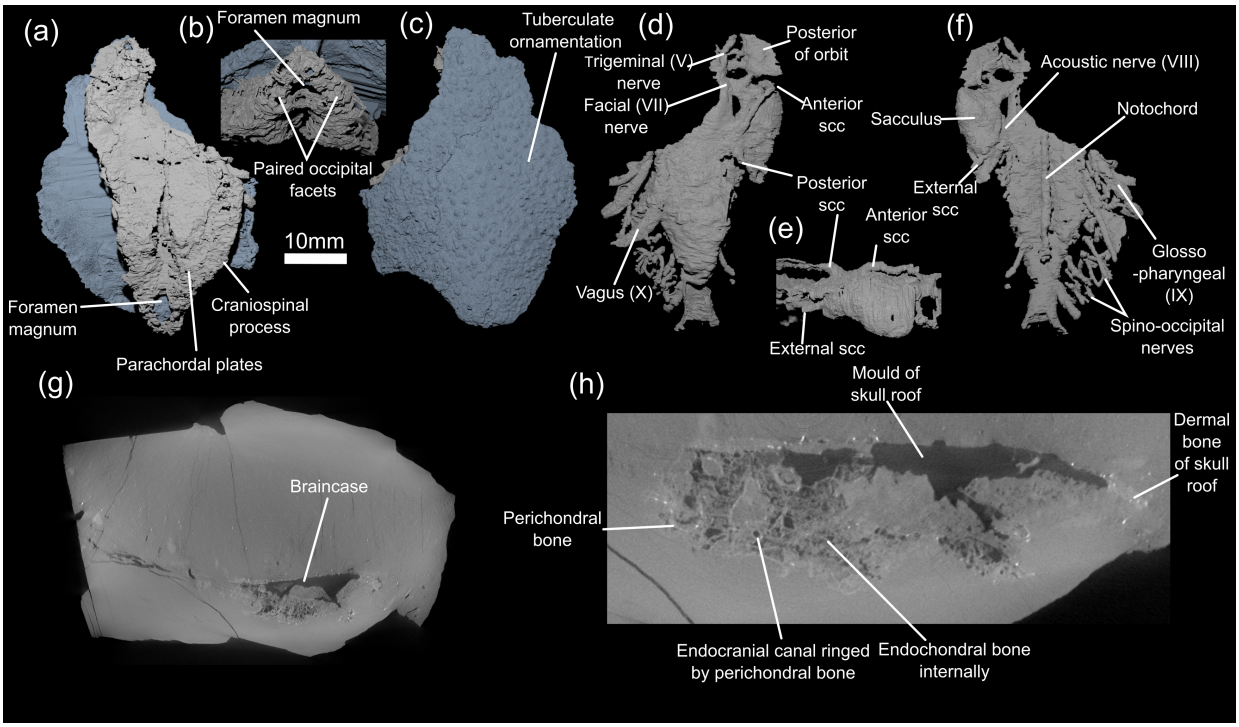


FIGURE 5.3: Endochondral bone in an arthrodire placoderm braincase. (a) ventral view; (b) posterior view of occipital region; (c) dorsal view; (d) endocast in dorsal view; (e) right labyrinth in lateral view; (f) endocast in ventral view, (g) specimen in matrix, (h) close up view of tomogram

5.4 DISCUSSION

5.4.1 **The evolution of tissues in chondrichthyans**

Tessellate prismatic calcified cartilage is a well-established apomorphy of chondrichthyans (Brazeau and Friedman, 2014; Maisey, 2013; Schaeffer, 1981). However the evolutionary transition between globular calcified cartilage (with or without a bony perichondrium) and a tessellate cartilage perichondrium is poorly characterised. This skeletal tissue comprises prismatic (ie. so dense as to be refractive) cartilage, which grades into globular calcified cartilage internally (Dean and Summers, 2006; Dean et al., 2009). The distinct tesserae of this type of calcification are easily visible on the surface of cartilages due to and are readily used to diagnose fossil mineralised elements as being chondrichthyan (Brazeau and Friedman, 2014). They are widely seen in "shark-like" fossil chondrichthyans in stem-elasmobranchs and stem-holocephalans, as well as the likely crown-group symmoriiforms (Coates and Sequeira, 2001a; Zangerl and Case, 1976; Coates et al., 2017a; Pradel et al., 2014), xenacanths (Schaeffer, 1981; Heidtke, 1999), and ctenacanths (Romer, 1964; Williams, 1998; Schaeffer, 1981). This distribution provides weighty evidence in favour of tessellate prismatic calcified cartilage being a chondrichthyan synapomorphy at some level (Brazeau and Friedman, 2014).

Prismatic calcified cartilage is absent in *Diplacanthus* and all other acanthodian-grade taxa in which the histological structure of the endoskeletal tissue is known. While there has been one account of this tissue in the acanthodian *Traquairichthys* by Fritsch (1895), the credibility of this is doubtful (Ørvig, 1951). It is also absent in *Doliodus* Long et al. (2015), despite reports in the articulated specimen's original description (Miller et al., 2003; Long et al., 2015). This creates quite a stark morphological gulf between cartilage types.

Recently two chondrichthyans have emerged which have cartilages that may fill this gap. The first of these, the Late Devonian *Gogoselachus* has a perichondrium with tesserae, but which lack the fibrous interconnections of modern chondrichthyans, instead being embedded in a lacunae-filled matrix (Long et al., 2015). However, the poorly understood relationships of *Gogoselachus* make using it as a comparison difficult. The second is *Gladbachus*, in which most of the perichondrium is lined with "wood-like" continuously calcified ridges (Coates et al., 2018; Heidtke and Krätschmer, 2001). However, in *Gladbachus* irregularly sized and spaced tesserae are found lining the semicircular canals, as well underneath the surface of parts of the continuous calcification. Another potentially important taxon may be *Pucapampella*. While it is also described as having tessellate prismatic calcified cartilage it is poorly figured in the literature. Tesserae are clearly present on the surface of the cartilages of *Pucapampella* (Alan Pradel, pers. comm. 2018), however closer investigation may reveal that it also has an unusually mineralised perichondrium (Maisey, 2001a; Maisey and Anderson, 2001).

On thing that *Diplacanthus* does seem to demonstrate is a preference for calcified cartilage to form towards the outer surface of skeletal elements. In certain parts of elements such as the palatoquadrate and braincase, only the outside surface is mineralised - this seems to also be the case in the jaws of *Climatius* (Burrow et al., 2015). In some stem-gnathostomes, as Coates et al. (2018) [supplementary] observe, the globular calcified cartilage is associated specifically with the perichondral bone rather than deeper within the element (Janvier, 1996), and so globular mineralisation of the cartilage may have originated associated with the perichondrium. Possibly this is linked to the later acquisition of tesselate prismatic calcified cartilage elements, where the inner part of the sheath of perichondral tesserae is formed from globular calcified cartilage with uncalcified cartilage deeper inside elements (Dean and Summers, 2006).

The globular calcified cartilage itself in *Diplacanthus* is consistent with frequent reports of the tissue in chondrichthyans. As well as comprising part of the cartilage of Recent chondrichthyans (Dean and Summers, 2006) globular calfied cartilage has been reported in the possible stem-holocephalan *Akmonistion* (Coates et al., 1998). Thin sections made by Ørvig (1951) showed that globular calcified cartilage formed the endochondral tissue in *Cheiracanthus*, *Acanthodes*, and an unidentified acanthodian from Scaumenac Bay. In the case of *Climatius* this has a granular surface texture (Burrow et al., 2015) which has also been reported and assumed to be globular calcified cartilage in other acanthodian-grade stem-chondrichthyans: *Euthacanthus* (Long et al., 2015), *Kathemacanthus*(Hanke and Wilson, 2010), *Ischnacanthus* (Burrow, 2004), *Parexus* (Burrow et al., 2013), and *Nostolepis* (Burrow and Turner, 2010). A very similar tissue forms the skeleton in in *Doliodus* (Long et al., 2015), *contra* the original report of tessellate calcified cartilage by Miller et al. (2003). Of these, only *Akmonistion* (Coates et al., 1998) and the sections made by Ørvig (1951) are figured in close histological detail - these appear similar in structure to *Diplacanthus*, with similarly sized globules growing concentrically around chondrocyte spaces.

Outside the chondrichthyan crown-group the structure of some globular calcified cartilages is more heterogeneous. Globular calcified cartilages in osteichthyans and in "placoderm-grade" stem-gnathostomes do seem quite similar to that of chondrichthyans in form, with similarly sized and distributed chondrocyte lacunae Ørvig (1951). The calcified cartilage in the likely stem-gnathostome *Eriptychius* also appears to have a similarly organised tissue (Johanson et al., 2010). However, a particularly unusual cartilage occurs in the stem-gnathostome *Euphanerops* (Janvier and Arsenault, 2002). This comprises cell nests, like those found characteristic of cyclostome cartilage (Janvier and Arsenault, 2002) (although note also that cell nests are figured in the tetrapod *Ambystoma* by (Johanson et al., 2010)). The tissue of the enigmatic *Palaeospondylus* is also very unusual, possibly being equivalent to

an ontogenetic stage in the development of endochondral bone (Johanson et al., 2010). The recent proposal that *Palaeospondylus* is a stem-chondrichthyan (Johanson et al., 2017) puts this tissue at odds with what is observed in *Diplacanthus*. If *Palaeospondylus* is a chondrichthyan it seems likely that it either branched off the stem-group before any known acanthodian, or had an a highly apomorphic tissue.

Perichondral bone is another tissue which is probably plesiomorphic for chondrichthyans, however its distribution is less clear. In his endochondral sections Ørvig (1951) identified perichondral bone in *Acanthodes* and the unidentified acanthodian from Scaumenac Bay. It is known on the basis of histology from a wide range of taxa (eg. *Diplacanthus*, (Burrow et al., 2016a), *Acanthodopsis* (Burrow, 2004), *Climatius* (Burrow et al., 2015), and *Akmonistion* (Coates et al., 1998)) and so is clearly widespread in the chondrichthyan stem-group. However its presence is often confidently asserted in acanthodians on the basis of external appearance alone (Burrow et al., 2012). The outward similarity in appearance between the perichondral bone and the globular calcified cartilage in *Diplacanthus* suggests that caution should be taken with this approach, and that some tissues described as bone may be calcified cartilage and *vice versa*.

5.4.2 **The plesiomorphic endochondral skeleton in crown-gnathostomes**

Cancellous endochondral tissues have been reported before in stem-gnathostomes, however these occurrences have been poorly documented and homology with that of osteichthyans met with scepticism (Smith and Hall, 1990; Gardiner, 1984; Friedman and Brazeau, 2010). Dunkle and Bungart (1940, 1942, 1943, 1945) reported cancellous tissues in the endoskeleton of various placoderm stem-gnathostomes from the Cleveland shale, however the tissue was not figured and Ørvig (1951) believed that the specimens may have been misinterpreted. Cancellous tissue has

also been reported in *Macropetalichthys* by Stensiö (1925a), and some arthrodires Goujet (1984). More recently *Bothriolepis* (Charest et al., 2018) was shown to have trabeculae, interpreted as endochondral bone, and some evidence of bone resorption in the pelvic girdle. Outside the placoderm-grade Wängsjö (1952) also described a cancellous endochondral tissue in the skeleton of *Boreaspis*, an osteostracan stem-gnathostome from Spitsbergen (although the diagnosis of this as endochondral bone has been disputed (Smith and Hall, 1990; Gardiner, 1984; Janvier, 1984; Wang et al., 2005)). These last two examples - *Boreaspis* and *Bothriolepis* are by far the most convincingly figured examples of putative endochondral bone. However, both examples are found in quite thin plates, with sparse trabeculae: neither shows a convincing network of trabecule like that found in osteichthyans.

This description of endochondral bone in a placoderm is the first well-characterised three-dimensional account an extensive endochondral trabecular matrix in a stem-gnathostome. Although the resolution of the data is insufficient to report small details, the bone appears generally consistent with its form in osteichthyans, with irregularly shaped spaces between trabeculae and perichondral bone coating the tissue. Although it is possible that this tissue is homoplasious this casts doubt on the veracity of endochondral bone as an osteichthyan synapomorphy (Friedman and Brazeau, 2010; Brazeau and Friedman, 2014). However, (Charest et al., 2018) are probably correct that widespread endochondral bone throughout the body is an osteichthyan synapomorphy (Charest et al., 2018).

If all of the reports of this tissue in placoderm-grade stem-gnathostomes are accurate, endochondral bone is remarkably widespread throughout the gnathostome stem-group. If placoderms are paraphyletic, as many recent analyses have recovered them, (eg. Brazeau (2009); Zhu et al. (2013); Giles et al. (2015c)) then endochondral bone is distributed in many different clades along the gnathostome stem-group, making the most parsimonious interpretation that it originated deep

in the gnathostome clade and as lost in chondrichthyans. Recently the hypothesis has re-emerged, supported by phylogenetic analyses, that placoderms are instead a clade King et al. (2016). In this scenario endochondral bone could be homologous in placoderms and osteichthyans. It could also be a synapomorphy uniting placoderms and osteichthyans to the exclusion of chondrichthyans, although this is somewhat unlikely on the basis of a suite of other characters Brazeau and Friedman (2014). A problem with distinguishing between scenarios of homology and homoplasy in this instance is the extremely sparse sampling of placoderm endoskeletons. To do so would require a far more widespread sampling of placoderm endoskeleton to determine if endochondral bone has been lost in some groups.

5.5 CONCLUSION

In the context of other work on tissues in early vertebrates, this new information helps to clarify conditions of the endoskeleton in the gnathostome total group. Globular calcified cartilage is widespread amongst gnathostomes and perichondrial tesserae unique to chondrichthyans and absent in most stem-group members. At some point in chondrichthyan evolutionary history these tesserae developed, likely directly on globular calcified cartilage without perichondral mineralisation. There is increasing evidence that endochondral bone originated in the gnathostome stem-group - however, extensive endochondral ossification throughout the bodyis only present in the osteichthyan clade. Endochondral tissues co-occur and are not mutually exclusive in the skeletons of gnathostomes - endochondral bone and globular calcified cartilage are both present in the skeletons of osteichthyans and placoderm-grade stem-gnathostomes. More endochondral tissue characters could possibly be worked into early vertebrate phylogenetic analyses, and assumptions of tissue presence or absence should be avoided without histological evidence.

CHAPTER 6

THE STEM-CHONDRICHTHYAN GENUS *Vernicomacanthus* AND THE EARLY EVOLUTION OF THE CHONDRICHTHYAN SHOULDER GIRDLE

6.1 INTRODUCTION

Amongst the acanthodian fauna of the Early Devonian ORS are various comparatively heavily armoured acanthodians, including *Climatius*, *Parexus*, *Euthacanthus*, *Brachyacanthus*, and *Vernicomacanthus*. In the past these taxa were grouped together into the "climatiids", on the basis of a heavily armoured shoulder girdle, a large number of spines, a tessera-roofed head and, often, tooth whorls (Miles, 1964b). However, many of the characters that link these taxa together are found outside the proposed group (eg. in Hanke and Davis (2008); Maisey et al. (2017)). Moreover many of the taxa within it exhibit morphologies which are more characteristic of animals outside the supposed group (eg. *Brachyacanthus*, *Vernicomacanthus*). Reflecting this, in recent phylogenetic analyses the "climatiid" grouping has decayed, and what were formerly a proposed clade are now understood to be a paraphyly on the chondrichthyan stem-group (eg. in Coates et al. (2018)). The placement of this grade, arrayed between the Acanthodii and "conventional" chondrichthyans, means that it is in a unique position to help us understand the stepwise evolution of chondrichthyan anatomy.

The character suite that ostensibly united these "climatiids" is instead probably a series of character states gained and lost in the chondrichthyan stem-group. Some of these characters are probably chondrichthyan plesiomorphies, inherited

from the ancestor of all chondrichthyans and shared by a broad range of stem-chondrichthyans. Others may denote smaller clades within the chondrichthyan stem-group. Particularly valuable however are characters which are shared with chondrichthyans in or closely related to the crown-group, to the exclusion of other stem-chondrichthyans. These are the most likely to bring resolution to chondrichthyan phylogeny. One area where you might particularly expect to find these is the shoulder girdle (Miles, 1973a), which is comparatively well preserved in many acanthodians and in chondrichthyans. Using these characters to resolve the phylogeny of the climatiids should provide us with a clear pattern of chondrichthyan character acquisition.

Amongst the ORS acanthodian fauna one taxon which may be particularly important is the Lochkovian (419-411Mya) "climatiid" *Vernicomacanthus uncinatus*. In many respects *Vernicomacanthus uncinatus* is typical for a climatiid-grade stem-chondrichthyan, having tooth whorls, a *Climatius*-like head skeleton, and an armoured shoulder girdle (Miles, 1973a). However its fin spines have a number of similarities with the gyracanthids, an unusual grade of large bodied, late occurring stem-chondrichthyans (Burrow et al., 2008). Its cogeneric, *Vernicomacanthus waynensis*, is broadly similar but has a highly unusual dermal pectoral girdle (Miles, 1973b). Despite its having been known since the 19th century (Powrie, 1864), *V. uncinatus* has only been cursorily described (Miles, 1973a). Moreover, material from the locality in which all articulated *V. uncinatus* have been found - Tillywhandland (or Turin Hill) - is conducive to new acid preparation techniques, resulting in prepared fossils having a similar information content to those from MOTH. This combination of factors make it a key target taxon for untangling the relationships of stem-chondrichthyans.

Here I redescribe *Vernicomacanthus uncinatus* using new material as well as a re-examination of specimens originally described by previous authors. I erect a new

genus, *Dobunnacanthus* n. gen., for specimens previously assigned to *V. waynensis*, on the basis of differences between the two taxa. I also review the evolution of the shoulder girdle in the chondrichthyan stem-group by comparison between *Vernicomacanthus* and new information on the shoulder girdles of *Ptomacanthus* and *Diplacanthus*.

6.2 MATERIALS AND METHODS

6.2.1 *Vernicomacanthus uncinatus*

All public *Vernicomacanthus uncinatus* material is housed in the National Museum of Scotland, Edinburgh (NMS), the Natural History Museum, London (NHM), the McManus Galleries and Museum, Dundee (DUNMG), and the Montrose Museum (NH), Montrose. All of this material comes from the ORS "Turin Hill" locality, most of which is probably originally from Tillywhandland Quarry, near Forfar in Angus Trewin and Davidson (1996). Tillywhandland is Lochkovian in age, and preserves a number of different species of osteostracan, acanthodian, and thelodont, as well as plants and arthropods, from what is interpreted as having been a lake bed (Trewin and Davidson, 1996). Specimens from the fish bed of Tillywhandland are preserved in a laminite with alternating carbonate and clastic layers (Trewin and Davidson, 1996).

A new, undescribed specimen of *V. uncinatus*, NMS 2001.7.4, was prepared out of the surrounding matrix using alternate washes of acetic acid, surfactant, and water. During this process the fossil itself was protected with paraloid. The residues from the preparation of this specimen were kept, and included several scales which had disarticulated from the body. Scanning electron microscopy of the surface of this specimen were carried out at the Natural History Museum, London, using a Zeiss Ultra Plus field emission SEM. Sections, between 40 and 50 microns thick, were

made of three scales from these residues. These were prepared by embedding the specimens in Buehler EpoThin resin, cutting on Buehler IsoMet slow speed saws, and imaged using a combination of plain polarised light, Nomarski Differential Interference Contrast (with and without a gypsum accessory plate) on a Zeiss Axioskop Pol polarizing microscope.

Before sectioning the most complete of the scales taken from the residues of *V. uncinatus* NMS 2001.7.4 was scanned using computed microtomography at the University of Bristol Life Sciences Department. We used a Nikon XT H 225 ST, scanning at 90kV and 78μA. We achieved a voxel size of 2μm. These data were segmented in with Mimics v.19 (biomedical.materialise.com/mimics; Materialise, Leuven, Belgium). Segmented models were then imported into Blender (blender.org) to acquire images.

Sectioning was carried out on NMS G.2018.18.1, an isolated *Vernicomacanthus uncinatus* pectoral fin spine from Balruddery Den. Nine sections were made, NMS G.2018.18.1.2-10, with the remnant designated NMS G.2018.18.1.1. These were made using epoxy resin and corundum grinding powder of various grain sizes. Sections were ground down to 4 microns, and were photogaphed using a Sony DSC-H2 camera on a Nikon Eclipse E 400 microscope.

Material and peels originally assigned to *Vernicomacanthus waynensis* were also studied as part of this. These are housed in the Natural History Museum, London (NHM).

6.2.2 *Ptomacanthus*

The *Ptomacanthus* pectoral girdle described here was obtained from the scan detailed in Chapter 3, carried out on NHM P.24919a. As with that dataset the resulting tomograms were then segmented using Mimics v.18 (biomedical.materialise.com/mimics; Materialise, Leuven, Belgium) and models were then imported into Blender (blender.org) to acquire images.

6.2.3 *Diplacanthus*

The *Diplacanthus* procoracoid described herein was obtained from NMS 1891.92.334, using the scan detailed in Chapter 4. The scan set from with it was segmented had a voxel size of 2.26 μA. As above Mimics v.18 and Blender were used for segmentation and imaging respectively.

6.3 THE ACANTHODIAN-GRADE GENUS *Vernicomacanthus*

Superclass: Gnathostomata, Gegenbaur 1874

Class: Chondrichthyes, Huxley 1880

REMARKS Miles (1973a) placed *Vernicomacanthus* in the family Climatiidae, part of the suborder Climatioidei, itself part of the order Climatiiformes. While *Vernicomacanthus* is anatomically similar to "climatiid" stem-chondrichthyans, recent phylogenetic analyses have failed to recover a consistent climatiid clade, and some or all climatiids are probably arrayed paraphyletically along the chondrichthyan stem-group rather than forming a monophyletic group. However, I consider the

wealth of evidence that "acanthodians" are in fact stem-chondrichthyans sufficient to place *Vernicomacanthus* in the class Chondrichthyes (Brazeau and de Winter, 2015; Davis et al., 2012; Maisey et al., 2017; Miller et al., 2003; Coates et al., 2018).

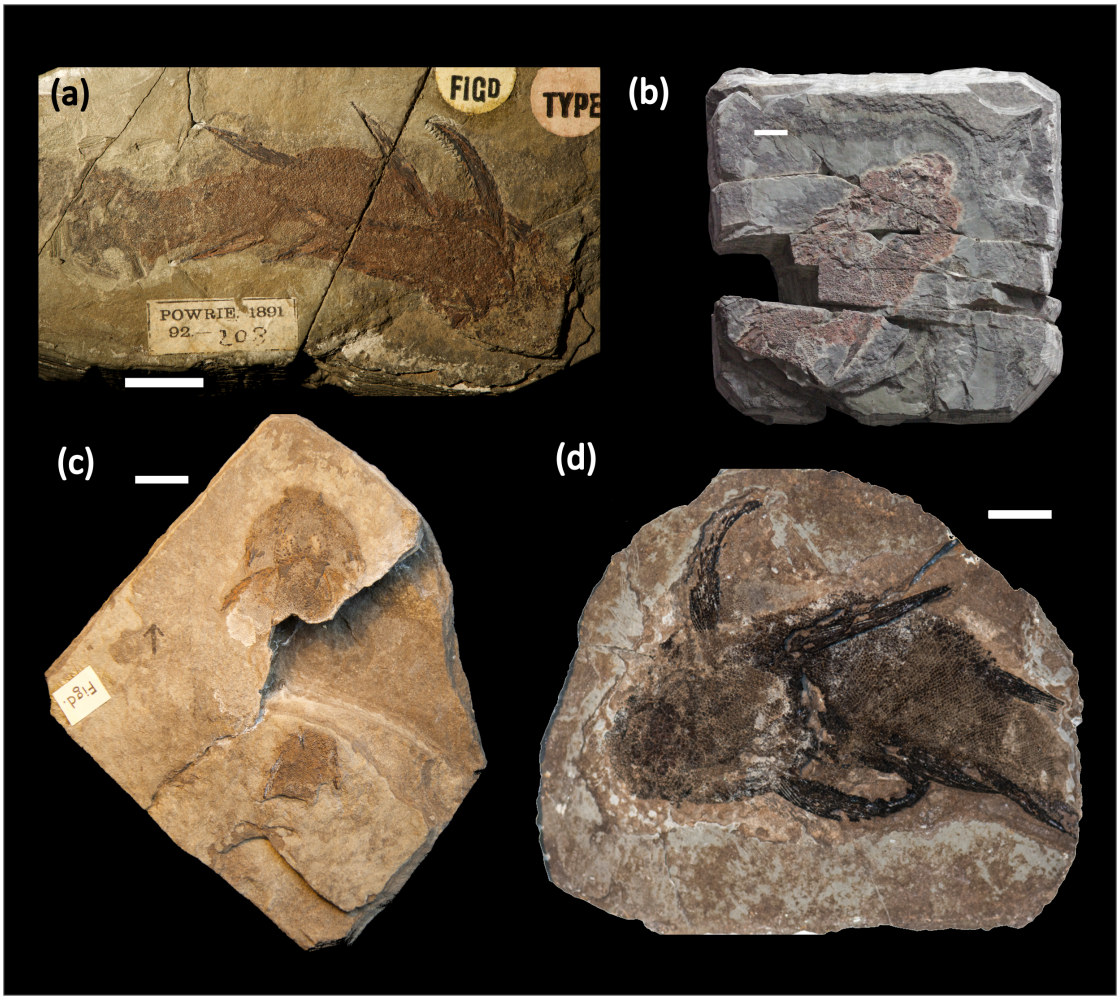


FIGURE 6.1: Four articulated specimens of *Vernicomacanthus uncinatus*: (a) NMS 1891.92.203; (b) NHM P.1342a; (c) DUNMG Kinnaird 82; (d) NMS 2001.7.4. Scale bar is 5mm in all cases.

Genus: *Vernicomacanthus*, Miles 1973

Type specimen: NMS 1891.92.208 is the lectotype

Type species:*Vernicomacanthus uncinatus* Powrie [*Climatius uncinatus*, (Powrie 1864)]

Emended diagnosis: Further to Miles' description these characters can be used to diagnose the genus *Vernicomacanthus*. Apomorphies:Pinnal plate with anterior edge oriented almost perpendicularly to lateral edge. Gnathostome symplesiomorphies: dorsoventrally closing jaws, teeth, sclerotic ring, lateral line on flank. Shared with certain total-group chondrichthyans: ascending process of scapulocoracoid, postero-lateral angle of scapulocoracoid, paired fin spines, anal fin spine, intermediate fin spines, microsquamose body integument, skull roofed by interlocking tesserae, scales comprising multiple laterally apposed odontodes, scales growing by antero-dorsal addition of odontodes. Shared with other "climatiid" acanthodians: dermal pectoral girdle with two prepectoral spines and a median spine, postorbital tesserae. Shared with gyracanthids and other stem-chondrichthyans: fin spine ornament oblique to leading edge, posterior denticles on paired fin spines.

Species: *Vernicomacanthus uncinatus* Powrie
1864 *Climatius uncinatus* ; Powrie (ex Egerton MS), p.422
1870 *Climatius uncinatus* ; Powrie p.296 pl. 14 fig. 11
1891 *Climatius uncinatus* ; Powrie, Woodward, p. 30
1973 *Vernicomacanthus uncinatus* Miles p. 140, pl. 7, fig. 33

6.3.1 *Vernicomacanthus uncinatus*

Material: NHM P.1342a, NHM P.6960, NHM P.1342, NMS 2001.7.4, counterparts NMS 1891.92.209 and DUNMG Kinnaird 82, and counterparts NMS 1891.92.210 and NH Mitchell 57
Locality: Tillywhandland ("Turin Hill"), near Forfar, Angus, Scotland
Horizon: Arbuthnott Group, Dundee Formation, Lower Old Red Sandstone
Emended diagnosis: as for genus

REDESCRIPTION OF *Vernicomacanthus uncinatus* —

Head skeleton The majority of specimens preserving a good view of the head are dorso-ventrally flattened (eg. NMS 2001.7.4, DUNMG Kinnaird 82). The head in these specimens is spread laterally well past the bounds of the pectoral region, suggesting a fairly tall head shape in life (Fig. 6.2a,e) . The head's proportions seem to be similar to those of other climatiid-grade animals, with anteriorly positioned eyes (Fig. 6.2a).

The roof of the head in *Vernicomacanthus uncinatus* is covered with interlocking tesserae (Fig. 6.2e,h,i), similar to those of other "climatiid" acanthodians such as *Climatius* and *Parexus* Burrow et al. (2015, 2013). These are fairly irregular in shape and pattern, but most plates have one larger, roughly central stellate tubercle, surrounded by radiating rows of smaller unornamented tubercles (Fig. 6.2h). These tesserae cover the roof of the skull between the level of the shoulder girdle and the snout(Fig. 6.2e). Towards the snout, the tesserae become larger and more densely packed with tubercles. Some of these anterior tesserae seem to have a more specialised shape, and could be something more like the circumnasal plates of *Climatius* (Miles, 1973a) than tesserae, although it is difficult make out exact borders of elements. The extreme anterior end of the snout is covered in very small stellate scales (Fig. 6.2g), similar to those described in *Obtusacanthus* Hanke and Wilson (2004).

The anteriorly placed orbits are marked by sclerotic rings on either side of the head (Fig. 6.2a,c,e). The dorsalmost two plates forming the ring are visible on either side of the head of NMS G 2001.7.4 (Fig. 6.2e). Both sclerotic rings are visible laterally in NHM P.1342a (Fig. 6.2c)- they are difficult to count but seem likely to number five like *Parexus* and *Climatius* (Burrow et al., 2013, 2015). Each bone is slightly convex and ornamented with tuberculate ridges radiating perpendicularly from the edge facing into the orbit. Posteriorly to each orbit is a large, spine-like postorbital

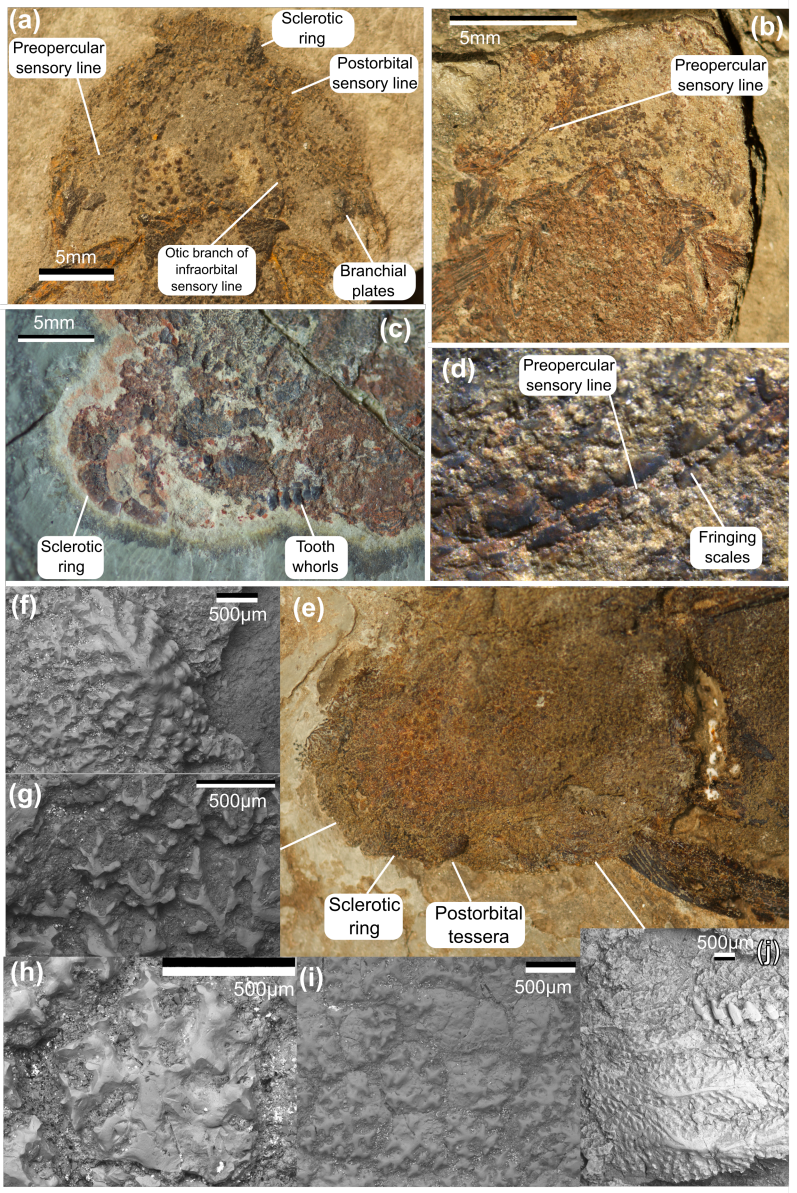


FIGURE 6.2: The head of *Vernicomacantus uncinatus*. (a) DUNMG Kinnaird 82, (b) NMS 1891.92.203, (c) NHM P.1342a, (d) Magnified picture of sensory line in NMS 1891.92.203, (e) CT rendered model surface model of NMS 2001.7.4, with SEMS of (f) Postorbital tessera, (g) rostral denticles, (h) head tessera, (i) several head tesserae in articulation, (j) branchial plates.

tessera. These have a pronounced peak and are ornamented with tuberculate ridges radiating outwards from the apex. Between these postorbital scales and the branchial plates, tesserae seem to be slightly smaller, although still tuberculate. Although no pattern can be discerned, markedly larger tesserae appear to be present on either side anterior to the lowermost visible branchial plate.

The branchial plates are best visible on the left-hand side of NMS G 2001.7.4 (Fig. 6.2e,j). The ventralmost visible plate is the largest and is ornamented with a large antero-dorsal ridge extending along the middle two thirds of its length. Smaller ridges extend dorsally and ventrally from this ridge. Around these ridges, particularly anteriorly, the plate is ornamented with tubercles. The whole plate, including the main ridge has a slight curve, with the convex side ventral. Other plates are similar in overall shape, but decrease in size dorsally. This makes their exact number difficult to count, but in NMS G 2001.7.4 there are at least four, and possibly as many as seven. The branchial integument posterior to the plates is difficult to observe. On the right hand side of NMS G. 2001.7.4 there are could be similar to the bones fringing the gill openings in *Climatius* (Watson, 1937), but it is difficult to make them out clearly.

The sensory lines are visible on certain specimens (Fig. 6.2a,c,d). The otic branch of the infraorbital sensory line is the most clearly visible. This is particularly so in DUNMG Kinnaird 82, where these are posteriorly continuous with the lateral lines, before they travel medially to form the otic branches, forming between them a lyre-shape in dorsal view (Fig. 6.2a). On this same specimen Miles (1973a) also identified preopercular canals - these are visible anterior to the branchial plates, where they swing anteriorly to meet the otic branch of the infraorbital sensory line (Fig. 6.2a,c,d). This canal is also clearly visible on NMS 1891.92.208 (Fig. 6.2b,d). Also visible on Kinnaird 82, but not figured by Miles, is the infraorbital sensory line (Fig. 6.2a). A possible supramaxilliary sensory line can also be seen on the left hand

side of NMS G 2001.7.4.

All sensory lines on the head appear to pass between the scales like in extant chondrichthyans (Janvier, 1996), rather than being carried in specialised canal scales like in acanthodians such as *Homalacanthus* and *Acanthodes* (Zidek, 1976; Gagnier, 1996). This is most clearly visible in the preopercular canal of NMS 1891.92.208 (Fig. 6.2d). The exact morphology of the scales is difficult to make out clearly, but they appear less broad and more rectangular than other head tesserae (also see Miles (1973a) Plate 7). Each also appears to be lightly offset along the course of the sensory line from its opposite number. In NMS 1891.92.208 the sensory line is almost invisible (also see Miles (1973a) Plate 7), whereas in the more heavily worn NMS 1891.92.208 a clear space is present (Fig. 6.2d). This suggests that the crowns of the scales covered the sensory lines themselves, like in recent elasmobranchs, although no pores are present.

Shoulder girdle The ventral dermal pectoral girdle has been described in detail by Miles (1973a). My observations and a CT scan of NMS2001.7.4 appears to confirm his account, that the dermal shoulder girdle comprises paired pinnal plates each with two prepectoral and a median prepectoral spine (Fig. 6.3a,b). A new observation is that dorsal to the pectoral fin spines are zones of small tesserae ornamented with small tubercles. These are visible in NMS 2001.7.4, as well as in NMS 1885.54.69 where they cover the distance between the scapulocoracoid ventral margin and the dorsal margin of the pectoral fin spine (Fig. 6.3c).

The scapulocoracoid is best preserved in NMS 1885.54.69, between the part and counterpart (Fig. 6.3c). The fish has been dorso-ventrally flattened, and the scapulocoracoid is split down the middle, with the inside of the medial face preserved in one part NMS 1885.54.69a and the scapulocoracoid in medial view with the medial face removed in the other NMS 1885.54.69b. It is formed from

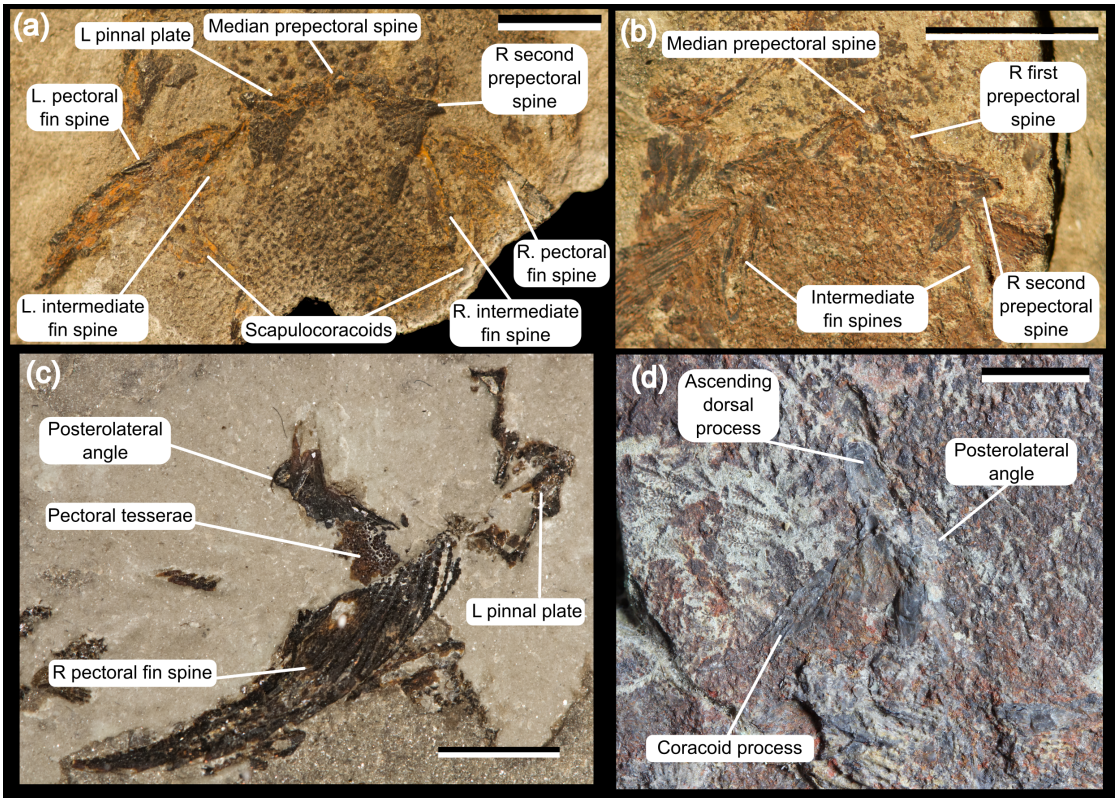


FIGURE 6.3: The shoulder girdle in *Vernicomacanthus uncinatus*: (a) DUNMG Kinnaird 82; (b) NMS 1891.92.203, (c) NMS 1885.54.69a, (d) NHM P.1342a. Abbreviations: R., right; L.,left. All scale bars 50mm.

a uniform, unperforated material - this lacks tesserae and isn't granular like endoskeletal tissues interpreted as mineralised cartilage in other acanthodians (Hanke and Wilson, 2010)). Instead it seems most likely to be perichondral bone (although I have reservations about this kind of diagnosis as discussed in Chapter 5).

The scapulocoracoid is L-shaped, with a prounounced ascending dorsal process, and is laterally flattened (Fig. 6.3c). The ascending dorsal process is slender with anterior and posterior margins which taper towards a rounded off dorsal tip. The ventral part of the spine meets the base of this ascending process at a 135 degree

angle. This ventral section is triangular and tapers to an anterior point. The ventral margin of the scapulocoracoid is flat, rising posteriorly to meet the ascending process. On the posterior edge of the ascending dorsal process is a prounced postero-lateral process. Although a postero-lateral process was not recorded by Miles (1973a), it can faintly made out in specimens such as NHM P.1342a (Fig. 6.3d). A posterolateral angle is common in the shoulder girdle of chondrichthyans (Coates and Gess, 2007).

Spines The pectoral fin spines are large and curve posteriorly (Fig. 6.3c). They are ornamented with rounded denticles (Fig. 6.4a), organised into oblique rows approaching the leading edge of the fin spine. Posteriorly the fin spine is ornamented with large, tooth-like denticles (Fig. 6.4b), which are very slightly inwardly curved pointing towards the insertion of the fin spine. These posterior denticles occur along the entire length of the fin spine's inside edge, from tip to insertion. The pelvic fin spines are slightly curved, and ornamented with oblique rows of denticles, but are shorter than the pectoral fin spines and lack posterior denticles. Although Burrow et al. (2008) reported a double row of denticles on the trailing edge, I cannot observe this in NMS 2001.7.4.

Two dorsal fin spines are present - these are longer relative to body length than those of *Climatius* and *Brachyacanthus*, and are slightly laterally flattened. The anterior dorsal fin spine is slightly longer than the posterior. They are ornamented with oblique rows of rounded denticles borne on ridges, converging on the leading edge of the spine (Fig. 6.4c). The anal fin spine is also ornamented with denticulated ridges, but is straight and shorter than the pectoral fin spine.

V. uncinatus has six pairs of intermediate, or pre-pelvic fin spines. These are best counted in specimen NMS 1891.92.208 and NMS 1891.92.210; in other specimens it is difficult to perform a full count It is possible that the exact number of intermediate

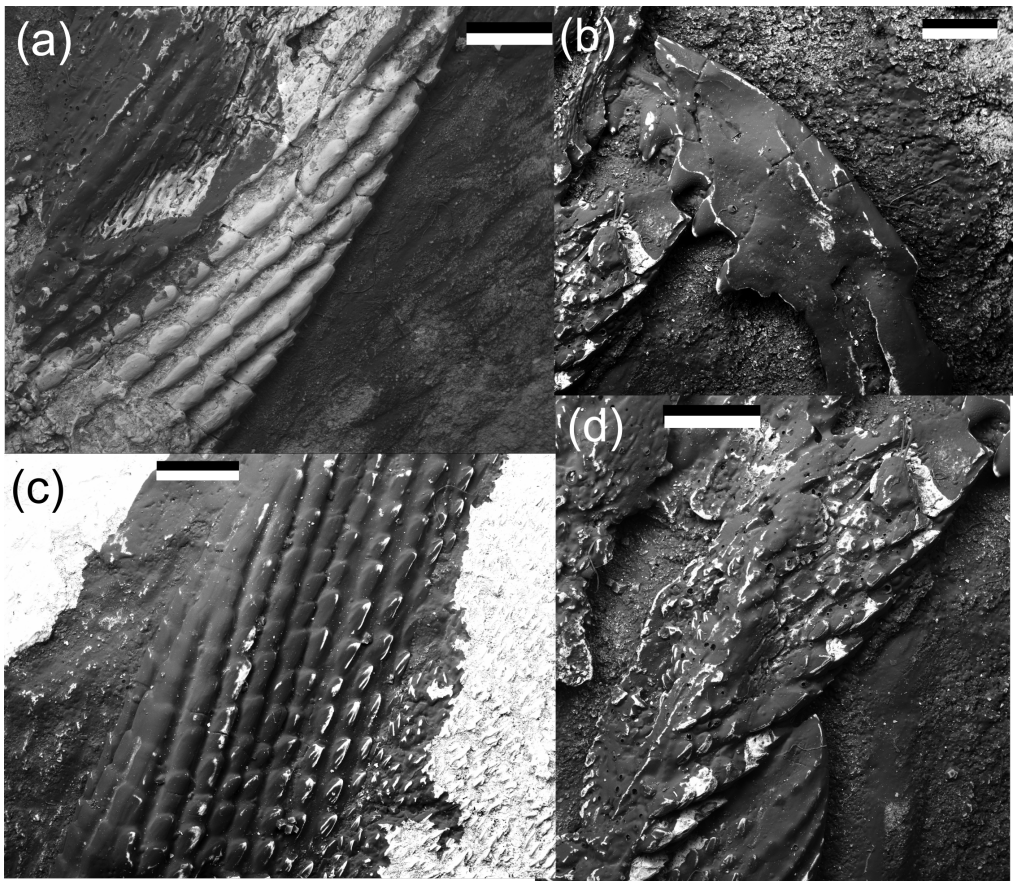


FIGURE 6.4: Details of fin spines in *V. uncinatus* NMS 2001.7.4 , using SEM. (a) the ornament at the proximal end of the right pectoral fin spine; (b) trailing edge denticles at the distal end of the pectoral fin spine; (c) Ornament at the proximal end of the anterior dorsal fin spine; (d) an intermediate fin spine. All scale bars 1mm.

fin spines may vary between specimens as reported in *Climatius* and *Euthacanthus* (Watson, 1937; Miles, 1973a). The anteriormost intermediate spine is located almost medially relative to the pectoral fin spines, while the posteriormost is situated close anteriorly to the pelvic girdle. In NMS G 2001.7.4 the intermediate spines have been pushed together making it difficult to perform a count. However, this specimen shows the best view of the individual intermediate spines themselves.

The spines are short, and are elliptical in cross-section - the inserting end is open (Fig. 6.4d). They are ornamented with oblique rows of small denticles - proximally these denticles are smaller and more pointed than those on the fin spines - distally they become more rounded, and more organised into ridges.

The histological structure of the sectioned pectoral fin spine NMS G.2018.18.1 is similar to that of other "climatiid" acanthodian fin spines such as *Climatius* and *Parexus* (Burrow et al., 2013, 2015) (Fig. 6.5). The pulp cavity is large, becoming relatively smaller towards the distal end of the spine (Fig. 6.5a). The outside of the cavity is bordered by a thin layer of lamellar tissue - this is so thin as to be invisible in some sections, but can be best seen in section 5 (Fig. 6.5b). Outside this lamellar layer is a thick layer of osteodentine (trabecular dentine), punctured by large vascular canals (Fig. 6.5b,c). These vascular canals become progressively smaller towards the surface of the spine, with some present inside the ornament ridges (Fig. 6.5b). Vascularisation also becomes less common towards the tip of the spine(Fig. 6.5d). The surface of the ornament is formed from mesodentine, with tubules linking the vascular canals and the surface (Fig. 6.5c). No enameloid is present. Osteocyte lacunae are present throughout the tissues(Fig. 6.5c,d). At its insertion the fin spine is open - in the sectioned spine there seems to be an opening halfway along the posterior of the spine, but this isn't visible in complete spines and is probably taphonomic (Fig. 6.5a).

Body squamation The body scales are organised into diagonal lines, and become gradually smaller posteriorly on the body. Scales are ridged, with a large central ridge flanked by two pairs of smaller ridges on the majority of scales (Fig. 6.6a). On occasional scales with six ridges, three shorter ridges are found ventrally to the large central ridge - this is seen in a zone immediately anterior to the first dorsal fin. Below the anterior dorsal fin spine is a region of scales which are more tessera-like, with horizontal ridges connecting the longtitudinal ridges (Fig. 6.6b). A similar

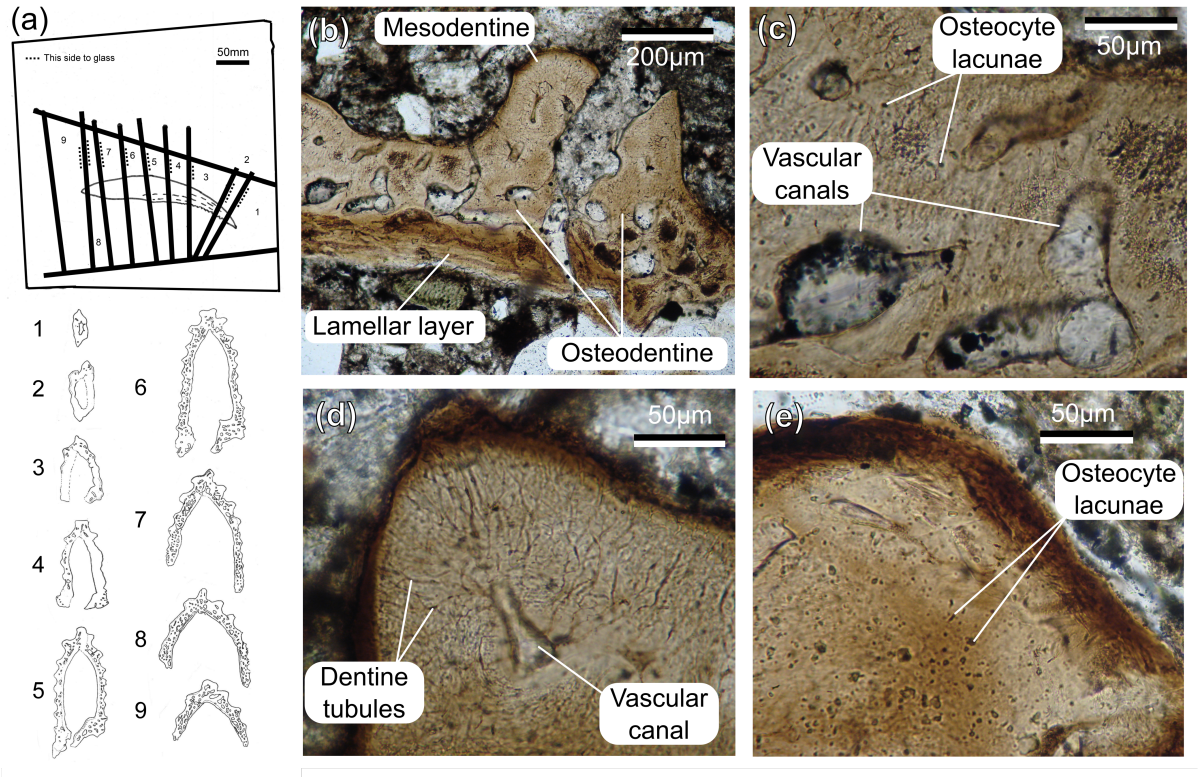


FIGURE 6.5: Histology in an isolated pectoral fin spine NMS G.2018.18.1 of *V. uncinatus*: (a) Plan of sections through fin spine, with drawings of sections below; (b) section no. 5 at 10x magnification, showing general architecture; (c) section no. 5 at 40x magnification, showing osteodentine; (d) section no. 5 at 40x magnification, showing an ornament ridge; (d) section no. 1 at 40x magnification, note reduced vascularisation and osteocyte lacunae.

condition was been described in the midline of *Dobunnacanthus* gen. nov.Miles (1973a). The right pectoral fin of NMS G 2001.7.4 also preserves scales - these are much like the body scales in all aspects except that they are smaller with only three or four ridges (Fig. 6.6c).

The transition between the head tesserae and the body scales is worthy of note, taking place through a gradual transformation rather than a sudden change..

Towards the back of the head the tubercles ornamenting the tesserae become progressively more antero-posteriorly oriented (Fig. 6.6d). However, they remain joined by perpendicular bars (Fig. 6.6d). These are slowly lost posteriorly, giving way to the antero-posteriorly ridged body squamation. A similar condition was reported in *Dobunnacanthus waynensis* gen. nov.Miles (1973a).

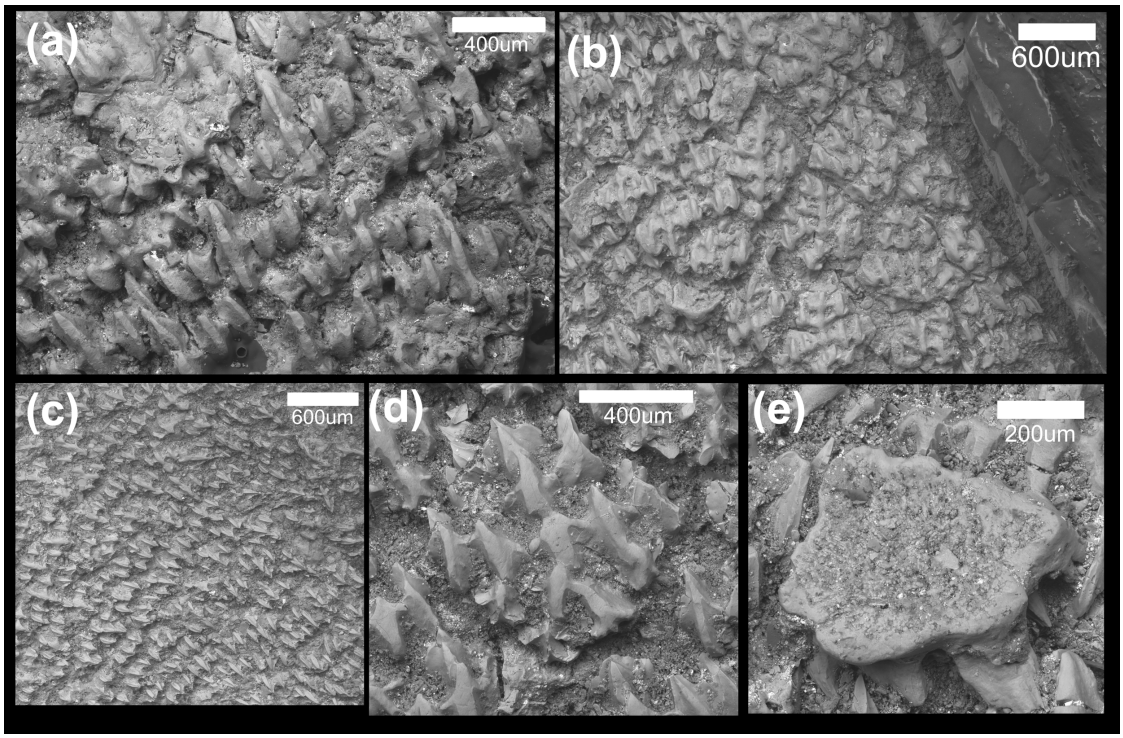


FIGURE 6.6: Scanning electron microscope images of scales from across the body of NMS 2001.7.4: (a) Typical flank squamation; (b) Tessera-like scales underneath dorsal fin spine; (c) Scales of the fin web; (d) transitional tessera on posterior of head; (e) exposed underside of flank scale.

The body scales of *Vernicomacanthus* comprise a polyodontode crown on a thin, convex base (Fig. 6.7). This base is polygonal, and wider than it is long (Fig. 6.6e). It accommodates the bases of the overlying crowns, and forms a slight anterior

lamina beyond the posterior extent of the crowns(Fig. 6.7a). The crowns of the body scales of Vernicomacanthus are formed from multiple antero-posteriorly elongate odontodes. Each odontode comprises an underlying leaf-shaped lateral lamina topped by a sharply defined, wedge-shaped crest, which tapers posteriorly. While the base of each odontode is firmly attached to the scale base, they extend posteriorly well past the scale base and in articulation the crown overlies the anterior laminae of the bases of the posterior two scales (Fig. 6.6a, Fig. 6.7d). The largest odontode is in the centre of the scale's crown, and is flanked laterally by symmetrically arranged pairs of odontodes, the lateral laminae of which are fused to their lateral counterparts(Fig. 6.7a,b). Anteriorly to the large odontode, on the central axis of the scale, is a smaller odontode (Fig. 6.7a,c,d). Like its larger fellows it has a pronounced dorsal ridge, but its underlying lamina is shaped into two posterior points flanking the dorsal ridge. Underlying the largest odontode is an additional odontode of similar size to it (Fig. 6.7c). The crest of this ventral odontode is obscured by the growth of the overlying central odontode, but its lamina can be seen projecting laterally. Sections through the scales show that the base is made from cellular bone. The crown of the scale is formed from mesodentine.

Internally each odontode has a separate pulp cavity (Fig. 6.7e-g). This cavity comprises an antero-posteriorly elongate chamber which runs most of the length of the odontode(Fig. 6.7e). The pulp cavity is restricted to the centre of the odontode, and does not extend into the dorsal ridge (Fig. 6.7f). The pulp cavities of the two lateral-most odontodes are far larger than those in the more medial odontodes, filling almost the entire odontode (Fig. 6.7e). Branching off the pulp cavity laterally are several neck canals of similar lumen size to the pulp cavity, which extend ventrolaterally out of the odontode (Fig. 6.7e-g). These canals are inconsistent in number in different odontodes, but odontode each has at least two pairs of neck canals. Because of the growth of the scale some of these neck canals end in dead ends within the crown, however, many remain open on the surface of the

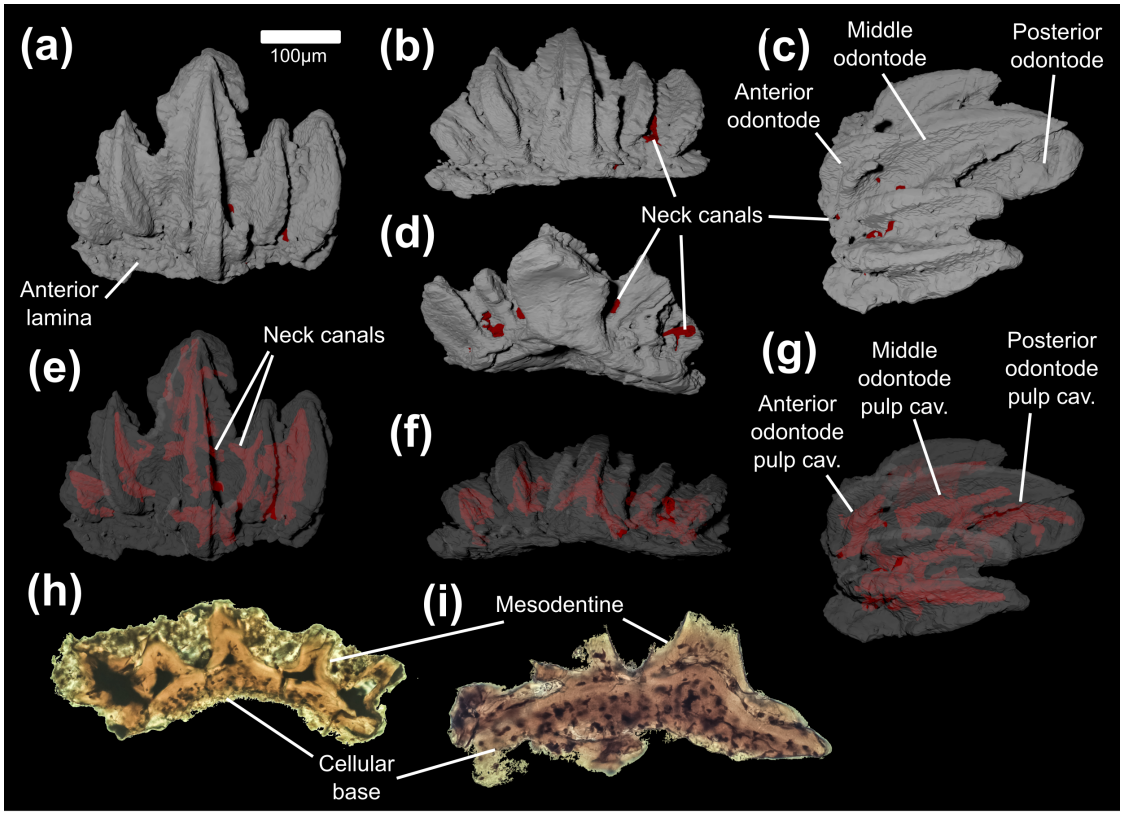


FIGURE 6.7: Histology of isolated scale from residues of NMS 2001.7.4: (a-d) CT rendered images in (a) dorsal view; (b) anterior view; (c) dorso-lateral view; (d) Posterior view; (e-g) CT rendered images with outside semi transparent, revealing pulp cavities in (e) dorsal view; (f) anterior view; (g) dorso-lateral view; (h) WRITE THIS BIT

scales (Fig. 6.7d,c). Most are visible on the posterior neck of the scale, fewer open between odontodes or anteriorly. While the pulp cavities are separate, some of them commune via meetings between neck canals within the scale - this can particularly be seen between the central large odontode and the large odontode underlying it (Fig. 6.7e-f). Base canals are entirely absent in the scanned specimen, and also

appear to be absent on exposed bases of scales on the surface of specimen NMS 2004.7.4 (Fig. 6.6a, Fig. 6.7).

Based on the relative positions of the odontodes in the *Vernicomacanthus* scale the first odontode to grow was the underlying large odontode (Fig. 6.7g). Following this, the largest odontode grew on top of this odontode, superpositionally, and obscuring the crown of the underlying odontode. It is not possible to tell which odontode grew next, but the small anterior odontode clearly grew after the large central odontode. Also following the central odontode, the lateral odontodes clearly grew outwards. It seems likely that the relatively large size of the pulp cavities in the lateralmost two odontodes is due to their relatively young age. Notably, the series of growth in the three odontodes along the central axis of the scale is reminiscent of the growth of chondrichthyan tooth whorls.

6.3.2 *Dobunnacanthus waynensis* Powrie n. gen.

Genus: *Dobunnacanthus* gen. nov.

Etymology: After the Dobunni, an Iron Age tribe whose territory extended into Southern Herefordshire (Allen, 1944; Van Arsdell, 1994), and akantha, Greek for a thorn.

Type specimen: NHM P.24938a, b

Type species: *Dobunnacanthus waynensis* Miles gen. nov. [*Vernicomacanthus waynensis* (Miles 1973)]

Diagnosis: Further to Miles' description these characters can be used to diagnose the genus Dobunnacanthus.

Autapomorphies: Ascending pinnal lamina over half as high as scapulocoracoid. Gnathostome symplesiomorphies: dorsoventrally closing jaws, teeth, sclerotic ring,

lateral line on flank. Shared with certain total-group chondrichthyans: ascending process of scapulocoracoid, paired fin spines, anal fin spine, intermediate fin spines, microsquamose body integument. Shared with other "climatiid" acanthodians: dermal pectoral girdle with two prepectoral spines and a median spine, head skeleton formed from interlocking tesserae. Shared with gyracanthids and other stem-chondrichthyans: fin spine ornament oblique to leading edge, scales with multiple laterally apposed odontodes. Differs from *Vernicomacanthus* in having a less ventrally extensive dermal shoulder girdle, a high ascending pinnal lamina, lacking a postero-lateral angle on the ascending process of the scapulocoracoid, and being significantly larger in size.

Remarks: I consider the differences between *Vernicomacanthus* and *Dobunnacanthus* gen. nov. to be sufficient to erect a new genus. I hope this will encourage workers to use both genera in their phylogenetic matrices.

Species: *Dobunnacanthus waynensis* Miles gen. nov.
1973: *Vernicomacanthus waynensis*; Miles p.140, pl. 1, 8-10, figs 1, 3

Material: NHM P.24938a,b [holotype]; NHM P.16614; NHM P.16615; NHM 52441a,b; P52443
Occurrence: Wayne Herbert Quarry, Herefordshire Allen and Tarlo (1963); White (1935)
Diagnosis: As for genus
Remarks: Unlike *Vernicomacanthus* Miles (1973a) described *Dobunnacanthus* gen. nov. in detail, based on peels made from a series of moulds from Wayne Herbert. No new material has been described since then, but I have a few observations to add by comparison of this material to *Vernicomacanthus*.

Squamation. The tesserae of the head are similar to those in other climatiids- roughly hexagonal in shape and tuberculated. As Miles (1973a) observes the flank scales of *Dobunnacanthus* gen. nov. are ornamented with antero-lateral ridges. These appear to be similar to the scales of *Vernicomacanthus*, with their laterally apposed odontodes. However it is impossible to confidently diagnose this from the mouldic preservation.

Shoulder girdle. *Dobunnacanthus* has a highly unusual morphology of the dermal shoulder girdle, noted by Miles (1973a). Despite the unusual nature of it the description of Miles appears to be accurate - the two prepectoral spines in life would have been in the same anatomical position as those in other stem-chondrichthyans.

The moulds of the scapulocoracoid appear not to have a postero-lateral angle, like that in *Vernicomacanthus*.

Spines. The pectoral fin spines of *Dobunnacanthus* as described by Miles (1973a). Miles implies, but does not explicitly state, that the ornamentation of the pectoral fin spine converges obliquely on the leading edge of the spine. I can confirm that this is the case.

6.4 COMPARATIVE ANATOMY OF TWO ACANTHODIAN SHOULDER GIRDLES

During the scanning detailed in Chapters 3 and 4 parts of the shoulder girdles of *Ptomacanthus* and *Diplacanthus* were found. These confirm in some ways the anatomy described by Miles (1973a) and Brazeau (2012), but provide some novel information. They are also notable in being as a fairly rare examples of three-dimensionally preserved stem-chondrichthyan shoulder girdles, particularly in the

light of recent new data on *Doliodus* (Maisey et al., 2017). Here I describe this new data.

6.4.1 **Shoulder girdle of *Ptomacanthus anglicus***

In *Ptomacanthus* NHM P.24919a both left and right sides of the dermal shoulder girdle of are preserved. Each side comprises a single, slightly convex, tuberculated pinnal plate, which is ventrally continuous with its corresponding pectoral fin spine (Fig. 6.8). The posterior border of this plate extends antero-medially from its junction with the spine's posterior, gently curving to create a slightly convex postero-medial margin. At the plate's lateral extent of the animal it curves anteriorly, and joins with the lateral margin of the plate to form an angular anterior margin. Between this anterior angle and the pectoral fin spine the plate bears two prepectoral spines, which are short, flattened and striated, with the posterior being slightly larger. These spines are not continuous with the base of the plate, but are instead obliquely embedded in a low pinnal lamina (Fig. 6.8c). On the basis of the *Ptomacanthus* shoulder girdle NMS P.17290-1 reconstructed by Miles (1973a), these prepectoral spines would have been situated on the coracoid process (Miles, 1973a). While the overall aspect of the shoulder girdle is similar to *Sabrinacanthus* and *Erriwacanthus* (Miles, 1973a), there is no intermediate spine incorporated into the shoulder girdle in *Ptomacanthus* (Fig. 6.8a). Posteriorly the structure continues dorsally, echoing the ascent of the scapulocoracoid - it is unclear whether this is actually the scapulocoracoid or dermal bone overlying it (Fig. 6.8c). Broken material between the two sides of the dermal girdle is probably the edge of the left dermal girdle and the median prepectoral spine (Fig. 6.8b).

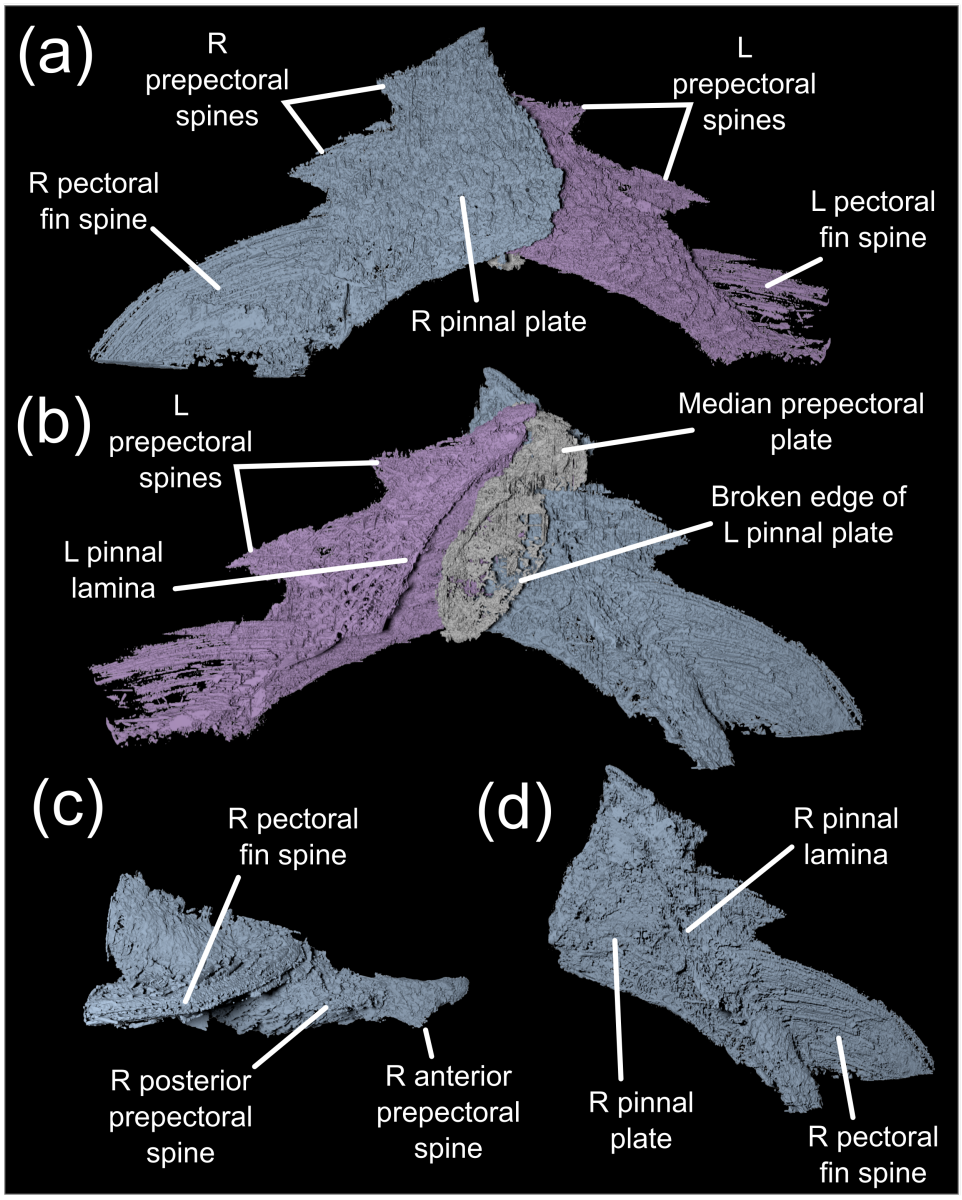


FIGURE 6.8: The dermal shoulder girdle of *Ptomacanthus* NHM P.24919a. (a) in ventral view; (b) in dorsal view; (c) in lateral view; (d) right pinnal plate in dorsal view. Colour scheme: Purple, left pinnal plate; Blue, right pinnal plate; Grey, material I interpret as the broken edge of the left pinnal plate and the median prepectoral plate

6.4.2 **Shoulder girdle of *Diplacanthus crassisimus***

ORIENTATION — Between the mould of the scapulocoracoid and the branchial skeleton in NMS 1891.92.334 lies a procoracoid element (Fig. 6.9a). The element is slightly worn at the surface of the specimen, but is otherwise preserved three-dimensionally. Its position on the left hand side of the animal suggests that it is a left procoracoid which has spun during preservation in such a way that its anterior end now points posteromedially. This conflicts with previous interpretations of the procoracoid of *Diplacanthus* (Watson, 1937; Miles, 1973a), in which this element would be interpreted as the right hand element. NHM P.1364-4311 was one of the main specimens used to reconstruct the bone by Miles (1973a) as it preserves moulds of both left and right elements of which casts were taken. However, my reexamination of this and other specimens observed suggest that the orientations in these previous reconstructions is incorrect and that the procoracoid in NMS 1891.92.334 is in fact the left hand one. Further evidence comes from specimens such as NHM P1357a, which both procoracoids *in situ*, oriented the way I interpret it here (Fig. 6.9i).

DENTICULATED PAD — The ventral part of the element comprises a denticulated pad (Fig. 6.9b,f,g). What remains of this pad has a teardrop-shape, with its pointed end oriented anteriorly. Although the lateral border of the element is worn, a ridge formed by denticles at the complete posterior and anterior ends of this border suggests its preserved shape is fairly accurate (Fig. 6.9b). The postero-lateral end of the pad curves dorso-laterally to form a "heel" (Fig. 6.9d) - anteriorly to this heel the pad is flat, with its anterior part slightly concave. The denticles are Phrygian cap shaped and ornamented by shallow ridges converging on the tip. The majority are directed posteriorly, but without any great organisation - a small subset are instead directed antero-medially. In life this pad would have lain antero-laterally relative to

the pectoral fin spine (Fig. 6.9j,k).

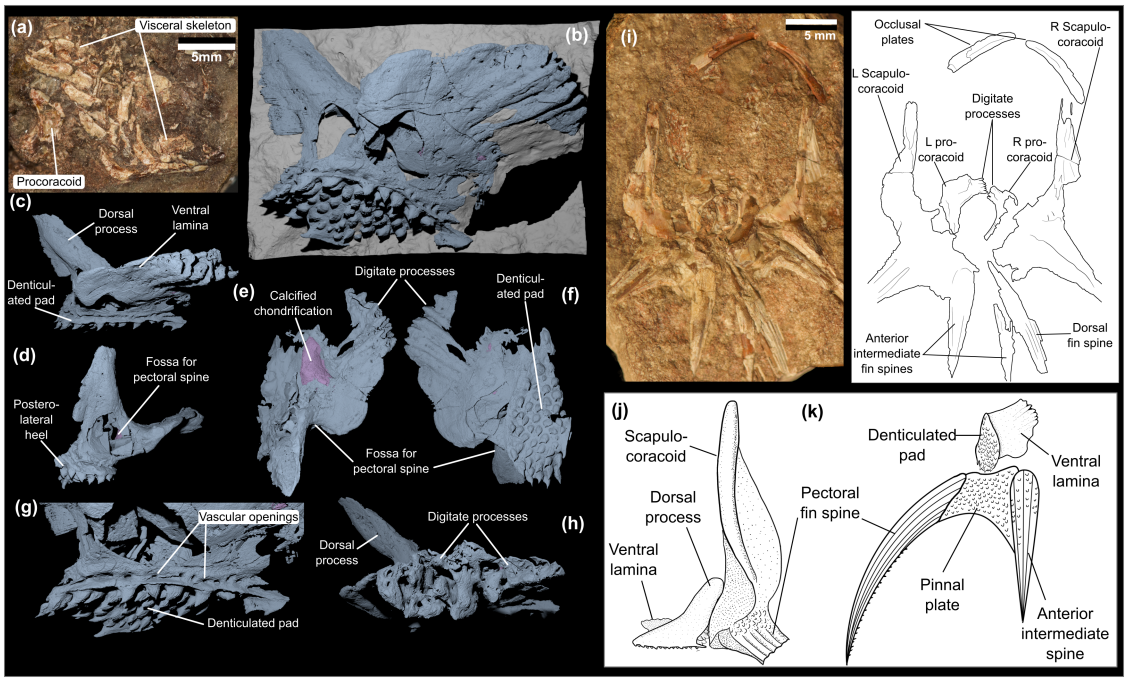


FIGURE 6.9: The procoracoid of *Diplacanthus*. (a) in the specimen; (b) rendered 3D model juxtaposed against specimen surface; (c-f) element in (c) medial, (d) posterior, (e) dorsal, and (f) ventral views; (g) medial view of top of denticulated pad, showing vasculature; (h) medial view of ventral lamina, showing digitate processes and vasculature; (i) photograph and drawing of NHM P.1357a, with articulated procoracoids showing inwards-pointed digitate processes; (j,k) updated reconstruction of the shoulder girdle of *Diplacanthus* in (j) lateral, and (k) ventral views.

ENDOSKELETAL PART — The endoskeletal part of the shoulder girdle consists of two parts, referred to here using the terminology of Miles (1973a): a ventral lamina and a dorsal process. The preserved medial side of the dorsal process forms a stout, upright rod, oriented dorso-posteriorly (Fig. 6.9). The lateral side of this process is worn making its overall shape, and exact upper limit, difficult to make

out - however, the medial side has a semi-elliptical cross-section. Ventrally this process meets the denticulated pad, and medially it meets the ventral lamina of the procoracoid. The junction between these three parts forms a posterior concavity at the base of the dorsal process, into which the scapulocoracoid likely inserted (Fig. 6.9d).

The ventral lamina forms a broad shelf, which extends antero-dorso-medially from where it meets the dorsal process and denticulated plate. This shelf's base meets with the denticulated pad along its full length - at the junction between the two are 12 foramina, just above the rim of the pad. These were presumably for vascularisation of the pad's tissue (Fig. 6.9g). The shelf itself is partly worn on the surface of the specimen - however the posterior and medial borders are preserved (Fig. 6.9b). The antero-medial rim of the shelf iforms a number of small digitate protruberances extend antero-medially (Fig. 6.9e,f,h). Between these protruberances are vascular foraminae, with ridges on both dorsal and ventral surfaces of the shelf marking the carriage of this vasculature through the ventral shelf .

While all the structures described so far seem to have been formed from either perichondral or dermal bone, part of the procoracoid takes the form of globular calcified cartilage, similarly to the rest of the endoskeleton of *Diplacanthus* (described in chapter 4). This is restricted to an L-shaped element sitting anteriorly to the base of the ascending process, dorsal to the ventral lamina. The significance of this is uncertain - presumably the entire procoracoid was filled with cartilage, and this is just a mineralised remnant.

6.5 DISCUSSION

6.5.1 **The endoskeletal shoulder girdle in stem-chondrichthyans**

A dorsal blade of the scapulocoracoid is widespread in chondrichthyans (eg. Coates and Sequeira (2001a); Coates and Gess (2007); Zangerl (1981)) (Fig. 6.10). Brazeau and Friedman (2014) noted that the dorsal blade is also present in all known acanthodian scapulocoracoids (see Miles (1973a)), and serves as evidence of acanthodians being early chondrichthyans. Several characters contingent on this dorsal blade also demarcate parts of the chondrichthyan total group. A laterally flattened ascending process, as opposed to a cylindrical or hemicylindrical one, seems to unite crown-chondrichthyans and some acanthodians to the exclusion of others (eg. Character 108 in Brazeau (2009)), although it is unclear which condition is derived due to the lack of a suitable outgroup. A posterolateral angle on this ascending process has been identified as a synapomorphy uniting some total-group chondrichthyans to the exclusion of "acanthodians" (Coates and Gess, 2007).

The presence of a posterolateral angle in *Vernicomacanthus* is consistent with a stem-chondrichthyan placement of acanthodians. In conventional chondrichthyans the posterolateral angle is broadly present in crown holocephalans as well as in many Palaeozoic "sharks" (Coates and Gess, 2007; Coates and Sequeira, 2001a; Dick, 1978). While it is absent in neoselachians this is probably secondarily derived, as it is present in stem-elasmobranchs (Coates and Gess, 2007). While this region of the scapulocoracoid is unknown in the stem-chondrichthyan *Doliodus*, the possible stem-chondrichthyan *Gogoselachus* exhibits one (Long et al., 2015). This distribution suggests that the morphology originated in the chondrichthyan stem-group.

A posterolateral angle has not been described in any other acanthodian-grade taxa (Fig. 6.10). Disregarding the posterolateral angle the overall shape of the scapulocoracoid in *Vernicomacanthus* is similar to that in other climatiids such as

Ptomacanthus, *Climatius*, and *Dobunnacanthus* gen. nov. in that it is comprises a laterally flat, lambda shape (Miles, 1973a). However a posterolateral angle is not observed in any of these other taxa. In gyracanthids scapulocoracoids are large, flat and triangular with no obvious posterolateral angle (Warren et al., 2000), although in *"Gyracanthus" sherwoodi* and *Gyracanthides hawkinsi* the apex of the scapulocoracoid is bent anteriorly in a manner that suggests perhaps a posterolateral angle is present but obscured by the wide, flat shape of the bone (see Turner et al. (2005); Snyder et al. (2017)). Ischnacanthids and acanthodids have tall columnar ascending processes which lack any kind of angle (Miles, 1973a). Diplacanthids such as *Diplacanthus* and *Uraniacanthus* have a posterior flange (Miles, 1973a; Hanke and Davis, 2008), which could be considered to be a posterolateral angle, but which is rather morphologically different to the angle in other chondrichthyans. As the difficulty in seeing the angle in other *Vernicomacanthus* specimens demonstrates, it is difficult to see in flattened specimens, and may be undersampled even in stem-chondrichthyans where the scapulocoracoid is to some extent known.

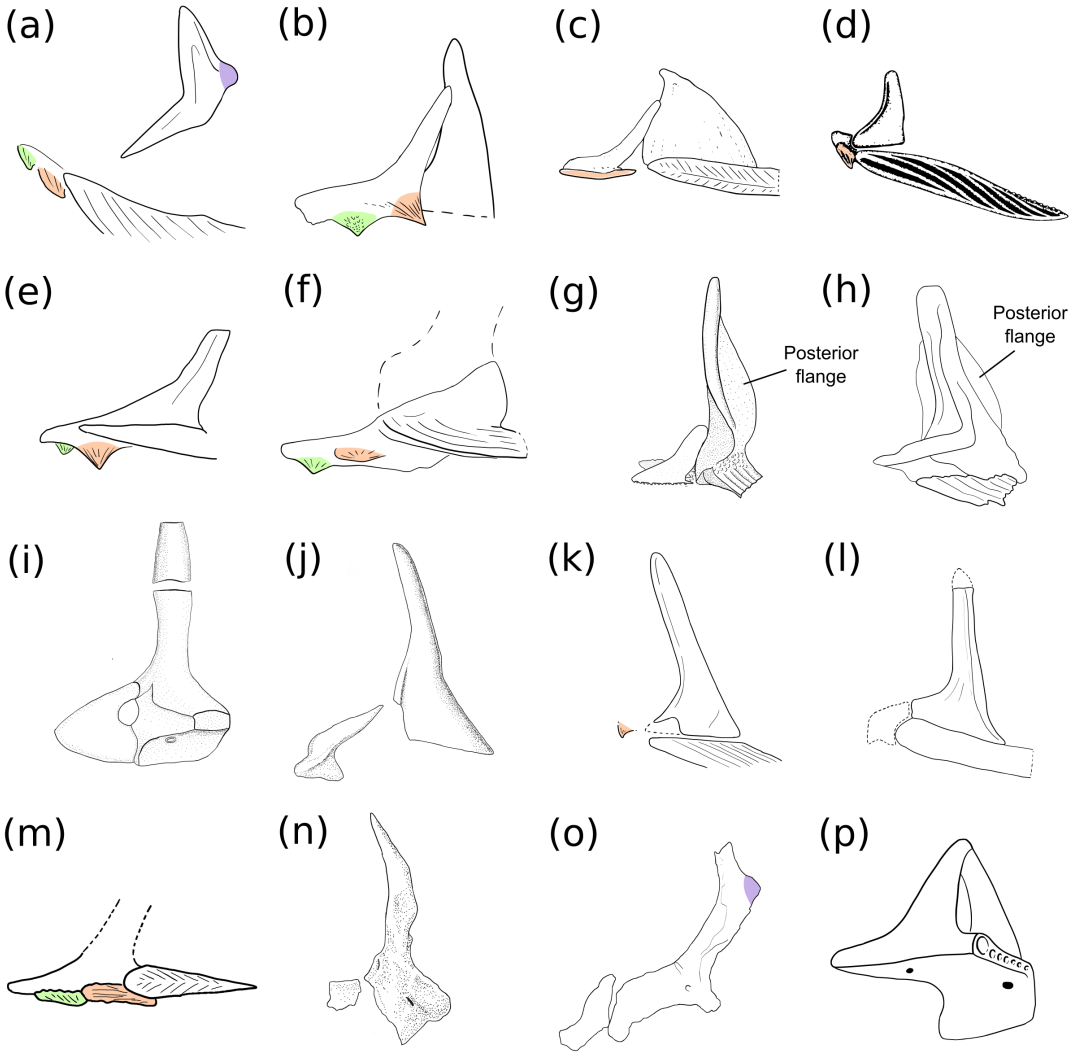


FIGURE 6.10: Caption on next page

If the presence of the posterolateral angle in *Vernicomacanthus* is homologous with that in crown-chondrichthyans there are two possible resolutions to its homology. If acanthodians are paraphyletic, as almost all recent analyses

FIGURE 6.10: Selected gnathostome shoulder girdles in lateral view. Depicted are (a) *Vernicomacanthus*, from this chapter; (b) *Dobunnacanthus* gen. nov., from Miles (1973a); (c) Gyracanthides, from Warren et al. (2000); (d) *Lupopsyrus*, from Hanke and Davis (2012); (e) *Climatius*, from Burrow et al. (2015); (f) *Ptomacanthus*, from this chapter, scapulocoracoid inferred from Miles (1973a); (g) *Diplacanthus*, from Miles (1973a) and this chapter; (h) *Uraniacanthus*, from Hanke and Davis (2008); (i) *Acanthodes*, from Miles (1973a); (j) *Cheiracanthus*, from Miles (1973a); (k) *Euthacanthus*, from Miles (1973a); (l) *Ischnacanthus*, from Miles (1973a) (procoracoid conjectural); (m) *Doliodus*, from Maisey et al. (2017); (n) *Onychoselache*, from Coates and Gess (2007); (o) *Akmonistion*, from Coates and Sequeira (2001a); (p) *Mimipiscis*, an osteichthyan, from Miles (1973a). Colours: Green, prepectoral spine 1; Orange, Prepectoral spine 2; Purple, posterolateral angle.

recover them (eg. Coates et al. (2018)), it may be evidence that *Vernicomacanthus* lies in a relatively crownwards position in the chondrichthyan stem-group. Alternatively, if acanthodians are monophyletic, it could instead provide evidence for Vernicomacanthus as a sister taxon to a larger acanthodian clade. More information on stem-chondrichthyan scapulocoracoids is required to resolve this.

The coracoid region provides another source of characters in the endoskeletal shoulder girdle. In acanthodians the coracoid region is often mineralised separately to the rest of the shoulder girdle, in what is known as a procoracoid (Miles, 1973a). Procoracoids are known in a range of acanthodian taxa: principally diplacanthids, gyracanths, acanthodiforms, and *Lupopsyrus* (Miles, 1973a; Hanke and Davis, 2012). In these taxa they differ slightly in shape, but appear to comprise the same part of the coracoid region. Procoracoids have also been reported in symmoriiforms such as *Akmonistion* and *Cobelodus* (Coates and Sequeira, 2001a; Zangerl and Case, 1976). Unusually, in these animals they co-occur with a coracoid process, with the procoracoid seemingly only forming the tip of the coracoid region. This, combined with the face procoracoids are absent in stem-chondrichthyans *Gladbachus* and *Doliodus*, suggests that this is probably a homoplasious occurrence.

Based on this distribution it might seem likely that the mineralisation of separate procoracoids is a plesiomorphic chondrichthyan character. However, in many stem-chondrichthyans they are absent, or at least the coracoid region is unmineralised (Miles, 1973a). Moreover in some stem-chondrichthyan taxa, such as *Ptomacanthus sp.* (Miles, 1973a) or in *Doliodus* (Maisey et al., 2017), the whole coracoid region is mineralised This may indicate a relatively crownwards position. Alternatively the presence or absence of mineralisation in the procoracoid region may just be quite a labile character.

My reinterpretation of the procoracoid in *Diplacanthus* allows us to identify a common architectural similarities between the procoracoids in a range of stem-chondrichthyans. In particular the procoracoid of *Diplacanthus* is very similar in structure to that in gyracanths, such as *Gyracanthides* and *Gyracanthus* (Snyder et al., 2017; Warren et al., 2000; Turner et al., 2005). Like these it comprises a dorsal process, a medial shelf and a dermal structure appended to the ventro-lateral surface. The procoracoids of *Acanthodes* and *Cheiracanthus* also appear to have some similarity to this, with dorsal processes, although it is difficult to assess the presence or absence of a medial shelf. Although it lacks a separate procoracoid mineralisation, this morphology also bears similarities with the procoracoid region of *Doliodus* (Maisey et al., 2017). This also seems to have a dorsal flange, a medial shelf, and a prepectoral spine attached to the ventro-lateral margin. Although not known in great detail, in *Gladbachus* the procoracoid region again has a similar structure (Mike Coates, personal communication). Although this does not provide any new characters, this recognition of a common architecture throughout the chondrichthyan stem-group may lead to them in future.

6.5.2 **The dermal shoulder girdle in stem-chondrichthyans**

The array of plates and spines which encases the ventral shoulder girdle in many acanthodians also provides a potential source of phylogenetic information (Fig. 6.11). Miles (1973a) considered that these originated from an armoured ancestor with a "full complement" of paired spines, paired plates, and median plates, which gradually were gradually lost throughout the evolution of acanthodians. Recent topologies (eg. Coates et al. (2018)) provide limited support for a similar idea, with the heavily armoured outgroup condition in osteichthyans and stem-gnathostomes suggesting that armoured shoulder girdles were gradually lost in chondrichthyans. Pectoral spines are also arguably plesiomorphic for gnathostomes, as there is no

a priori reason to preclude homology with the spinal plates observed in early osteichthyans (eg. Choo et al. (2017)) and stem-gnathostomes (eg. Long (1997)). However, some aspects of the dermal shoulder girdle do appear to be unique to chondrichthyans.

Uniquely stem-chondrichthyans possess prepectoral spines (also see Chapter 2 of this thesis). Principally, prepectoral spines are found in climatiid-like acanthodians - often they are associated with a dermal plate like in *Climatius*, *Vernicomacanthus*, *Euthacanthus*, *Dobunnacanthus* gen. nov., *Ptomacanthus*, and *Parexus* (Miles, 1973a) (Fig. 6.11). Spines are also found in the acanthodiform *Promesacanthus*, the diplacanthiform *Uraniacanthus* and the ischnacanthiform *Acritolepis*, suggesting they are probably plesiomorphic for "acanthodians" (Hanke, 2008; Hanke and Davis, 2008; Newman et al., 2012; Valiukevičius, 2003). This broad distribution suggests that these spines are probably a plesiomorphic feature of stem-chondrichthyans.

Prepectoral spines were also recently described in the relatively more crownward stem-chondrichthyan *Doliodus* (Maisey et al., 2017). These are unaccompanied by dermal plates, and are particularly informative as they are preserved mounted in their life position on the endoskeletal shoulder girdle. Two spines are present in *Doliodus*: - one immediately ventral and anterior to the fin spine, and the other anterior to this with a slightly more ventrally oriented apex. Maisey et al. (2017) primarily argue that the posterior of these spines is an admedian spine, although concede that it could be a second prepectoral. Comparison with the dermal pectoral girdle of *Ptomacanthus* suggests that it is instead a second prepectoral, as it occupies the same position and orientation relative to the pectoral fin spine and the anterior prepectoral (Fig. 6.11, 6.10). More broadly it suggests that the prepectoral spines can be strictly defined as spines that are situated on the

corocoid region of the shoulder girdle.

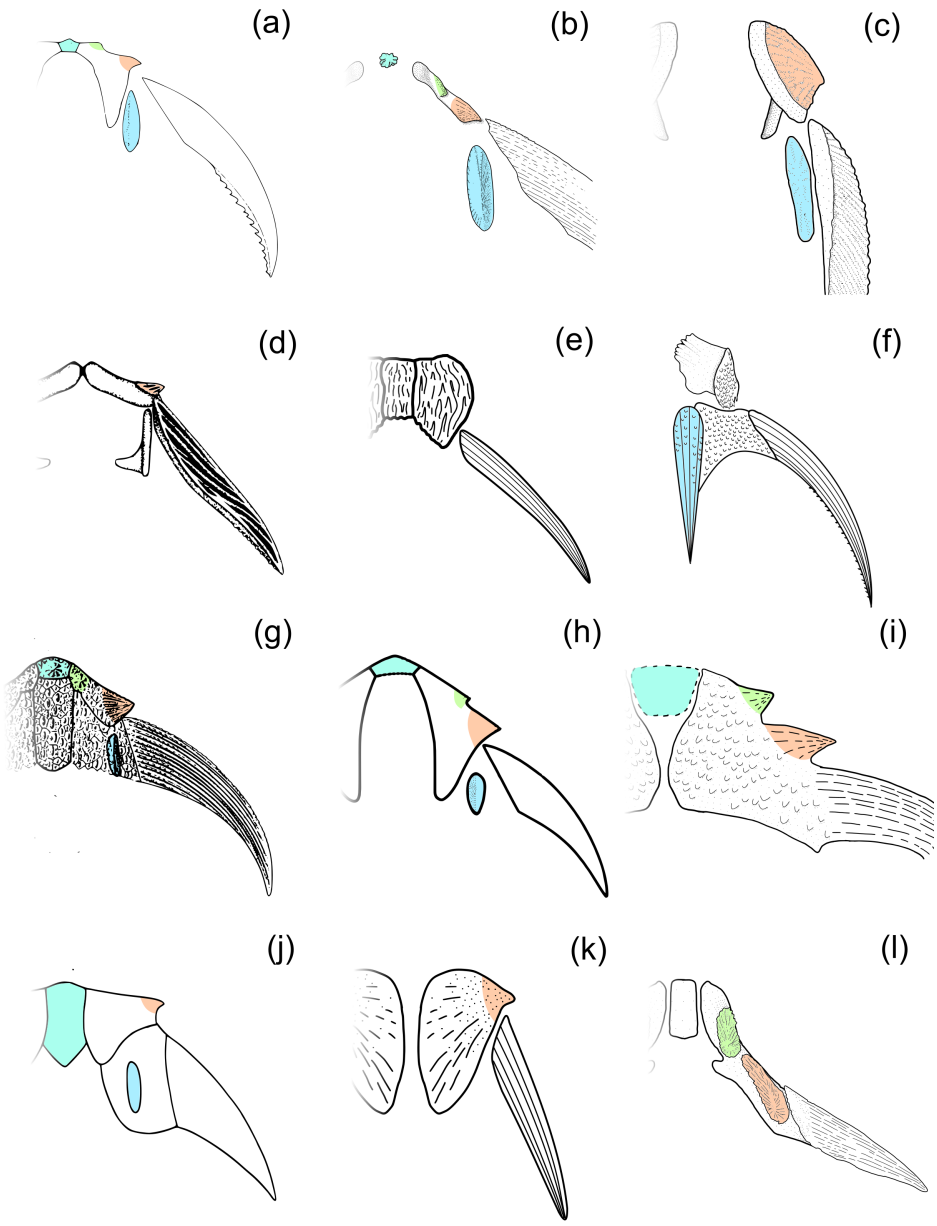


FIGURE 6.11: Caption on next page

FIGURE 6.11: Selected gnathostome shoulder girdles in ventral view. Depicted are (a) *Vernicomacanthus*, from this chapter; (b) *Dobunnacanthus* gen. nov., from Miles (1973a); (c) Gyracanthides, from Warren et al. (2000); (d) *Lupopsyrus*, from Hanke and Davis (2012); (e) *Culmacanthus*, from Long (1983); (f) *Diplacanthus*, from Miles (1973a) and this chapter; (g) *Climatius*, from Burrow et al. (2015); (h) *Parexus*, from Miles (1973a); (i) *Ptomacanthus*, from this chapter; (j) *Brachyacanthus*, from Miles (1973a); (k) *Euthacanthus*, from Miles (1973a);(m) *Doliodus*, from Maisey et al. (2017). Colour scheme as for Fig. 6.10 with: Cyan, median plate/spine; Blue, first intermediate ("admedian") spine.

This definition of prepectoral spine placement allows a clarification of the evolution of prepectoral spines in stem-chondrichthyans. The three paired fin spines in the hypothetical acanthodian ancestor of (Miles, 1973a) seems unlikely when conditions are mapped onto current phylogenetic topologies. The only taxa with three paired prepectoral spines are (possibly) *Kathemacanthus* and *Seretolepis*, both of which are "shark-like" taxa (Hanke and Wilson, 2010), and *Erriwacanthus*, a genus based on isolated armoured dermal shoulder girdles (Miles, 1973a). Instead by far the most common pattern is two prepectoral spines, and this seems likely to be plesiomorphic for chondrichthyans.

Accompanying the prepectoral spine in some chondrichthyan taxa is a median prepectoral spine (Fig. 6.11). This is present in a number of climatiids, such as *Climatius*, *Vernicomacanthus*, *Parexus*, *Ptomacanthus*, *Dobunnacanthus* gen. nov., and possibly *Brachyacanthus* and *Lupopsyrus* (Miles, 1973a; Hanke and Davis, 2012; Gagnier and Wilson, 1996b). It is absent in all known acanthodiforms, diplacanthiforms and ischnacanthiforms - however, a spineless median plate is present in the likely diplacanthiform *Culmacanthus* (Long, 1983). While a median dermal ossification is absent in *Doliodus*, a median endoskeletal component of the shoulder girdle does exist, which Maisey et al. (2017) observe could be homologous with the perichondral lining of the lorical plate in *Climatius*. This median prepectoral

spine could be a character uniting a subset of "climatiid" stem-chondrichthyans. However, as a character it can be problematic as it is often small and difficult to observe amidst the squamation, for example in the case of *Lupopsyrus* (Hanke and Davis, 2012). Moreover, median plates are also present in various osteichthyan and stem-gnathostome taxa (eg. interclavicles in osteichthyans (Gardiner, 1984), median ventral plates in placoderms (Denison, 1978)), and could be a crown-gnathostome plesiomorphy (noted by King et al. (2016)).

Another feature unique to stem-chondrichthyans is a row of intermediate, or pre-pelvic, spines - spines seemingly unassociated with any endoskeletal structure, and which form a paired series between the pectoral and pelvic fins. In some taxa the anterior pair of these spines is associated with the pectoral girdle, termed admedian spines by Burrow et al. (2016a) (Fig. 6.11). While the classification of these spines as intermediates is disputed (Burrow et al., 2016a), it seems most sensible to consider them to be intermediates as they are invariably in series with posterior intermediates. Admedian spines are most pronounced in diplacanthids, in which they are huge and attached to the pectoral fin spines by dermal sheets (Burrow et al., 2016a; Miles, 1973a). They are also present in a number of climatiids where they are either embedded in the dermal armour (eg. *Brachyacanthus*, *Sabrinacanthus*, and *Erriwacanthus falcatus* (Miles, 1973a)) or in the same position but free of armour (eg. *Vernicomacanthus*, *Dobunnacanthus*, *Parexus*, *Gyracanthides*, and Burrow *et als'* redecription of Climatius (Burrow et al., 2015; Miles, 1973a)). *Ptomacanthus* lacks admedian spines, as do ischnacanthiforms and acanthodiforms (Brazeau, 2012; Miles, 1973a). On the basis of my interpretation, *Doliodus* lacks evidence of admedian fin spines (*contra* Maisey et al. (2017)). The absence of these spines could indicate a placement in the chondrichthyan stem-group crownwards relative to acanthodian-grade animals - the paucity of intermediate spines in ischnacanths and acanthodids is presumably independently derived.

6.5.3 **Vernicomacanthus and possible kin**

Amongst stem-chondrichthyans *Vernicomacanthus* and *Dobunnacanthus* gen. nov. bear a number of anatomical similarities with gyracanths, a poorly understood group of unusually large acanthodians known mainly from isolated pectoral fin spines (Burrow et al., 2008). Like gyracanths the fin spines of *Vernicomacanthus* and *Dobunnacanthus* gen. nov. are ornamented with oblique, nodulate ridges converging on the leading edge of the spine, forming a chevron pattern when the spine is viewed anteriorly. *Vernicomacanthus*, although not *Dobunnacanthus* gen. nov., also possess posterior denticles on the inside edge of pectoral spines. The scales of all three taxa also appear to comprise multiple laterally apposed odontodes on a single base plate, although a similar morphology is also present in several "conventional" chondrichthyans (eg. *Gogoselachus* and *Tamiobatis* (Long et al., 2015; Williams, 1998)). This suite of characters could plausibly unite these taxa to the exclusion of other acanthodian-grade taxa.

Similar characteristics are found in a number of other acanthodians which may also be associated with these animals. As Burrow et al. (2008) observed, the isolated spines of *Ankylacanthus* are extremely similar to those of *Vernicomacanthus*, with oblique, nodulate ridges and trailing edge denticles. Scales associated with *Ankylacanthus* are also formed from laterally positioned odontodia (Burrow et al., 2008). The fin spines of *Lupopsyrus* also exhibit both oblique striations and trailing edge denticles (Hanke and Davis, 2012). While the scales of *Lupopsyrus* are monodontode, the crowns are markedly similar in shape to the individual crowns in *Vernicomacanthus* (Hanke and Davis, 2012). Combined with its comparatively small size, this could mean that the taxon *Lupopsyrus* represents either young animals related to *Vernicomacanthus* and these other taxa, or a taxon which has undergone some level of paedomorphosis in scale growth.

Another notable similarity can be found between the scales of *Vernicomacanthus* and those of *Altholepis*, a putatively chondrichthyan scale-based taxon originally described from the Lochkovian of Podolia (Karatajūtė-Talimaa, 1997). Since its original description *Altholepis* has also been found in the Early Devonian of Spain, the UK, and Canada (Martinez-perez et al., 2010; Turner et al., 2017; Hanke et al., 2013) amongst a similar collection of taxa to those from Podolia. *Altholepis* is a growing scale type, with younger odontodes growing laterally and posteriorly to the primordium in a series of lateral antero-posteriorly oriented ridges, very similarly to what we describe in *Vernicomacanthus*. Further building the link between *Vernicomacanthus* and *Altholepis* is an undescribed articulated *Altholepis* from the MOTH locality which has markedly *Vernicomacanthus*-like fin spines (pers. obs., figured in the PhD thesis of Gavin Hanke). Scales assigned to *Altholepis* are fairly divergent in form, and so probably belong to a range of general, quite possibly not all gyracanthid-like animals. However, at least some seem likely to belong to similar animals to *Vernicomacanthus*.

6.6 CONCLUSION

Vernicomacanthus uncinatus shows similarities in finspines and scales with gyracanths and other similar taxa, which may constitute evidence of a group on the chondrichthyan stem. This includes *Dobunnacanthus waynensis* gen. nov.. New information has been presented on the shoulder girdle of *Ptomacanthus* and *Diplacanthus* Combined in particular with the recent description of an acanthodian-like soulder girdle in *Doliodus* this has led to a more coherent picture of shoulder girdle in stem-chondrichthyans.

CHAPTER 7

A PHYLOGENETIC EXPLORATION OF THE CHONDRICHTHYAN STEM-GROUP

7.1 INTRODUCTION

As has been reiterated throughout this thesis, relationships on the chondrichthyan stem-group remains poorly understood. It can now be stated with reasonable confidence that acanthodians are all stem-group chondrichthyans, and it seems unlikely that they form a single clade. As Coates et al. (2018) note, a dichotomy appears to exist between in this stem-group between the Acanthodii and conventional chondrichthyans + climatiids. However, the interrelationships between taxa in this stem-group remains poorly known, as does support for proposed clades within it. In this chapter I attempt to address this with a phylogenetic analysis targeting the chondrichthyan stem-group. I discuss the results of this analysis and its implications for the evolution of chondrichthyans.

7.2 METHODS

7.2.1 **Character list**

This character list was assembled from a variety of recent phylogenetic analyses. Primarily these were Giles et al. (2015c) and Coates et al. (2018, 2017a), but characters were also taken from other sources, detailed in Appendix B. Details of changes to the character list and notes are available in Appendix B

7.2.2 **Taxon selection**

I have tried to select a broad range of stem-chondrichthyans for this analysis, on the basis of having a reasonably complete articulated skeleton and a plausibly useful set of morphological characters. Taxa comprising only isolated dermal elements were not included in the analysis. I have also attempted to select a representative, broad range of crown-group chondrichthyans and Palaeozoic "sharks". Outside the chondrichthyan total group taxa were selected to try to reflect a broad swathe of gnathostome phylogeny.

Ptomacanthus, *Diplacanthus*, *Vernicomacanthus*, and *Dobunnacanthus* have had data scored on the basis of unpublished data within this thesis. Coates et al. (2017a) make a convincing argument that the *"Cobelodus"* braincase described by Maisey (2007) is in fact cospecific with the pharynx and skull of *Ozarcus* described by Pradel et al. (2014): both are considered together here in the taxon *Ozarcus*. *Ligulalepis* is scored only on the basis of the cranial materal described by Basden et al. (2000); Basden and Young (2001), and Clement et al. (2018). Osteostraci and Galeaspida are composites of available information on both putative groups (summarised in Janvier (1996)).

Taxa were mainly scored from published data, but some scorings were made from my own observations of material. These are noted in Appendix B, in which full details of sources for taxa are also provided. The matrix is provided in Appendix C.

7.2.3 **Parsimony analysis**

Parsimony analysis of the dataset was carried out in TNT version 1.5 (Goloboff and Catalano, 2016). A parsimony ratchet was used with TBR branch swapping. 10,000 iterations of were carried out, holding 100 trees each iteration. The topological

constraint (Galeaspida(Osteostraci(Mandibulate gnathostomes))) was enforced, with Galeaspida designated as the outgroup. Bremer support values for each node of the strict consensus tree were also calculated in TNT using the script `Bremer.run`. Lists of unambiguous synapomorphies for the strict consensus tree were calculated in PAUP* (Swofford, 2003) while a graphic representation of these on the agreement subtree of all most parsimonious trees (MPTs) was generated using Macclade (Maddison and Maddison, 1992). The matrix, all MPTs recovered, a file to run the tnt analysis, and the Bremer support value script are provided in Appendix C, along with all character changes under ACCTRAN and DELTRAN optimisations mapped onto the strict consensus tree.

7.2.4 **Bayesian analysis**

Bayesian analysis was carried out in MrBayes v.3.2.6 (Huelsenbeck and Ronquist, 2001; Ronquist and Huelsenbeck, 2003). As a prior I constrained mandibulate gnathostomes as a monophyletic group, with Galeaspida set as the outgroup. An Mkv model was used, with rate heterogeneity modelled with a gamma distribution with 5 discrete rate categories. The search was carried out for 1000000 generations, sampling a tree every 1000 generations. From this sample a majority rule consensus was calculated using a relative burn-in of 25%. This matrix is provided in Appendix C.

7.3 RESULTS

The parsimony analysis resulted in 29463 MPTs of 842 steps in length. The topology of the chondrichthyan total-group from both this and the Bayesian tree are summarised below, with reference to support values.

Both parsimony and Bayesian analyses recover a monophyletic Chondrichthyes including all acanthodian-grade taxa (Figs. 7.1, 7.3, 7.2), strongly supported by node support values. Both also recover the acanthodian grade as a paraphyletic array of stem-chondrichthyans. As in previous analyses, a grade comprising ischnacanthiforms, acanthodiforms, and diplacanthiforms subtends a clade including crown-chondrichthyans, stem-group "conventional" chondrichthyans, and "climatiid" acanthodians.

Support for a monophyletic Acanthodii, comprising ischnacanthiforms, acanthodiforms, and diplacanthiforms, is limited. The strict consensus lacks almost all resolution in this grade, recovering only small clades of ishnacanthids and diplacanthids (Fig. 7.1). The Adams consensus (Fig. 7.1b) and the agreement subtree (Fig. 7.5) reveal that there is some support for Acanthodii in the MPTs, with a clade of diplacanthids and acanthodids to the exclusion of ischnacanthids in a polytomy with *Euthacanthus*, *Latviacanthus*, and more crownwards chondrichthyans. However, the Bayesian analysis also fails to recover Acanthodii, instead recovering paraphyletic ischnacanthids subtending a polytomy between acanthodiforms, diplacanthiforms, *Cassidiceps*, *Latviacanthus*, and more crownwards chondrichthyans (Fig. 7.2). Here *Euthacanthus* is recovered as lying more crownwards, as the sister-group to crown-chondrichthyans and more crownwards stem-chondrichthyans.

There is some resolution to putative groups within this grade. Diplacanthids *Uraniacanthus*, *Culmacanthus*, *Diplacanthus*, and *Rhadinacanthus* are recovered in all three consensus trees shown, with some support from the Adams consensus for *Tetanopsyrus* and *Milesacanthus* joining them in a clade. A clade of acanthodids, including *Promesacanthus*, *Mesacanthus*, *Cheiracanthus*, *Homalacanthus*, *Acanthodes*, and *Halimacanthodes* is also recovered by the Bayesian trees, although is not supported by parsimony results. Ischnacanthids - *Poracanthodes*, *Ischnacanthus*, and *Nerepisacanthus* group together in parsimony results but not in the Bayesian tree.

Latviacanthus, *Cassidiceps*, and *Euthacanthus* are also all associated with this grade.

Crownwards relative to these taxa, "climatiid" acanthodians are recovered as a paraphyly along with "conventionally chondrichthyan" stem-chondrichthyans (Figs. 7.1, 7.3, 7.2). There is some evidence for a clade of Early Devonian "climatiids" within this from the Bayesian tree and Adams consensus, although exact membership varies and it is unresolved in the strict consensus. Others form a series of clades leading to the crown-group. Particularly strongly supported, by both Bremer support and posterior probability, is the node subtending *Brochoadmones* and all more crownwards chondrichthyans.

Resolution of the chondrichthyan crown-group differs in both analyses. The Bayesian tree fairly strongly supports symmoriiformes as being part of the holocephalan total group (Fig. 7.2). However, in the parsimony analysis elasmobranchs, definite holocephalans and symoriiformes are recovered in a three-way polytomy (Figs. 7.1, 7.3). Iniopterygians are recovered as stem-group holocephalans. In both sets of results ctenacanths, and xenacanths are recovered as stem-group elasmobranchs with limited supported, as is *Gogoselachus*. Hybodonts are more strongly supported as members of the elasmobranch stem-group.

The parsimony agreement subtree with unambiguous character state changes is shown in Figs. 7.4 and 7.5. These state changes listed for the parsimony strict consensus are given in `Synapomorphy_List.txt` in the supplement.

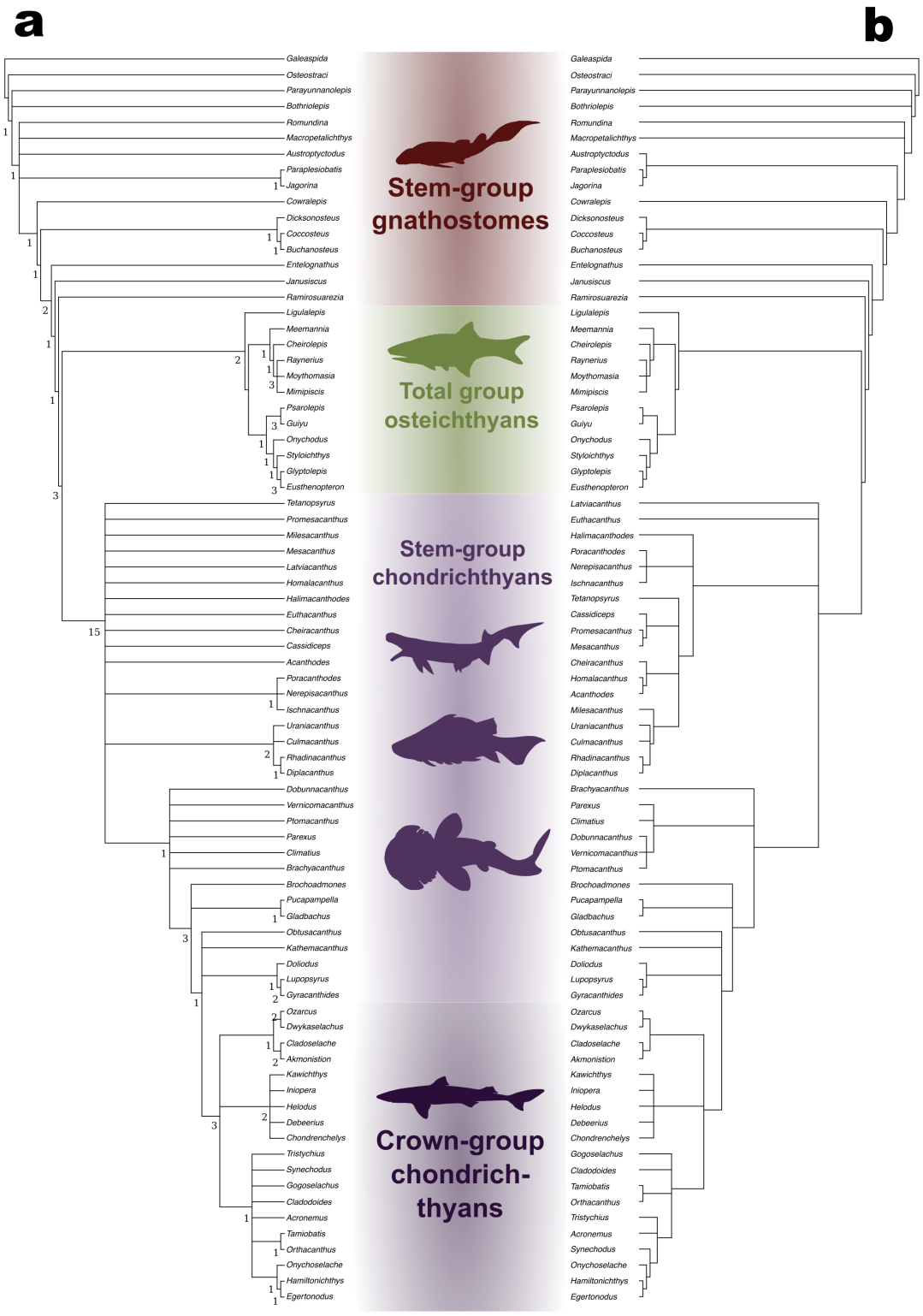


FIGURE 7.1: (Caption next page.)

FIGURE 7.1: Results of parsimony analysis: (a) strict consensus tree, with Bremer decay indices for each node (b) Adams consensus tree

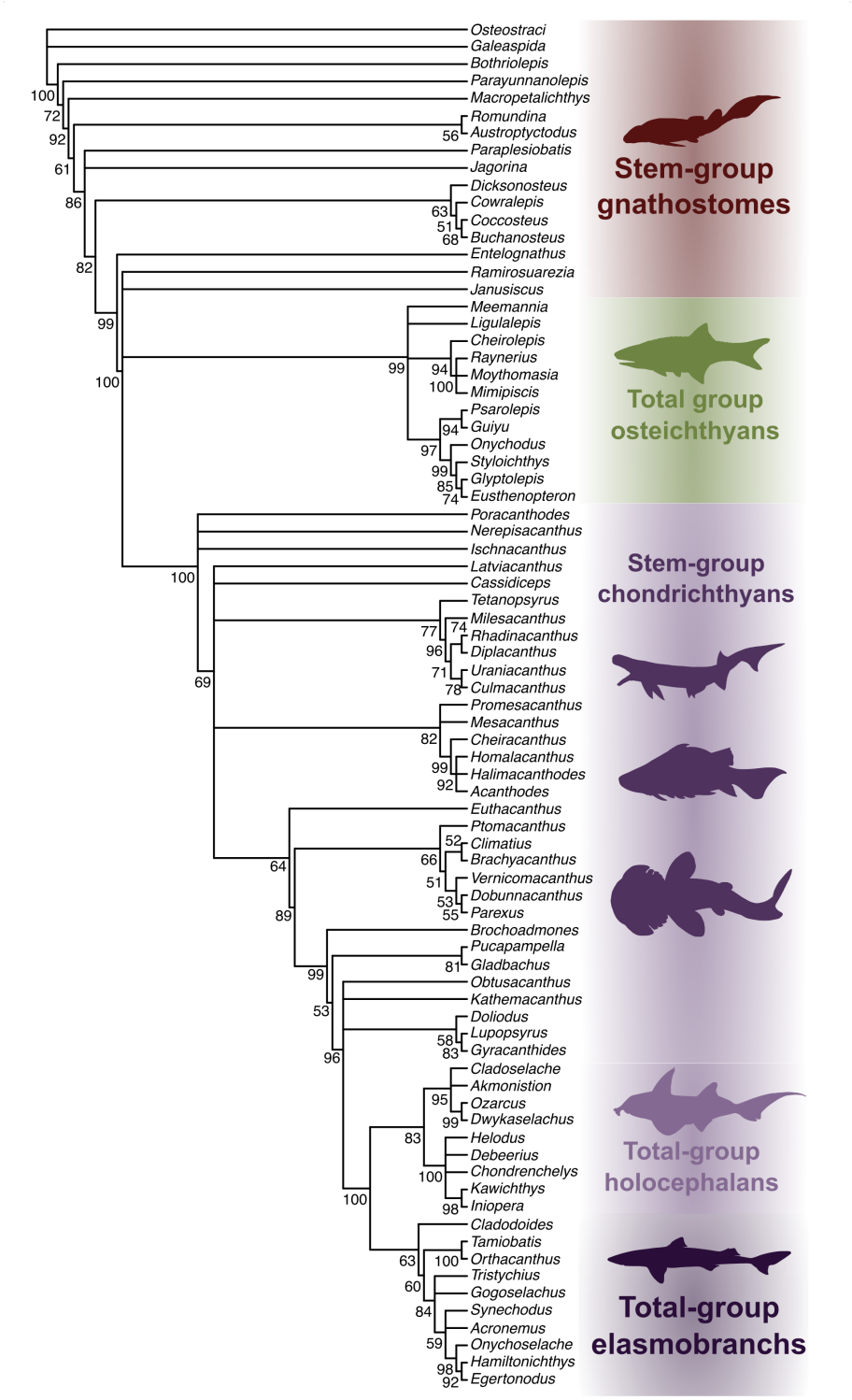


FIGURE 7.2: (Caption next page.)

FIGURE 7.2: Majority rule consensus from the Bayesian analysis: node numbers are posterior probabilities as percentages

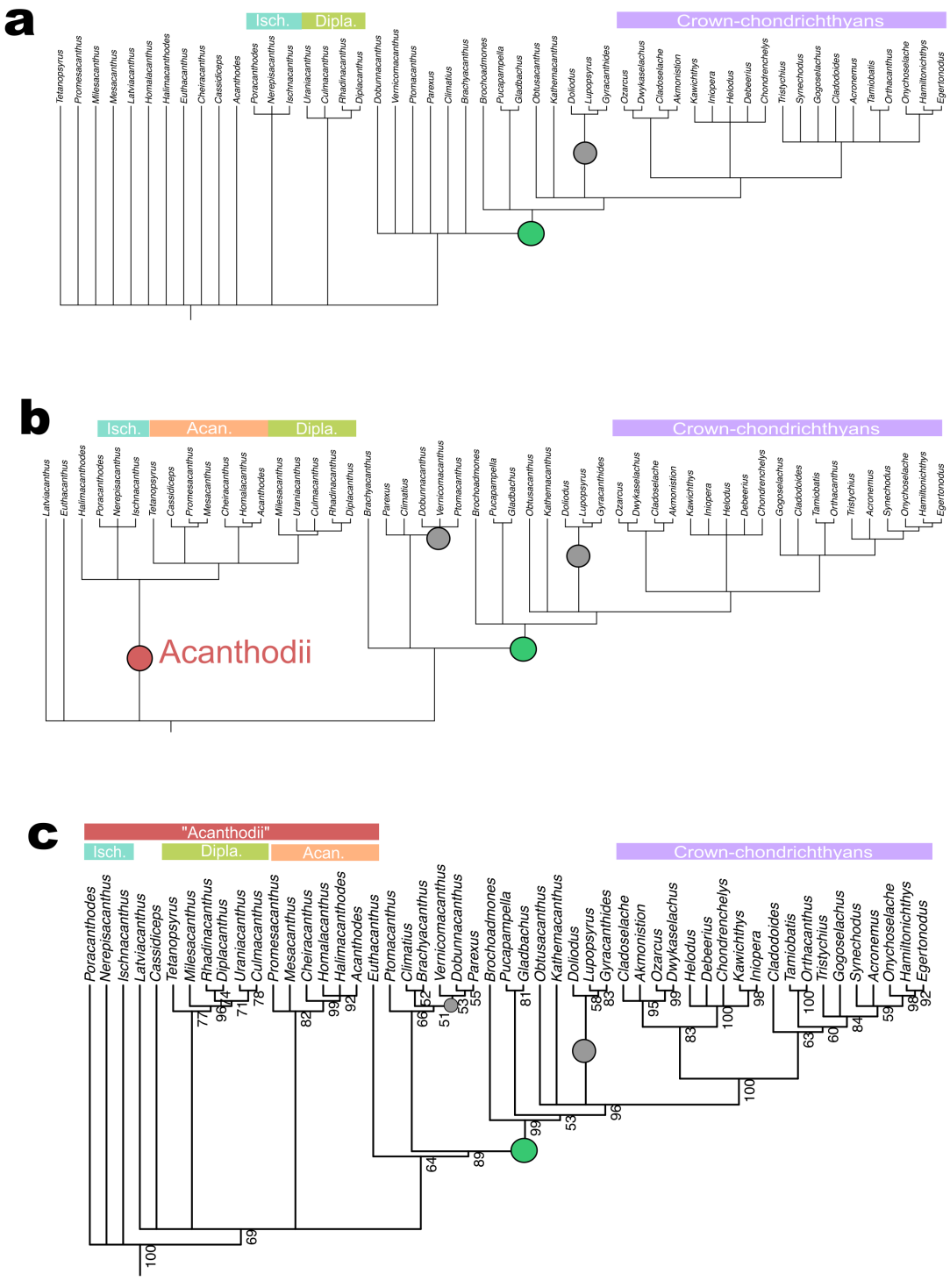


FIGURE 7.3: (Caption next page.)

FIGURE 7.3: Chondrichthyan total-group from results of different analyses, with different parts labelled. (a) parsimony strict consensus; (b) parsimony Adams consensus; (c) Bayesian result. Abbreviations: Acantho: acanthodiforms; Dipla, diplacanthiforms; Isch, ischnacanthiforms. Grey blobs are clades with "gyracanthid" characters, Green blob is inferred position of posterior shift of branchial skeleton

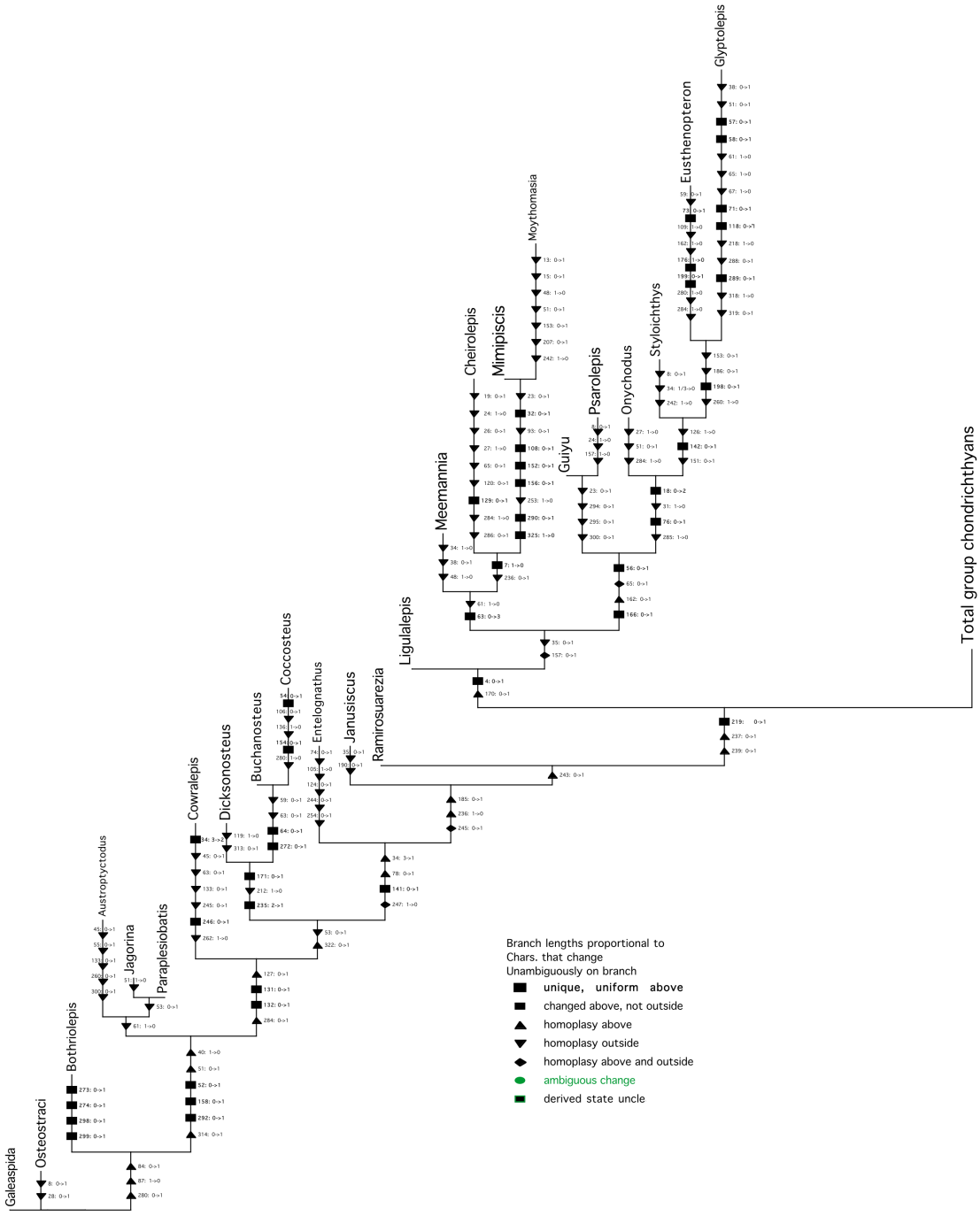


FIGURE 7.4: Unambiguous synapomorphies plotted on agreement subtree, excluding the chondrichthyan total group.

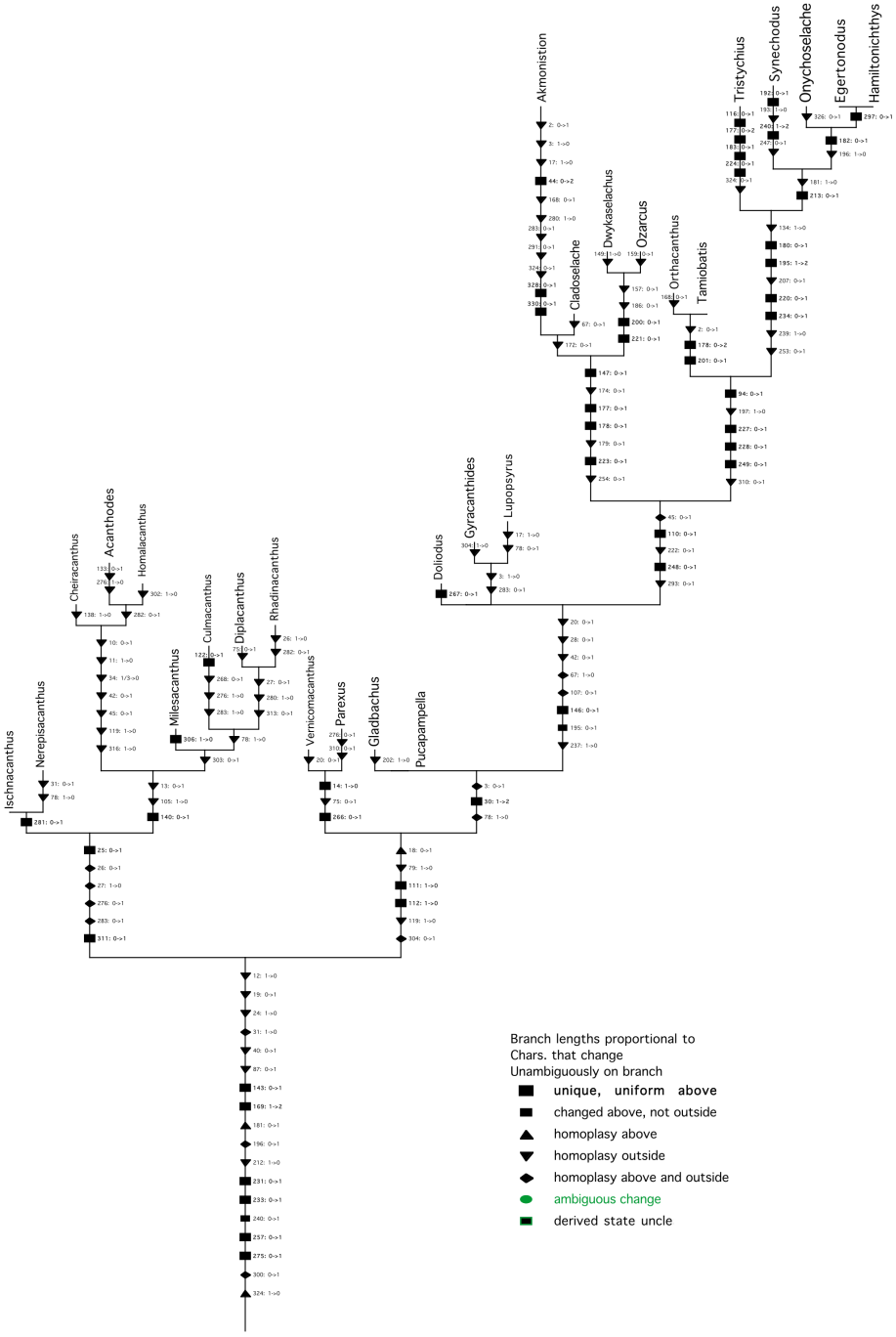


FIGURE 7.5: Unambiguous synapomorphies of the chondrichthyan total group, plotted on agreement subtree.

7.4 DISCUSSION

7.4.1 **Relationships of the chondrichthyan stem-group**

My results strongly support all acanthodians being stem-group chondrichthyans, now the predominant view of early vertebrate workers. More generally the tree also conforms with the general view of early vertebrates, with a paraphyletic placoderms-grade stem-gnathostomes and a monophyletic osteichthyans as the sister group to chondrichthyans. This is supported by a host of characters (Fig. 7.5) across their anatomy. This includes several characters discussed in Chapter 2, such as the absence of an osteonal vascular middle layer of the dermal integument, the antero-dorsal addition of odontodes, a dermal skull roof made from tesserae or scales, the articulation of the hyoid ventral to the jugular vein, and a scapular process of the shoulder girdle (Fig. 7.5). I recover no indication that acanthodian-grade taxa form a clade.

Only limited support is found for the Acanthodii forming a clade, as suggested by Coates et al. (2018). In the agreement subtree (Fig. 7.5), where this clade is recovered, it is supported by anvil-like scales with bulging bases, and flattened fin spines. However, there is strong support for these taxa forming a grade subtending all other total group chondrichthyans. Although the Adams consensus (Fig. 7.1b) and Bayesian consensus (Fig. 7.2) show different topologies, both show a closer association between diplacanthids and acanthodids than either has with ischnacanthids, which differs from some previous results (see Coates et al. (2018) Supplementary fig. 9). They are grouped by the absence of bone cell lacunae in scale bases, a lack of teeth, and a perforate metapterygoid. The positions of *Euthacanthus* and *Latviacanthus* in association with this group suggests that they may be intermediate taxa, with a combination of "Acanthodii"-like and "climatiid"-like character states. The recovery of diplacanthids as a distinct clade within the Acanthodii suggests that their distinct morphology developed from a more

generalised, possibly somewhat acanthodiform-like morphology, with *Tetanopsyrus* and *Milesacanthus* possibly acting as a morphological bridge between diplacanthids and other Acanthodii. The unusual *Culmacanthus* is recovered well within this clade, suggesting that its high degree of armouredness is secondarily derived rather than primitive.

The lack of resolution for acanthodiforms in my parsimony analysis is unusual compared to other recent analyses, although the Bayesian result recovers an acanthodiform clade. There seems to be a rough split between *Acanthodes*-like and mesacanthid-like taxa. Particularly odd is the recovery of *Halimacanthodes*, which is extremely like *Acanthodes* in form (Burrow et al., 2012), outside the "acanthodiforms" by the parsimony analysis. I suspect this reflects the lack of information on the dermal skeleton of the head of *Halimacanthodes* rather than its true phylogenetic position, as was borne out in the Bayesian analysis. This specimen would be a prime candidate for CT-scanning, given its three dimensionally preserved branchial skeleton, and which may also reveal details of the dermal head skeleton.

Similarly to other recent analyses I find no evidence that "climatiid" acanthodians form a clade. Instead, as in other analyses, they appear to reflect the gradual loss of ostensibly climatiid plesiomorphic states throughout the chondrichthyan stem-group. The clade they form with crown-group members is distinct from the Acanthodii clade in the agreement subtree on the basis of characters including areal scale growth, and *contra* my predictions in Chapter 6 I recover no "gyracanth"-like clade in the climatiid part of the chondrichthyan stem-group. However, I do resolve two separate clades based on gyracanth-like characters: of *Parexus*, *Dobunnacanthus* and *Vernicomacanthus* on the one hand, and *Doliodus*, *Gyracanthides*, and *Lupopsyrus* on the other. What appears to be separating *Parexus*, *Dobunnacanthus* and *Vernicomacanthus* from the ingroup is their relatively heavily armoured shoulder girdles. The group including *Parexus* is not

present in the parsimony result. Several characters from my scheme in Chapter 2 support nodes thorughout this "climatiid" stem-group. The addition of odontodes in bilateral symmetry (Fig. 7.5) supports *Doliodus* and all more crownwards taxa. Supporting taxa crownwards of *Doliodus* is tooth whorls with separated bases (Fig. 7.5).

The poor resolution of more crownwards stem-chondrichthyans in both analyses possibly reflects the fact that many of them are based on fairly non-comparable information. These taxa are excluded from the chondrichthyan crown-group by a lack of tessellate calcified cartilage and pushed up by the gill skeleton and their lack of shoulder armour. It comprises animals such *Pucapampella* and *Doliodus*, which are known almost entirely from their endoskeletons (Maisey and Anderson, 2001; Maisey, 2001a; Miller et al., 2003; Maisey et al., 2009, 2017), and animals such a *Kathemacanthus* and *Brochoadmones* which are known almost entirely from dermal information (Hanke and Wilson, 2010, 2006). Attempting to bridge this informational gap may be key to resolve their relationships.

No clear conclusions can be drawn about the chondrichthyan crown-group from the results of this analysis. The elasmobranch total group, including hybodonts, is well-supported. This support includes characters from my scheme in Chapter 2, including a medial capsular wall, an anhedral angle, an isolated posterior canal, and perilymphatic fenestrae (Fig. 7.5). However, the relationship between elasmobranchs, holocephalans, and symoriiformes is unclear. No definite holocephalans are present in the agreement subtree and so no unambiguous characters are present in the figured tree, suggesting that the characters discussed in Chapter 2 are not all that clearly supportive in this tree.

7.4.2 **Implications for character evolution along the chondrichthyan stem-group**

Because of the disagreement between consensus results the implications for the ancestral chondrichthyan are not clear cut. However it likely had some of the character states previously associated with the supposed "climatiids". Paired pelvic and pectoral fin spines are a symplesiomorphy for crown-gnathostomes, being present both in stem-gnathostomes (Zhu et al., 2013) and in stem-osteichthyans (Zhu et al., 2009). Intermediate, prepectoral and anal fin spines are probably plesiomorphic for chondrichthyans, having evolved somewhere on earliest stem-chondrichthyan branch. A skull roofed by tesserae also evolved somewhere on this branch. Body scales are uncertain, but probably grew as some kind of polyodontodium, having lost an osteonal middle layer - it is uncertain whether areal growth was present. This entire character set is quite different to that in osteichthyans and placoderms, suggesting the record of a lot of morphological change is unknown.

As Maisey et al. (2017) showed, aspects of the "climatiid"-like shoulder girdle are actually retained almost to the divergence of crown-chondrichthyans. My analysis supports this, with several members of the polytomy immediately stemwards to the crown-group having spinose pectoral girdles. However, a dermally plated shoulder girdle appears to have been lost prior to this, being absent in all animals in this polytomy. As the description of *Doliodus* showed, Maisey et al. (2017) information on shoulder girdles in *Cladodoides* and *Pucapampella* might be more climatiid-like than previously imagined.

A tessellate "acanthodian-like" head skeleton is retained into the chondrichthyan crown-group. These are common in the chondrichthyan stem-group, and based on their distribution are probably plesiomorphic for total-group chondrichthyans. Head tesserae like those in early stem-chondrichthyans are

retained as late as the chondrichthyan crown-group (in *Tamiobatis* (Williams, 1998)). They are also present in *Gogoselachus* (Long et al., 2015), which we recover as a stem-group elasmobranch. I have however seen no report of tesserae in anything I recover as a holocephalan. In the topology I recover a tesselate head was presumably lost in the early holocephalan total-group. Alternatively if, as is possible, these taxa are stem-chondrichthyans, the absence of a tessellate head skeleton may be a crown-chondrichthyan character.

Another major change is the shift from typically "acanthodian" scales to polyodontode "ctenacanthid"-like morphologies over the course of the chondrichthyan stem-group. The latter is notable for its broad presence across the chondrichthyan total group: as well as in actual ctenacanths like *Tamiobatis*, similar scales are present in for example *Doliodus* (Miller et al., 2003), *Gogoselachus* (Long et al., 2015), *Vernicomacanthus* (Chapter 6), and possibly gyracanths (Turner et al., 2005). These are markedly different from the monodontode scales in most of the crown-group animals in this analysis. However, this analysis gives no clear indication of exactly when this transition took place. Scale type varies quite widely, and seem to have little correlation with dermal shoulder armour. As with head tesserae, scale morpholgies (again with the notable exception of *Gladbachus*) are extremely poorly known in articulated early "shark-like" taxa. However, "ctenacanthid"-type scales are present in animals displaying otherwise plesiomorphic chondrichthyan character traits (eg. *Vernicomacanthus*, *Doliodus*) and are probably plesiomorphic form the chondrichthyan crown-group. This suggests an ancestral crown-chondrichthyan which is possibly more acanthodian-like than previously appreciated - it will be important to collect data on the dermal skeletons of Palaeozoic chondrichthyans to resolve this.

A notable implication of this topology lies in what it means for the evolution of the chondrichthyan skull. Osteichthyans (eg. Gardiner (1984)), *Janusiscus*

(Giles et al., 2015c), *Acanthodes* Davis et al. (2012); Miles (1973b), *Diplacanthus* (see Chapter 4), and possibly *Milesacanthus* (Young and Burrow, 2004) all have a laterally restricted basioccipital relative to the otic region. Contrastingly, all other chondrichthyans have a laterally broad basioccipital region (sometimes considered a hypotic lamina): for example in *Doliodus* (Maisey et al., 2009), *Pucapampella* (Maisey and Anderson, 2001; Maisey, 2001a), *Cladodoides* (Maisey, 2005), and possibly *Ptomacanthus* (Brazeau, 2009). This could also be associated with a posterior shift of the divergence of the dorsal aorta, although based on the distribution of this character this is equivocal (see Chapter 7, Figure 4.6). The evolution of a broad basioccipital region appears to be a major morphological difference denoting crown-group chondrichthyans and some stem-group members.

Another major endoskeletal shift in the chondrichthyan stem-group concerns the posterior shift of the branchial skeleton behind the head (Coates et al., 2018). I have already discussed this at length in Chapter 3: the results of the analysis of this chapter corroborate the analysis described therein. The subcranial position of the gill basket in *Diplacanthus* and *Ptomacanthus* (and osteichthyans and placoderms (Gardiner, 1984; Brazeau et al., 2017)) suggests instead that the elasmobranch branchial skeleton evolved somewhere on the chondrichthyan stem-group, before the divergence of *Gladbachus* and all more crown-wards chondrichthyans. This supports what I argued in Chapter 3, that the posterior extension of the branchial skeleton in acanthodiforms is homoplasious with that of more crownwards chondrichthyans and, as Miles (1968) suggests, part of a suite of characteristics associated with their anguiliform body-shape. An elasmobranch-like branchial skeleton denotes a subset of total-group chondrichthyans including at least some of the stem-group.

Another uncertainty arising from this topology is on the ancestral state of the chondrichthyan dentition. Individual, symphyseal tooth whorls are found in several

osteichthyans (eg. *Onychodus*, *Guiyu* (Andrews et al., 2006; Zhu et al., 2009)), and these are possibly homologous with the symphyseal tooth whorls of ischnacanths. However, in the parsimony topology the state at the base of the Acanthodii is complete toothlessness, while the state at the base of all other chondrichthyans is to have tooth whorls. If, as recovered by the Bayesian analysis, ischnacanthiforms are the sister group to all other chondrichthyans, their dentigerous jaw bones may be homologous with the tooth-bearing dental plates of stem-gnathostomes and osteichthyans. However the homology of osteichthyan and chondrichthyan tooth whorls remains in doubt and merits more investigation to clarify the state of the dentition at the crown-gnathostome node.

7.5 CONCLUSION

My analysis supports the status of all acanthodian-grade animals as a paraphyletic array of stem-chondrichthyans. I find only limited support for the clade Acanthodii from the parsimony analysis, comprising ischnacanthids, acanthodids, and diplacantids, and associated with some problematic taxa. The dichotomy between the "Acanthodii" rump grade and remaining chondrichthyans reflects characters of dermal integument, as well as a reorganisation of the basicranium. "Climatiid" acanthodians are recovered as a paraphyly, with many ostensibly climatiid states reflecting plesiomorphic states for chondrichthyans. I find support for the development of a posteriorly placed chondrichthyan pharynx relatively crownwards on the stem-group, confirming that the relationships of *Gladbachus* lie crownwards of the acanthodian grade. The relationships of the crownwards part of the chondrichthyan stem-group remain poorly resolved, possibly reflecting distinct types of morphological information in the members of this paraphyly.

CHAPTER 8

CONCLUSION

In this thesis I have attempted to bring together several strands of evidence on the anatomy of acanthodian-grade stem-chondrichthyans to develop a clearer picture of the evolution of chondrichthyan anatomy. The branchial skeleton of *Ptomacanthus* allows us to constrain the evolution of an elasmobranch-like pharynx in the chondrichthyan stem-group. The data on *Diplacanthus* provides a valuable third "acanthodian" endoskeleton, and suggests that the development of a broad chondrichthyan basioccipital occurred somewhere between the acanthodian rump grade and "climatiids". Its tissue and that of the Mongolian placoderm help contrain endoskeletal tissues in vertebrates. *Vernicomacanthus* provides a valuable additional "climatiid" anatomy, and I hope the creation of the genus *Dobunnacanthus* will encourage people to use both in their phylogenetic analyses. My phylogenetic analysis provides support for the idea that stem-chondrichthyans fall out in a rump "Acanthodii" grade and a "climatiid" paraphyly, and that most ostensibly "climatiid" characters are chondrichthyan plesiomorphies. From this work I would predict that a particularly useful course of direction (notwithstanding the discovery of a pristine acanthodian braincase!) would be to attempt to mine comparable dermal data to that in acanthodians in stem-group and putative crown-group chondrichthyans such as *Doliodus* and *Tamiobatis*.

BIBLIOGRAPHY

Adrain, J. M. and Wilson, M. V. H. (1994). Early Devonian cephalaspids (Vertebrata: Osteostraci: Cornuata) from the southern Mackenzie Mountains. *Journal of Vertebrate Paleontology*, 14(3):301–319.

Ahlberg, P. E. (1989). Paired fin skeletons and relationships of the fossil group Porolepiformes (Osteichthyes : Sarcopterygii). *Zoological Journal of the Linnean Society*, 96:119–166.

Ahlberg, P. E., Trinajstic, K., Johanson, Z., and Long, J. A. (2009). Pelvic claspers confirm chondrichthyan-like internal fertilization in arthrodires. *Nature*, 460:888–9.

Alekseeva, R. E. (1993). *Biostratigraphy of the Devonian of Mongolia*. Nauka, Moscow.

Allen, D. (1944). The Belgic dynasties of Britain and their coins. *Archaeologia*, 90:1–46.

Allen, J. R. L. and Tarlo, L. B. (1963). The Downtonian and Dittonian Facies of the Welsh Borderland. *Geological Magazine*, 100:129–155.

Allis, E. P. (1897). The cranial muscles of Amia. *Journal of Morphology*, XII(3).

Allis, E. P. (1917). The prechordal portion of the chondrocranium of Chimaera colliei. *Proceedings of the Zoological Society of London*, VIII(December).

Allis, E. P. (1922). The Cranial Anatomy of Polypterus, with Special Reference to Polypterus bichir. *Journal of anatomy*, 56(Pt 3-4):189–294.

Allis, E. P. (1926). On the homologies of the prechordal portion of the skull of the holocephali. *Journal of anatomy*.

Andreev, P. S., Coates, M. I., Karatajūtė-talimaa, V., Shelton, M., Cooper, P. R., and Sansom, I. J. (2017). Elegestolepis and its kin , the earliest monodontode chondrichthyans. *Journal of Vertebrate Paleontology*, 37(1).

Andreev, P. S., Coates, M. I., Karatajūtė-Talimaa, V., Shelton, R. M., Cooper, P. R., Wang, N.-Z., and Sansom, I. J. (2016). The systematics of the Mongolepidida (Chondrichthyes) and the Ordovician origins of the clade. *PeerJ*, 4:e1850.

Andreev, P. S., Coates, M. I., Shelton, R. M., Cooper, P. R., Smith, M. P., and Sansom, I. J. (2015). Upper Ordovician chondrichthyan-like scales from North America. *Palaeontology*, 58(4).

Andrews, S. M., Long, J. A., Ahlberg, P. E., Barwick, R. E., and Campbell, K. (2006). The structure of the sarcopterygian Onychodus jandemarrai n. sp. from Gogo, Western Australia: with a functional interpretation of the skeleton. *Transactions of the Royal Society of Edinburgh: Earth Sciences*, 96:197–307.

Andrews, S. M. and Westoll, T. S. (1970). XII-The postcranial skeleton of Rhipidistian fishes excluding Eusthenopteron. *Transactions of the Royal Society of Edinburgh*, 68(12):391–489.

Basden, A. M. and Young, G. C. (2001). A primitive actinopterygian neurocranium from the Early Devonian of southeastern Australia. *Journal of Vertebrate Paleontology*, 21(4):754–766.

Basden, A. M., Young, G. C., Coates, M. I., and Ritchie, A. (2000). The most primitive osteichthyan braincase? *Nature*, 403(January):185–188.

Beck, K. G., Soler-gijón, R., Carlucci, J. R., and Willis, R. A. Y. E. (2016). Morphology and histology of dorsal spines of the xenacanthid shark Orthacanthus platypternus from the Lower Permian of Texas , USA : Palaeobiological and palaeoenvironmental implications. *Acta Palaeontologica Polonica*, 61(1):97–117.

Bendix-Almgreen, S. E. (1975). The paired fins and shoulder girdle in Cladoselache, their morphology and phyletic significance. *Colloques Internationaux du Centre National de la Recherche Scientifique*, 218:111–123.

Benton, M. J., Donoghue, P. C. J., Asher, R. J., Friedman, M., Near, T. J., and Vinther, J. (2015). Constraints on the timescale of animal evolutionary history. *Palaeontologica Electronica*, (18.1.1FC):1–107.

Berg, L. (1940). *Classification of fishes both Recent and fossil*. Trav. Inst Zool. Acad. Sci. URSS.

Bernacsek, G. M. and Dineley, D. L. (1977). New acanthodians from the Delorme Formation (Lower Devonian) of N.W.T., Canada. *Palaeontographica, Abteilung A*, 159:1–25.

Beznosov, P. (2009). A redescription of the Early Carboniferous acanthodian Acanthodes lopatini Rohon, 1889. *Acta Zoologica*, 90(May):183–193.

Blais, S. A. (2017). Precise occlusion and trophic niche differentiation indicate specialized feeding in Early Devonian jawed vertebrates. *Facets*, 2(1):513–530.

Blais, S. A., Hermus, C. R., and Wilson, M. V. H. (2015). Four new Early Devonian ischnacanthid acanthodians from the Mackenzie Mountains, Northwest Territories, Canada: an early experiment in dental diversity. *Journal of Vertebrate Paleontology*, 35(1):37–41.

Blais, S. A., MacKenzie, L. A., and Wilson, M. V. H. (2011). Tooth-like scales in Early Devonian eugnathostomes and the outside-in hypothesis for the origins of teeth in vertebrates. *Journal of Vertebrate Paleontology*, 31(6):1189–1199.

Botella, H. (2006). The oldest fossil evidence of a dental lamina in sharks. *Journal of Vertebrate Paleontology*, 26(4):1002–1003.

Botella, H., Donoghue, P. C. J., and Martínez-Pérez, C. (2009). Enameloid microstructure in the oldest known chondrichthyan teeth. *Acta Zoologica*, 90:103–108.

Brazeau, M. D. (2009). The braincase and jaws of a Devonian 'acanthodian' and modern gnathostome origins. *Nature*, 457(7227):305–308.

Brazeau, M. D. (2012). A revision of the anatomy of the Early Devonian jawed vertebrate Ptomacanthus anglicus Miles. *Palaeontology*, 55:355–367.

Brazeau, M. D. and de Winter, V. (2015). The hyoid arch and braincase anatomy of Acanthodes support chondrichthyan affinity of 'acanthodians'. *Biology letters*, 282.

Brazeau, M. D. and Friedman, M. (2014). The characters of Palaeozoic jawed vertebrates. *Zoological Journal of the Linnean Society*, 170(4):779–821.

Brazeau, M. D., Friedman, M., Jerve, A., and Atwood, R. (2017). A three-dimensional placoderm (stem-group gnathostome) pharyngeal skeleton and its implications for primitive gnathostome pharyngeal architecture. *Journal of Morphology*, 278(9):1–9.

Burrow, C. J. (2004). Acanthodian fishes with dentigerous jaw bones : the Ischnacanthiformes and Acanthodopsis. *Fossils and Strata*, (50):8–22.

Burrow, C. J. (2007). Early Devonian (Emsian) acanthodian faunas of the western USA. *Journal of Paleontology*, 81(5):824–840.

Burrow, C. J. (2011). A partial articulated acanthodian from the Silurian of New Brunswick, Canada. *Canadian Journal of Earth Sciences*, 48:1329–1341.

Burrow, C. J., Blaauwen, J. D., Newman, M. J., and Davidson, R. G. (2016a). The diplacanthid fishes (Acanthodii , Diplacanthiformes , Diplacanthidae) from the Middle Devonian of Scotland. *Palaeontologica Electronica*, (February):1–83.

Burrow, C. J., Davidson, R. G., Den Blaauwen, J. L., and Newman, M. J. (2015). Revision of Climatius reticulatus Agassiz, 1844 (Acanthodii, Climatiidae), from the Lower Devonian of Scotland, based on new histological and morphological data. *Journal of Vertebrate Paleontology*, 35(3):e913421.

Burrow, C. J., Hu, Y., and Young, G. C. (2016b). Placoderms and the evolutionary origin of teeth: a comment on Rücklin and Donoghue (2015). *Biology Letters*, 12.

Burrow, C. J., Newman, M. J., Davidson, R. G., and Den Blaauwen, J. L. (2011). Sclerotic plates or circumorbital bones in early jawed fishes? *Palaeontology*, 54(1):207–214.

Burrow, C. J., Newman, M. J., Davidson, R. G., and den Blaauwen, J. L. (2013). Redescription of Parexus recurvus , an Early Devonian acanthodian from the Midland Valley of Scotland. *Alcheringa: An Australasian Journal of Palaeontology*, 37(3):392–414.

Burrow, C. J. and Rudkin, D. (2014). Oldest near-complete acanthodian: The first vertebrate from the silurian bertie formation Konservat-Lagerstätte, Ontario. *PLoS ONE*, 9(8):e104171.

Burrow, C. J., Trinajstic, K., and Long, J. A. (2012). First acanthodian from the Upper Devonian (Frasnian) Gogo Formation , Western Australia. *Historical Biology*, 24(4):349–357.

Burrow, C. J. and Turner, S. (1998). Devonian Placoderm Scales from Australia. *Journal of Vertebrate Paleontology*, 18(4):677–695.

Burrow, C. J. and Turner, S. (1999). A review of placoderm scales, and their significance in placoderm phylogeny. *Journal of Vertebrate Paleontology*, 19(2):204–219.

Burrow, C. J. and Turner, S. (2010). Reassessment of "Protodus" scoticus from the Early Devonian of Scotland. In *Morphology, Phylogeny and Paleobiogeography of Fossil Fishes*, pages 123–144.

Burrow, C. J. and Turner, S. (2013). Scale structure of putative chondrichthyan Gladbachus adentatus Heidtke & Krätschmer, 2001 from the Middle Devonian Rheinisches Schiefergebirge, Germany. *Historical Biology*, 25(3):385–390.

Burrow, C. J., Turner, S., Desbiens, S., and Miller, R. F. (2008). Early Devonian putative gyracanthid acanthodians from eastern Canada. *Canadian Journal of Earth Sciences*, 45(8):897–908.

Burrow, C. J., Turner, S., Maisey, J. G., Desbiens, S., and Miller, R. F. (2017). Spines of the stem chondrichthyan Doliodus latispinosus. *Canadian Journal of Earth Sciences*, 15(October):1–15.

Burrow, C. J. and Young, G. C. (2012). New Information on Culmacanthus (Acanthodii: Diplacanthiformes) from the ?Early-Middle Devonian of Southeastern Australia. *Proceedings of The Linnean Society of New South Wales*, 134:21–29.

Cappetta, H. (1987). Handbook of Paleoichthyology. Volume 3B. Chondrichthyes II. Mesozoic and Cenozoic Elasmobranchii.

Carr, R., Johanson, Z., and Ritchie, A. (2009). The phyllolepid placoderm Cowralepis mclachlani: insights into the evolution of feeding mechanisms in jawed vertebrates. *Journal of morphology*, 270(7):775–804.

Carvalho, M., Bockmann, F. A., and de Carvalho, M. R. (2013). Homology of the fifth epibranchial and accessory elements of the ceratobranchials among Gnathostomes: Insights from the development of ostariophysans. *PLoS ONE*, 8(4).

Chang, M.-m. (1982). *A Lower Devonian Crossopterygian from Yunnan, South-Western China*. PhD thesis, University of Stockhom, and Section of Palaeozoology, Swedish Museum of Natural History.

Charest, F., Johanson, Z., and Cloutier, R. (2018). Loss in the making: absence of pelvic fins and presence of paedomorphic pelvic girdles in a Late Devonian antiarch placoderm (jawed stem-gnathostome). *Biology Letters*, 14(6).

Choo, B. (2011). Revision of the actinopterygian genus Mimipiscis (=Mimia) from the Upper Devonian Gogo Formation of Western Australia and the interrelationships of the early Actinopterygii. *Earth and Environmental Science Transactions of the Royal Society of Edinburgh*, 102(02):77–104.

Choo, B., Zhu, M., Qu, Q., Yu, X., Jia, L., and Zhao, W. (2017). A new osteichthyan from the late Silurian of Yunnan, China. *Plos One*, 12(3):e0170929.

Clement, A. M., King, B., Giles, S., Choo, B., Ahlberg, P. E., and Gavin, C. (2018). Neurocranial anatomy of an enigmatic Early Devonian fish sheds light on early osteichthyan evolution. *eLife*, pages 1–28.

Cloutier, R. and Schultze, H.-p. (1996). Porolepiform fishes (Sarcopterygii). In Schultze, H.-p. and Cloutier, R., editors, *Devonian fishes and plants of Miguasha, Quebec, Canada*, pages 248–270. Verlag Dr Friedrich Pfeil, München, Germany.

Coates, M. I., Finarelli, J. A., Sansom, I. J., Andreev, P. S., Criswell, K. E., Tietjen, K., Rivers, M. L., Riviere, P. J. L., and Coates, M. I. (2018). An early chondrichthyan and the evolutionary assembly of a shark body plan. *Proceedings of the Royal Society B: Biological Sciences*, 285(1870).

Coates, M. I. and Gess, R. W. (2007). A new reconstruction of Onychoselache traquairi, comments on early chondrichthyan pectoral girdles and hybodontiform phylogeny. *Palaeontology*, 50(6):1421–1446.

Coates, M. I., Gess, R. W., Finarelli, J. A., Criswell, K. E., and Tietjen, K. (2017a). A symmoriiform chondrichthyan braincase and the origin of chimaeroid fishes. *Nature*, 541(7636):1–16.

Coates, M. I., Gess, R. W., Finarelli, J. A., Criswell, K. E., and Tietjen, K. (2017b). A symmoriiform chondrichthyan braincase and the origin of chimaeroid fishes. *Nature*, 541(7636):208–211.

Coates, M. I. and Sequeira, S. E. K. (1998). The braincase of a primitive shark. *Transactions of the Royal Society of Edinburgh: Earth Sciences*, 89(02):63–85.

Coates, M. I. and Sequeira, S. E. K. (2001a). A new stethacanthid chondrichthyan from the lower Carboniferous of Bearsden , Scotland. *Journal of Vertebrate Paleontology*, (October 2014):37–41.

Coates, M. I. and Sequeira, S. E. K. (2001b). Early sharks and primitive gnathostome interrelationships. In Ahlberg, P. E., editor, *Major events in early vertebrate evolution*, chapter 15, pages 241–262. Taylor and Francis, London.

Coates, M. I., Sequeira, S. E. K., Sansom, I. J., and Smith, M. M. (1998). Spines and tissues of ancient sharks. *Nature*, 396(December).

Coates, M. I. and Tietjen, K. (2018). The neurocranium of the Lower Carboniferous shark Tristychius arcuatus (Agassiz , 1837). *Earth and Environmental Science Transactions of the Royal Society of Edinburgh*, pages 1–17.

Cunningham, J. A., Rahman, I. A., Lautenschlager, S., Rayfield, E. J., and Donoghue, P. C. J. (2014). A virtual world of paleontology. *Trends in ecology & evolution*, 29(6):347–57.

Cuny, G., Srisuk, P., Khamha, S., Suteethorn, V., and Tong, H. (2009). A new elasmobranch fauna from the Middle Jurassic of southern Thailand. *Geological Society, London, Special Publications*, 315(1):97–113.

Davis, S. P., Finarelli, J. A., and Coates, M. I. (2012). Acanthodes and shark-like conditions in the last common ancestor of modern gnathostomes. *Nature*, 486(7402):247–250.

De Beer, G. R. and Moy-Thomas, J. A. (1935). On the Skull of Holocephali. *Philosophical transactions of the Royal Society of London. Series B, Biological Sciences*, 224(514):287–312.

Dean, M. N., Mull, C. G., Gorb, S. N., Summers, A. P., Sciences, B., State, C., and Beach, L. (2009). Ontogeny of the tessellated skeleton : insight from the skeletal growth of the round stingray Urobatis halleri. *Journal of Anatomy*, 215:227–239.

Dean, M. N. and Summers, A. P. (2006). Mineralized cartilage in the skeleton of chondrichthyan fishes. *Zoology*, 109:164–168.

Denison, R. (1978). Handbook of paleoichthyology. Volume 2. Placodermi.

Denison, R. (1979). *Handbook of Palaeoichthyology: Acanthodii*. Verlag Dr. Friedrich Pfeil.

Dick, J. R. F. (1978). On the Carboniferous shark Tristychius arcuatus Agassiz from Scotland. *Transactions of the Royal Society of Edinburgh*, 70(04):63–109.

Dick, J. R. F. (1981). Diplodoselache woodi gen. et sp. nov., an early Carboniferous shark from the Midland Valley of Scotland. *Transactions of the Royal Society of Edinburgh: Earth Sciences*, 72(02):99–113.

Dick, J. R. F. and Maisey, J. G. (1980). The Scottish Lower Carboniferous shark Onychoselache traquairi. *Palaeontology*, 23(2):363–74.

Didier, D. A. (1995). Phylogenetic Systematics of Extant Chimaeroid Fishes (Holocephali, Chimaeroidei). *American Museum Novitates*, (3119).

Dineley, D. L. and Metcalf S J (1999). *Fossil Fishes of Great Britain*. Joint Nature Conservation Committee, Peterborough.

Donoghue, P. C. J., Sansom, I. J., and Downs, J. P. (2006). Early evolution of vertebrate skeletal tissues and cellular interactions, and the canalization of skeletal development. *Journal of Experimental Biology*, 306B:1–14.

Downs, J. P. and Donoghue, P. C. J. (2009). Skeletal histology of bothriolepis canadensis (placodermi, antiarchi) and evolution of the skeleton at the origin of jawed vertebrates. *Journal of Morphology*, 270(11):1364–1380.

Duff, P. (1842). *Sketch of the Geology of Moray*. Forsyth and Young, Elgin.

Dunkle, D. J. and Bungart, P. A. (1940). On one of the least known of the Cleveland Shale arthrodira. *Scientific Publications of the Cleveland Museum of Natural History*, 8(3).

Dunkle, D. J. and Bungart, P. A. (1942). The infero-gnathal plates of Titanichthys. *Scientific Publications of the Cleveland Museum of Natural History*, 8(4).

Dunkle, D. J. and Bungart, P. A. (1943). Comments on Diplognathus mirabilis NEWBERRY. *Scientific Publications of the Cleveland Museum of Natural History*, 8(7):6–9.

Dunkle, D. J. and Bungart, P. A. (1945). A new arthrodiran fish from the Upper Devonian Ohio Shales. *Scientific Publications of the Cleveland Museum of Natural History*, 8(8).

Dupret, V., Sanchez, S., Goujet, D., and Ahlberg, P. E. (2017). The internal cranial anatomy of Romundina stellina Ørvig , 1975 (Vertebrata , Placodermi , Acanthothoraci) and the origin of jawed vertebrates - Anatomical atlas of a primitive gnathostome. *PLoS ONE*.

Dupret, V., Sanchez, S., Goujet, D., Tafforeau, P., and Ahlberg, P. E. (2014). A primitive placoderm sheds light on the origin of the jawed vertebrate face. *Nature*, 507(7493):500–3.

Enault, S., Guinot, G., Koot, M. B., and Cuny, G. (2015). Chondrichthyan tooth enameloid: past, present, and future. *Zoological Journal of the Linnean Society*, 174(3):549–570.

Finarelli, J. A. and Coates, M. I. (2012). First tooth-set outside the jaws in a vertebrate. *Proceedings of the Royal Society B: Biological Sciences*, 279(1729):775–779.

Finarelli, J. A. and Coates, M. I. (2014). Chondrenchelys problematica (Traquair, 1888) redescribed: a Lower Carboniferous, eel-like holocephalan from Scotland. *Earth and Environmental Science Transactions of the Royal Society of Edinburgh*, 105(01):35–59.

Friedman, M. (2007). Styloichthys as the oldest coelacanth: Implications for early osteichthyan interrelationships. *Journal of Systematic Palaeontology*, 5(3):289–343.

Friedman, M. and Brazeau, M. D. (2010). A reappraisal of the origin and basal radiation of the Osteichthyes. *Journal of Vertebrate Paleontology*, 30(1):36–56.

Fritsch, A. (1895). *Fauna der Gaskohle und der Kalksteine der Permformation Böhmens*, volume 3. Prague.

Fritsch, A. (1907). *Miscellanea palaeontologica. I. Palaeozoica*. Fr. Rivnác, Prague.

Gagnier, P.-Y. (1996). Acanthodii. In *Devonian fishes and plants of Miguasha, Quebec, Canada*, pages 149–164.

Gagnier, P.-y., Hanke, G. F., and Wilson, M. V. H. (1999). Tetanopsyrus lindoei gen. et sp. nov., an Early Devonian acanthodian from the Northwest Territories, Canada. *Acta Geologica Polonica*, 49(2):81–96.

Gagnier, P.-Y., Paris, F., Racheboeuf, P., Janvier, P., and Suarez-Riglos, M. (1989). Les vertebres de Bolivie: donees biostratigraphiques et anatomiques complementaires. *Bulletin de l'Institut Francais d'Etudes Andines*, 18(75-93).

Gagnier, P.-Y. and Wilson, M. V. H. (1995). New evidences on jaw articulations in acanthodians. *Geobios*, 19:137–143.

Gagnier, P.-y. and Wilson, M. V. H. (1996a). An unusual acanthodian from Northern Canada: revision of Brochoadmones milesi. *Modern Geology*, 20:235–251.

Gagnier, P.-y. and Wilson, M. V. H. (1996b). Early Devonian acanthodians from Northern Canada. *Palaeontology*, 39(2):241–258.

Gagnier, P.-Y. and Wilson, M. V. H. (1996c). Early Devonian acanthodians from Northern Canada. *Palaeontology*, 39(2):241–258.

Gai, Z., Donoghue, P. C. J., Zhu, M., Janvier, P., and Stampanoni, M. (2011). Fossil jawless fish from China foreshadows early jawed vertebrate anatomy. *Nature*, 476(7360):324–7.

Gardiner, B. G. (1984). The relationships of the palaeoniscid fishes, a review based on new specimens of Mimia and Moythomasia from the Upper Devonian of Western Australia. *Bulletin of the British Museum (Natural History), Geology*, 37(4):175–418.

Gardiner, B. G. and Bartram, A. W. H. (1977). The homologies of ventral cranial fissures in osteichthyans. In Andrews, S. M., Miles, R. S., and Walker, A. D., editors, *Problems in Vertebrate Evolution*, pages 227–245. Academic Press, Linnean Symposium Series, London.

Garman, S. (1913). The Plagiostomia: Sharks, skates and rays. *Memoirs of the Museum of Comparative Zoology at Harvard College*, 36:1–528.

Gegenbaur, C. (1878). *Elements of Comparative Anatomy*. Macmillan.

Giles, S., Coates, M. I., Garwood, R. J., Brazeau, M. D., Atwood, R., Johanson, Z., and Friedman, M. (2015a). Endoskeletal structure in Cheirolepis (Osteichthyes, Actinopterygii), An early ray-finned fish. *Palaeontology*, 58(5).

Giles, S., Darras, L., Clément, G., Blieck, A. R. M., and Friedman, M. (2015b). An exceptionally preserved Late Devonian actinopterygian provides a new model for primitive cranial anatomy in ray-finned fishes. *Proceedings of the Royal Society B: Biological Sciences*, 282.

Giles, S. and Friedman, M. (2014). Virtual reconstruction of endocast anatomy in early ray-finned fishes (Osteichthyes, Actinopterygii). *Journal of Paleontology*, 88(4):636–651.

Giles, S., Friedman, M., and Brazeau, M. D. (2015c). Osteichthyan-like cranial conditions in an Early Devonian stem gnathostome. *Nature*, 520:82–175.

Giles, S., Rücklin, M., and Donoghue, P. C. J. (2013). Histology of "placoderm" dermal skeletons: Implications for the nature of the ancestral gnathostome. *Journal of morphology*, 274(6):627–44.

Gillis, J. A., Alsema, E. C., and Criswell, K. E. (2017). Trunk neural crest origin of dermal denticles in a cartilaginous fish. *Proceedings of the National Academy of Sciences*, 18(21):1–6.

Gillis, J. A., Dahn, R. D., and Shubin, N. H. (2009). Shared developmental mechanisms pattern the vertebrate gill arch and paired fin skeletons. *Proceedings of the National Academy of Sciences*, 106(14):5720–5724.

Gillis, J. A. and Donoghue, P. C. J. (2007). The homology and phylogeny of chondrichthyan tooth enameloid. *Journal of Morphology*, 268:33–49.

Gillis, J. A., Modrell, M. S., and Baker, C. V. H. (2013). Developmental evidence for serial homology of the vertebrate jaw and gill arch skeleton. *Nature Communications*, 4:1436–1438.

Goloboff, P. A. and Catalano, S. A. (2016). TNT version 1.5, including a full implementation of phylogenetic morphometrics. *Cladistics*, 32:221–238.

Goujet, D. (1973). Sigaspis, un nouvel arthrodire du Dévonien inférieur du Spitsberg. *Palaeontographica, Abteilung A*, 143:73–88.

Goujet, D. (1975). Dicksonosteus, un nouvel arthrodire du Dévonien du Spitsberg. Remarques sur le squelette viscéral des Dolichothoraci. *Colloques Internationaux du Centre National de la Recherche Scientifique*, 218:81–99.

Goujet, D. (1984). Les Poissons placodermes du Spitsberg. Arthrodires Dolichothoraci de la Formation de Wood Bay (Dévonien inférieur). In *Cahiers de Paléontologie (section Vertébrés)*. Éditions du CNRS, Paris.

Grogan, E. D. and Lund, R. (2000). Debeerius ellefseni (fam. nov., gen. nov., spec. nov.), an autodiastylic chondrichthyan from the Mississippian Bear Gulch Limestone of Montana (USA), the relationships of the Chondrichthyes, and comments on gnathostome evolution. *Journal of Morphology*, 245:219–245.

Grogan, E. D., Lund, R., and Greenfest-Allen, E. (2012). The Origin and relationships of early chondrichthyans. *Biology of Sharks and their Relatives*, (June 2016):3–30.

Gross, W. (1935). Histologischen Studien am Aussenskelett fossiler Agnathen und Fische. *Palaeontographica, Abteilung A*, 83:1–60.

Gross, W. (1937). Das Kopfskelett con Cladodus wildungensis JAEKEL. 1. Teil. Endocranium und Palatoquadratum. *Senckenbergiana*, 19:80–107.

Gross, W. (1938). Das kopfskelett von Cladodus wildungensis Jaekel: 2. Teil. Der Kieferbogen. *Senckenbergiana*, 20:123–145.

Gross, W. (1947). Die Agnathen und Acanthodier des obersilurischen Beyrichienkalks. *Palaeontographica, Abteilung A*, 96:91–158.

Gross, W. (1962). Neuuntersuchung der Stensiöellida (Arthrodira, Unterdevon). *Notizblatt des Hessischen Landesamtes für Bodenforschung zu wiesbaden*, 90:48–86.

Gross, W. (1973). Kleinschuppen, Flossenstacheln und Zähne von fishen aus Europäischen und Nordamerikanischen bonebeds des Devons. *Palaeontographica, Abteilung A*, 142:51–55.

Hall, B. K. (2015). *Bones and cartilage*. Academic Press, 2nd edition.

Hanke, G. F. (2002). Paucicanthus vanelsti gen. et sp. nov., an Early Devonian (Lochkovian) acanthodian that lacks paired fin-spines. *Canadian Journal of Earth Sciences*, 39:1071–1083.

Hanke, G. F. (2008). Promesacanthus eppleri n. gen., n. sp., a mesacanthid (Acanthodii, Acanthodiformes) from the Lower Devonian of northern Canada. *Geodiversitas*, 30(2):287–302.

Hanke, G. F. and Davis, S. P. (2008). Redescription of the acanthodian Gladiobranchus probaton Bernacsek &Dineley, 1977, and comments on diplacanthid relationships. *Geodiversitas*, 30(2):303–330.

Hanke, G. F. and Davis, S. P. (2012). A re-examination of Lupopsyrus pygmaeus Bernacsek & Dineley , 1977 Pisces , Acanthodii). *Geodiversitas*, 34(3):469–487.

Hanke, G. F., Davis, S. P., and Wilson, M. V. H. (2001a). New species of the acanthodian genus Tetanopsyrus fron northern Canada, and comments on related taxa. *Journal of Vertebrate Paleontology*, 21(4):740–753.

Hanke, G. F. and Wilson, M. V. H. (2004). New teleostome fishes and acanthodian systematics. In Arratia, G. and Wilson, M. V. H., editors, *Recent Advances in the Origin and Early Radiation of Vertebrates*, pages 189–216. München, Germany.

Hanke, G. F. and Wilson, M. V. H. (2006). Anatomy of the early Devonian acanthodian Brochoadmones milesi based on nearly complete body fossils , with comments on the evolution and development of paired fins. *Journal of Vertebrate Paleontology*, 26(3):526–537.

Hanke, G. F. and Wilson, M. V. H. (2010). The putative stem-group chondrichthyans Kathemacanthus and Seretolepis from the Lower Devonian MOTH locality, Mackenzie Mountains, Canada. In Elliott, D. K., Maisey, J. G., Yu, X., and Miao, D., editors, *Phylogeny and Paleobiogeography of Fossil Fishes*, pages 159–182. Verlag Dr. Friedrich Pfeil, München, Germany.

Hanke, G. F., Wilson, M. V. H., and Lindoe, L. A. (2001b). New species of Silurian acanthodians from the Mackenzie Mountains , Canada. *Canadian Journal of Earth Sciences*, 1529:1517–1529.

Hanke, G. F., Wilson, M. V. H., and Saurette, F. J. (2013). Partial articulated specimen of the Early Devonian putative chondrichthyan Polymerolepis whitei Karatajūtė-Talimaa, 1968, with an anal fin spine. *Geodiversitas*, 35(3):529–543.

Harris, J. E. (1938). The dorsal spine of Cladoselache and The neurocranium and jaws of Cladoselache. *Scientific Publications of the Cleveland Museum of Natural History*, VIII(1).

Heidtke, U. H. J. (1999). Orthacanthus (Lebachacanthus) senckenbergianus FRITSCH 1889 (Xenacanthida: Chondrichthyes): Revision, Organisation und Phylogenie. *Freiburger Forschungsheft*, 481:63–106.

Heidtke, U. H. J. (2011). Neue Erkenntwisse über Acanthodes bronni AGASSIZ 1833. *Mitt. Pollichia*, 95:1–14.

Heidtke, U. H. J. (2015). Acanthodes bronni; weitere Exemplare von der Typlokalität Berchweiler bei Kirn. *Mitt. Pollichia*, 97:5–18.

Heidtke, U. H. J. and Krätschmer, K. (2001). Gladbachus adentatus nov. gen. et sp., ein primitiver Hai aus dem Oberen Givetium (Oberes Mitteldevon) der Bergisch Gladbach - Paffrath-Mulde (Rheinisches Schiefergebirge). *Mainzer Geowissenschaftliche Mitteilungen*, 30:105–122.

Heidtke, U. H. J., Schwind, C., and Krätschmer, K. (2004). Über die Organisation des Skelettes und die verwandschaftlichen Beziehungen der Gattung Triodus JORDAN 1849 (Elasmobranchii: Xenacanthida). *Mainzer Geowissenschaftliche Mitteilungen*, 32:9–54.

Hotton, N. (1952). Jaws and teeth of American xenacanth sharks. *Journal of Paleontology*, 26(3):489–500.

Hu, Y., Lu, J., and Young, G. C. (2017). New findings in a 400 million-year-old Devonian placoderm shed light on jaw structure and function in basal gnathostomes. *Scientific Reports*, 7:1–12.

Huelsenbeck, J. P. and Ronquist, F. (2001). MRBAYES: Bayesian inference of phylogenetic trees. *Bioinformatics*, 17(8):754–755.

Hussakof, L. and Bryant, W. L. (1918). Catalog of the fossil fishes in the Museum of Buffalo Society of Natural Sciences. *Bulletin of the Buffalo Society of Natural Sciences*, 12:5–178.

Inoue, J. G., Miya, M., Lam, K., Tay, B.-H., Danks, J. A., Bell, J., Walker, T. I., and Venkatesh, B. (2010). Evolutionary origin and phylogeny of the modern holocephalans (Chondrichthyes: Chimaeriformes): a mitogenomic perspective. *Molecular biology and evolution*, 27(11):2576–86.

Janvier, P. (1984). The relationships of the Osteostraci and Galeaspida. *Journal of Vertebrate Paleontology*, 4(3):344–358.

Janvier, P. (1985). Les Céphalaspides du Spitsberg. Anatomie, phylogénie et systématique des Ostéostracés siluro-dévoniens. Révision des Ostéostracés de la Formation de Wood Bay (Dévonien inférieur du Spitsberg). *Cahiers de Paléontologie, Section Vertebres, Centre National de la Recherche Scientifique*.

Janvier, P. (1996). *Early Vertebrates*. Clarendon.

Janvier, P. (2004). Calcified cartilage in the paired fins of the osteostracan Escuminaspis laticeps (Traquair 1880), from the Late Devonian of Miguasha (Québec , Canada), with a consideration of the early evolution of the pectoral fin endoskeleton in vertebrates. *Journal of Vertebrate Paleontology*, 24(4):773–779.

Janvier, P. (2015). Facts and fancies about early fossil chordates and vertebrates. *Nature*, 520(7548):483–489.

Janvier, P. and Arsenault, M. (2002). Calcification of early vertebrate cartilage. *Nature*, 417:609.

Janvier, P. and Maisey, J. G. (2010). The Devonian vertebrates of South America and their biogeographical relationships. In *Morphology,Phylogeny and Paleobiogeography of Fossil Fishes*.

Janvier, P. and Pradel, A. (2015). Elasmobranchs and Their Extinct Relatives: Diversity, Relationships, and Adaptations Through Time. (October):1–17.

Janvier, P. and Suarez-Riglos, M. (1986). The Silurian and Devonian vertebrates of Bolivia. *Bulletin de l'Institut Francais d'Etudes Andines*, 15:73–114.

Jarvik, E. (1953). On the visceral skeleton in Eusthenopteron with a discussion of the parasphenoid and palatoquadrate in fishes. *Kungl. Svenska Vetenskakad. Handl.*, 5(1).

Jarvik, E. (1972). Middle and Upper Devonian Porolepiformes from East Greenland with special reference to Glyptolepis groenlandica n. sp. *Meddr. Grønland*, 187(2).

Jarvik, E. (1977). The systematic position of acanthodian fishes. In Andrews, S. M., Miles, R. S., and Walker, A., editors, *Problems in vertebrate Evolution*, pages 199–225. Academic Press, London, UK.

Jarvik, E. (1980). *Basic structure and evolution of vertebrates*. Academic Press, London.

Johanson, Z., Kearsley, A., den Blaauwen, J., Newman, M. J., and Smith, M. M. (2010). No bones about it: An enigmatic Devonian fossil reveals a new skeletal framework-A potential role of loss of gene regulation. *Seminars in Cell and Developmental Biology*, 21(4):414–423.

Johanson, Z., Smith, M. M., Sanchez, S., Senden, T., Trinajstic, K., and Pfaff, C. (2017). Questioning hagfish affinities of the enigmatic Devonian vertebrate Palaeospondylus. *Royal Society Open Science*, 4.

Karatajūtė-talimaa, V. (1973). Elegestolepis grossi gen. et sp. nov., ein neuer Typ der Placoidschuppe aus dem Oberen Silur der Tuwa. *Palaeontographica, Abteilung A*, (143):35–50.

Karatajūtė-Talimaa, V. (1995). The Mongolepidida: Scale structure and systematic position. *Geobios*, (19):35–37.

Karatajūtė-Talimaa, V. (1997). Chondrichthyan scales from Lochkovian (Lower Devonian) of Podolia (Ukraine). *Geologija*, (22):5–17.

Karatajūtė-Talimaa, V., Novtistkaya, L. I., Rozman, K. S., and Sodov, J. (1990). Mongolepis, a new genus of Elasmobranchii from the Lower Silurian of Mongolia. *Paleontologicheskii zhurnal 1,*, 1:76–86.

Karatajūtė-Talimaa, V. and Smith, M. M. (2003). Early acanthodians from the Lower Silurian of Asia. *Transactions of the Royal Society of Edinburgh; Earth Sciences*, 93:277–299.

Keating, J. N. and Donoghue, P. C. J. (2016). Histology and affinity of anaspids, and the early evolution of the vertebrate dermal skeleton. *Proceedings of the Royal Society B: Biological Sciences*.

Keating, J. N., Marquart, C. L., and Donoghue, P. C. J. (2015). Histology of the heterostracan dermal skeleton: Insight into the origin of the vertebrate mineralised skeleton. *Journal of Morphology*, 276:657–680.

King, B., Qiao, T., Lee, M. S. Y., Zhu, M., and Long, J. A. (2016). Bayesian Morphological Clock Methods Resurrect Placoderm Monophyly and Reveal Rapid Early Evolution in Jawed Vertebrates. *Systematic Biology*, 66(4).

Lane, J. A. (2010). Morphology of the Braincase in the Cretaceous Hybodont Shark Tribodus limae (Chondrichthyes: Elasmobranchii), Based on CT Scanning. *American Museum Novitates*, 3681(3681):1–70.

Lane, J. A. and Maisey, J. G. (2009). Pectoral anatomy of Tribodus limae (Elasmobranchii: Hybodontiformes) from the Lower Cretaceous of northeastern Brazil. *Journal of Vertebrate Paleontology*, 29(1):25–38.

Lane, J. A. and Maisey, J. G. (2012). The Visceral Skeleton and Jaw Suspension In The Durophagous Hybodontid Shark Tribodus limae from the Lower Cretaceous of Brazil. *Journal of Paleontology*, 86(5):886–905.

Lemey, P., Salemi, M., and Vandamme, A.-M. (2009). *The Phylogenetic Handbook*. Second edition.

Long, J. A. (1983). A new diplacanthoid acanthodian from the Late Devonian of Victoria. *Memoirs of the Association of Australasian Palaeontologists*, 1:51–65.

Long, J. A. (1986a). A new Late Devonian acanthodian fish from Mt. Howitt, Victoria, Australia, with remarks on acanthodian biogeography. *Proceedings of the Royal Society of Victoria*, 98:1–17.

Long, J. A. (1986b). New ischnacanthid acanthodians from the Early Devonian of Australia, with comments on acanthodian interrelationships. *Zoological Journal of the Linnean Society*, 87:321–339.

Long, J. A. (1997). Ptyctodontid fishes (Vertebrata, Placodermi) from the Late Devonian Gogo Formation, Western Australia, with a revision of the European genus Ctenurella Ørvig, 1960. *Geodiversitas*.

Long, J. A. and Barwick, R. E. (1997). Osteology and Functional Morphology of the Osteolepiform Fish Gogonasus andrewsae Long, 1985, from the Upper Devonian Gogo Formation, Western Australia by. *Records of the Western Australian Museum*, 53:1–89.

Long, J. A., Burrow, C. J., Ginter, M., Maisey, J. G., Trinajstic, K. M., Coates, M. I., Young, G. C., and Senden, T. J. (2015). First Shark from the Late Devonian (Frasnian) Gogo Formation, Western Australia Sheds New Light on the Development of Tessellated Calcified Cartilage. *Plos One*, 10(5):e0126066.

Long, J. A., Mark-Kurik, E., Johanson, Z., Lee, M. S. Y., Young, G. C., Zhu, M., Ahlberg, P. E., Newman, M. J., Jones, R., Blaauwen, J. L. D., Choo, B., and Trinajstic, K. (2014). Copulation in antiarch placoderms and the origin of gnathostome internal fertilization. *Nature*, 517.

Long, J. a., Trinajstic, K., and Johanson, Z. (2009). Devonian arthrodire embryos and the origin of internal fertilization in vertebrates. *Nature*, 457(7233):1124–7.

Lu, J., Giles, S., Friedman, M., Blaauwen, J. L. D., and Zhu, M. (2016). The Oldest Actinopterygian Highlights the Cryptic Early History of the Hyperdiverse Ray-Finned Fishes Report The Oldest Actinopterygian Highlights the Cryptic Early History of the Hyperdiverse Ray-Finned Fishes. *Current Biology*, 26(12):1–7.

Lu, J., Giles, S., Friedman, M., and Zhu, M. (2017). A new stem sarcopterygian illuminates patterns of character evolution in early bony fishes. *Nature Communications*, 8.

Lund, R. (1982). Harpagofutator volsellorhinus new genus and species (Chondrichthyes, Chondrenchelyformes) from the Naurian Bear Gulch Limestone, Chondrenchelys problematica Traquair (Visean) and their sexual dimorphism. *Journal of paleontology*, 56(4):938–958.

Lund, R. (1985). The morphology of Falcatus falcatus (St . John and Worthen), a Mississippian stethacanthid chondrichthyan from the Bear Gulch Limestone of Montana. *Journal of Vertebrate Paleontology*, 5(1):1–19.

Lund, R. and Grogan, E. D. (2004). Two tenaculum-bearing Holocephalimorpha (Chondrichthyes) from the Bear Gulch Limestone (Chesterian, Serpukhovian) of Montana, USA. In Arratia, G., Wilson, M., and Cloutier, R., editors, *Recent Advances in the Origin and Early Radiation of Vertebrates*, pages 171–187. Verlag Dr. Friedrich Pfeil, München, Germany.

Maddison, W. P., Donoghue, M. J., and Maddison, D. R. (1984). Outgroup analysis and parsimony. *Systematic Zoology*, 33(1):83–103.

Maddison, W. P. and Maddison, D. R. (1992). MacClade: Analysis of Phylogeny and Character Evolution.

Maisey, J. G. (1977). The fossil selachian fishes Palaeospinax Egerton, 1872 and Nemacanthus Agassiz, 1837. *Zoological Journal of the Linnean Society*, 60:259–273.

Maisey, J. G. (1980). An Evaluation of Jaw Suspension in Sharks. *American Museum Novitates*, (2706):1–17.

Maisey, J. G. (1982). The Anatomy and Interrelationships of Mesozoic Hybodont Sharks. *American Museum Novitates*, (2724):1–48.

Maisey, J. G. (1983). Cranial anatomy of Hybodus basanus Egerton from the Lower Cretaceous of England. *American Museum Novitates*, (2758):1–64.

Maisey, J. G. (1984). Chondrichthyan phylogeny: a look at the evidence. *Journal of Vertebrate Paleontology*, 4(3):359–371.

Maisey, J. G. (1985). Cranial Morphology of the Fossil Elasmobranch Synechodus dubrisiensis. *American Museum Novitates*, 2804(2804):1–28.

Maisey, J. G. (1986). Heads and Tails: a Chordate Phylogeny. *Cladistics*, 2(4):201–256.

Maisey, J. G. (1989a). Hamiltonichthys mapesi, g. & sp. nov. (Chondrichthyes; Elasmobranchii) from th Upper Pennsylvanian of Kansas. *American Museum Novitates*, (2931):1–42.

Maisey, J. G. (1989b). Visceral skeleton and musculature of a Late Devonian shark. *Journal of Vertebrate Paleontology*, 9(2):174–190.

Maisey, J. G. (2001a). A primitive chondrichthyan braincase from the Middle Devonian of Bolivia. In Ahlberg, P. E., editor, *Major events in early vertebrate evolution*, pages 263–288. Taylor and Francis, London, UK.

Maisey, J. G. (2001b). Remarks on the inner ear of elasmobranchs and its interpretation from skeletal labyrinth morphology. *Journal of morphology*, 250(3):236–64.

Maisey, J. G. (2004). Morphology of the Braincase in the Broadnose Sevengill Shark Notorynchus (Elasmobranchii, Hexanchiformes), Based on CT Scanning. *American Museum Novitates*, 3429(3429):1–52.

Maisey, J. G. (2005). Braincase of the Upper Devonian Shark Cladodoides Wildungensis (Chondrichthyes, Elasmobranchii), With Observations on the Braincase in Early Chondrichthyans. *Bulletin of the American Museum of Natural History*, 288(288):1–103.

Maisey, J. G. (2007). The Braincase in Paleozoic Symmoriiform and Cladoselachian Sharks. *Bulletin of the American Museum of Natural History*, 307(307):1–122.

Maisey, J. G. (2009). The Spine-Brush Complex in Symmoriiform Sharks (Chondrichthyes; Symmoriiformes), with Comments on Dorsal Fin Modularity. *Journal of Vertebrate Paleontology*, 29(1):14–24.

Maisey, J. G. (2011). The braincase of the Middle Triassic shark Acronemus tuberculatus (Bassani, 1886). *Palaeontology*, 54(2):417–428.

Maisey, J. G. (2013). The diversity of tessellated calcification in modern and extinct chondrichthyans. *Revue de paléobiologie*, 32(2):355–371.

Maisey, J. G. and Anderson, M. E. (2001). A primitive chondrichthyan braincase from the Early Devonian of South Africa. *Journal of Vertebrate Paleontology*, 21(4):702–713.

Maisey, J. G. and Denton, J. S. S. (2016). Dermal denticle patterning in the Cretaceous hybodont shark Tribodus limae (Euselachii, Hybodontiformes), and its implications for the evolution of patterning in the chondrichthyan dermal skeleton. *Journal of Vertebrate Paleontology*, 36(5).

Maisey, J. G. and Lane, J. A. (2010). Labyrinth morphology and the evolution of low-frequency phonoreception in elasmobranchs. *Comptes Rendus Palevol*, 9(6-7):289–309.

Maisey, J. G., Miller, R. F., Pradel, A., Denton, J. S. S., and Janvier, P. (2017). Pectoral Morphology in Doliodus : Bridging the âĂŸAcanthodian'- Chondrichthyan Divide. *American Museum Novitates*, (3875):1–15.

Maisey, J. G., Miller, R. F., and Turner, S. (2009). The braincase of the chondrichthyan Doliodus from the Lower Devonian Campbellton Formation of New Brunswick, Canada. *Acta Zoologica*, 90(May):109–122.

Maisey, J. G., Turner, S., Naylor, G. J. P., and Miller, R. F. (2014). Dental patterning in the earliest sharks: Implications for tooth evolution. *Journal of morphology*, 275(5):586–96.

Mallatt, J. (1996). Ventilation and the origin of jawed vertebrates: a new mouth. *Zoological Journal of the Linnean Society*, 117:329–404.

Märss, T. and Gagnier, P.-Y. (2001). A new chondrichthyan from the Wenlock, Lower Silurian, of Baillie-Hamilton Island, the Canadian Arctic. *Journal of Vertebrate Paleontology*, 21(4):693–701.

Märss, T., Turner, S., and Karatajūtė-Talimaa, V. (2007). *âĂŸâĂŸAgnatha" II: Thelodonti. Handbook of Paleoichthyology, Vol. 1B.* Verlag Dr. Friedrich Pfeil, München, Germany.

Märss, T., Wilson, M. V. H., and Thorsteinsson, R. (2002). New thelodont (Agnatha) and possible chondrichthyan (Gnathostomata) taxa established in the Silurian and Lower Devonian of the Canadian Arctic Archipelago. *Proceedings of the Estonian Academy of Sciences: Geology*, 51(2):88–120.

Märss, T., Wilson, M. V. H., and Thorsteinsson, R. (2006). Silurian and Lower Devonian thelodonts and putative chondrichthyans from the Canadian Arctic Archipelago. *Special Papers in Palaeontology*, 75:1–144.

Martinez-perez, C., Dupret, V., Manzanares, E., and Botella, H. (2010). New Data on the Lower Devonian Chondrichthyan Fauna from Celtiberia (Spain) New data on the Lower Devonian chondrichthyan fauna. *Journal of Vertebrate Paleontology*, 30(5).

Miles, R. S. (1964a). A reinterpretation of the visceral skeleton of Acanthodes. *Nature*, 204:457–459.

Miles, R. S. (1964b). The acanthodian fishes of the Devonian Plattenkalk of the Paffrath Trough in the Rhineland. *Arkiv för zoologi*, 18(9):147–194.

Miles, R. S. (1965). Some features in the cranial morphology of acanthodians and the relationships of the Acanthodii. *Acta Zoologica*, 46:233–255.

Miles, R. S. (1968). Jaw articulation and suspension in Acanthodes and their significance. In Ørvig, T., editor, *Current problems of lower vertebrate phylogeny. Proc. Fourth Nobel Symp.*, pages 109–127. Armqvist and Wiksell, Stockholm.

Miles, R. S. (1970). Remarks on the vertebral column and caudal fin of acanthodian fishes. *Lethaia*, 3(4):343–362.

Miles, R. S. (1973a). Articulated acanthodian fishes from the Old Red Sandstone of England, with a review of the structure and evolution of the acanthodian shoulder girdle. *Bulletin of the British Museum (Natural History). Geology.*, 24(2).

Miles, R. S. (1973b). Relationships of acanthodians. In Greenwood, P., Miles, R. S., and Patterson, C., editors, *Interrelationships of fishes*, pages 63–103. London: Zoological Journal of the Linnean Society.

Miles, R. S. (1977). Dipnoan (lungfish) skulls and the relationships of the group : a study based on new species from the Devonian of Australia. *Zoological Journal of the Linnean Society*, 61:1–328.

Miles, R. S. and Westoll, T. S. (1968). IX . - The Placoderm Fish Coccosteus cuspidatus Miller ex Agassiz from the Middle Old Red Sandstone of Scotland. Part I. Descriptive Morphology. *Transactions of the Royal Society of Edinburgh*, LXVII(9):374–476.

Miles, R. S. and Young, G. C. (1977). Placoderm interrelationships reconsidered in the light of new ptyctodontids from Gogo, Western Australia. In Andrews, S. M., Miles, R. S., and Walker, T. I., editors, *Problems in vertebrate Evolution*, pages 123–198. Academic Press, Linnean Symposium Series, London.

Miller, H. (1841). *The Old Red Sandstone*. Edinburgh.

Miller, R. F., Cloutier, R., and Turner, S. (2003). The oldest articulated chondrichthyan from the Early Devonian period. *Nature*, 425(6957):501–504.

Moy-Thomas, J. A. (1936). On the structure and affinities of the Carboniferous cochliodont Helodus simplex. *Geological Magazine*, 73:488–503.

Mutter, R. J., Blanger, K. D. E., Neuman, A. G., Sciences, E., Building, W. M., and Road, Q. (2007). Elasmobranchs from the Lower Triassic Sulphur Mountain Formation near Wapiti Lake (BC , Canada). *Zoological Journal of the Linnean Society*, 149:309–337.

Nelson, G. J. (1966). Gill Arches of Teleostean Fishes of the Order Anguilliformes. *Pacific Science*, 20:391–408.

Nelson, G. J. (1968). Gill-arch structure in Acanthodes. In Ørvig, T., editor, *Current problems of lower vertebrate phylogeny. Proc. Fourth Nobel Symp.*, pages 129–143. Armqvist and Wiksell, Stockholm.

Nelson, G. J. (1969). Gill arches and the phylogeny of fishes, with notes on the classification of vertebrates. *Bulletin of the American Museum of Natural History*, 141(4):475–552.

Newman, M. J., Burrow, C. J., Den Blaauwen, J. L., and Davidson, R. G. (2014). The Early Devonian Acanthodian Euthacanthus macnicoli from the Midland Valley of Scotland. *Geodiversitas*, 36(2):321–348.

Newman, M. J., Davidson, R. G., Blaauwen, J. L. D., and Burrow, C. J. (2012). The Early Devonian Acanthodian Uraniacanthus curtus (Powrie , 1870) n . comb . from the Midland Valley of Scotland. *Geodiversitas*, 34(4):739–759.

Newman, M. J., Davidson, R. G., Den Blaauwen, J. L., and Burrow, C. J. (2011). The Early Devonian Acanthodian Euthacanthus gracilis from the Midland Valley of Scotland. *Scottish Journal of Geology*, 47(2):101–111.

Oelofsen, B. W. (1986). A Fossil Shark Neurocranium from the Permo-Carboniferous (Lowermost Ecca Formation) of South Africa. In Uyeno, T., Arai, R., Taniuchi, T., and Matsuura, K., editors, *Indo-Pacific fish biology: Proceedings of the second international conference on Indo-Pacific fishes*, pages 107–124. Ichthyological Society of Japan, Tokyo.

Ørvig, T. (1951). Histologic studies of placoderms and fossil elasmobranchs. I: The endoskeleton, with remarks on the hard tissues of lower vertebrates in general. *Arkiv för zoologi*, 2(2):321–454.

Ørvig, T. (1973). Acanthodian dentition and its bearing on the relationships of the group. *Palaeontographica, Abteilung A*, 143:119–150.

Patterson, C. (1965). The phylogeny of the chimaeroids. *Philosophical transactions of the Royal Society of London. Series B, Biological Sciences*, 249(757):101–219.

Patterson, C. (1982). Morphological characters and homology. In Joysey, K. A. and Friday, A. E., editors, *Problems of phylogenetic reconstruction*, chapter 2, pages 21–74. Academic Press, London.

Pearson, D. M. and Westoll, T. S. (1979). The Devonian actinopterygian Cheirolepis Agassiz. *Transactions of the Royal Society of Edinburgh*, 70(13-14):337–399.

Peignoux-Deville, J., Lallier, F., and Vidal, B. (1982). Evidence for the presence of osseous tissue in dogfish vertebrae. *Cell and tissue research*, 222:605–614.

Powrie, J. (1864). On the fossiliferous rocks of Forfarshire and their contents. *Quarterly Journal of the geological society of London*, xvii:413–429.

Pradel, A. (2010). Skull and brain anatomy of Late Carboniferous Sibyrhynchidae Skull and brain anatomy of Late Carboniferous Sibyrhynchidae (Chondrichthyes, Iniopterygia) from Kansas and Oklahoma (USA). *Geodiversitas*, 32(4):595–661.

Pradel, A., Didier, D. A., Casane, D., Tafforeau, P., and Maisey, J. G. (2013). Holocephalan Embryo Provides New Information on the Evolution of the Glossopharyngeal Nerve, Metotic Fissure and Parachordal Plate in Gnathostomes. *PLoS ONE*, 8(6):e66988.

Pradel, A., Langer, M., Maisey, J. G., Geffard-Kuriyama, D., Cloetens, P., Janvier, P., and Tafforeau, P. (2009a). Skull and brain of a 300-million-year-old chimaeroid fish revealed by synchrotron holotomography. *Proceedings of the National Academy of Sciences of the United States of America*, 106(13):5224–5228.

Pradel, A., Maisey, J. G., Mapes, R. H., and Kruta, I. (2016). First evidence of an intercalar bone in the braincase of "palaeonisciform" actinopterygians, with a virtual reconstruction of a new braincase of Lawrenciella Poplin, 1984 from the Carboniferous of Oklahoma. *Geodiversitas*, 38(4):489–504.

Pradel, A., Maisey, J. G., Tafforeau, P., and Janvier, P. (2009b). An enigmatic gnathostome vertebrate skull from the Middle Devonian of Bolivia. *Acta Zoologica*, 90(May):123–133.

Pradel, A., Maisey, J. G., Tafforeau, P., Mapes, R. H., and Mallatt, J. (2014). A Palaeozoic shark with osteichthyan-like branchial arches. *Nature*, 509(7502):608–11.

Pradel, A., Tafforeau, P., and Janvier, P. (2010). Study of the pectoral girdle and fins of the Late Carboniferous sibyrhynchid iniopterygians (Vertebrata, Chondrichthyes, Iniopterygia) from Kansas and Oklahoma (USA) by means of microtomography, with comments on iniopterygian relationships. *Comptes Rendus Palevol*, 9(6-7):377–387.

Pradel, A., Tafforeau, P., Maisey, J. G., and Janvier, P. (2011). A new paleozoic symmoriiformes (chondrichthyes) from the late carboniferous of Kansas (USA) and cladistic analysis of early chondrichthyans. *PLoS ONE*, 6(9).

Puttick, M. N., O'Reilly, J. E., Pisani, D., and Donoghue, P. C. J. (2018). Probabilistic methods outperform parsimony in the phylogenetic analysis of data simulated without a probabilistic model. *Palaeontology*, pages 1–17.

Qiao, T., King, B., Long, J. A., Ahlberg, P. E., and Zhu, M. (2016). Early Gnathostome Phylogeny Revisited : Multiple Method Consensus. *Plos One*, pages 1–23.

Qu, Q., Blom, H., Sanchez, S., and Ahlberg, P. E. (2015a). Three-dimensional virtual histology of silurian osteostracan scales revealed by synchrotron radiation microtomography. *Journal of Morphology*, 276(8):873–888.

Qu, Q., Haitina, T., Zhu, M., and Ahlberg, P. E. (2015b). New genomic and fossil data illuminate the origin of enamel. *Nature*, 526:108–111.

Qu, Q., Sanchez, S., Blom, H., Tafforeau, P., and Ahlberg, P. E. (2013a). Scales and Tooth Whorls of Ancient Fishes Challenge Distinction between External and Oral 'Teeth'. *PLoS ONE*, 8(8).

Qu, Q., Zhu, M., and Wang, W. (2013b). Scales and Dermal Skeletal Histology of an Early Bony Fish Psarolepis romeri and Their Bearing on the Evolution of Rhombic Scales and Hard Tissues. *PLoS ONE*, 8(4).

Qu, Q., Zhu, M., and Wang, W. (2013c). Scales and dermal skeletal histology of an early bony fish Psarolepis romeri and their bearing on the evolution of rhombic scales and hard tissues. *PloS one*, 8(4):e61485.

Rayner, D. H. (1951). III.âĂŤOn the Cranial Structure of an Early Palæoniscid, Kentuckia, gen. nov. *Transactions of the Royal Society of Edinburgh*, 62(1):53–83.

Reif, W. E. (1978). Types of morphogenesis of the dermal skeleton in fossil sharks. *Paläeontologische Zeitschrift*, 52(1-2):110–128.

Reif, W. E. (1979). Morphogenesis and histology of large scales of batoids (Elasmobranchii). *Paläeontologische Zeitschrift*, 53(1-2):26–37.

Reif, W. E. (1982). Evolution of dermal skeleton and dentition in vertebrates: the odontode regulation theory. *Evolutionary Biology*, (15):287–368.

Reilly, J. E. O., Puttick, M. N., Parry, L., Tanner, A. R., Tarver, J. E., Fleming, J., Pisani, D., and Donoghue, P. C. J. (2016). Bayesian methods outperform parsimony but at the expense of precision in the estimation of phylogeny from discrete morphological data. *Biology Letters*, 12.

Richter, M., Neis, P. A., and Smith, M. M. (1999). Acanthodian and actinopterygian fish remains from the Itaituba Formation, Late Carboniferous of the Amazon Basin, Brazil, with a note on acanthodian ganoin. *Neues Jahrbuch für Geologie und Paläontologie*, 12:729–744.

Richter, M. and Smith, M. M. (1995). A microstructural study of the ganoine tissue of selected lower vertebrates. *Zoological Journal of the Linnean Society*, 114:173–212.

Rieppel, O. (1982). A new genus of shark from the Middle Triassic of Monte San Giorgio, Switzerland. *Palaeontology*, 25(2):399–412.

Ritchie, A. (2005). Cowralepis, a new genus pf phyllolepid fish (Pisces, Placodermi) from the Late Middle Devonian of New South Wales, Australia. *Proceedings of The Linnean Society of New South Wales*, 126:215–259.

Romer, A. S. (1964). The braincase of the Palaeozoic elasmobranch Tamiobatis. *Bulletin of the Museum of Comparative Anatomy at Harvard College*, 131(4):87–105.

Ronquist, F. and Huelsenbeck, J. P. (2003). MrBayes 3: Bayesian phylogenetic inference under mixed models. *Bioinformatics*, 19(12):1572–1574.

Rosen, D. E., Forey, P. L., Gardiner, B. G., and Patterson, C. (1981). Lungfishes, tetrapods, paleontology, and plesiomorphy. *Bulletin of the American Museum of Natural History*, 167(4):159–276.

Rücklin, M., Donoghue, P. C. J., Johanson, Z., Trinajstic, K., Marone, F., and Stampanoni, M. (2012). Development of teeth and jaws in the earliest jawed vertebrates. *Nature*, 491.

Sanchez, S., Tafforeau, P., and Ahlberg, P. E. (2014). The humerus of Eusthenopteron : a puzzling organization presaging the establishment of tetrapod limb bone marrow. *Proceedings of the Royal Society B: Biological Sciences*, 281.

Sansom, I. J., Davies, N. S., Coates, M. I., Nicoll, R. S., and Ritchie, A. (2012). Chondrichthyan-like scales from the Middle Ordovician of Australia. *Palaeontology*, 55(2):243–247.

Sansom, I. J., Sansom, I. J., Wang, N.-z., Wang, N.-z., and Smith, M. M. (2005). The histology and affinities of sinacanthid fishes: primitive gnathostomes from the Silurian of China. *Zoological Journal of the Linnean Society*, (1998):379–386.

Sansom, R. S. (2009). Phylogeny, classification and character polarity of the Osteostraci (Vertebrata). *Journal of Systematic Palaeontology*, 7(1):95–115.

Sansom, R. S., Gabbott, S. E., and Purnell, M. A. (2013). Unusual anal fin in a Devonian jawless vertebrate reveals complex origins of paired appendages. *Biology letters*, 9(3):20130002.

Sansom, R. S., Randle, E., and Donoghue, P. C. J. (2014). Discriminating signal from noise in the fossil record of early vertebrates reveals cryptic evolutionary history. *Proceedings of the Royal Society B: Biological Sciences*, 282(1800):20142245–20142245.

Schaeffer, B. (1968). The origin and basic radiation of the Osteichthyes. In Ørvig, T., editor, *Current problems of lower vertebrate phylogeny. Proc. Fourth Nobel Symp.*, pages 207–222. Armqvist and Wiksell, Stockholm.

Schaeffer, B. (1981). The xenacanth shark neurocranium, with comments on elasmobranch monophyly. *Bulletin of the American Museum of Natural History*, 169(1).

Schaeffer, B. and Williams, M. E. (1977). Relationships of fossil and living elasmobranchs. *Integrative and Comparative Biology*, 17:293–302.

Schmitz, B., Werdelin, L., Forey, P. L., and Bendix-almgreen, S. E. (1991). Sr/ 86 Sr, Na, F, Sr, and La in skeletal fish debris as a measure of the paleosalinity of fossil-fish habitats. *Geological Society of America bulletin*, (June):786–794.

Schultze, H.-p. and Zidek, J. (1982). Ein primitiver acanthodier (pisces) aus dem unterdevon lettlands. *Paläeontologische Zeitschrift*, 56(1/2):95–105.

Smith, M. M. and Hall, B. K. (1990). Vertebrate skeletogenic and odontogenic tissues. *Biological Reviews*, 65:277–373.

Smith, M. M. and Sansom, I. J. (1997). Exoskeletal micro-remains of an Ordovician fish from the Harding Sandstone of Colorado. *Palaeontology*, 40(3):645–658.

Snyder, D., Turner, S., Burrow, C. J., and Daeschler, E. B. (2017). "Gyracanthus" sherwoodi (Gnathostomata , Gyracanthidae) from the Late Devonian of North America. *Proceedings of the Academy of Natural Sciences of Philadelphia*, 165:195–219.

Stahl, B. J. (1967). Morphology and relationships of the Holocephali with special reference to the venous system. *Bull. Mus. Camp. Zool. 135, 141.*

Stensiö, E. (1925a). On the head of Macropetalichthyids with certain remarks on the head of the other arthrodires. *Field Museum of Natural History Geological Series*, 4(4):87–197.

Stensiö, E. (1925b). On the head of the macropetalichthyids with certain remarks on the head of the other arthrodires. *Publications of the Field Museum of Natural History*, 4:87–197.

Stensiö, E. (1969). Elasmobranchiomorphi; Placodermata, Arthrodires. In Piveteau, J., editor, *Traité de paleontologie*, volume 4, pages 71–692. Masson et Cie., Paris.

Summers, A. P. (2000). Stiffening the stingray skeleton-an investigation of durophagy in myliobatiod stingrays (Chondrichythes Batiodea, Myliobatiodae). *Journal of Morphology*, 243:113–126.

Sutton, M., Rahman, I. A., and Garwood, R. J. (2014). *Techniques for virtual palaeontology*. Wiley.

Swofford, D. L. (2003). PAUP*: Phylogenetic Analysis Using Parsimony (*And Other Methods).

Thorsteinsson, R. (1973). Dermal elements of a new lower vertebrate from Middle Silurian (Upper Wenlockian) rocks of the Canadian arctic archipelago. *Palaeontographica, Abteilung A*, (143):51–57.

Traquair, R. H. (1899). XXI.- On Thelodus Pagei, Powrie, sp. from the Old Red Sandstone of Forfarshire. *Transactions of the Royal Society of Edinburgh; Earth Sciences*, 39:595–602.

Trewin, N. H. and Davidson, R. G. (1996). An Early Devonian Lake and its associated biota in the Midland Valley of Scotland. *Transactions of the Royal Society of Edinburgh-Earth Sciences*, 86(November 2011):233–246.

Trinajstic, K., Boisvert, C., Long, J. A., Maksimenko, A., and Johanson, Z. (2014). Pelvic and reproductive structures in placoderms (stem gnathostomes). *Biological Reviews*, 90:467–501.

Turner, S., Burrow, C. J., and Warren, A. (2005). Gyracanthides hawkinsi sp. nov. (Acanthodii, gyracanthidae) from the lower carboniferous of Queensland, Australia, with a review of gyracanthid taxa. *Palaeontology*, 48(Turner 1982):963–1006.

Turner, S., Burrow, C. J., Williams, R. B., and Tarrant, P. (2017). Welsh Borderland bouillabaisse: Lower Old Red Sandstone fish microfossils and their significance. *Proceedings of the Geologists' Association*, 128:460–479.

Turtletaub, J. (2018). The Meg.

Valiukevičius, J. (1992). First articulated Poracanthodes from the Lower Devonian of Severnaya Zemlya. In *Fossil Fishes as Living Animals*, pages 193–213.

Valiukevičius, J. (2003). Devonian acanthodians from Severnaya Zemlya Archipelago (Russia). 25(1):131–204.

Valiukevičius, J. (2004). New Wenlock-Pridoli (Silurian) acanthodian fishes from Lithuania. *Acta Palaeontologica Polonica*, 49(1):147–160.

Van Arsdell, R. D. (1994). *The coinage of the Dobunni. Money supply and coin circulation in Dobunnic territory (Studies in Celtic coinage)*. Oxford University Committee for Archaeology, Oxford.

Wang, N.-z., Donoghue, P. C. J., Smith, M. M., Sansom, I. J., and Nian-zhong, W. (2005). Histology of the Galeaspid Dermoskeleton and Endoskeleton, and the Origin and Early Evolution of the Vertebrate Cranial Endoskeleton. *Journal of Vertebrate Paleontology*, 25(4):745–756.

Wängsjö, G. (1952). The Downtonian and Devonian vertebrates of Spitsbergen. IX. Morphologic and systematic studies of the Spitsbergen cephalaspids. Results of Th. Vogt's Expedition 1928 and the English- Norwegian-Swedish Expedition in 1939. *Norsk Polarinstitutt Skrifter*, 97:1–611.

Warren, A., Currie, B. P., Burrow, C. J., and Turner, S. (2000). A redescription and reinterpretation of Gyracanthides murrayi Woodward 1906 (Acanthodii, Gyracanthidae) from the Lower Carboniferous of the Mansfield Basin, Victoria, Australia. *Journal of Vertebrate Paleontology*, 20(2):225–242.

Watson, D. M. S. (1937). The Acanthodian Fishes. *Philosophical transactions of the Royal Society of London. Series B, Biological Sciences*, 228(549):49–146.

White, E. I. (1935). The ostracoderm Pteraspis KNER and the relationships of the agnathous vertebrates. *Philosophical Transactions of the Royal Society of London B*, 225(527):381–456.

Wilga, C. D. (2002). A functional analysis of jaw suspension in elasmobranchs. *Biological Journal of the Linnean Society*, 75(4):483–502.

Williams, M. E. (1998). A new specimen of Tamiobatis vetustus (Chondrichthyes, Ctenacanthoidea) from the Late Devonian Cleveland Shale of Ohio. *Journal of Vertebrate Paleontology*, 18(2):251–260.

Williams, M. E. (2001). Tooth retention in cladodont sharks: with a comparison between primitive grasping and swallowing, and modern cutting and gouging feeding mechanisms. *Journal of Vertebrate Paleontology*, 21(2):214–226.

Woodward, A. S. (1891). *Catalogue of the fossil fishes in the British Museum (Natural History) - Part II*.

Woodward, A. S. (1919). On two new elasmobranch fishes (Crossorhinus jurassicas sp. nov., and Protospinax annectans, ge. et sp. nov.) from the Upper Jurassic Lithographic Stone of Bavaria. *Zool Soc Proc*, 13:231–235.

Woodward, A. S. and White, E. I. (1938). The Dermal tubercles of the Upper Devonian shark, Cladoselache. *Annals and Magazine of Natural history*, 11:367–368.

Wright, A. M. and Hillis, D. M. (2014). Bayesian analysis using a simple likelihood model outperforms parsimony for estimation of phylogeny from discrete morphological data. *PloS one*, 9(10):e109210.

Young, G. C. (1979). New information on the structure and relationships of Buchanosteus (Placodermi: Euarthrodira) from the Early Devonian of New South Wales. *Zoological Journal of the Linnean Society*, 66:309–352.

Young, G. C. (1982). Devonian sharks from South-Eastern Australia and Antarctica. *Palaeontology*, 25(4):817–843.

Young, G. C. (1984). Reconstruction of the jaws and braincase in the Devonian placoderm Bothriolepis. *Palaeontology*, 27(3):635–661.

Young, G. C. (1986). The relationships of placoderm fishes. *Zoological Journal of the Linnean Society*, 88(1):1–57.

Young, G. C. and Burrow, C. J. (2004). Diplacanthid acanthodians from the Aztec Siltstone (late Middle Devonian) of southern Victoria Land, Antarctica. *Fossils and Strata*, (50).

Young, G. C., Lelièvre, H., and Goujet, D. (2001). Primitive jaw structure in an articulated brachythoracid arthrodire (placoderm fish; Early Devonian) from southeastern Australia. *Journal of Vertebrate Paleontology*, 21(4):37–41.

Yu, X. (1998). A new porolepiform-like fish, Psarolepis romeri , gen. et sp. nov. (Sarcopterygii, Osteichthyes) from the Lower Devonian of Yunnan, China. *Journal of Vertebrate Paleontology*, 18(2):261–274.

Zangerl, R. (1966). A new shark of the family Edestidae , Ornithoprion hertwigi , from the Pennsylvanian Mecca and Logan quarry shales of Indiana. *Fieldiana*, 16(1):1–43.

Zangerl, R. (1981). *Handbook of Paleoichthyology, Chondrichthyes I, Paleozoic Elasmobranchii*. Gustav Fischer Verlag, Stuttgart.

Zangerl, R. and Case, G. (1973). Iniopterygia, a new order of chondrichthyan fishes from the Pennsylvanian of North America. *Fieldiana*, 6.

Zangerl, R. and Case, G. (1976). Cobelodus aculeatus (Cope), an anacanthous shark from Pennsylvanian black shales of North America. *Palaeontographica. Abteilung A, Palaeozoologie-Stratigraphie*, 154:107–157.

Zhang, G., Wang, J., and Wang, N. (2001). The structure of pectoral fin and tail of Yunnanolepidoidei, with a discussion of the pectoral fin of chuchinolepids. *Vertebrata PalAsiatica*, 39:1–13.

Zhu, M., Ahlberg, P. E., Pan, Z., Zhu, Y., Qiao, T., and Zhao, W. (2016). A new Silurian maxillate placoderm illuminates jaw evolution. *Science*.

Zhu, M. and Schultze, H.-p. (1997). The oldest sarcopterygian fish. *Lethaia*, 30:293–304.

Zhu, M. and Yu, X. (2002). A primitive fish close to the common ancestor of tetrapods and lungfish. *Nature*, 21:767–770.

Zhu, M. and Yu, X. (2004). Lower jaw character transitions among major sarcopterygian groups - a survey based on new materials from Yunnan, China. In *Recent Advances in the Origin and Early Radiation of Vertebrates*, pages 271–286. Verlag Dr. Friedrich Pfeil, München.

Zhu, M., Yu, X., and Ahlberg, P. E. (2001). A primitive sarcopterygian fish with an eyestalk. *Nature*, 73(1981):1999–2002.

Zhu, M., Yu, X., Ahlberg, P. E., Choo, B., Lu, J., Qiao, T., Qu, Q., Zhao, W., Jia, L., Blom, H., and Zhu, Y. (2013). A Silurian placoderm with osteichthyan-like marginal jaw bones. *Nature*, 502(7470):188–93.

Zhu, M., Yu, X., Choo, B., Wang, J., and Jia, L. (2012). An antiarch placoderm shows that pelvic girdles arose at the root of jawed vertebrates. *Biology letters*, 8(3):453–6.

Zhu, M., Yu, X., and Janvier, P. (1999). A primitive fossil fish sheds light on the origin of bony fishes. *Nature*, 6004(1978):607–610.

Zhu, M., Zhao, W., Jia, L., Lu, J., Qiao, T., and Qu, Q. (2009). The oldest articulated osteichthyan reveals mosaic gnathostome characters. *Nature*, 458(7237):469–74.

Zidek, J. (1976). Kansas Hamilton Quarry (Upper Pennsylvanian) Acanthodes, with remarks on the previously reported North American occurrences of the Genus. *The University of Kansas Palaeontological Contributions*, (83).

Zidek, J. (1992). Geology and paleontology of the Kinney Brick Quarry, Late Pennsylvanian, central New Mexico. In Zidek, J., editor, *Geology and paleontology of the Kinney Brick Quarry, Late Pennsylvanian, central New Mexico*, pages 199–214.

APPENDIX A

APPENDIX A: DETAILS OF PHYLOGENETIC ANALYSIS FOR CHAPTER 3

Phylogenetic dataset

A.0.1 **(i) Notes on taxa**

For our phylogenetic analysis we added additional information to the dataset of Coates et al. (2018). *Ptomacanthus* was scored for branchial characters on the basis of this work. Two additional taxon were added: *Paraplesiobatis*, a "placoderm' with three dimensionally preserved branchial arches, to increase sampling of stem-gnathostome branchial arches, and *Euthacanthus*, an acanthodian with a potentially important combination of climatiid-like and acacnthodiform-like traits. *Nereipisacanthus* was modified for a number of characters - notably character 225 from 0 to ?

Additional sources used to score characters are as follows:

- *Euthacanthus* Watson (1937); Newman et al. (2011, 2014)
- *Paraplesiobatis* - Gross (1962); Brazeau et al. (2017), KGM 1983/294
- *Ptomacanthus* - NHM P 24919a

Institutional abbreviations: **KGM** - Schlossparkmuseum (Karl-Geib-Museum), Bad Kreuznach, **NHM** - Natural History Museum, London

A.0.2 **(ii) Notes on characters**

I modified and added a number of characters from the original matrix, several of which relate to the pharyngeal skeleton: these are detailed below. Also included are recodings.

MODIFIED Character 17 - Scale sensory line of body: (0) passes between or beneath scales, (1) passes over scales and/or is partially enclosed or surrounded by scales, (2) perforates or passes through scales

This replaces character 17 of Coates et al. (2018) "Sensory line canal...". The original character attempts to capture the different morphologies of in the sensory line canals in (1) most chondrichthyans, where it passes between scales (Brazeau and Friedman, 2014), (2) those of some early chondrichthyans (eg. *Akmonistion* (Coates and Sequeira, 2001a)) which are carried by c-shaped scales, and of some acanthodians (eg. *Homalacanthus* (Gagnier, 1996)) where the head sensory lines are carried in open gutter-like scales, and (3) those of osteichthyans and stem-gnathostomes, where the canal passes through the scales themselves.

However, in doing so it conflates states in the head and body which can differ in the same animal, particularly in acanthodians. In *Homalacanthus* for example the state on the head is (1), but the state on the body (0) (Gagnier 1996). Here we have attempted to remedy this by distinguishing between two characters - one covering body squamation (17) and one for head squamation (18)

ADDED Character 18 - Scale sensory line of head: (0) passes between or beneath scales, (1) passes over scales and/or is partially enclosed or surrounded by scales, (2) perforates or passes through scales

See above.

RECODED Character 64

MODIFIED Character 67 Gill skeleton extends posteriorly beyond occiput: (0) absent, (1) present

The branchial arches of osteichthyans and stem-gnathostomes are located beneath the neurocranium, whereas those of chondrichthyans have a pronounced posterior extension beyond the occiput (a notable, and certainly derived, exception to this being holocephalans). Coates et al. (2018) capture this with their character number 66, present in conventional chondrichthyans and some acanthodians (eg. *Acanthodes*). As discussed in the main text, here I consider that there is a subtlety to this character that is not considered - the anterior and posterior extents of the branchial skeleton. This is covered by this and the next character.

ADDED Character 68 First branchial arch meets neurocranium (1) ventral to otic region (1) posterior to otic region

See above

MODIFIED Character 73 - Anteriormost unpaired element of branchial skeleton contacted by: (0) one branchial arch only, (1) two or more branchial arches

A basihyal is a median unpaired component of the hyoid arch - in living gnathostomes it is only present in chondrichthyans, where it articulates with the hyoid arch, and sometimes the hyoid arch and first branchial arch (Garman, 1913; Pradel et al., 2014). This is a morphologically distinct from the basibranchial/s of osteichthyans, which is an unpaired element or group of elements onto which the hyoid arch (via hypohyals) and branchial arches articulate (eg. *Glyptolepis*

(Jarvik, 1972), or *Raynerius* (Giles et al., 2015b)). Amongst extinct gnathostomes a basihyal is usually considered present in chondrichthyans - both crown-group (eg. *Egertonodus* (Maisey, 1983), and *Debeerius* (Grogan and Lund, 2000)) and stem-group (eg. *Gladbachus* (Coates et al., 2018)) - as well as in various stem-gnathostomes (for example, *Paraplesiobatis* (Brazeau et al., 2017)).

The actual diagnosis for what constitutes a basihyal as opposed to a basibranchial in a fossil is slightly opaque - compare codings for (Giles et al., 2015c) character 73 with (Coates et al., 2018) character 71. In their discussion of basihyals Coates et al. (2018) (in the supplementary material) state that the "position, connectedness, and separation from other basibranchials" are what distinguish a basihyal from a basibranchial/copula. This diagnosis is a compound combination of traits. Notwithstanding this the relative position of basihyals and basibranchials actually often differs little - the basibranchial of *Raynerius* for example (Giles et al., 2015b), is in much the same position relative to the hyoid arch as that of *Paraplesiobatis* (Brazeau et al., 2017) or *Ptomacanthus* (Chapter 3).

Here I attempt to break the remainder of this diagnosis down into characters - this character and the following. One aspect of the connectedness of a "basihyal" is the absence of hypohyals - these are captured in another character. We also note that there are two additional characters one could try, but which are uninformative with the current dataset. The first could attempt to capture the spacing aspect of the basihyal definition *sensu* Coates et al. (2018) a basihyal is usually well separated from the posterior basibranchial copulae in chondrichthyans - this is not observed in osteichthyans with posterior basibranchials (eg. *Amia* (Allis, 1897)), *Eusthenopteron*(Jarvik, 1980)).). The second could attempt to code for the articulation of only the hyoid arch onto the basihyal, a state which at least present in some holocephalans (pers. obvs).

This character distinguishes an attribute of connectedness that separates a basihyal *sensu* Coates et al. (2018)from basibranchials/copulae - the number of branchial arches articulating with it in addition to the hyoid arch. In taxa with a "basihyal" this is either one or none, whereas in osteichthyans it is typically two or more.

ADDED Character 74 - Multiple unpaired branchial mineralisations (0) absent, (1) present

Often gnathostomes have a chain of unpaired elements running along the base of the branchial basket - whether these be the copulae of chondrichthyans or the basibranchials of osteichthyans. *Ptomacanthus* lacks any kind of mineralised unpaired structure posterior to its basihyal. It shares this in common with placoderms such as *Paraplesiobatis* (Brazeau et al., 2017) and *Cowralepis* (Carr et al., 2009). Contrastingly, in most chondrichthyans a basibranchial copula is present, eg. *Ozarcus* (Pradel et al., 2014) and *Gladbachus* (Coates et al., 2018). Osteichthyans vary between having a chain of elements (eg. *Amia* (Allis 1897)) or a single element or complex of elements onto which all arches articulate (eg. *Mimipiscis* (Gardiner, 1984) or *Eusthenopteron* (Jarvik, 1980)). *Ozarcus* has been scored present despite the apparent absence of a basihyal as its elongate posterior ossification seems likely to equate to the basibranchial copulae of other chondrichthyans.

ADDED Character 80: Posterior two ventral branchial arches (0) separate, (1) articulate ventrally

In the "placoderm" stem-gnathostome *Paraplesiobatis*, the posterior two branchial arches articulate ventrally (Brazeau et al., 2017). A similar state is also observed in various sarcopterygians, such as *Glyptolepis* (Jarvik, 1972) and *Gryphognathus* (Miles, 1977). Contrastingly, no such state is found in chondrichthyans, such as

Ozarcus (Pradel et al., 2014), *Gladbachus* (Coates et al., 2018), and now, *Ptomacanthus*. It is possible that having fully separated ventral paired branchial arches is autapomorphic for chondrichthyans.

ADDED Character 81: Posterior two dorsal branchial arches (0) separate, (1) articulate dorsally

In living chondrichthyans the posteriormost (fifth) epibranchial forms a fused complex with the fourth pharyngobranchial (Carvalho et al., 2013). *Ptomacanthus* has a separate fifth epibranchial: however, rather than having its own expanded end (presumed pharyngobranchial) it articulates with the posterior of the fourth pharyngobranchial. A similar state is observed in the stem-holocephalan *Ozarcus* Pradel et al. (2014). Thus this possibly constitutes an autapomorphy, at some level, of chondrichthyans.

MODIFIED Character 262: Anteriormost intermediate spine associated with shoulder girdle (0) absent, (1) present

This replaces Coates et al. (2018) character Admedian pectoral spines present/absent. I have coded *Doliodus* absent for this - this is discussed in Appendix B Character 264.

A.0.3 **(iii) Notes on analysis**

To allow exact replication of the tnt analysis I have included a list of tnt commands used in the text file `PtomCommands.txt`. If a directory contains both the tnt matrix (`PtomCoates18_v2.tnt`) and this text file (`PtomCommands.txt`) then these commands can be automatically run in tnt using:

```
cdir INSERT DIRECTORY HERE;
proc PtomCommands.txt;
```

The commands used for MrBayes are included in a Bayes block in the NEXUS file `PtomCoates18_v2Bayes.nex`.

APPENDIX B

APPENDIX B: DETAILS OF PHYLOGENETIC ANALYSIS FOR CHAPTER 7

B.1 TAXA AND REFERENCES

TABLE B.1: Taxa included in phylogenetic analysis with references used for morphological information

Genus	**References**
Galeaspida	Janvier (1996); Wang et al. (2005); Gai et al. (2011)
Osteostraci	Janvier (1996, 1985, 2004); Sansom (2009); Adrain and Wilson (1994)
Acanthodes	Ørvig (1951); Beznosov (2009); Davis et al. (2012); Gardiner (1984); Miles (1973a,b, 1970, 1968, 1964a); Watson (1937); Heidtke (2011), NMS 1950.38.9, NHM casts
Acronemus	Maisey (2011); Rieppel (1982)
Akmonistion	Coates and Sequeira (1998, 2001a); Coates et al. (1998)
Austroptyctodus	Miles and Young (1977); Long (1997)
Bothriolepis	Janvier (1996); Denison (1978); Young (1984, 1986); Downs and Donoghue (2009)
Brachyacanthus	Watson (1937) NMS 1891.92.220
Brochoadmones	Bernacsek and Dineley (1977); Hanke and Wilson (2006)
Buchanosteus	Young (1979, 1986); Burrow and Turner (1998); Young et al. (2001)
Cassidiceps	Gagnier and Wilson (1996b)
Cheiracanthus	Watson (1937); Denison (1979); Miles (1973a)

Cheirolepis	Pearson and Westoll (1979); Giles et al. (2015a); Giles and Friedman (2014); Lu et al. (2016)
Chondrenchelys	Finarelli and Coates (2012, 2014)
Cladodoides	Gross (1938); Maisey (2005)
Cladoselache	Hussakof and Bryant (1918); Harris (1938); Maisey (1989b, 2007); Schaeffer (1981); Williams (2001); Woodward and White (1938); Zangerl (1981); Bendix-Almgreen (1975)
Climatius	Watson (1937); Miles (1973a); Burrow et al. (2015)
Cobelodus	Zangerl and Case (1976); Zidek (1992)
Cowralepis	Carr et al. (2009); Long et al. (2009); Ritchie (2005)
Culmacanthus	Long (1983); Burrow and Young (2012) and peels of specimens from Long (1983)
Debeerius	Grogan and Lund (2000)
Dicksonosteus	Goujet (1975, 1984)
Diplacanthus	Watson (1937); Burrow et al. (2016a), NMS specimens discussed in chapter 4
Dobunnacanthus	Miles (1973a) specimens discussed in chapter 6
Doliodus	Miller et al. (2003); Maisey et al. (2009, 2014, 2017); Long et al. (2015)
Dwykaselachus	Coates et al. (2017a); Oelofsen (1986)
Egertonodus	Maisey (1982, 1983); Lane (2010)
Entelognathus	Zhu et al. (2013)
Eusthenopteron	Jarvik (1980)
Euthacanthus	Watson (1937); Newman et al. (2011, 2014); Long et al. (2015)
Gladbachus	Heidtke and Krätschmer (2001); Coates et al. (2018); Burrow and Turner (2013)

Glyptolepis	Jarvik (1972); Andrews and Westoll (1970); Cloutier and Schultze (1996); Ahlberg (1989)
Guiyu	Zhu et al. (2009)
Gyracanthides	Warren et al. (2000); Turner et al. (2005); Miles (1973a)
Halimacanthodes	Burrow et al. (2012)
Hamiltonichthys	Maisey (1982)
Helodus	Moy-Thomas (1936); Patterson (1965)
Homalacanthus	Gagnier (1996); Miles (1964b)
Iniopera	Zangerl and Case (1973); Pradel et al. (2010); Pradel (2010); Pradel et al. (2009a)
Ischnacanthus	Watson (1937); Miles (1973a); Gross (1947)
Jagorina	Stensiö (1969); Denison (1978); Young (1986); Giles et al. (2015c)
Janusiscus	Giles et al. (2015c)
Kathemacanthus	Gagnier and Wilson (1996b); Hanke and Wilson (2010)
Kawichthys	Pradel et. al (2011)
Latviacanthus	Schultze and Zidek (1982)
"Ligulalepis"	Basden et al. (2000); Basden and Young (2001); Clement et al. (2018)
Lupopsyroides	Hanke and Wilson (2004)
Lupopsyrus	Bernacsek and Dineley (1977); Hanke and Davis (2012)
Macropetalichthys	Stensiö (1925b, 1969); Denison (1978); Gross (1935)
Mesacanthus	Watson (1937); Miles (1973a)
Milesacanthus	Young and Burrow (2004)
Mimipiscis	Gardiner (1984); Giles and Friedman (2014); Choo (2011); Gardiner and Bartram (1977)
Nereipisacanthus	Burrow (2011); Burrow and Rudkin (2014)
Obtusacanthus	Hanke and Wilson (2004)

Onychodus	Andrews et al. (2006)
Onychoselache	Dick and Maisey (1980); Coates and Gess (2007)
Orthacanthus	Schaeffer (1981); Maisey (1983); Heidtke (1999); Lane and Maisey (2009)
Ozarcus	Pradel et al. (2014); Maisey (2007); Coates et al. (2017b)
Paraplesiobatis	Brazeau et al. (2017); Gross (1962)
Parayunnanolepis	Zhang et al. (2001); Zhu et al. (2012)
Parexus	Watson (1937); Burrow et al. (2013)
Paucicanthus	Hanke (2002)
Poracanthodes	Denison (1979); Valiukevičius (1992)
Promesacanthus	Hanke (2008)
Psarolepis	Yu (1998); Zhu and Schultze (1997); Zhu et al. (1999); Qu et al. (2013c)
Ptomacanthus	Miles (1973a); Brazeau (2012, 2009), specimens discussed in chapter 3
Pucapampella	Maisey and Anderson (2001); Maisey (2001a); Maisey and Lane (2010); Janvier and Maisey (2010)
Ramirosuarezia	Pradel et al. (2009b)
Rhadinacanthus	Burrow et al. (2016a)
Romundina	Dupret et al. (2014, 2017)
Styloichthys	Zhu and Yu (2002, 2004); Friedman (2007)
Synechodus	Maisey (1985)
Tamiobatis	Schaeffer (1981); Williams (1998)
Tetanopsyrus	Gagnier et al. (1999); Gagnier and Wilson (1995); Hanke et al. (2001a)
Tristychius	Dick (1978); Coates and Tietjen (2018); Coates and Gess (2007)
Trizeugacanthus	Gagnier (1996)

Uraniacanthus	Miles (1973a); Hanke and Davis (2008); Bernacsek and Dineley (1977); Newman et al. (2012); Burrow et al. (2016a)
Vernicomacanthus	Miles (1973a) specimens discussed in chapter 6

B.2 NOTES ON CHARACTER DERIVATION

B.3 ABBREVIATIONS FOR CHARACTER SOURCES

Abbreviation	**Character source**
BdeW15	Brazeau and de Winter (2015)
B16	Burrow et al. (2016a)
C17	Coates et al. (2017b)
C18	Coates et al. (2018)
GFB15	Giles et al. (2015c)
HW04	Hanke and Wilson (2004)
Keatetal16	Keating and Donoghue (2016)
K16	King et al. (2016)
L16	Lu et al. (2016)
L17	Lu et al. (2017)

B.4 CHARACTER LIST

B.4.1 **Histology**

1. **[Modified from C18:1] Calcified cartilage tesserae in perichondrium**

   This character is based on a well established synapomorphy of crown-group chondrichthyans - a perichondral layer of tessellate calcified cartilage (Brazeau and Friedman, 2014). In living chondrichthyans each of these tesserae is formed from prismatic (ie. so dense as to be refractive) calcified cartilage externally, which grades into globular calcified cartilage internally (Dean and Summers, 2006). As Burrow et al. (2016a) note, histological study of

these tesserae in Palaeozoic chondrichthyans is extremely limited, and so it is unknown if tesserae include prismatic cartilage except in a few rare instances (eg. Long et al. (2015)). However, the tesserae themselves are readily visible without sectioning: following Burrow et al. (2016a) and subsequent analyses (Coates et al., 2017b,b) I have omitted the term prismatic from the character definition.

Coates et al. (2018) considered that *Gladbachus* lacked this character as the tesserae in its labyrinth did not interlock. However, while the perichondrial tesserae in *Gladbachus* are not like those of living chondrichthyans even non-interlocking tesserae are not observed in any acanthodian-grade stem-chondrichthyans, and they may provide evidence of a relatively crownwards position in the chondrichthyan stem-group for *Gladbachus*. Correspondingly I have scored *Gladbachus* as present for this character. If more taxa are described with *Gladbachus*-like tesserae this could be accounted for with an additional character for "interlocking tesserae", but currently this would be uninformative.

Despite the original description of the endoskeleton of *Doliodus* describing tessellate calcified cartilage (Miller et al., 2003), the cartilage lacks discrete tesserae and is actually far more similar in morphology to the globular calcified cartilage of acanthodian-grade chondrichthyans (Long et al., 2015). *Pucapampella* is described as having tessellate prismatic calcified cartilage, but it is never adequately figured (Maisey and Anderson, 2001; Maisey, 2001a; Gagnier et al., 1989; Janvier and Suarez-Riglos, 1986), and should probably be reassessed in the light of recent descriptions of atypical tesserae in early chondrichthyans (Long et al., 2015; Coates et al., 2018). Because of this it is

scored ?.

0. *absent*
1. *present*

2. **[C17: 2] Multilayered tesserae in the outer wall of the neurocranium**

   In several Palaeozoic chondrichthyans the tesserae that form the perichondrium of cartilages form multiple layers (eg.*Akmonistion*, *Orthacanthus* (Coates and Sequeira, 2001a; Schaeffer, 1981), discussed by Maisey (2013)) In Recent elasmobranchs the same morphology has been described and seems to be linked to areas of high mechanical force (Summers, 2000), however, it may be a phylogenetic signal in Palaeozoic chondrichthyans so I have kept the character.

   0. *absent*
   1. *present*

3. **[GFB15: 3] Perichondral bone**

   0. *present*
   1. *absent*

4. **[GFB15: 4] Extensive endoskeletal ossification**

   0. *absent*
   1. *present*

5. **[GFB15: 5] Enamel(oid) present on dermal bones and scales**

Layers of enameloid-like biorefringent tissue are reported in some isolated acanthodian scales assigned to *Acanthodes sp.* (Richter and Smith, 1995; Richter et al., 1999). However as these are not associated with an articulated animal *Acanthodes* is scored 0 for this character, following Giles et al. (2015c). The scales of *Halimacanthodes*, an articulated acanthodiform, do however display this (Burrow et al., 2012) and so it is scored 1.

0. *absent*

1. *present*

6. **[GFB15: 6] Enamel**

0. *single-layered*

1. *multi-layered*

7. **[GFB15: 7] Enamel layers**

Guiyu has been changed from - to 1 on basis of Lu et al. (2016) (Supp. fig. 9b) which appears to show enamel separated by dentinous layers.

0. *applied directly to one another (ganoine)*

1. *separated by layers of dentine*

8. **[L16: 8] Pore-canal network**

I have adopted the formulation of this character used by Lu et al. (2017, 2016).

0. *absent*

1. *present*

9. **[GFB15: 9] Dentinous tissues**

Cassidiceps, and *Lupopsyrus* have been scored 1 following Burrow et al. (2016b) and Coates et al. (2018).

0. *absent*

1. *present*

10. **[Modified from GFB15: 10] Dentine tubules in dermal integument**

This replaces previous characters distinguishing between types of dentine - instead it explicitly refers to the arrangement of tubules to clarify scoring. As spine dentine type sometimes differs from scale and plate dentine type (eg. in *Climatius* (Burrow et al., 2015)) I have considered only the latter in this character. Teeth are not considered by this character.

Brochoadmones is reported as having mesodentine (Hanke and Wilson, 2006) - I have scored it as such, but note the misgivings of (Coates et al., 2018) regarding the illustration. *Uraniacanthus* is considered by Burrow et al. (2016a) and Newman et al. (2012) to have mesodentine, *contra* Hanke and Davis (2008) - it is scored for mesodentine here. *Onychodus* is described as having branching dentine tubules in the scale ornament (Andrews et al., 2006); however this is not figured, so I have scored it ?.

0. *reticulate tubules (mesodentine)*

1. *unipolar tubules (orthodentine/semidentine)*

11. **[Modified from GFB15: 10] Cell lacunae within dentine of dermal integument**

This attempts to code for semidentine, a tissue found only in placoderms where cell lacunae are present within the dentine Burrow and Turner (1999). Although lacunae are only present in semidentine in this matrix, which has reticulate dentine tubules, it is logically possible for a combination of lacunae and orthogonal tubules to be present so this character is scored for all taxa with dentinous tissues. In effect this means that it is identical to the Coates et al. (2018) character 6, which only distinguishes between orthodentine and mesodentine/semidentine, albeit with a reversed polarity.

0. *absent*

1. *present*

12. **[Keatetal16] Osteonal vascular middle layer of the dermal integument**

Plesiomorphically, the crown-gnathostome skeleton comprises three layers: a lamellar basal layer, a vascular middle layer and superficial outer layer (Giles et al., 2013; Keating and Donoghue, 2016). In chondrichthyan body scales the middle layer has seemingly been lost (Andreev et al., 2016; Giles et al., 2013).

Arguably, this middle layer is present in the fin spines of many acanthodian-grade stem-chondrichthyans; typically these comprise an inner lamellar layer, a trabecular middle layer, and a superficial dentine layer forming the ornament (eg. *Parexus* Burrow et al. (2013)). However, I have restricted scoring to body

and head integument.

0. *absent*
1. *present*

13. **[GFB15: 11] Bone cell lacunae in body scale bases**

Akmonistion has been scored absent following Coates and Sequeira (2001a). .

0. *present*
1. *absent*

14. ***Dentine forming fin spine ornament**

Previously a character was present in a number of character matrices "Main dentinous tissue forming fin spine: osteodentine/orthodentine" (Burrow and Turner, 2010; Giles et al., 2015c; Lu et al., 2016, 2017). This character was never explained or defined in great detail, but attempted to capture the difference between the internal architecture of different chondrichthyan fin spines. However, while orthodentine, in the sense used in most descriptions, refers to ornamental dentine with orthogonal tubules (Burrow and Turner, 1999), osteodentine refers to the trabecular nature of the internal dentine. Some of the spines scored as comprising orthodentine had a large osteodentine component (eg. *Orthacanthus* (Beck et al., 2016))

However, spines do differ in their ornament dentine composition. I have replaced it with a new character distinguishing between the type of dentine tubulation forming the ornament in different chondrichthyan fin spines: comprising either orthogonal tubules (orthodentine) or a reticulate network of

tubules (mesodentine).

Acanthodes is scored ? *Climatius* has been scored 0 following Burrow et al. *Euthacanthus* is scored 0 following Newman et al. (2014). In *Gyracanthides* the "pallial dentine" has orthodentine tubules at the surface (Turner et al., 2005). *Rhadinacanthus* appears to have parallel tubules so I have coded it 1 (Burrow et al., 2016a).

0. *reticulate tubules (mesodentine)*
1. *orthogonal tubules (orthodentine)*

B.4.2 Squamation

15. **[GFB15: 13] Longitudinal scale alignment in fin web**

0. *present*
1. *absent*

16. **[GFB15: 14] Differentiated lepidotrichia**

0. *absent*
1. *present*

17. **[GFB15: 15] Body scale growth pattern**

Coates et al. (2017a, 2018) instead formulate this character as trunk scales: monocuspid/multicuspid. The purpose of this is in part to eliminate the use to the problematic term "odontode" from the definition, which is difficult to define. However, this fails to capture the generational growth of some single cusped scales (ie. "acanthodian"-type onion-skin growth) : instead I have

settled on a definition that refers to scale generations.

0. *comprising single generation of growth ("monodontode")*
1. *comprising a complex of multiple generations of growth ("polyodontode")*

18. **[GFB15: 17] Generations of odontodes**

0. *buried*
1. *areally growing*
2. *resorbed*

19. **[Novel] Odontode generations added in antero-dorsal axis**

In scales with multiple generations of growth new generations are added on and around the previous generation of growth. In stem-chondrichthyans such as *Seretolepis* (Hanke and Wilson, 2010), *Parexus* (Burrow et al., 2013), and those with "onion-skin" style scale growth (eg. *Diplacanthus* (Burrow et al., 2016a)), these generations are added strictly in the antero-dorsal axis, in a manner unique to chondrichthyans.

Previously "onion-skin" type growth was coded for with a "Scale growth concentric" character (Giles et al., 2015c; Coates et al., 2017a, 2018). Now this state is covered by a combination of superpositional and buried growth, and this character has been removed.

This character is inapplicable for taxa with only a single generation of scale growth. *Doliodus* and *Tamiobatis* are scored present despite the lack of histological sections as "ctenacanth-type" scales figured appear to grow in a manner similar to *Vernicomacanthus* (see Chapter 6) (Miller et al., 2003;

Williams, 1998). *Ptomacanthus* is scored 1, as superpositional scales are present (although not ubiquitous) (Brazeau, 2012). *Gladbachus* is scored 1 as figured body scale crowns have a row of odontodes oriented antero-posteriorly (Coates et al., 2018).

0. *absent*
1. *present*

20. **[Novel] Odontode generations grow in bilateral symmetry around original odontode**

Polyodontode chondrichthyan flank scales are unique in that new odontodes are added symmetrically, laterally to the primordial odontode Andreev et al. (2016). This is not observed in osteichthyan or stem-gnathostome scales, or in chondrichthyan head tesserae. Monodontode taxa are considered inapplicable.

The *Cladoselache* scale figured by Woodward and White (Woodward and White, 1938) is only shown in one plane; it probably is bilaterally symmetrical by comparison with other chondrichthyan scales and so is scored 1. The same is true of sections of *Gyracanthides* scales (Turner et al., 2005; Warren et al., 2000). Moulds of *Dobunnacanthus* scales are polyodontode and appear to conform to this state.

0. *absent*
1. *present*

21. **[GFB15: 18] Body scales with peg-and-socket articulation**

0. *absent*

1. *present*

22. **[GFB15: 19] Scale peg**

0. *broad*

1. *narrow*

23. **[GFB15: 20] Anterodorsal process on scale**

I have changed the scorings of *Cowralepis* and *Jagorina* from 0 to ? as I could not find adequately well-figured scales.

0. *absent*

1. *present*

24. **[GFB15: 21] Body scale profile**

Akmonistion has been changed from - to ? as the profile of its "miniscule body scales" is not shown (Coates and Sequeira, 2001a). I have scored *Obtusacanthus* 1 for this (change from ?) as in figure 10c (Hanke and Wilson, 2004) a scale is illustrated with a neck, even though the text says it is not present. Buchanosteus is scored 0 following Burrow and Turner (1998) - a scale neck appears to be present in some scales.

0. *distinct crown and base demarcated by a constriction ("neck")*

1. *flattened*

25. **[GFB15: 22] Profile of scales with constriction between crown and base**

Buchanosteus scored 0 following Burrow and Turner (1998)

0. *neck similar in width to crown*

1. *neck greatly constricted resulting in anvil-like shape*

26. **[GFB15: 23] Body scales with bulging base**

Diplacanthus has both flat and bulging based scales (Burrow et al., 2016a).

0. *absent*

1. *present*

27. **[GFB15: 24] Body scales with flattened base**

Glyptolepis was scored 0 for both this and the previous character: I have scored it 1 for this character.

0. *absent*

1. *present*

28. **[C17: 14] Body scales with basal canal or open basal vascular cavity**

Osteostracans scored 1 following Qu et al. (2015a).

0. *absent*

1. *present*

29. **[C17: 15] Neck canal**

Polybranchiaspid scales figures by Wang et al. (2005) show no evidence of neck canals - I have scored Galeaspida 0. *Acanthodes* has been scored 1 for this following Coates et al. (2018). *Climatius*, *Cheirolepis* I've left as ? as can not find any explicit mention of it. *Chondrenchelys* and *Cladoselache* are scored 1 following reports in Coates et al. (2018). *Onychoselache* is scored ?. *Rhadinacanthus* is scored 1 due to a report of ascending canals between the crown and the base (ie. the neck) Burrow et al. (2016a). Although *Obtusacanthus* is described as lacking a scale neck, a section through a scale with an apparent neck is figured by Hanke and Wilson (2004).

0. *absent*

1. *present*

30. **[GFB15: 26] Flank scale alignment**

0. *vertical rows oblique rows or hexagonal*

1. *rhombic packing*

31. **[GFB15: 27] Scute-like ridge scales (basal fulcra)**

0. *absent*

1. *present*

32. **[C18: 20] Fringing fulcra**

This is inapplicable for taxa with a heavily reduced squamation.

0. *absent*

1. *present*

33. **[Modified from C17:17] Lateral lines**

This is modified from the sense of the character in Coates et al. (2018) to explicitly refer to sensory lines on the body (ie. lateral lines). The previous formulation of the character failed to account for taxa in which the carriage of the sensory lines differs between the head and the body; an example of this is in the acanthodian *Homalacanthus* in which the lateral lines pass between scales but the sensory lines of the head are carried in semicircular ossicles (Gagnier, 1996). Sensory lines of the head are instead covered by Characters 35 and 36.

Taxa in which nothing of the lateral lines are known are scored ?. The portions of sensory line preserved in *Akmonistion* lie between the neural arches and spine plate and so comprise the lateral line (Coates and Sequeira, 2001a). *Gladbachus* is scored ? as no lateral lines are actually figured on the specimen (Coates et al., 2018).

0. *pass between or beneath scales*
1. *pass over scales and/or is partially enclosed or surrounded by scales*
2. *perforate and pass through scales*

B.4.3 Dermal bones of the skull

34. **[GFB15: 29] Dermal ornamentation of plates**

This character was originally erected to code for the ornamentation of the head skeleton. While states were clearly codeable in osteichthyans and stem-gnathostomes, many acanthodian-grade animals have a combination of ornamentation on different parts of the head skeleton, for example the roofing tesserae and branchial plates (eg. *Promesacanthus* Hanke (2008),

Uraniacanthus Hanke and Davis (2008)). Moreover, some of the states are logically inapplicable for the head tesserae of acanthodians (it is hard to conceive of concentric or vermiform ridges on a head tessera). For this reason the scoring of this character has here been restricted to macromeric plates, being inapplicable for taxa lacking them. In effect this means that most acanthodian-grade chondrichthyans are scored on the basis of their branchiostegal plates. I have removed character 65 of Giles et al. (2015c), which coded for ornamented/unornamented branchiostegals, as it is now covered by this character. The ornamentation of head tesserae is now covered by Character 43.

Although osteostracans and galeaspids have a headshield formed from tesserae I have scored them for this and the next character as the tesserae cover the whole head.

Austroptyctodus scored 3 on basis of tuberculated anterior lateral plate in Long (1997). *Uraniacanthus* has a tuberculate postorbital plate, but branchiostegals with vermiform ornament; as the "postorbital plate" is probably a large tessera it is scored 1.

0. *smooth*
1. *parallel, vermiform ridges*
2. *concentric ridges*
3. *tuberculate*

35. **[Modified from C17:17] Sensory line canal relationship with dermal head plates**

Because of the completely different set of possibilities for sensory lines of the head I have elected to code their morphology on the basis of the head

squamation. This character covers the relationship between macromeric dermal bones and sensory lines. It is inapplicable for taxa which have no large dermal plates, or in which sensory lines do not interact with large dermal plates.

Diplacanthus has been reported as having had a sensory line crossing the cheek plate - I can see no evidence of such a sensory line (see Chapter 4).

0. *passes over scales and/or is partially enclosed or surrounded by dermal bone*
1. *perforates and passes through dermal bone*

36. **[Modified from C17:17] Sensory line canal relationship with head scales/tesserae**

Because of the completely different set of possibilities for sensory lines of the head I have elected to code their morphology on the basis of the head squamation. This character covers the relationship between scales/tesserae and sensory lines. It is inapplicable for taxa which have a head skeleton entirely comprising large dermal plates.

Coates et al. (2018) code *Acanthodes* as having the sensory canal pass over scales in their equivalent character. *Acanthodes lopatini*, figured by Beznosov (2009), appears to have small c-shaped scales on the head (Figure 5A), and this also seems to be the case in specimens of *Acanthodes confusus* (eg. NMS 1950.38.9). Watson (1937) describes *Brachyacanthus* as having a "lateral series of bones with a deeply grooved lower surface" related to the sensory canal - in specimens I have examined (eg.NMS 1891.92.220) this looks like the morphology in other climatiids (eg. *Climatius, Vernicomacanthus*) where the line passes between scales and so I have scored it 0. In *Cheiracanthus* the

sensory lines are difficult to observe (Watson, 1937) and so I have scored it ? - however it is possible that more careful examination might reveal small c-shaped scales as in the otherwise very similar *Homalacanthus* (Gagnier, 1996). *Gladbachus* scored ? as no sensory lines are actually figured on the specimen (Coates et al., 2018). *Uraniacanthus* scored 1 on basis of suborbital scales.

Part of the infraorbital sensory line is carried past the orbit posteroventrally in *Promesacanthus*(fig 5C of Hanke (2008)) anteriorly to the triangular patch of cheek scales- this appears to pass between scales so I have scored it 0. *Cassidiceps* appears to have a similar morphology (Gagnier and Wilson, 1996b). In *Cheiracanthus* the sensory lines are difficult to observe (Watson, 1937) and so I have scored it 0 - however it is possible that closer examination might reveal small c-shaped scales as in the very similar fish *Homalacanthus* (Gagnier, 1996). I have not observed any specialised sensory line scales in *Tetanopsyrus* (Gagnier et al., 1999; Hanke et al., 2001a). Burrow *et al.* report rows of umbellate scales lining the cranial sensory canals of *Parexus*, and Coates et al. (2018) score it as state 1. It appears to me that the sensory line runs between scales - I have scored it state 0.

0. *passes between or beneath scales*
1. *carried in specialised scales*

37. **[Modified from GFB15: 61] Scales flanking sensory line on head**

This is contingent upon the previous character (state 0). It aims to capture the head scales of some acanthodian-grade taxa, which are apposed across the sensory line (eg. *Brochoadmones* (Hanke and Wilson, 2006)). A fourth state in the original character (semicylindrical c-shaped ring scales) is inapplicable to

taxa where the sensory line passes between scales.

0. *unspecialized*
1. *apposed growth*

38. **[GFB15: 31] Sensory canals/grooves**

This is contingent upon having sensory lines that pass through or over dermal bones. Buchanosteus has been changed from - > 0.

0. *contained within the thickness of dermal bones*
1. *contained in prominent ridges on visceral surface of bone*

39. **[GFB15: 32] Jugal portion of infraorbital canal joins supramaxillary canal**

0. *present*
1. *absent*

40. **[GFB15: 33] Dermal skull roof**

0. *includes large dermal plates*
1. *includes undifferentiated plates or tesserae*

41. **[GFB15: 34] Anterior pit line of dermal skull roof**

0. *absent*
1. *present*

42. **Modified from [GFB15: 27] Tessera morphology**

Coates et al. (2018) make the point that the cranial roof tesserae of *Gladbachus* do not interlock and so score it 1 for this character. It is true that in *Gladbachus* the head tesserae do not appear to form regular interlocking hexagons like some climatiids (eg. *Vernicomacanthus* Chapter 6), and have unusually bulging bases. However they are still larger than and clearly differentiated from the body integument (Coates et al., 2018), and interlock to the same extent as any other continuous shagreen of the head (eg. *Cassidiceps*, *Promesacanthus* (Gagnier and Wilson, 1996c; Hanke, 2008)). Some stem-chondrichthyans also have tesserae which are no larger than the body squamation. To distinguish between the tesserae of many stem-chondrichthyans and scaled heads of crown-chondrichthyans I have removed the words "interlocking" and "large" from state 0 of this character. In future, if more animals with non-polygonal head tesserae are described, it might be worth introducing further tessera-based characters based on relative size and nature of interlocking.

Gladbachus has been scored 1 on basis of explanation above. *Milesacanthus* is scored 1 on basis of Young and Burrow (2004). *Euthacanthus* scored 1 on basis of Newman et al. (2014). *Ischnacanthus* has been scored 0 on basis of ischnacanthids figured from MOTH (Blais et al., 2011). *Nerepisacanthus* scored 0 as has tesserae on head. *Culmacanthus* has been scored ?

0. *polygonal plates*
1. *indistinguishable from body scales*

43. *** Tessera ornament**

In the majority of acanthodian-grade stem-chondrichthyans, the tesserae that roof the head have an ornament of stellate tuberculae (eg. *Climatius* (Miles, 1973a), *Vernicomacanthus* (see Chapter 6)). In the acanthodiform fishes

Promesacanthus (Hanke, 2008) and *Cassidiceps* (Gagnier and Wilson, 1996b) these tesserae instead have a distinct vermiform ornament, which may be a character grouping "mesacanthid" acanthodiforms. Although the ornament is poorly preserved in all *Mesacanthus* specimens I have seen, the tesserae seem to lack a stellate ornament and may be like those in *Promesacanthus* and *Cassidiceps*. Nonetheless I have conservatively coded it ?.

0. *tuberculate*

1. *vermiform*

44. **[GFB15: 36] Cranial spines**

0. *absent*

1. *present, multicuspid*

2. *present, monocuspid*

45. **[GFB15: 37] Extent of dermatocranial cover**

0. *complete*

1. *incomplete (limited to skull roof)*

46. **[C18:28] Large unpaired median skull roofing bone anterior to the level of nasal capsules**

0. *present*

1. *absent*

47. **[C18: 29] Anterior or mesial edge of nasal notched for anterior nostril**

Cheirolepis scored present following Coates et al. (2018).

0. *absent*

1. *present*

48. **[GFB15: 38] Openings for endolymphatic ducts in dermal skull roof**

0. *present*

1. *absent*

49. **[GFB15: 39] Endolymphatic ducts with oblique course through dermal skull bones**

0. *absent*

1. *present*

50. **[GFB15: 40] Endolymphatic duct relationship to median skull roof bone (i.e. nuchal plate)**

0. *within median bone*

1. *on bones flanking median bone (eg. paranuchals)*

51. **[GFB15: 41] Pineal opening perforation in dermal skull roof**

0. *present*

1. *absent*

52. **[GFB15: 42] Dermal plate associated with pineal eminence or foramen**

0. *contributes to orbital margin*

1. *plate bordered laterally by skull roofing bones*

53. **[GFB15: 43] Series of paired median skull roofing bones that meet at the dorsal midline of the skull (rectilinear skull roof pattern)**

0. *absent*

1. *present*

54. **[GFB15: 44] Broad supraorbital vaults**

0. *absent*

1. *present*

55. **[GFB15: 45] Median commisure between suprorbital sensory lines**

0. *absent*

1. *present*

56. **[GFB15: 46] Dermal cranial joint at level of sphenoid-otic junction**

0. *absent*

1. *present*

57. **[GFB15: 47] Otic canal extends through postparietals**

0. *absent*

1. *present*

58. **[GFB15: 48] Number of bones of skull roof lateral to postparietals**

0. *two*

1. *one*

59. **[GFB15: 49] Suture between paired skull roofing bones (centrals of placoderms, postparietals of osteichthyans)**

0. *straight*

1. *sinusoidal*

60. **[C18: 32] Lateral plates**

0. *absent*

1. *present*

61. **[C18:33] Large median bone contributes to posterior margin of skull roof**

0. *absent*

1. *present*

62. **[C18:34] Contact of nuchal or centronuchal plate with paired preorbital plates**

0. *absent*

1. *present*

63. **[GFB15: 50] Medial processes of paranuchal wrapping posterolateral corners of nuchal plate**

0. *absent*

1. *present*

64. **[GFB15: 51] Paired pits on ventral surface of nuchal plate**

0. *absent*

1. *present*

65. **[C18:30] Supraorbital**

0. *absent*

1. *present*

66. *** Enlarged antero-dorsal circumorbital tessera**

The diplacanthid acanthodians *Diplacanthus* and *Rhadinacanthus* have a pair of large, curved circum-orbital tesserae that line the antero-dorsal margin of the orbit (Watson, 1937; Burrow et al., 2016a). A similar curved plate is present on the anterior part of the orbit in *Tetanopsyrus* (Hanke et al., 2001a), and may be a diplacanthid synapomorphy. The putative diplacanthid *Uraniacanthus* also has a large spinose tessera in this position in the circum-orbital series (Hanke and Davis, 2008). The likely diplacanthid *Milesacanthus* is scored ? for this character, as the antero-dorsal part of its orbit is crushed and it is difficult to verify the presence or absence of this bone (Young and Burrow, 2004).

Another possible diplacanthid, *Culmacanthus*, has a series of bones surrounding the orbit, originally described as circumorbitals (specimen NMV P159838 (Figure 3, 4 Long (1983))). Since this original description Burrow and Young (2012) reinterpreted this specimen as being described upside down, on the basis that the "pectoral" fin spine of Long (1983) has the deep, striated insertion characteristic of diplacanthid dorsal fin spines (Burrow et al., 2016a). The "circumorbitals" that Long describes surrounding the orbit in this specimen have a marked curvature, and a position and ornament like

that of the sclerotic ring in other stem-chondrichthyans (Burrow et al., 2011) - I believe this to be a more plausible identification. On this basis the tuberculated plate identified by Long as part of the circumorbital ring, but lying outside the orbit, is probably instead an enlarged antero-dorsal circumorbital tessera as in other diplacanthids (particularly similar to that in *Uraniacanthus* Hanke and Davis (2008)). *Culmacanthus* has been scored for this and the next character following this interpretation.

0. *absent*

1. *present*

67. **[GFB15: 52] Sclerotic ring**

Culmacanthus scored 1 following above interpretation of the "circumorbital ring". Following Coates et al. (2018) *Brochoadmones* and *Cladoselache* have been scored 1. The anterior "circumorbital bones" of *Cassidiceps* Gagnier and Wilson (1996b)are likely to instead be a sclerotic ring: it has been scored 1. *Diplacanthus* is scored present by Coates et al. (2018) there is no description of a sclerotic ring (Burrow et al., 2016a; Watson, 1937), nor have I observed one: it is scored 0.

0. *absent*

1. *present*

68. **[C18: 23] Number of sclerotic plates**

This is inapplicable for all taxa without a sclerotic ring.

0. *four or less*

1. *more than four*

69. **[GFB15: 53] Consolidated cheek plates**

Rhadinacanthus and *Culmacanthus* arguably have cheek plates Burrow et al. (2016a); Long (1983)- they are scored 1. As discussed elsewhere in the list, I do not consider the large plates of *Diplacanthus* and *Uraniacanthus* to lie over the cheek.

0. *absent*

1. *present*

70. **[GFB15: 54] Cheek plate**

0. *undivided*

1. *squamosal (i.e. squamosal and preopercular)*

71. **[GFB15: 55] Subsquamosals in taxa with divided cheek**

0. *absent*

1. *present*

72. **[C18:43] Preopercular bone**

0. *absent*

1. *present*

73. **[GFB15: 56] Preopercular shape**

Following Giles et al. (2015c) this applies only to taxa with subdivided cheek plates (formed from an preopercular and a squamosal).

0. *rhombic*

1. *bar-shaped*

74. **[GFB15: 57] Vertical canal associated with preopercular/suborbital canal**

0. *absent*

1. *present*

75. **[GFB15: 58] Enlarged postorbital tessera separate from orbital series**

A large postorbital tessera is well-documented in some climatiid-grade stem-chondrichthyans (eg. *Parexus*, *Climatius*, *Brachyacanthus*, and now *Vernicomacanthus* (Watson, 1937; Miles, 1973a; Burrow et al., 2013)). A very similar tessera (the "postorbital bone")is present in the diplacanthiform acanthodian *Uraniacanthus* (Newman et al., 2012; Hanke and Davis, 2008; Bernacsek and Dineley, 1977). Although originally described as being homologous with the "climatiid" postorbital tessera (Bernacsek and Dineley, 1977) this has since been rejected on the basis of either the participation of the bone in the orbital series (Hanke and Davis, 2008) or its proposed homology instead with the cheek plate of other diplacanthiforms (Burrow et al., 2016a). However, it is not clear that the bone definitely is in the circumorbital series, as figures of MOTH material appear to show smaller bones between it and the orbit: furthermore, it is not entirely clear that it does not flank the orbit directly in *Vernicomacanthus* (NMS 2004.7.1). As seen in Chapter 4 of this thesis, the cheek plate of *Diplacanthus* instead overlays the branchial chamber, and so was presumably opercular and in an entirely different position to the postorbital bone in *Uraniacanthus*.

Correspondingly *Uraniacanthus* has been scored 1 for this character. *Diplacanthus* has a large postorbital bone in addition to its operculum (Burrow et al., 2016a) and so is scored 1. *Culmacanthus* has a large plate postorbitally that could correspond either to a cheek plate or to a postorbital plate (or both) (Long, 1983): it is scored ?. In the putative diplacanthiforms *Rhadinacanthus* and *Tetanopsyrus* postorbital tesserae are absent (Burrow et al., 2016a; Hanke et al., 2001a).

0. *absent*

1. *present*

76. **[GFB15: 59] Extent of maxilla along cheek**

0. *to posterior margin of cheek*

1. *cheek bones exclude maxilla from posterior margin of cheek*

77. **[GFB15: 60] Dermal neck joint**

0. *overlap*

1. *ginglymoid*

78. **[GFB15: 62] Bony hyoidean gill-cover series (branchiostegals)**

0. *absent*

1. *present*

79. **[GFB15: 63] Branchiostegal plate series along ventral margin of lower jaw**

0. *absent*

1. *present*

80. **[GFB15: 64] Branchiostegal ossifications**

Euthacanthus has been changed from 1 to 0 on the basis of Newman et al. (2011). *Halimacanthodes* is scored ? as not clearly visible (Burrow et al., 2012).

0. *plate-like*

1. *narrow and ribbon-like*

1. *filamentous*

81. **[GFB15: 66] Proximal margins of branchiostegal ossifications imbricated**

Due to confusion between different phylogenetic studies as to the meaning of this character (see Davis et al. (2012); Giles et al. (2015c)), I have changed the wording. The definition remains the original definition of Brazeau (2009): that is the proximal margins of the branchiostegals are curved and overlap, rather than that of Davis et al. (2012), that the whole plates overlap.

Halimacanthodes is scored ? as they are not clearly visible.

0. *absent*

1. *present*

82. **[GFB15: 67] Median gular**

0. *absent*

1. *present*

83. **[GFB15: 68] Lateral gular**

0. *absent*

1. *present*

84. **[C18:: 55] Submarginal (dermohyal) ossification**

Brazeau (2009) and most subsequent datasets versions of this character equated the submarginal of placoderms to the opercular of osteichthyans (eg.)Brazeau (2009); Giles et al. (2015c)). Coates et al. (2018) modified it and instead argued that the submarginal is more likely to be homologous to the dermohyal of osteichthyans, as it is fused to an underlying, possibly hyomandibula, cartilage (Gardiner, 1984), and that the opercular plate is an osteichthyan novelty. Here I have used the reformulation of Coates et al. (2018) as it seems to rely on less assumptions.

The opercular plate of some diplacanthids is unlikely to be homologous with the submarginal: it overlies the branchial skeleton and shows no evidence of having been fused to an underlying visceral cartilage (See Chapter 4). It is likely an apomorphic branchial cover, as several diplacanthids, and the majority of other "acanthodians" instead have branchiostegal rays (Hanke and Davis, 2008). *Diplacanthus* and *Rhadinacanthus* are scored 0 (Burrow et al., 2016a).

0. *absent*

1. *present*

85. **[C18:: 56] Shape of submarginal (dermohyal) ossification**

0. *broad plate that tapers towards its proximal end*

1. *narrow, rod-shaped*

86. **[GFB15: 71] Size of lateral gular plates**

0. *extending most of the length of the jaw*

1. *restricted to the anterior third of the jaw*

87. **[Modified from C18: 63] * Gill openings in dermal integument**

Living elasmobranchs exhibit multiple separate gill slits on either side of the pharynx. In osteichthyans (and holocephalans) there is instead a single pair of gill openings, covered by an operculum. This is also the case in "placoderm" grade stem-gnathostomes.

The previous formulation of this character considered it in terms of a partial/complete dermal covering vs separate uncovered slits. However, a dermal operculum is already accounted for with character 78, which records the presence or absence of bony hyoidean gill covers. Many "acanthodian" grade chondrichthyans (for example *Ptomacanthus*) have both a bony hyoidean gill cover, and multiple gill slits in the dermal integument (Brazeau, 2012), while living holocephalans have no dermal bony covering, but a single fleshy operculum (Didier, 1995). For this reason I have explicitly linked this character to the number of openings to avoid redundancy. I have coded it conservatively - in some stem-chondrichthyans, such as *Acanthodes*, not enough of the dermal skeleton is preserved to be able to tell if multiple openings were present.

0. *single pair*

1. *multiple pairs*

88. *** Branchial openings fringed with rod-like scales**

A common feature of acanthodian-grade stem-chondrichthyan head skeletons is a series of short rod-like scales fringing each gill slit, patterned into a series parallel to the slit and another perpendicular to it. These are seen in a wide range of taxa including *Climatius*(Miles, 1973a), *Mesacanthus* (Watson, 1937), *Euthacanthus* Watson (1937), and ischnacanthids (pers. obvs - see figs in Blais et al. (2011).). These scales are absent in diplacanthids (Watson, 1937; Burrow et al., 2016a), crown-chondrichthyans (Coates and Sequeira, 2001a), and stem-chondrichthyans such as *Gladbachus* (Coates et al., 2018), *Ptomacanthus* (Brazeau, 2012), and *Brochoadmones* (Hanke and Wilson, 2006).

Plates considered to be homologous to branchiostegals, however rod-like (eg. *Acanthodes*), are not considered for this character.

0. *absent*
1. *present*

B.4.4 Hyoid and branchial arches

89. **[Modified from C18: 66] Gill skeleton extends posterior to occipital region**

The branchial arches of osteichthyans and stem-gnathostomes are located beneath the neurocranium, whereas those of chondrichthyans have a pronounced posterior extension beyond the occiput (a notable, and certainly derived, exception being holocephalans) (Janvier, 1996). Phylogenetic analyses typically capture this with a single character (eg. Coates et al. (2018, 2017a); Giles et al. (2015c). However, as discussed in Chapter 3 I consider that there is a subtlety to this character that isn't covered by a single character. While the stem-chondrichthyan *Acanthodes* has a posteriorly elongate branchial skeleton

like that of chondrichthyans, the gill arches extend anteriorly to the same extent as osteichthyans (Miles, 1973b). To capture this I have split it into two: this and the next character.

Brochoadmones is scored 1 on the basis of the relative positions of the gill openings and the otic infill (Hanke and Wilson, 2006).

0. *absent*
1. *present*

90. **[Modified from C18: 66] Anteriormost branchial arch meets neurocranium**

See previous character for explanation. For scoring purposes I have considered facets for branchial arches on the ventral surface of the neurocranium to be sufficient evidence for state 0.

0. *ventral to otic region*
1. *posterior to otic region*

91. ***Anterior unpaired element contacts**

A basihyal is a median unpaired component of the hyoid arch - in living gnathostomes it is only present in chondrichthyans, where it articulates with the hyoid arch, and sometimes the hyoid arch and first branchial arch (Garman (1913); Pradel et al. (2014)). This is a morphologically distinct from the basibranchial/s of osteichthyans, an unpaired element or group of elements onto which the hyoid arch (via hypohyals) and branchial arches articulate (eg. *Glyptolepis* (Jarvik, 1972), or *Raynerius* (Giles et al., 2015b)). Amongst extinct gnathostomes a basihyal is usually considered present in chondrichthyans -

both crown-group (eg. *Egertonodus* (Maisey, 1983), and *Debeerius* (Grogan and Lund, 2000)) and stem-group (eg. *Gladbachus* (Coates et al., 2018)) - as well as in various stem-gnathostomes (for example, *Paraplesiobatis* (Brazeau et al., 2017)).

The actual diagnosis for what constitutes a basihyal as opposed to a basibranchial in a fossil is slightly opaque - compare codings for (Giles et al., 2015c) character 73 with (Coates et al., 2018) character 71. In their discussion of basihyals Coates et al. (2018) - (supplementary material) state that the "position, connectedness, and separation from other basibranchials" are what distinguish a basihyal from a basibranchial/copula. This diagnosis is a compound combination of traits. Notwithstanding this the relative position of basihyals and basibranchials actually often differs little - the basibranchial of *Raynerius* for example (Giles et al., 2015b), is in much the same position relative to the hyoid arch as that of *Paraplesiobatis* (Brazeau et al., 2017) or *Ptomacanthus* (Chapter 3).

Here I attempt to break the remainder of this diagnosis down into characters - this character and the following. One aspect of the connectedness of a "basihyal" is the absence of hypohyals - these are captured in another character. We also note that there are two additional characters one could try, but which are uninformative with the current dataset. The first could attempt to capture the spacing aspect of the basihyal definition *sensu* Coates et al. (2018) a basihyal is usually well separated from the posterior basibranchial copulae in chondrichthyans - this is not observed in osteichthyans with posterior basibranchials (eg. *Amia* (Allis, 1897)), *Eusthenopteron*(Jarvik, 1980)).). The second could attempt to code for the articulation of only the hyoid arch onto

the basihyal, a state which at least present in some holocephalans (pers. obvs).

This character distinguishes an attribute of connectedness that separates a basihyal *sensu* Coates et al. (2018)from basibranchials/copulae - the number of branchial arches articulating with it in addition to the hyoid arch. In taxa with a "basihyal" this is either one or none, whereas in osteichthyans it is typically two or more. It replaces characters coding for the presence/absence of a basihyal in previous matrices (eg.Giles et al. (2015c), Character 73.

Egertonodus is coded 0 as the element is impossibly far anterior to articulate with more than one element in Maisey (1983) (fig. 2B)

0. *two or fewer visceral arches*
1. *three or more visceral arches*

92. ***Posterior basibranchial elements mineralised**

Often gnathostomes have a chain of unpaired elements running along the base of the branchial basket - whether these be the copulae of chondrichthyans or the basibranchials of osteichthyans. *Ptomacanthus* lacks any kind of mineralised unpaired structure posterior to its basihyal. It shares this in common with placoderms such as *Paraplesiobatis* (Brazeau et al., 2017) and *Cowralepis* (Carr et al., 2009). Contrastingly, in most chondrichthyans a basibranchial copula is present, eg. *Ozarcus* (Pradel et al., 2014) and *Gladbachus* (Coates et al., 2018). Osteichthyans vary between having a chain of elements (eg. *Amia* (Allis, 1897)) or a single element or complex of elements onto which all arches articulate (eg. *Mimipiscis* (Gardiner, 1984)) or *Eusthenopteron* (Jarvik, 1980)). *Ozarcus* has been scored 1 despite the apparent absence of a basihyal as its elongate posterior ossification seems likely to equate to the basibranchial

copulae of other chondrichthyans. *Acanthodes* is coded from Gardiner (1984), which I think is the most plausible interpretation of the ventral branchial skeleton on the basis of my own observations of moulds kept in the NHM.

0. *absent*

1. *present*

93. **[C18: 67] Perforate hyomandibula**

0. *absent*

1. *present*

94. **[C18: 69] Ceratohyal smooth with posterior, lateral fossa**

0. *absent*

1. *present*

95. **[GFB15: 74] Interhyal**

This appears to be present in *Acanthodes* (NHM P.49990) (Miles, 1973b), and in *Ischnacanthus* (NHM P.6996).

0. *absent*

1. *present*

96. **[GFB15: 75] Hypohyal**

0. *absent*

1. *present*

97. **[C17: 36] Hypohyals directed**

0. *anteriorly*

1. *posteriorly*

98. **[GFB15: 76] Endoskeletal urohyal**

0. *absent*

1. *present*

99. **[C17: 34] Separate supra- and infra- pharyngobranchials**

0. *absent*

1. *present*

100. **[C17: 35] Pharyngobranchials directed**

Acanthodes is coded following Miles (1973b), which seems to me to be the most plausible interpretation on the basis of the moulds I have observed (NHM P.34914).

0. *anteriorly*

1. *posteriorly*

101. *** Posteriormost ventral paired arches**

In the "placoderm" stem-gnathostome *Paraplesiobatis*, the posterior two branchial arches articulate ventrally (Brazeau et al., 2017). A similar state is also observed in various sarcopterygians, such as *Glyptolepis* (Jarvik, 1972) and *Gryphognathus* (Miles, 1977). Contrastingly, no such state is found in chondrichthyans, such as *Ozarcus* (Pradel et al., 2014), *Gladbachus* (Coates et al.,

2018), and *Ptomacanthus* (Chapter 3). It is possible that having fully separated ventral paired branchial arches is autapomorphic for chondrichthyans.

0. *separate*
1. *articulate*

102. *** Posteriormost dorsal paired arches**

In living chondrichthyans the posteriormost (fifth) epibranchial forms a fused complex with the fourth pharyngobranchial (Carvalho et al., 2013). *Ptomacanthus* has a separate fifth epibranchial: however, rather than having its own expanded end (presumed pharyngobranchial) it articulates with the posterior of the fourth pharyngobranchial. A similar state is observed in the stem-holocephalan *Ozarcus* (Pradel et al., 2014). Thus this possibly constitutes an autapomorphy, at some level, of chondrichthyans.

In *Gladbachus* and *Debeerius* the posterior epibranchials appear to share a pharyngobranchial - I have scored these taxa present for this character (Coates et al., 2018; Grogan and Lund, 2000).

0. *separate*
1. *articulate on same pharyngobranchial*

103. **[C18:74] Posteriormost branchial arch bears epibranchial unit**

0. *absent*
1. *present*

104. **[C18: 75] Epibranchials bear posterior flange**

0. *absent*

1. *present*

B.4.5 Mandibular arch

105. **[GFB15: 77] Oral dermal tubercles borne on jaw cartilages or on margins of mouth**

Although tubercles are reported on a set of jaws attributed to *Tetanopsyrus*, there is no clear link between these and a *Tetanopsyrus* body fossil - the *Tetanopsyrus* body fossil they were found near has a full articulated mandibular arch (Hanke et al., 2001a). *Tetanopsyrus* is the only taxon known from the MOTH locality with high, stout Meckelian cartilages, and so they may well belong to a member of the genus, but I have conservatively scored it ?.

0. *absent*

1. *present*

106. **[GFB15: 78] Oral dermal tubercles patterned into distinct rows (teeth)**

0. *absent*

1. *present*

107. **[GFB15: 79] Enamel(oid) on teeth**

0. *absent*

1. *present*

108. **[GFB15: 80] Cap of enameloid restricted to upper part of teeth (acrodin)**

0. *absent*

1. *present*

109. **[GFB15: 81] Tooth whorls**

I have coded Chondrenchelys absent, following Coates et al. (2018).

0. *absent*

1. *present*

110. **[GFB15: 82] Bases of tooth whorls**

0. *single continuous plate*

1. *some or all whorls consisting of separate tooth units*

111. **[GFB15: 83] Distribution of tooth whorls**

0. *Entire length of tooth row*

1. *restricted to symphyseal region*

112. **[GFB15: 84] Distribution of tooth whorls**

Climatius changed from 0>1 on basis of Burrow et al. (2015)

0. *Upper and lower jaws*

1. *lower jaws only*

2. *upper jaws only*

113. **[C17: 38] Pharyngeal teeth or denticles**

In a specimen of *Parexus* (NMS 1891.92.207) the lorical plate is preserved in dorsal view, with small denticles unlike those forming the integument covering its dorsal surface. Since these presumably originated in the overlying pharynx I have scored *Parexus* 1.

0. *absent*

1. *present*

114. **[C17: 41] Lingual torus**

0. *absent*

1. *present*

115. **[C17: 42] Basolabial shelf**

0. *absent*

1. *present*

116. **[C18: 84] Number of tooth families/whorls per jaw ramus**

0. *15 or fewer*

1. *20 or more*

117. **[GFB15: 85] Teeth ankylosed to dermal bone**

0. *absent*

1. *present*

118. **[GFB15: 86] Plicidentine**

0. *absent*

1. *present*

119. **[GFB15: 87] Dermal jaw plates on biting surfaces of jaw cartilages**

0. *absent*

1. *present*

120. *** Dermal jaw plates**

Modified from Hanke and Wilson character 13 and 14 Hanke and Wilson (2004). Dermal jaw plates in stem-group gnathostomes, osteichthyans, ischacanthid "acanthodians", and *Tetanopsyrus* line both upper and lower margins of the gape. Uniquely, in the diplacanthid "acanthodians" *Diplacanthus*, *Rhadinacanthus*, *Uraniacanthus*, and *Culmacanthus* a dermal plate is only present on the ventral margin of the jaw.

0. *upper and lower jaws*

1. *lower jaw only*

121. **[B16: 261] Dental plates with smooth occlusal surface**

The dermal jaw plates of diplacanthid stem-chondrichthyans are smoothly convex bones with a completely unornamented surface. This character is inapplicable for taxa without dermal jaw plates.

0. *absent*

1. *present*

122. **[Modified from GFB15: 105] Pronounced dorsal process on lower dermal jaw plate**

This character was originally erected to capture a similar dorsal process between the "Meckelian elements" of *Tetanopsyrus* and *Uraniacanthus* (Brazeau, 2009; Hanke and Wilson, 2004). However, while the "Meckelian element" of *Uraniacanthus* is an occlusal plate like that seen in other diplacanthids (Newman et al., 2012) the "Meckelian element" of *Tetanopsyrus* is instead the back of Meckel's cartilage (Giles et al., 2015c), confirmed by comparison with *Diplacanthus* (Chapter 4). Dorsal processes of the two types of element are non-comparable: while this has been recognised by some authors (Giles et al., 2015c) confusion continues with others continuing to score this character on the basis of Meckel's cartilage (Burrow et al., 2016a). This character has been redefined to explicitly refer to a lower dermal jaw plate rather than a "Meckelian bone or cartilage". It is inapplicable for taxa without a dermal jaw plate of the lower jaw.

Dorsal processes of the dermal jaw plate are only present in *Uraniacanthus* (Hanke and Davis, 2008) and *Culmacanthus* (Burrow and Young, 2012). *Tetanopsyrus* is coded 0 as its "dorsal process" is of the Meckelian element - the lower dental plate has no process (Hanke et al., 2001a). *Diplacanthus* has in the past been scored present for this character (Davis et al., 2012): this is likely due to observation of the articular part of the Meckelian cartilage in NMS 1891.92.334: its occlusal plate lacks a dorsal process (see Chapter 4) and so it is scored 0. The problematic putative stem-gnathostome *Ramirosuarezia* has been scored present for this character (eg by Coates et al. (2018)) on the basis of a dorsal process on what is interpreted as its Meckel's cartilage (Pradel et al., 2009b). However this is non-homologous with the dermal plate of diplacanthids, evidenced by the fact that it bears tooth plates. *Ramirosuarezia*

is here scored 0 for this character.

0. *absent*

1. *present*

123. **[Modified from C17: 44] Adjacent tooth families fused**

As Coates *et al.* note Coates et al. (2018), tooth plates in holocephalans are understood to have formed from the fusion of adjacent tooth families. The formulation of this character has been changed to clearly reflect this. This is only scored applicable for animals with tooth whorls extending along the jaw ramus.

0. *absent*

1. *present*

124. **[GFB15: 88] Maxillary and dentary marginal bones of mouth**

0. *absent*

1. *present*

125. **[GFB15: 89] Premaxilla**

0. *extends under orbit*

1. *restricted anterior to orbit*

126. **[GFB15: 90] Maxilla shape**

0. *splint-shaped*

1. *cleaver-shaped*

127. **[GFB15: 91] Pair of tooth plates (anterior supragnathals or vomers) on ethmoidal plate**

This is only scored applicable for taxa with macromeric head skeletons. *Ligulalepis* is scored 1 on the basis of the area of attachment for the vomer figured by Clement et al. (2018).

0. *absent*

1. *present*

128. **[GFB15: 92] Strong posterior flexion of dentary symphysis**

This is scored as applicable in taxa with dentaries.

0. *absent*

1. *present*

129. **[GFB15: 93] Extent of infradentaries**

0. *along much of ventral margin of dentary*

1. *restricted to posterior half of dentary*

130. **[GFB15: 94] Coronoid fangs**

0. *absent*

1. *present*

131. **[GFB15: 95] Position of upper mandibular arch cartilage (and associated cheek plate where present)**

0. *entirely suborbital*

1. *with a postorbital extension*

132. **[GFB15: 96] Position of mandibular arch articulations**

I have scored *Kathemacanthus* ? on the basis of its difficult to interpret endoskeleton (Hanke and Wilson, 2010).

0. *terminal*

1. *subterminal*

133. **[GFB15: 97] Autopalatine and quadrate**

0. *comineralised*

1. *separate mineralisations*

134. **[GFB15: 98] Large otic process of the palatoquadrate**

The palatoquadrate of *Tetanopsyrus* is interpreted by Brazeau (2009) as being low and placoderm-like. I consider it more likely that what is preserved is the quadrate. However I have conservatively scored it ? for this and the previous character.

0. *absent*

1. *present*

135. **[GFB15: 99] Insertion area for jaw adductor muscles on palatoquadrate**

0. *ventral or medial*

1. *lateral*

136. **[GFB15: 100] Palatoquadrate relationship to dermal cheek bones**

0. *broad articulation*

1. *articulation narrow and restricted*

137. **[GFB15: 101] Palatoquadrate fused with neurocranium**

0. *absent*

1. *present*

138. **[GFB15: 102] Oblique ridge or groove along medial face of palatoquadrate**

Climatius scored 0>1 for this on basis of Burrow et al. (2015)

0. *absent*

1. *present*

139. **[GFB15: 103] Fenestration of palatoquadrate at basipterygoid articulation**

0. *absent*

1. *present*

140. **[GFB15: 104] Perforate or fenestrate anterodorsal (metapterygoid) portion of palatoquadrate**

Tetanopsyrus scored ?.

0. *absent*

1. *present*

141. **[C18: 102] Commissural lamina of palatoquadrate**

0. *absent*

1. *present*

142. **[GFB15: 106] Number of coronoids**

0. *four or more*

1. *three or fewer*

143. **[GFB15: 107] Preglenoid process**

Cladodoides ?>1 from Gross

0. *absent*

1. *present*

144. ***Preglenoid process shape**

The preglenoid process in most chondrichthyans is rounded (the mandibular knob). In *Acanthodes* it instead forms a flange (Coates et al., 2018). This flange-like shape is also present in *Diplacanthus* (See Chapter 4).

0. *knob-like*

1. *oblique flange*

145. **[GFB15: 108] Jaw articulation located on rearmost extremity of mandible**

0. *absent*

1. *present*

146. **[C17:57] Dental trough or sulcus adjacent to oral rim of Meckel's cartilage and palatoquadrate**

0. *absent*

1. *present*

147. **[C17:58] Scalloped oral margin on Meckel's cartilage or palatoquadrate**

0. *absent*

1. *present*

148. **[C17:59] Mandibular symphysis fused**

0. *absent*

1. *present*

B.4.6 Neurocranium

149. **[GFB15: 109] Precerebral fontanelle**

0. *absent*

1. *present*

150. **[GFB15: 110] Median dermal bone of palate (parasphenoid)**

Coded this ? for *Romundina* due to Dupret et al. (2017).

0. *absent*

1. *present*

151. **[GFB15: 111] Paraspenoid shape**

0. *lozenge shaped*

1. *splint shaped*

152. **[GFB15: 112] Multifid anterior margin of parasphenoid denticle plate**

0. *absent*

1. *present*

153. **[GFB15: 113] Enlarged ascending process of parasphenoid**

0. *absent*

1. *present*

154. **[GFB15: 114] Buccohypophyseal canal in parasphenoid**

0. *single*

1. *paired*

155. **[GFB15: 115] Nasal opening(s)**

0. *dorsal, placed between orbits*

1. *ventral and anterior to orbits*

156. **[GFB15: 116] Posterior nostril**

0. *separated from orbital fenestra*

1. *confluent with orbital fenestra*

157. **[C17: 67] Canal or channel for the olfactory tracts and telencephalon elongate**

0. *absent*

1. *present*

158. **[K16: 22] Extended preorbital region between eyes and nasal capsule**

Following King et al. (2016) this replaces Giles et al. (2015c) character 118.

0. *present*

1. *absent*

159. **[GFB15: 119] Pronounced sub-ethoidal keel**

0. *absent*

1. *present*

160. **[C17:65] Internasal groove**

0. *absent*

1. *present*

161. **[C17:66] Orbitonasal lamina dorsoventrally deep**

0. *absent*

1. *present*

162. **[GFB15: 120] Internasal vacuities**

0. *absent*

1. *present*

163. **[GFB15: 121] Discrete division of the ethmoid and more posterior braincase at the level of the optic tract canal**

0. *absent*

1. *present*

164. **[GFB15: 122] Position of myodome for superior oblique eye muscles**

0. *posterior and dorsal to foramen for nerve II*

1. *anterior and dorsal to foramen*

165. **[C17:73] Ophthalmic foramen in anterodorsal extremity of orbit communicates with cranial interior**

0. *absent*

1. *present*

166. **[GFB15: 123] Endoskeletal intracranial joint**

0. *absent*

1. *present*

167. **[GFB15: 124] Spiracular groove on basicranial surface**

0. *absent*

1. *present*

168. **[GFB15: 125] Transverse otic process**

In the majority of recent analyses this character has been used to test a putative homology between the transverse otic process of osteichthyans and

the anterior postorbital process of placoderms, and the lateral otic processes of some chondrichthyans (eg.(Giles et al., 2015c; Lu et al., 2016; Brazeau and de Winter, 2015; King et al., 2016)). The recent analysis of Coates et al. (2018) instead reinstituted a separate character for the lateral otic process of chondrichthyans, arguing that the two processes were anatomically dissimilar enough to merit it. They also rejected the presence of the described lateral otic process in *Akmonistion* (Coates and Sequeira, 1998) and *Acanthodes* (Brazeau and de Winter, 2015). Here I have elected to instead test the homology between the processes and taxa with lateral otic processes are scored present for this character (including *Acanthodes* and *Akmonistion*).

Gladbachus has been scored ?.

0. *present*
1. *absent*

169. **[GFB15: 126] Jugular canal**

0. *long (invested in otic region along length of skeletal labyrinth)*
1. *short (restricted to region anterior of skeletal labyrinth)*
2. *absent (jugular vein univested in otic region)*

170. **[GFB15: 127] Spiracular groove on lateral commisure**

0. *absent*
1. *present*

171. **[GFB15: 128] Subpituitary fenestra**

0. *absent*

1. *present*

172. **[GFB15: 129] Supraorbital shelf broad with convex lateral margin**

0. *absent*

1. *present*

173. **[GFB15: 130] Orbit dorsal or facing dorsolaterally, surrounded laterally by endocranium**

Coates et al. (2018) modify this character to "Orbit directed mostly laterally and free of flanking endocranial cartilage or bone", but in their matrix it remains coded for the original character (ie. all codings are reversed). I have kept it as the original formulation: following Coates et al. (2018). *Jagorina* is coded as present.

0. *present*

1. *absent*

174. **[C17:80] Orbit larger than otic capsule**

0. *absent*

1. *present*

175. **[GFB15: 131] Eyestalk attachment area**

0. *absent*

1. *present*

176. **[GFB15: 132] Postorbital process**

0. *absent*

1. *present*

177. **[C17: 53] Palatoquadrate articulation with the postorbital process directed**

0. *anteriorly*

1. *laterally*

1. *dorsally*

178. **[C18: 144] Postorbital process and arcade**

Contra Coates et al. (2018) *Tamiobatis* is scored 2: while the postorbital process is more slender and curved than that in *Orthacanthus* it is still notably more robust than that in most other taxa (Schaeffer, 1981).

0. *short and deep - width not more than maximum braincase width (excluding arcade)*

1. *process and arcade wide - width exceeds maximum width of braincase, and anteroposteriorly narrow*

2. *process and arcade massive*

3. *arcade forms postorbital pillar*

179. **[C17: 84] Jugular canal in postorbital arcade**

0. *small*

1. *large*

1. *absent*

180. **[C18: 145] Postorbital process downturned, with anhedral angle relative to braincase**

0. *absent*

1. *present*

181. **[C18: 147] Canal, likely for trigeminal nerve (V) mandibular ramus, passes through the postorbital process from proximal dorsal entry to distal and ventral exit**

0. *absent*

1. *present*

182. **[C18: 148] Postorbital process expands anteroposteriorly**

0. *absent*

1. *present*

183. **[C18: 152] C-bout notch separates postorbital process from supraotic shelf**

0. *absent*

1. *present*

184. **[GFB15: 134] Series of perforations for innervation of supraorbital sensory canal in supraorbital shelf**

Changed *Eusthenopteron* from ?->0.

0. *absent*

1. *present*

185. **[GFB15: 135] Extended prehypophyseal portion of sphenoid**

0. *absent*

1. *present*

186. **[GFB15: 136] Narrow interorbital septum**

0. *absent*

1. *present*

187. **[GFB15: 137] The main trunk of facial nerve (N. VII)**

0. *elongate and passes anterolaterally through orbital floor*

1. *stout divides within otic capsule at the level of the transverse otic wall*

188. **[GFB15: 138] Course of hyoid ramus of facial nerve (N. VII) relative to jugular canal**

0. *traverses jugular canal, with separate exit in otic region*

1. *intersects jugular canal, with exit through posterior jugular foramen*

189. **[GFB15: 140] Relationship of cranial endocavity to basisphenoid**

0. *endocavity occupies full depth of sphenoid*

1. *endocavity dorsally restricted*

190. **[GFB15: 141] Subcranial ridges**

0. *absent*

1. *present*

191. **[GFB15: 142] Ascending basisphenoid pillar pierced by common internal carotid**

0. *absent*

1. *present*

192. **[C17: 74] Bucco-hypophyseal duct**

0. *open*

1. *closed*

193. **[GFB15: 144] Entrance of internal carotids**

Helodus has been scored ? Cladoseache has been changed from 1 > ? as the condition seems to vary on Maisey (2007) figs. 58+59.

0. *through separate openings flankin the hypophyseal opening or recess*

1. *through a common opening at the central midline of the basicranium*

194. **[GFB15: 145] Canal for efferent pseudobranchial artery within basicranial cartilage**

Doliodus has been scored ?

0. *absent*

1. *present*

195. **[C18: 124] Palatobasal (or orbital) articulation**

0. *posterior to the optic foramen*

1. *anterior to the optic foramen, and overlapped by process or flange of palatoquadrate*

2. *anterior to the optic foramen, and overlaps or flanks articular surface on*

palatoquadrate

196. **[GFB15: 147] Articulation between neurocranium and palatoquadrate posterodosal to orbit (suprapterygoid artic.)**

0. *absent*

1. *present*

197. **[GFB15: 148] Labyrinth cavity**

0. *Separated from the main neurocranial cavity by a cartilaginous or ossified capsular wall*

1. *skeletal capsular wall absent*

198. **[GFB15: 149] Basipterygoid process (basal articulation) with vertically oriented component**

0. *absent*

1. *present*

199. **[GFB15: 150] Pituitary vein canal**

0. *dorsal to level of basipterygoid process*

1. *flanked posteriorly by basipterygoid process*

200. **[C17: 89] Periotic process**

0. *absent*

1. *present*

201. **[C17: 91] Sub-otic occipital fossa**

0. *absent*

1. *present*

202. **[C17: 94] Otic capsules**

0. *widely separated*

1. *approaching dorsal midline*

203. **[C17: 95] Endocranial cavity (infill) anterior to otic capsules smoothly convex dorsally and anteriorly**

0. *absent*

1. *present*

204. **[C17: 96] Roof of skeletal cavity for cerebellum and mesencephalon significantly higher than dorsal-most level of semicircular canals**

Acanthodes is scored 0 following Coates et al. (2018) - this seems highly likely given the relationship of the labyrinth and the cranial roof.

0. *absent*

1. *present*

205. **[C17: 97] Roof of the endocranial space for telencephalon and olfactory tracts offset ventrally relative to level of mesencephalon**

Acanthodes scored ?.

0. *absent*

1. *present*

206. **[GFB15: 151] External (horizontal) semicircular canal**

0. *absent*

1. *present*

207. **[C17: 99] *Crus commune* connecting anterior and posterior semicircular canals**

0. *present*

1. *absent*

208. **[C17: 100] Sinus superior**

0. *absent or indistinguishable from union of anterior and posterior canals with saccular chamber*

1. *present, elongate, and nearly vertical*

209. **[C17: 101] Angle of external semicircular canal: in lateral view, straight line projected through canal intersects anterior ampulla, external ampullae, and base of foramen magnum**

0. *absent*

1. *present*

210. **[C17: 102] Left and right external semicircular canals approach or meet the posterodorsal midline of the hindbrain roof**

0. *absent*

1. *present*

211. **[GFB15: 153] External (horizontal) semicircular canal**

0. *joins the vestibular region dorsal to posterior ampulla*

1. *joins level with posterior ampulla*

212. **[GFB15: 154] Horizontal semicircular canal in dorsal view**

0. *medial to path of jugular vein*

1. *dorsal to jugular vein*

213. **[GFB15: 155] Lateral cranial canal**

0. *absent*

1. *present*

214. **[C18: 168] Otic capsules project anteriorly between postorbital processes**

0. *absent*

1. *present*

215. **[C18:173] Double octaval nerve foramena in chondrified mesial wall of otic capsule**

0. *absent*

1. *present*

216. **[C18:174] Semicircular canals describe wide arcs**

0. *absent*

1. *present*

217. **[C18:179] Preampullary portion of posterior semicircular canal**

0. *absent*

1. *present*

218. **[GFB15: 156] Trigemino-facial recess**

0. *absent*

1. *present*

219. **[GFB15: 157] Posterior dorsal fontanelle**

0. *absent*

1. *present*

220. **[C17: 103] Perilymphatic fenestra**

0. *absent*

1. *present*

221. **[C17: 105] Posterior dorsal fontanelle/external opening for endolymphatic ducts anterior to crus commune**

0. *absent*

1. *present*

222. **[C17: 106] Posterior dorsal fontanelle**

0. *connected to persistent otico-occipital fissure*

1. *posterior tectum separates fontanelle from fissure*

223. **[C17: 107] Subcircular endolymphatic foramen**

0. *absent*

1. *present*

224. **[C18:187] Supraotic shelf broad**

0. *absent*

1. *present*

225. **[GFB15: 160] Dorsal ridge**

Changed Cladoselache 1 > ? due to poor visibility in flattened specimens.

0. *absent*

1. *present*

226. **[C17: 108] Dorsal ridge forms a horizontal crest posteriorly, and flanks the anterior rim of the endolymphatic fossa**

0. *absent*

1. *present*

227. **[C17: 109] Dorsal ridge divided posteriorly by an anteroposteriorly elongate recess enclosing the exits of the endolymphatic ducts**

0. *absent*

1. *present*

228. **[C17: 110] Endolymphatic or parietal fossa**

0. *absent*

1. *present*

229. **[GFB15: 162] Endolymphatic ducts in neurocranium**

0. *posteriodorsally angled tubes*

1. *tubes oriented vertically through median endolymphatic fossa*

230. **[GFB15: 163] Position of hyomandibula articulation on neurocranium**

This and following characters coded for *Dwykaselachus* on basis that hyoid articulated on unpreserved region (Coates et al., 2018).

0. *below or anterior to orbit, on ventrolateral angle of braincase*

1. *on otic capsule, posterior to orbit*

231. **[GFB15: 164] Position of hyomandibula articularion relative to structure of skeletal labyrinth**

0. *anterior or lateral to skeletal labyrinth*

1. *at level of posterior semicircular canal*

232. **[GFB15: 165] Hyoid arch articulation on braincase**

0. *single*

1. *double*

233. **[BdeW15: 237] Relative position of jugular groove and hyomandibular articulation**

0. *hyomandibula dorsal or same level, (ie. on bridge)*

1. *jugular vein passing dorsal or lateral to hyomandibula*

234. **[C18: 162] Hyomandibula articulates with neurocranium beneath otic shelfs**

0. *absent*

1. *present*

235. **[GFB15: 166] Branchial ridges**

0. *present*

1. *reduced to vagal process*

2. *absent (articulation with cranial wall*

236. **[GFB15: 167] Craniospinal process**

0. *absent*

1. *present*

237. **[GFB15: 168] Ventral cranial fissure**

0. *absent*

1. *present*

238. **[GFB15: 169] Basicranial fenestra**

0. *absent*

1. *present*

239. **[GFB15: 170] Metotic (otico-occipital) fissure**

0. *absent*

1. *present*

240. **[C17: 115] Glossopharyngeal nerve path**

0. *directed laterally, across floor of the saccular chamber and exits via foramen in side wall of otic capsule*

1. *directed posteriorly, and exits through metotic fissure or foramen in posteroventral wall of otic capsule,*

2. *exits laterally through a canal contained ventrally (floored) by the hypotic lamina*

3. *exits through a foramen anterior to the posterior ampulla*

241. **[GFB15: 171] Vestibular fontanelle**

0. *absent*

1. *present*

242. **[GFB15: 173] Spino-occipital nerve foramina**

0. *two or more, aligned horizontally*

1. *one or two, dorsoventrally offset*

243. **[GFB15: 174] Ventral notch between parachordals**

0. *present or entirely unfused*

1. *absent*

244. **[GFB15: 175] Parachordal shape**

0. *forming a flat, broad surface as wide as the otic capsules*

1. *mediolaterally constrained relative to the otic capsules*

245. **[GFB15: 176] Stalk-shaped parachordal/occipital region**

0. *absent*

1. *present*

246. **[GFB15: 177] Paired occipital facets**

0. *absent*

1. *present*

247. **[C17: 119] Ventral portion of occipital arch wedged between rear of otic capsules**

0. *absent*

1. *present*

248. **[C17: 120] Dorsal portion of occipital arch wedged between rear of otic capsules**

Changed Buchanosteus from - to 0 for this and previous

0. *absent*

1. *present*

249. **[C17: 121] Occipital crest anteroposteriorly elongate, and extends from the roof of the posterior tectum**

0. *absent*

1. *present*

250. **[C17: 122] Unconstricted basicranial notochord**

0. *absent*

1. *present*

251. **[GFB15: 178] Size of aperture to notochordal canal**

0. *much smaller than foramen magnum*

1. *as large or larger than foramen magnum*

252. **[C17: 117] Channel for dorsal aorta and/or lateral dorsal aortae**

Acanthodes scored 1 following the interpretation of Miles (1973b). *Chondrenchelys* scored ?. *Pucapampella* scored 0 following Coates et al. (2018). *Diplacanthus* scored for this and the next character following Chapter 4.

0. *passes through basicranium*

1. *external to braincase*

253. **[C17: 118] Dorsal aorta divides into lateral dorsal aortae**

0. *posterior to occipital level*

1. *anterior to level of the occiput*

254. **[GFB15: 180] Hypotic lamina (and dorsally directed glossopharyngeal canal)**

0. *absent*

1. *present*

B.4.7 Paired fins

255. **[GFB15: 181] Macromeric dermal shoulder girdle**

This explicitly refers to plates, rather than other macromeric structures (ie. fin spines and prepectoral spines). Polarities of character states have been reversed so as to be simpler to score. *Gyracanthides* is scored absent - the prepectoral spine is spinose, and the "basal plates" are in exactly the same location as intermediate spines (Warren et al., 2000). *Milesacanthus* is scored ? as there is only one specimen and the pectoral region is disrupted (Young and Burrow, 2004).

0. *absent*

1. *present*

256. **[GFB15: 182] Dermal shoulder girdle composition**

0. *ventral and dorsal (scapular) components*

1. *ventral components only*

257. ***Ascending pinnal lamina**

In some acanthodian grade taxa the shoulder girdle has a lamina that wraps around the ventro-lateral corners of the shoulder girdle.

This character is only applicable for taxa with a dermal shoulder girdle comprising ventral components

0. *absent*

1. *present*

258. ***Ascending pinnal lamina forms dorsal process**

The acanthodian-grade taxon *Dobunnacanthus* has a prounounced ascending process on the dermal shoulder girdle Miles (1973a), the ascending pinnal lamina. A similar, but less tall process is also present on the dermal shoulder girdle of *Parexus* (Miles, 1973a), *contra* Watson (1937) and the reconstruction by Burrow et al. (2013).

This character is only applicable for taxa with an ascending pinnal lamina.

0. *absent*

1. *present*

259. **[GFB15: 183] Shape of dorsal blade of dermal shoulder girdle (either cleithrum or anterodorsal plate**

0. *spatulate*

1. *pointed*

260. **[GFB15: 184] Dermal shoulder girdle forming a complete ring around the trunk**

Polarities reversed.

0. *absent*

1. *present*

261. **[GFB15: 185] Pectoral fenestra completely encircled by dermal shoulder girdle**

Polarities reversed.

0. *absent*

1. *present*

262. **[Modified from GFB15: 215] Paired pectoral fin spines**

This character has been changed to explicitly code for pectoral fin spines - another character covers pelvic fin spines.

0. *absent*

1. *present*

263. **[HW04: 50] Pectoral fin spine relationship with dermal shoulder girdle**

In all stem-gnathostomes and osteichthyans with paired fin spines, the fin spines are fused to the dermal pectoral girdle (eg. *Guiyu* Zhu et al. (2009)). This is true in some stem-chondrichthyans, for example *Ptomacanthus* (Chapter 6) - in others however they are detached from these plates, for example in *Euthacanthus* (Miles, 1973a). This character is inapplicable for taxa without both pectoral fin spines and macromeric dermal shouder girdle plates.

0. *not attached to dermal plates*

1. *fused to dermal plates*

264. **[GFB15: 220] Prepectoral spines**

On the basis of chapter 6 these spines are defined as those borne on the coracoid part of the shoulder girdle. Correspondingly I agree with Hanke and Wilson (2010) that the "necklace" of spines in *Kathemacanthus* are prepectoral (*contra* Burrow et al. (2016a)), as the coracoid process can be seen extending below them. The high placement of the pectoral fins is probably the reason for

the unusual placement of the prepectoral spines.

Brochoadmones is also problematic to score, again because of the high placement of its pectoral spine. Hanke and Wilson (2004) consider it to have no prepectoral spines, and that all spines are one series of intermediate spines. Phylogenetic analyses since have however scored them as present (eg. Giles et al. (2015c); Coates et al. (2018); Burrow et al. (2016a). I judge that the first two "intermediate spines" in *Brochoadmones*probably are prepectoral: they are far smaller than the posterior intermediate spines, and could conceivable be borne on a long coracoid process. The third "prepectoral spine is probably an intermediate spine - it is directly underneath the pectoral fin spine, and in is similar to the posterior intermediate fin spines in size, shape, and in having an accompanying web of scales. This interpretation gives *Brochoadmones* a typical stem-chondrichthyan spine compliment of two prepectoral spines. I have scored it on the basis of this.

Milesacanthus has a similar procoracoid but it is unclear if spine is present (Young and Burrow, 2004): it is scored ?. Similarly the "patch of scales" on the procoracoid of *Tetanopsyrus* may in fact be a prepectoral spine like that of *Diplacanthus*: it is conservatively scored ?.

Burrow and Rudkin (2014) identify a prepectoral spine in *Nerepisacanthus*: however this is poorly preserved and far from certain to be a prepectoral spine. It is scored ?.

0. *absent*
1. *present*

265. *** Number of prepectoral spine pairs**

Based on Hanke and Wilson (2004) character number 48.

I consider that the "admedian" spine described in *Doliodus* (Maisey et al., 2017) is in fact a prepectoral spine, as it is mounted on the coracoid process of the shoulder girdle: thus it is scored 1. *Kathemacanthus* is the only taxon in our matrix to have three prepectoral spines, a state also seen in some other isolated acanthodian shoulder girdles (Miles, 1973a) but in this matrix the state is uninformative. *Brochoadmones* is scored 1 following the above interpretation of its spines.

0. *one*

1. *two*

2. *three*

266. *** Median, unpaired endoskeletal component in shoulder girdle**

A median endoskeletal element was described in the shoulder girdle of *Doliodus* (Maisey et al., 2017). An "intercoracoid" element is also present in the shoulder girdle of *Iniopera*, as well as several other putative stem-holocephalans (Pradel et al., 2010). Possible perichondral bone has been described in the lorical plate in *Climatius* (Burrow et al., 2015), however this is scored ?, as have other taxa where the coracoid region on the pectoral girdle is unknown or incompletely known.

0. *absent*

1. *present*

267. **[K16: 447] Median ventral trunk plates**

Following King et al. (2016) this captures osteichthyan interclavicles, stem-gnathostome median ventral plates, and acanthodian lorical plates (and spines).

0. *absent*

1. *present*

268. *** Median ventral trunk plate/s reduced to anterior spinose plate**

In some acanthodians, eg. *Culmacanthus* (Long, 1983), *Brachyacanthus* (Miles, 1973a), *Climatius* (Burrow et al., 2015)) the lorical dermal structure extends posteriorly to the level of the pectoral fin spines. In others *Vernicomacanthus* (Miles, 1973a), *Parexus* (Burrow et al., 2013)) it is reduced to a very small anterior element, which essentially constitutes only a spine.

0. *absent*

1. *present*

269. **[GFB15: 186] Median dorsal plate**

0. *absent*

1. *present*

270. **[GFB15: 187] Posterior dorsolateral (PDL) plate or equivalent**

0. *absent*

1. *present*

271. **[GFB15: 188] Pronounced internal crista (keel) on median dorsal surface of shoulder girdle**

0. *absent*

1. *present*

272. **[GFB15: 189] Crista internalis of dermal shoulder girdle**

0. *absent*

1. *present*

273. **[GFB15: 190] Scapular infundibulum**

0. *absent*

1. *present*

274. **[GFB15: 191] Scapular process of shoulder endoskeleton**

Changed *Guiyu* to ? for this as I can't see them in the figured material (Zhu et al., 2009).

0. *absent*

1. *present*

275. **[GFB15: 192] Ventral margin of separate scapular ossification**

Changed Euthacanthus to 0 following Newman et al. (2014).

0. *horizontal*

1. *deeply angled*

276. **[GFB15: 193] Cross-sectional shape of scapular process**

0. *flattened or strongly ovate*

1. *subcircular*

277. **[GFB15: 194] Flange on trailing edge of scapulocoracoid**

Culmacanthus scored 1 following Long (1983).

0. *absent*

1. *present*

278. **[GFB15: 195] Scapular process with posterodorsal angle**

0. *absent*

1. *present*

279. **[GFB15: 196] Endoskeletal postbranchial lamina on scapular process**

0. *absent*

1. *present*

280. **[GFB15: 197] Mineralisation of internal surface of scapular blade**

0. *mineralised all round*

1. *Unmineralised on internal face forming a hemicylindrical cross-section*

281. **[GFB15: 198] Coracoid process mineralised**

Contrary to the original coding of this by Brazeau (2009), and subsequent codings, I consider the procoracoid element in "acanthodian" stem-chondrichthyans to be homologous to the coracoid process in "conventional" chondrichthyans, as Miles (1973a) thought. Recent evidence in support of

this comes from *Doliodus* in which the coracoid clearly bears the prepectoral spines (Maisey et al., 2017)), in a manner consistent with the position they are borne in climatiids and in particular with a *Ptomacanthus* specimen in which the coracoid process is preserved but with the overlying armour lost (Miles, 1973a). Acanthodians with dermal ossifications attached to a mineralised procoracoid bear these structures in an equivalent place (eg. *Diplacanthus* in Chapter 6, and gyracanthids (Warren et al., 2000; Snyder et al., 2017). Other acanthodians with prepectoral spines (eg. *Vernicomacanthus*, *Dobunnacanthus*) presumably had a coracoid process or procoracoid extending into that region of the dermal shoulder girdle - however, as this is unpreserved they are scored ?.

0. *absent*

1. *present*

282. **[Modified from GFB15: 199] Part of coracoid mineralised separately ("procoracoid")**

In many "acanthodians" the coracoid region of the pectoral girdle is mineralised as a separate "procoracoid" element Miles (1973a). This character captures that separate mineralisation, as opposed to many "conventional" chondrichthyans in which it is fused to the rest of the scapulocoracoid by mineralised tissue (eg. *Doliodus* (Maisey et al., 2017)). The likely crown-chondrichthyans *Akmonistion* (Coates and Sequeira, 2001a), *Cobelodus* (Zangerl and Case, 1976), and *Orthacanthus* (Heidtke, 1999), also possess separate "procoracoid" mineralisations: they have been scored 1 for this character, although as their procoracoids are in addition to a pronounced coracoid process their condition may well not be directly homologous with that of "acanthodians".

I have changed *V. waynensis* from 1>?.

0. *absent*

1. *present*

283. **[GFB15: 200] Fin base articulation on scapulocoracoid**

Doliodus scored ?

0. *deeper than wide (stenobasal)*

1. *wider than deep (eurybasal)*

284. **[GFB15: 201] Pectoral fin articulation**

Doliodus scored ?

0. *monobasal*

1. *polybasal*

285. **[GFB15: 202] Number of basals in polybasal pectoral fins**

0. *three or more*

1. *two*

286. **[GFB15: 203] Branching radials in paired fins**

0. *absent*

1. *present*

287. **[GFB15: 204] Number of mesomeres in metapterygial axis**

0. *five or fewer*

1. *seven or more*

288. **[GFB15: 205] Biserial pectoral fin endoskeleton**

0. *absent*

1. *present*

289. **[GFB15: 206] Perforate propterygium**

0. *absent*

1. *present*

290. **[GFB15: 207] Filamentous extension of pectoral fin from axial region**

0. *absent*

1. *present*

291. **[GFB15: 208] Pelvic fins**

0. *absent*

1. *present*

292. **[[GFB15: 209] Pelvic claspers**

0. *absent*

1. *present*

293. **[Modified from K16: 433] Pelvic girdle with substantial dermal component**

Polarities reversed.

0. *absent*

1. *present*

294. **[K16: 434] Pelvic fin spines**

0. *absent*

1. *present*

295. **[GFB15: 210] Dermal pelvic clasper ossification**

0. *absent*

1. *present*

296. **[C17: 131] Pelvic girdle with fused puboischiadic bar**

0. *absent*

1. *present*

297. **[GFB15: 211] Pectoral fins covered in macromeric dermal armour**

0. *absent*

1. *present*

298. **[GFB15: 212] Pectoral fin base has large, hemispherical, dermal component**

0. *absent*

1. *present*

B.4.8 Axial skeleton

299. **[GFB15: 213] Dorsal fin spines**

0. *absent*

1. *present*

300. **[GFB15: 214] Anal fin spine**

0. *absent*

1. *present*

301. **[GFB15: 216] Median fin spine insertion**

Parexus scored 0 following Burrow et al 2013 Burrow et al. (2013).

0. *shallow, not greatly deep*

1. *deep*

302. **[B16: 257] Fin spine insertion with fine parallel longitudinal ridges:**

This is common to the fin spine insertions of diplacanthids (Burrow, 2007; Burrow and Young, 2012). It also appears to be present on the insertion in *Onychoselache* (Fig 7a of Coates and Gess (2007)).

0. *absent*

1. *present*

303. **[GFB15: 217] Intermediate fin spines**

Intermediate, or prepelvic, fin spines form a paired series between the pelvic and pectoral fins of many stem-chondrichthyans (eg. *Climatius, Doliodus*) (Burrow et al., 2015; Miles, 1973a; Maisey et al., 2017). In some animals an anterior pair of spines is positioned anteriorly, between the pectoral fin spines

(eg.*Vernicomacanthus* (Miles, 1973a)). These were considered by Miles (1973a) to be the first pair of intermediate fin spines - more recently Burrow et al. (2016a) argued that they should instead be considered to be separate "admedian" fin spines. Given that these spines are in series with the intermediate spines where present and are not fixed to an endoskeletal element like other spines of the shoulder girdle I consider that they are most conservatively interpreted as being intermediate fin spines, and so have coded taxa with only these spines and no other intermediate spines as "present" for this character. The "series" of admedian fin spines Burrow et al. (2016a) identify in *Kathemacanthus* are instead prepectoral, as evidenced by their position on the coracoid part of the shoulder girdle. The "admedian" fin spine of *Doliodus* are topologically consistent with second prepectoral spines in other acanthodian-grade stem-chondrichthyans (see Chapter 6) and are scored as such (Maisey et al., 2017).

0. *absent*

1. *present*

304. *** Anteriormost intermediate spine pair lies between pectoral fin spines**

In some stem-chondrichthyans with intermediate fin spines the anteriormost pair of these lies between the two pectoral fin spines, where it is sometimes incorporated into the ventral armour of the shoulder girdle (Miles, 1973a). In others, such as *Ptomacanthus Euthacanthus*, and *Doliodus* the intermediate spines instead all lie well posterior to the pectoral girdle (Newman et al., 2014; Brazeau, 2012; Maisey et al., 2017). Although *Doliodus* is described by Maisey *et al.* (Maisey et al., 2017) as having admedian spines, comparing its position on the scapulocoracoid to other "climatiids" I consider their second suggestion, that it is a prepectoral spine, far more likely - it is scored absent. *Brochoadmones* is coded as present, as following my interpretation of its spine array (see prepectoral spines character 264) its most anterior intermediate spine is directly

ventral to the pectoral fins (Hanke and Wilson, 2006). The most anterior intermediate fin spine in *Kathemacanthus* is also beneath the pectoral girdle (Hanke and Wilson, 2010).

0. *absent*

1. *present*

305. **[GFB15: 219] Intermediate spines when present**

On the basis of my previous argument, taxa with only one pair of "admedian" intermediate spines have been scored 0.

0. *one pair*

1. *multiple pairs*

306. **[GFB15: 218] Dorsal fin spine cross-section**

0. *Round or horseshoe-shaped*

1. *Flat sided, with rectangular profile*

307. **[GFB15: 221] Fin spines with ridge**

0. *absent*

1. *present*

308. **[GFB15: 222] Fin spines with nodes**

0. *absent*

1. *present*

309. ***Dorsal fin spines with rows of large retrose denticles**

Modified from Giles and Burrow

0. *absent*

1. *present*

310. **[GFB15: 224] Expanded spine rib on leading edge of spine**

0. *absent*

1. *present*

311. **[GFB15: 225] Spine ridges**

As discussed in Chapter 6 this is a character present in some stem-chondrichthyan taxa which could plausible unite them to the exclusion of some others. It is well documented in *Gyracanthides* (Warren et al., 2000; Turner et al., 2005), as well as in *Vernicomacanthus* and *Dobunnacanthus* (Miles, 1973a). It also appears to be present in *Lupopsyrus* (Hanke and Davis, 2012). Burrow et al. (2013, 2017) also report the condition in *Parexus* and in *Doliodus*.

0. *Converging at distal end of spine*

1. *Converging on leading edge*

312. **[B16: 258] Retrorse denticles on pectoral spine**

0. *absent*

1. *present*

313. **[GFB15: 226] Synarcual**

0. *absent*

1. *present*

314. **[GFB15: 227] Series of thoracic supraneurals**

0. *absent*

1. *present*

315. **[GFB15: 228] Number of dorsal fins, if present**

Check this against Coates dorsal character222

0. *one*

1. *two*

316. **[GFB15: 229] Posterior dorsal fin shape**

Cheiracanthus changed from 0>- as it has only 1 dorsal fin (Watson, 1937).

0. *base approximately as broad as tall, not broader than all of other median fins*

1. *base much longer than the height of the fin, substantially longer than any of the other dorsal fins*

317. **[GFB15: 230] Basal plate in dorsal fin**

0. *absent*

1. *present*

318. **[GFB15: 231] Branching radial structure articulating with dorsal fin base plate**

0. *absent*

1. *present*

319. **[C17: 136] Dorsal fin spine at pectoral level only**

This is coded inapplicable for taxa with only one dorsal fin.

0. *absent*

1. *present*

320. **[C17: 142] Posterior dorsal fin with delta-shaped cartilage**

0. *absent*

1. *present*

321. **[GFB15: 232] Anal fin**

0. *absent*

1. *present*

322. **[GFB15: 233] Basal plate in anal fin**

0. *absent*

1. *present*

323. **[GFB15: 234] Caudal radials**

0. *extend beyond level of body wall and deep into hypochordal lobe*

1. *radials restricted to axial lobe*

324. **[GFB15: 236] Epichordal lepidotrichia in caudal in**

0. *absent*

1. *present*

325. **[C17: 144] Caudal neural and/or supraneural spines**

0. *short*

1. *long*

326. **[C17: 145] Caudal axis upturned steeply supposting high aspect ratio (lunate) tail**

0. *absent*

1. *present*

327. **[C18: 240] Brush complex of bilaterally distributed calcified tubes flanking or embedded in calcified cartilage core**

0. *absent*

1. *present*

328. **[C18: 245] Anal fin base narrow, posteriormost proximal segments radials broad**

Tetanopsyrus changed - to 0.

0. *absent*

1. *present*

329. **[C18: 251] Anterior dorsal fin spine leading edge concave in lateral view**

0. *absent*

1. *present*

APPENDIX C: DETAILS OF SUPPLEMENTARY INFORMATION

Data that I was unable to make available within the thesis itself, for example videos of specimens, models, tomographic datasets, is available on Figshare at the following links:

1. **Chapter 3 - The visceral skeleton of the stem-chondrichthyan *Ptomacanthus* - Supplementary videos**: `https://figshare.com/s/00ea7c23349f20126ced`
2. **Chapter 3 - The visceral skeleton of the stem-chondrichthyan *Ptomacanthus* - Phylogenetic supplement**: `https://figshare.com/s/fc56cd82ccbecf541f85`
3. **Chapter 3 - The visceral skeleton of the stem-chondrichthyan *Ptomacanthus* - 3D models**: `https://figshare.com/s/5c94d1ccced395cdeb07`
4. **Chapter 4 - A third "acanthodian" endoskeleton in *Diplacanthus crassisimus* - Supplementary videos**: `https://figshare.com/s/ba83aedc59fbe24c4ae3`
5. **Chapter 4 - A third "acanthodian" endoskeleton in *Diplacanthus crassisimus* - 3D models**: `https://figshare.com/s/63723c0d9589cfc79bfe`
6. **Chapter 5 - Endochondral tissues in early vertebrates - Supplementary videos**: `https://figshare.com/s/246c458ea29dc13eeea8`
7. **Chapter 5 - Endochondral tissues in early vertebrates - 3D models**: `https://figshare.com/s/90bf90ca1612cea4f384`
8. **Chapter 6 - The stem-chondrichthyan genus *Vernicomacanthus* and the early evolution of the chondrichthyan shoulder girdle - Supplementary videos**: `https://figshare.com/s/e4105cd1c51ccea47c0b`

9. **Chapter 6 - The stem-chondrichthyan genus *Vernicomacanthus* and the early evolution of the chondrichthyan shoulder girdle - 3D models**: `https://figshare.com/s/66383ec298c8925862c9`

10. **Chapter 7 - A phylogenetic exploration of the chondrichthyan stem-group - Phylogenetic supplement**: `https://figshare.com/s/3635d1cb3b81c8015875`